UNIVERSITY OF LIVERPOOL

The role of Nuclear Lamins in regulating the circadian molecular clockwork; daily oscillations and response to mechanical stimulation.

Thesis submitted in accordance with the requirements of the University of Liverpool for the degree of Doctor in Philosophy

By

Miss Clare Amy Roskell

March 2019

Abstract

Circadian rhythms are evolutionarily conserved ~24h biological cycles in physiology, metabolism, and behaviour, including locomotor activity. Musculoskeletal cells contain cell-autonomous, self-sustainable circadian clocks; synchronised by a central clock located in the suprachiasmatic nuclei. The nuclear lamina underlies the nuclear envelope and consists of type-V intermediate filament proteins called lamins. Laminopathies are a spectrum of clinical diseases with a mutation in *Lmna*, often including tissue-specific pathogenesis; musculoskeletal pathology is characterised by muscle wasting and cardiac defects. Lamin A is an important regulator of genome organisation, nuclear support and tethering of transcription factors, such as those involved in differentiation and stress response signalling pathways. Accordingly, in musculoskeletal cells, lamin A is crucial for acute responses to mechanical stimulation.

The aims of this thesis investigated whether the molecular clock and lamin A bi-directionally regulate one another in musculoskeletal cells, and whether the circadian clock is responsive to mechanical stimuli, and then constructed a mathematical model to begin elucidating potential mechanisms of regulation.

To determine whether lamin A oscillates with a circadian rhythm, circadian time-courses were collected from C2C12 myoblasts and myotubes, primary myotubes, and mouse muscle samples. Lamin A circadian oscillations were identified in mRNA, protein, and immunocytochemistry time-course data. To determine whether lamin A exerts feedback regulation on the circadian clock, lamin A was manipulated in musculoskeletal cells, and had a direct effect on core clock gene expression. siRNA knockdown of lamin A significantly decreased the expression of the core clock genes *Per1*, *Per2*, *Bmal1*, and *Cry1*; overexpression of lamin A increased the expression of core clock genes *Per1*, *Per2*, and *Bmal1*, and decreased the expression of *Cry1.* Furthermore, in response to *in vitro* strain by the Flexcell system, primary myoblasts and C2C12 myotubes demonstrated a decrease in *Cry1* expression, and an increase in *Cry1* and *Bmal1* expression, respectively. Additionally, *Clock* gene expression was upregulated in Gastrocnemius and Quadricep muscle from mice subject to acute and chronic *in vivo* loading, respectively. Finally, 4 mathematical models were generated to investigate potential regulatory feedback pathways that may link the circadian clock and lamin A.

These results revealed that lamin A oscillates with a circadian rhythm in musculoskeletal tissues, that the circadian clock is disrupted in response to lamin A knockdown and overexpression, and that the circadian clock is responsive to mechanical strain. Future studies may include deciphering whether this mechanism conveys mechanical stimulation and myogenic differentiation signals to the clock, and determining if the musculoskeletal clock is disrupted in laminopathy patients. Knowledge of the circadian clock and lamin A regulatory mechanisms can direct therapeutic strategies to reset altered clocks in patients with musculoskeletal disorders.

Acknowledgements

I would like to thank my supervisors Dr Simon Tew, Dr Vanja Pekovic-Vaughan, Prof. Pete Clegg, and Dr Daryl Shanley. Simon, thank you for being kind enough to supervise my work and for providing invaluable support and expertise. Vanja, thank you for securing the funding for this project and for your intellectual contribution. Pete, thank you for your guidance and encouragement, without it this thesis would not have been possible. Daryl, thank you for your help and enthusiasm in developing my mathematical model.

Thank you to the BBSRC DTP for providing the funding for my PhD and for all of the opportunities that came with it.

Thank you to all of the staff and students at IACD who have taken the time to help me during my PhD. In particular, thank you to Ben McDermott, Rachel McCormick, and Caroline Staunton for your advice on experiments. A special thank you to Niamh Horton and Rhiannon Morgan for always being there to listen, for providing countless pep talks, and for keeping me motivated to finish.

To all of my family and friends, thank you for supporting me throughout my PhD.

Harry, thank you for your patience and for continuing to keep me smiling when I needed it most.

Last but not least, I would like to thank my parents and my brother Paul for your love and endless support. You believed in me when I was struggling to believe in myself.

I would like to dedicate this thesis to my parents, without your help and encouragement, I never would have succeeded.

Contents

List of Figures

List of Tables

Abbreviations

Ankrd2	Ankyrin repeat protein 2
BAF	Barrier-to-autointegration factor
bHLH	Basic helix-loop-helix
Bmal1	Brain and Muscle Arnt-Like 1
BOS	Buschke-Ollendorff syndrome
CLC	Cardiolipin-Like Cytokine
Cry	Cryptochrome
CT	Circadian Time
CTCF	CCCTC-binding factor
DAPI	4’,6-diamidino-2-phenylindole
DCM	Dilated cardiomyopathy
DCM-CD	Dilated cardiomyopathy with conduction defects
Dex	Dexamethasone
DMEM	Dulbecco’s Modified Eagle's Medium
DSPS	Delayed Sleep Phase Syndrome
ECM	Extracellular Matrix
EDMD	Emery Dreifuss Muscular Dystrophy
ERK	Extracellular Regulated Kinases
FA	Focal Adhesion
FACs	Fluorescence Activated Cell Sorting
FAK	Focal Adhesion Kinase
FASPS	Familial Advanced Sleep-Phase Syndrome
FBS	Foetal Bovine Serum
FPLD	Familial Partial Lipodystrophy
FTase	Farnesyltransferase
GHT	Geniculohypothalamic tract
HGPS	Hutchinson-Gilford Progeria Syndrome
HS	Horse Serum
Icmt	Isoprenylcysteine carboxyl methyltransferase
IGL	Intergeniculate leaflet
JNK	c-Jun NH2-terminal Kinases
KASH	Klarsicht, ANC-1, and Syne Homology
L-Glu	L-Glutamine
LADs	Lamina-Associated Domains
LAP	Laminin-associated polypeptides
LBR	Lamin-B Receptor
LEM	LAP2β-Emerin-MAN1
LGMD 1B	Limb girdle muscular dystrophy type 1B
MAP	Mitogen-Activated Protein
MEF	Mouse Embryonic Fibroblasts
MR	Midbrain Raphe Nucleus
mRNA	Messenger RNA
MSC	Mesenchymal Stem Cell
NETs	Nuclear Envelope Transmembrane proteins

NLS	Nuclear Localisation Signal
NPC	Nuclear Pore Complex
NPY	Neuropeptide Y
Nups	Nucleoporin proteins
PARP1	Poly [ADP-ribose] Polymerase 1
PAS	Period-Arnt-Single-Minded
Pen/Strep	Penicillin/Streptomycin
Per	Period
PBS	Phosphate Buffered Saline
PFA	Paraformaldehyde
qRT-PCR	Quantitative Real-Time PCR
Rb	Retinoblastoma protein
RHT	Retinohypothalamic tract
RNAi	RNA interference
ROS	Reactive Oxygen Species
SCN	Suprachiasmatic Nucleus
siRNA	Small interfering RNA
SREBP1	Sterol Response Element-Binding Protein 1
SRF	Serum Response Factor
SUN	Sad1 and UNC-84
TGF-β	Transforming growth factor-beta
TTFL	Transcriptional Translational Feedback Loop
VIP	Vasoactive Intestinal Peptide
ZT	Zeitgeber Time

1 General Introduction

1.1 Lamin A

1.1.1 The Nucleus

Within eukaryotic cells, chromatin is packaged and organised into the nucleus, a membrane enclosed organelle, separating nucleic and cytoplasmic functions. Prokaryotic cells do not contain a nucleus; the evolution of this organelle was likely due to the increasing genome size of more complex organisms, which led to a requirement for further regulation and organisation (Newport and Forbes, 1987). The nuclear envelope is the membrane that surrounds the nucleus, acting as a partition; it also has a wider role, through meditating cytoplasmic and nuclear interactions, it can regulate functions within each compartment. The nucleus is connected to the cytoplasm through nuclear pores which regulate nuclear entry and exit.

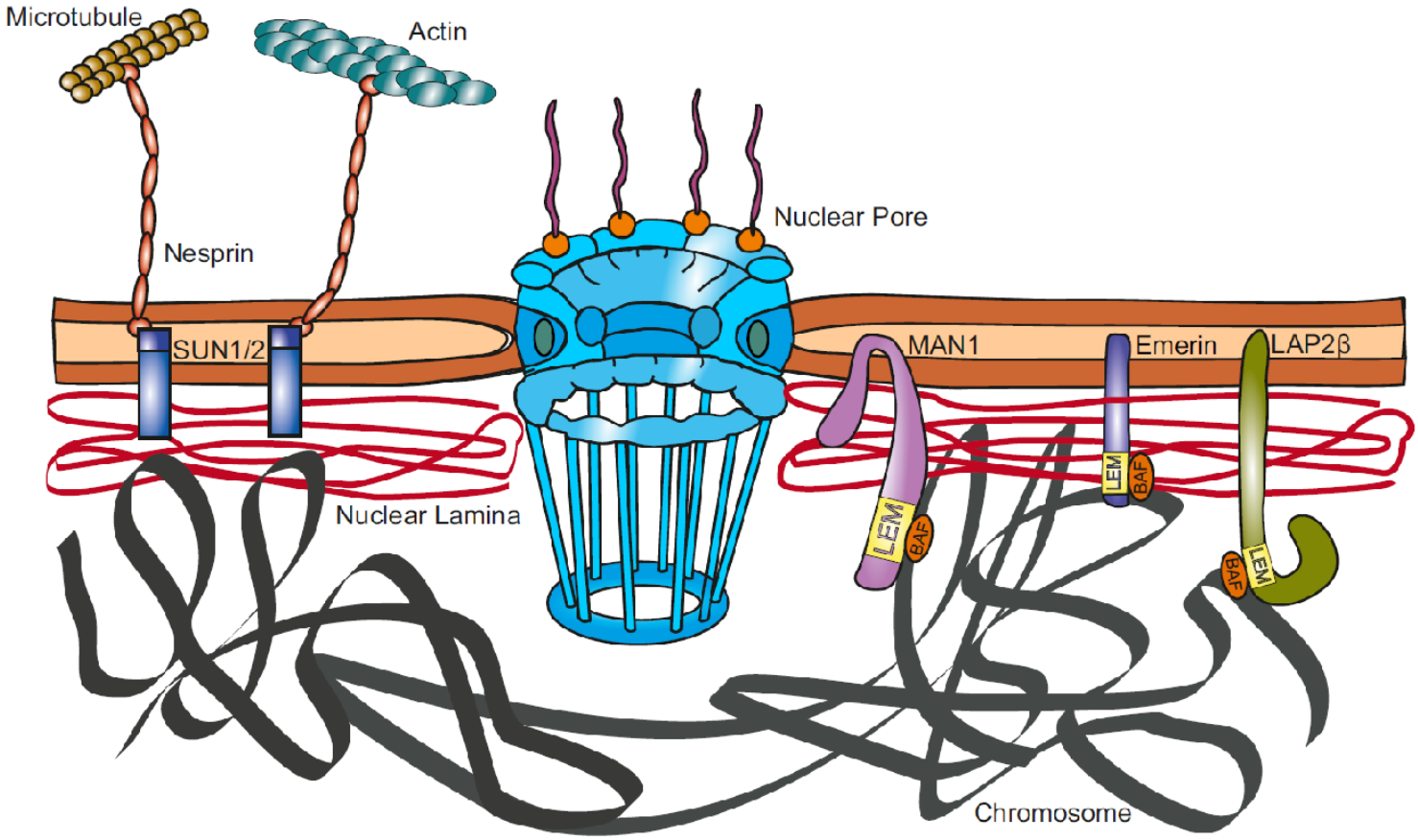

Figure 1.1. Schematic diagram of the nuclear envelope and the nuclear pore.

The cell nucleus is composed of nucleoplasm and is surrounded by a nuclear envelope that consists of four elements, shown in Figure 1.1: the inner nuclear membrane, outer nuclear membrane, nuclear pores, and the underlying nuclear lamina (Callan and Tomlin, 1950; Fawcett, 1966). The inner and outer nuclear membranes are phospholipid bilayers, which are separated from one another by the perinuclear cisternal space, roughly 30-50 nm in size. The outer nuclear membrane has ribosomes attached to its cytoplasmic surface and is continuous with the endoplasmic reticulum. The perinuclear space, of the inner and outer nuclear membrane, is continuous with the lumen of the endoplasmic reticulum.

Within the nucleus there are sub-compartments that localise the nuclear machinery for processes such as transcription and DNA replication, creating microenvironments specific for these essential functions. In 1885, experiments visualising interphase chromosomes in the salamander larvae first documented that chromosomes maintain individuality and occupy distinct territories (Rabl, 1885). Further research in 1888 and 1909 involving experiments with *Ascaris megalocephala* supported the individuality of chromosomes and also noted that the telomeres of chromosomes associate with the nuclear envelope (Boveri, 1888; Boveri, 1909). These observations on the interphase order of chromosomes were later confirmed in Chinese hamster fibroblasts, through utilising premature chromosome condensation and microirradiation with pulse-labelling in G1 (Cremer, *et al*., 1982). This research demonstrated that organisation within the nucleus is non-random; underpinning further research into the spatial organisation of chromosomes and what importance this may play in nuclear activities, such as transcriptional regulation.

1.1.2 Lamins

Lamins were first identified in 1975 and it was realised that they acted as structural proteins within the nucleus, organising into a meshwork of fibres roughly 15-20 nm thick called the nuclear lamina. Lamins are very closely associated with the inner nuclear membrane and are attached to both chromatin and the periphery of the nuclear pores (Aaronson and Blobel, 1975; Gerace, *et al*., 1978;

Paddy, *et al*., 1990). They are type V intermediate filament proteins and are classified into two subgroups, A-type or B-type, based on both biochemical properties and their primary sequences (Franke, 1987; Nigg, 1989). Like all proteins of the intermediate filament family, lamins are composed of three well-conserved domains: Head (NH2-terminal), Rod, and Tail (C-terminal) (Hanukoglu and Fuchs, 1982; Fisher, Chaudhary, and Blobel, 1986; Krohne, *et al*., 1987). The Head domain is globular, positively charged, and much shorter in lamins compared to other intermediate filaments. The Rod domain is composed of four α-helical coiled coil domains – coils 1A, 1B, 2A, and 2B, which represent the structural hallmarks of intermediate filament proteins and are separated by linker regions – L1, L12, and L2 (Conway and Parry, 1990). The Tail domain is globular and contains a Nuclear Localisation Signal (NLS), an s-type immunoglobulin (Ig) fold motif, and a CaaX (Cysteine-aliphatic-aliphatic- any amino acid) motif at the carboxyl-terminal end (Clarke, *et al*., 1988; Dhe-Paganon, *et al*., 2002). The tail domain is larger in lamins in comparison with other intermediate filament proteins, is highly positively charged, and is involved in binding to nuclear membrane and inner nuclear membrane binding proteins (Senior and Gerace, 1988; Belmont, *et al*., 1993).

It was first characterised in amphibian oocytes that Lamin proteins form higher-order polymers. Monomers of Lamin dimerise in a parallel formation through coiling of the α-helical coiled coil, located in the rod domain, and head-to-tail association of two or more dimers results in the formation of polymers (Aebi, *et al*., 1986; Strelkov, *et al*., 2004). Protofilaments are produced through the anti-parallel association of two polymers, and a complete intermediate filament is formed by three or four protofilaments associating and layering together, depicted in Figure 1.2 (Ben-Harush, *et al*., 2009).

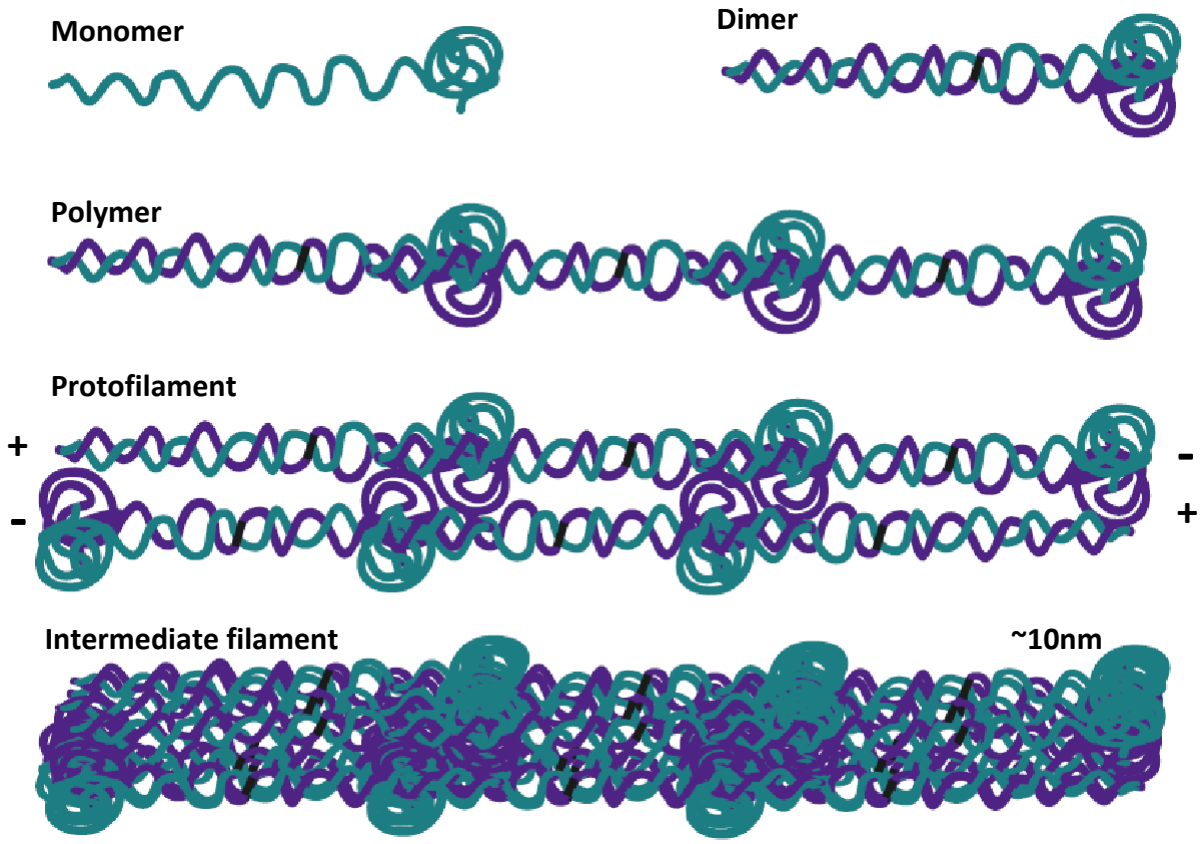

Figure 1.2. Diagram of Lamin intermediate filament formation from lamin monomers.

There are three Lamin genes in mammals: *Lmna*, *Lmnb1*, and *Lmnb2*, which each encode major and minor isoforms. A-type lamins are encoded by *Lmna*; located on chromosome 1q21.1-1q21.3, spanning 24kb, and are composed of 12 exons. Alternative splicing of the pre-mRNA transcript, within exon 10, gives rise to the two major isoforms that are 1992bp and 1716bp – pre-lamin A and lamin C mRNA, respectively (McKeon, *et al*., 1986; Lin and Worman, 1993). Minor isoforms include lamin AΔ10 and C2 (Machiels, *et al*., 1996; Smith and Benavente, 1992). The first 556 amino acids comprising human lamin A and lamin C are identical; however, they differ in the carboxyl-terminal ends, lamin C has six carboxyl terminal acids that are different to lamin A. Lamin A protein is 664 amino acids long and 74kDa, and lamin C is 572 amino acids long and 64kDa (Sakaki, *et al*., 2001).

All Lamin proteins undergo a range of post-translational modifications, including farnesylation, methylation, phosphorylation, sumoylation, ADP-ribosylation, and glycosylation (Farnsworth, *et al*., 1989; Ottaviano and Gerace, 1985; Zhang and Sarge, 2008; Adolph, 1987; Ferraro, *et al*., 1989). Pre-

lamin A undergoes a routine order of processing before lamin A is produced, including: farnesylation, proteolysis, methylation, and endoproteolysis, depicted in Figure 1.3.

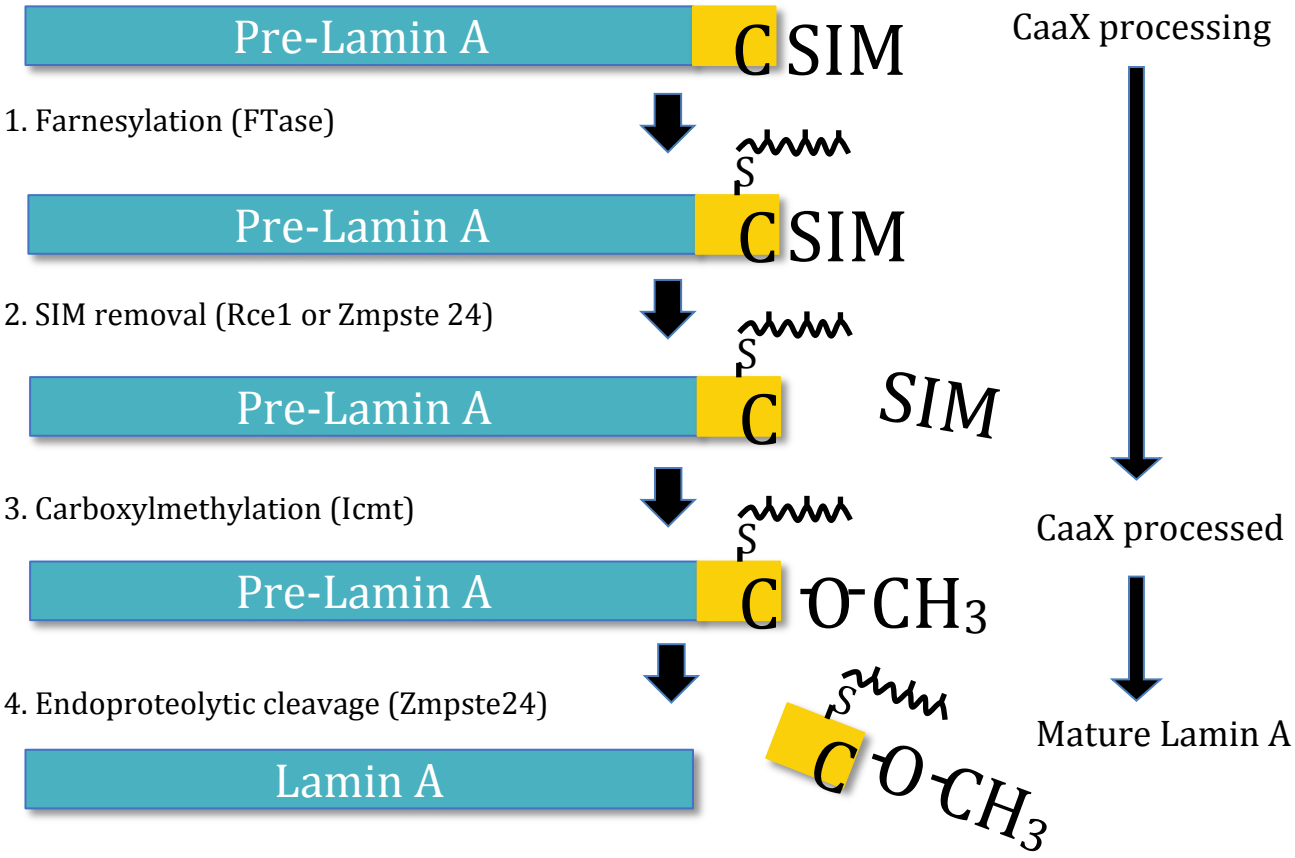

Figure 1.3. Schematic diagram of post-translational modifications to pre-lamin A to produce mature lamin A protein.

First, the pre-lamin A mRNA undergoes lipidation at the C residue of its CaaX box (CISM); the C is a cysteine amino acid, the two A residues are often aliphatic amino acids and the X can be multiple different residues. This is completed by protein farnesyltransferase (FTase) (Lutz, *et al.*, 1992). The endoproteolytic cleavage of the SIM amino acids (or the aaX of the CaaX) is completed by either RCE1 or ZMPSTE24 (Boyartchuk, Ashby, and Rine, 1997; Otto, *et al.*, 1999; Bergo, *et al.*, 2002). The final stage of CaaX processing includes the methylation of the carboxylate anion of the carboxyl-terminal farnesylcysteine by isoprenylcysteine carboxyl methyltransferase (Icmt), an integral membrane protein located in the endoplasmic reticulum (Clarke, *et al.*, 1988; Dai, *et al.*, 1998). Zempst24 performs the final pre-lamin A processing stage, undergoing site-specific cleavage at the

putative endoproteolysis site RSYLLG, with cleavage occurring between the Y and L amino acids (Sinensky, *et al*., 1994; Pendás, *et al*., 2002).

A-type lamins are developmentally regulated and are mainly expressed in differentiated cells, including in striated muscle (Broers, *et al*., 1997). Studies of mouse embryogenesis revealed that the expression of lamin A/C is not observed until day 11, with the onset of tissue-specific expression-primarily in primordial muscle cells (Stewart and Burke, 1987; Röber, Weber, and Osborn, 1989). It is suggested that lamin A/C expression may be accompanied by relevant adaptations to nuclear architecture, chromosome location, and transcriptional regulation (Constantinescu, *et al*., 2006; Paulsen, *et al*., 2017). The involvement of lamin A interactions to coordinate and regulate these functions is proposed, supported by recent research identifying that stem cell differentiation into stiffer, musculoskeletal tissues was enhanced through higher levels of lamin A (Swift, *et al*., 2013).

1.1.3 Lamin Binding Proteins

Lamin A binds to proteins at the nuclear lamina, including regulatory proteins responsible for both intracellular and extracellular signals. The interaction of lamin A with binding proteins can reinforce mechanical stability, anchor nuclear pores, tether chromatin or regulate protein localisation and activity (Wilson and Foisner, 2010; Naetar, Ferraioli, and Foisner, 2017).

1.1.3.1 Emerin

Emerin is an integral protein of the inner nuclear membrane and is ubiquitously expressed (Ostlund, *et al*., 1999). Emerin co-localises with lamin A and B, lamin A anchors emerin at the inner nuclear membrane by its hydrophobic tail (Vaughan, *et al*., 2001). Lamin A is essential for correct emerin localisation; in lamin A/C null mice, emerin becomes incorrectly located at the Endoplasmic Reticulum (Sullivan, *et al*., 1999). The LEM (LAP2-Emerin-MAN1) domain - a HLH fold roughly 40 residues long - containing proteins can bind to both barrier-to-autointegration factor (BAF), a DNA-bridging protein, and lamin A, linking chromatin to the nuclear periphery (Lee, *et al*., 2001;

Shumaker, *et al.*, 2001; Cai, *et al*., 2001; Solovei, *et al*., 2013). Through the LEM domain, emerin is able to self-assemble, forming oligomers with structural organisation, and bind to BAF, linking chromatin with the nuclear envelope (Samson, *et al*., 2017). Emerin was discovered in 1994 as the gene responsible for causing X-linked Emery Dreifuss Muscular Dystrophy (EDMD) located at Xq28 (Nagano, *et al*., 1996).

1.1.3.2 Lamin-B Receptor

Lamin-B Receptor (LBR) was the first binding partner to be identified and characterised, it is a 58kD protein and the N-terminal domain binds to DNA, heterochromatin protein HP1, and lamins (Worman, *et al*., 1988; Lin, *et al*., 1996). LBR binds to DNA through preferentially binding to linker DNA; DNA supercoiling and curvature result in enhanced binding (Duband-Goulet and Courvalin, 2000). LBR and lamin A/C are important for the localisation of chromatin at the nuclear periphery during development and in differentiated cells, respectively (Solovei, *et al*., 2013). These two proteins are important during the early stages of myoblast differentiation, loss of LBR or LMNA results in an increase or decrease of muscle-specific gene expression, respectively (Solovei, *et al*., 2013). This demonstrates the importance of correct heterochromatin localisation at the nuclear periphery, and how its loss impacts gene expression and developmental differentiation. Mutations in LBR are linked to Pelger-Huet anomaly and Greenberg skeletal dysplasia (Borovik, *et al*., 2013).

1.1.3.3 Lamin-associated polypeptides

Lamin-associated polypeptides (LAP) were first identified in isolated rat liver nuclear envelope protein extracts; three transmembrane proteins of sizes 75 kDa, 68 kDa, and 55 kDa were discovered representing LAP1A, LAP1B, and LAP1C, respectively (Senior and Gerace, 1988; Foisner and Gerace, 1993). All LAP1 isoforms are produced from alternative splicing of the same gene and all have a single transmembrane segment (Martin, Crimaudo, and Gerace, 1995). Shin *et al*. demonstrated that the LAP1 interaction with emerin is essential and plays a selective role in the maintenance of skeletal muscle (Shin, *et al*., 2013). LAP2 is located on chromosome 12q22 and alternative RNA splicing

produces 6 isoforms that are able to bind to lamin B and chromatin (Dechat, Vlcek, and Foisner, 2000). LAP2β and γ are transmembrane proteins located in the inner nuclear membrane, and LAP2α is located in the nuclear interior, as it does not have a transmembrane domain (Furukawa, *et al*., 1995; Vlcek, *et al*., 1999). LAP2α has the LEM domain and therefore, through BAF, binds to chromatin and lamin A (Brachner and Foisner, 2014). A mutation in LAP2α is linked to dilated cardiomyopathy (DCM) with pathological characteristics resembling lamin A-linked DCM (Taylor, *et al*., 2005).

1.1.3.4 MAN1

In 2000, MAN1 was characterised in humans, it is located on chromosome 12q14 and forms an 82.3kDa protein (Lin, *et al*., 2000). MAN1 transfected into cells is targeted exclusively to the nuclear envelope (Lin, *et al*., 2000). A study in 2014 found that MAN1, LBR, and lamin B1 oscillate with a circadian rhythm, and MAN1 regulates the circadian clock through binding to the Bmal1 promoter – enhancing transcription (Lin, *et al*., 2014). This demonstrates a link between the nuclear envelope and the circadian clock; proteins located at the nuclear periphery may be under clock control and can feedback to regulate the clock. Moreover, MAN1 contains the LEM domain, directly linking a protein with rhythmic oscillatory expression and a mechanism of feedback regulation to the circadian clock, with lamin A (Mansharamani and Wilson, 2005). *Man1* mutations result in Osteopoikilosis, Buschke-Ollendorff syndrome (BOS), and melorheostosis, these disorders are characterised by an increase in bone density due to loss of Smad and Transforming Growth Factor-beta (TGF-β) regulation (Hellemans, *et al*., 2004).

1.1.3.5 Nesprin

Nesprin 1 and 2 proteins are a large family encoded by the *Syne* genes; they are large, type II integral membrane proteins and cross the outer nuclear membrane to link the outer nuclear membrane to actin and the cytoskeleton (Zhang, *et al*., 2001). Nesprin and lamin A are important proteins in the LINC complex; LINC facilitates the communication of mechanical signals from the cytoplasm into the

nucleus (Crisp, *et al*., 2006). Mutations in *Nesprin* result in slowly progressive cerebellar ataxia, and disorders with an Emery-Dreifuss muscular dystrophy-like phenotype (Puckelwartz, *et al*., 2009; Fanin, *et al*., 2015; Synofzik, *et al*., 2016).

1.1.3.6 Why Lamin A?

The nuclear envelope is extremely complex, many nuclear envelope proteins and lamin-binding proteins may be under circadian clock control and may be involved in collectively regulating the core circadian clock. This is emphasised by previous research that identified feedback regulation between MAN1 and the circadian clock (Lin, *et al*., 2014). Research in this thesis focused on lamin A because it is important in regulating musculoskeletal tissue-specific gene expression and regulates nuclear mechanisms that may be responsible for providing feed-back regulation to the circadian clock.

1.1.4 Lamins and disease

Mutations in *Lmna* lead to a broad spectrum of diseases, now collectively known as laminopathies; these can affect muscle, skin, neurons, and fat. These diseases suggest a pleiotropic importance in the role played by nuclear lamins (Ho and Hegele, 2019). The disorders can be grouped in accordance with which organs and tissues they affect: striated muscle, adipose, peripheral nerve or multisystem (Worman, 2012). Since *Lmna* mutations are able to cause a clinical spectrum of myopathies and premature ageing disorders, which also affect muscle, lamin A/C proteins clearly play a pivotal role in both muscle development and maintenance.

1.1.4.1 Muscular Dystrophy

Emery Dreifuss Muscular Dystrophy

X-linked Emery Dreifuss Muscular Dystrophy (EDMD), caused by a mutation in *Emd*, was the first disease discovered to be caused by a mutation in a nuclear envelope protein (Bione, *et al*., 1994). Autosomal dominant and autosomal recessive forms of the disease, due to *Lmna* mutations, were subsequently identified in 1999 and 2000 (Bonne, *et al*., 1999; di Barletta, *et al*., 2000). EDMD is

characterised by weakness, slow, progressive muscle wasting, cardiac conduction defects, and early contractures of elbows, Achilles tendons, and post-cervical muscles (Helbling-Leclerc, Bonne, and Schwartz, 2002).

LGMD1B and DCM-CD

Limb girdle muscular dystrophy type 1B (LGMD 1B) and dilated cardiomyopathy with conduction defects (DCM-CD) are muscle disorders characterised by muscle wasting in voluntary and lower limbs, and cardiac defects, respectively (Muchir, *et al*., 2000; Fatkin, *et al*., 1999). They can be caused by the same *Lmna* mutations as EDMD and can be found in families who also have individuals suffering with EDMD. On observing how *Lmna* mutations are able to cause these overlapping disorders, myopathies associated with *Lmna* mutations can be considered a clinical spectrum rather than distinct disorders.

1.1.4.2 Lipodystrophy

A mutation in *Lmna* has been described that causes Dunnigan-type familial partial lipodystrophy (FPLD), this is a rare, autosomal dominant disorder and is characterised by a partial or complete absence of adipose tissue (Köbberling and Dunnigan, 1986; Cao and Hegele, 1999). Patients are born with normal fat distribution but after the onset of puberty begin to lose subcutaneous fat in the torso, extremities, and gluteal region, and accumulate fat in the neck, face, labia majora, and back (Garg, Peshock, and Fleckenstein, 1999). Additionally, later in life, patients can develop insulin resistance with secondary metabolic complications, such as diabetes, glucose intolerance, dyslipidaemia, and coronary heart disease, and have a predisposition to polycystic ovaries and atherosclerosis (Haque, Vuitch and Garg, 2002).

1.1.4.3 Peripheral Neuropathy

Mutations in *Lmna* are linked to Charcot-Marie-Tooth disorder type 2, this disease is characterised by distal muscle weakness and atrophy, foot deformities, electrophysiological changes, and mild

sensory loss (De Sandre-Giovannoli, *et al*., 2002; Chaouch, *et al*., 2003). Some patients can develop a more severe phenotype and roughly 4 years after onset, may have pelvic muscle wasting, leading to a mixed gait and difficulty standing up (Chaouch, *et al*., 2003).

1.1.4.4 Hutchinson-Gilford Progeria Syndrome

In addition, Hutchinson-Gilford Progeria Syndrome (HGPS) is a premature ageing disease caused by point mutations in *Lmna*, most frequently G608G, activating a cryptic splice site and producing a mutant protein (progerin) with an internal deletion of 50 amino acids (De Sandre-Giovannoli, *et al*., 2003). HGPS is characterised by accelerated ageing through growth retardation, hair loss, lipodystrophy, skin wrinkling, arteriosclerosis, and osteoporosis (Merideth, *et al*., 2008). On average, death occurs at roughly 13-years of age from a stroke or heart attack (Stables and Morley, 1994).

1.1.4.5 Pathology Progression

Although A-type lamins are ubiquitously expressed and can be found in most differentiated cell-types and tissues, it is notable that these laminopathies have tissue-specific disease phenotypes, such as EDMD that is characterised by muscle wasting. The mechanisms leading to this tissue-specific phenotype are currently still unknown and the subject of a great deal of study. There are two main hypotheses surrounding current research: the “gene expression” hypothesis and the “mechanical stress” hypothesis (Hutchinson, Alvarez-Reyes, and Vaughan, 2001; Worman and Courvalin, 2004; Briand and Collasa, 2018; Harris, Wirtz, and Wu, 2018). These hypotheses are not mutually exclusive but have emerged as research began to identify functional roles for lamin A and examined the loss of these roles in cells harbouring lamin A mutations. Both hypotheses encompass cellular functions that are known to be important in musculoskeletal-specific development and maintenance.

1.2 Function of the Nuclear Lamina

Research has identified many roles for lamin A that can be grouped into and support the "gene expression" or "mechanical stress" hypotheses. To begin unravelling how the circadian clock may contribute to disease progression, the main functions of lamin A and their response to lamin A mutations or knockout are discussed.

1.2.1 Gene Expression Hypothesis:

The following roles for lamin A can be grouped into the 'Gene Expression Hypothesis'.

1.2.1.1 Transcription Factor Sequestering

TF Sequestering

Through direct interaction, lamin A regulates transcription factors such as Retinoblastoma protein (Rb), MOK2, AP-1, and Sterol Response Element-Binding Protein 1 (SREBP1) (Ozaki, *et al*., 1994; Dreuillet, *et al*., 2002; Ivorra, *et al*., 2006; Lloyd, *et al*.,2002). These interactions sequester the transcription factor at the nuclear periphery, and by doing so, regulates their location and activity, preventing any DNA-binding and transcriptional activity (Dreuillet, *et al*., 2002; Lloyd, *et al*.,2002; Ivorra, *et al*., 2006; Markiewicz, *et al*., 2002a; Johnson, *et al*., 2004). Studies have shown that this regulation can be dynamic, to fine-tune transcriptional repression or activation according to cellular conditions. In response to serum stimulation, and in an ERK1/2 dependent manner, AP-1 is rapidly released from the nuclear periphery, enabling it to upregulate AP-1 responsive genes (González, *et al*., 2008).

Lamin A is central to the activity of these transcription factors; accordingly, *Lmna* knockout or mutation directly affects their localisation, activity, and downstream gene expression. In lamin A knockout fibroblasts, Rb is mis-localised and degraded (Nitta, *et al*., 2006). Muscular satellite cells isolated from lamin A knockout mice have a loss of Rb stabilisation and functional activation, resulting in compromised differentiation capacity (Frock, *et al*., 2006). Likewise, mouse embryonic

fibroblasts with lamin A knockout have increased levels of AP-1 bound to DNA and increased AP-1-dependant gene expression (González, *et al*., 2008). In addition, an EDMD autosomal dominant mutation prevents lamin A from binding to the adipose differentiation factor SREBP1 (Lloyd, *et al*., 2002). In contrast, the expression of pathogenic *Lmna* mutations does not alter the direct binding capacity of lamin A to MOK2 *in vitro* or *in vivo*. Instead, aberrant mis-localisation of the transcription factor into nuclear aggregates is observed (Dreuillet, *et al*., 2008). Thus, mutation or loss of lamin A results in dysregulated control of the localisation or stability of these transcription factors, which may affect many downstream pathways and processes within the cell.

Muscle and Mechanosensitive Pathway Regulation

Lamin A and its binding partner emerin regulate the expression and activity of Wnt/β-catenin and Notch (Wheeler, *et al*, 2010; Lee, Lee, and Shim, 2017). Wnt is mechanosensitive and its activation promotes the accumulation of β-catenin in the nucleus (Brunt, *et al*., 2017). Emerin is responsible for interacting with β-catenin and sequestering it at the nuclear periphery; thus, preventing its nuclear accumulation (Markiewicz, *et al*., 2006). Similarly, knockdown of emerin or lamin A increases Notch signalling due to a loss of retention at the nuclear periphery (Lee, Lee, and Shim, 2017). Notch is a mechanosensitive signalling molecule (Loerakker, 2018). Therefore, lamin A and emerin negatively regulate these mechanosensitive pathways through sequestering transcription factors at the nuclear periphery. Additionally, recent studies have identified a link between NRF2 activity and laminopathy diseases, although a mechanism of regulation is yet to be uncovered (Kubben, *et al*., 2016; Dialynas, *et al*., 2015).

Cardiomyopathic hearts from *Lmna*$^{H222P/H222P}$ mice demonstrate decreased Wnt/β-catenin signalling; pharmaceutical activation of β-catenin improved cardiac contractility and ventricular dysfunction (Le Dour, *et al*., 2017). Conversely, Notch signalling is increased in mesenchymal stem cells (MSC) expressing the HGPS mutant lamin A progerin (Scaffidi and Misteli, 2008). Additionally in HGPS, NRF2 is sequestered and antioxidant pathways are repressed, *in vivo* restoration of these NRF2 pathways

in HGPS-iPSC-MSCs rescues their viability (Kubben, *et al*., 2016). In addition, other laminopathy mutations cause reductive stress through increased activation of NRF2 (Dialynas, *et al*., 2015).

Furthermore, RNA interference (RNAi) down-regulation for lamin A in myoblast cells reduces the expression of the differentiation factors MyoD, M-cadherin, and desmin, and increases the expression of Myf5 (Frock, *et al*., 2006). Lamin A/C directly controls myogenic transcription factor activity and its loss affects muscle differentiation and maintenance (Markiewicz, Ledran, and Hutchison, 2005). Overall, there is strong evidence that lamin A can dynamically regulate transcription factors, including musculoskeletal tissue-specific gene expression, and this is clearly a plausible mechanism incorporated in the gene expression hypothesis.

1.2.1.2 Cell Cycle Control

During progression of the cell cycle, the nuclear lamina is depolymerised and disassembled during prophase, and reassembled following cytokinesis. Lamin A is phosphorylated by cdc2 kinase to induce disassembly during M phase (Peter, *et al*., 1990). The importance of this is demonstrated following mutation of the phosphorylation sites on lamin A at serine 22 and serine 392, which prevents the disassembly of nuclear lamina during mitosis (Heald and McKeon, 1990). Following mitosis, lamins are dephosphorylated and the nuclear lamina is reassembled as the nuclear envelope is formed. DNA replication is tightly controlled temporally and spatially during the cell cycle and lamin A is essential for DNA replication and mRNA transcription (O'Keefe, Henderson, and Spector, 1992; Goldman, *et al*., 2002). *Xenopus* nuclei depleted of lamin A or incorporating a mutant human *Lmna* transcript, are unable to initiate DNA replication, although there is no disruption occurring to nuclear import; indicating that the DNA replication machinery is incorrectly localised and targeted within the nucleus (Meier, *et al*., 1991; Spann, *et al*., 1997). In addition to a structural role, lamin A directly interacts with c-fos (part of the AP-1 complex) and Rb transcription factors, which are involved in regulating cell cycle progression (Johnson, *et al*., 2004; Ivorra, *et al*., 2006). Lamin A

dynamically regulates these transcription factors and can fine-tune cell cycle progression dependent upon cues provided by the cellular environment (González, *et al*., 2008; Pekovic, *et al*., 2007).

Genetic diseases caused by *Lmna* mutations disrupt cell cycle regulation, muscle development, and maintenance; these processes require coordination and control of the cell cycle. In muscle cells from patients affected by EDMD, the interactions between lamin A, Rb, and MyoD are abnormal, and the phosphorylation and acetylation steps in the cell cycle are uncoordinated (Bakay, *et al*., 2006). HGPS mutations, on the other hand, affect cell cycle progression by altering the distribution and solubility of lamin A, which prevents progression into M phase, and by causing defects in the Rb protein, preventing regulated transition into S-phase (Dechat, *et al*., 2007). Hence, lamin A is vital for correct cell cycle progression at a structural level by allowing nuclear membrane disassembly and assembly, and by directly regulating factors that coordinate cell cycle progression. Cell cycle control is vital in muscle development and maintenance; differentiation of skeletal myoblasts depends on increased levels of hypo-phosphorylated pRb and its interaction with MyoD, through deacetylase HDAC1, to arrest and withdraw from the cell cycle (Walsh, 1997; Puri, *et al*., 2001). Therefore, loss of coordinated cell cycle control in myoblasts has severe consequences on muscle development and maintenance.

1.2.1.3 Nuclear-cytoplasmic shuttling of protein

The separation of nuclear and cytoplasmic functions permits the regulation small polar molecules and macromolecules that pass into the nucleus. Through regulating this passage, lamin A can control the availability of transcription factors within the nucleus. These molecules can pass into the nucleus through nuclear pores, enabling the nucleus to become its own distinct and regulated biochemical environment. The nuclear pores are supramolecular complexes composed of multiple nucleoporin proteins (Nups), a total of 29 Nups and 18 nuclear pore-associated proteins have been identified (Cronshaw, *et al*., 2002). The nuclear pores are involved in bidirectional trafficking and are selective in the uptake of proteins (Bonner, 1975). The nuclear pore complex (NPC) binds to Lamin filaments,

which are involved in the trafficking of cargo and the positioning of the NPC (Goldberg and Allen, 1996). The soluble proteins of the nuclear basket bind to cargo about to be imported and also exhibit multiple binding sites for the Ig-fold of lamin A (Shah, Tugendreich, and Forbes, 1998; Al-Haboubi, *et al*., 2011).

Further evidence comes from both *Lmna* knockout and DCM mutant mouse embryonic fibroblasts, which demonstrate impaired nuclear-cytoplasmic shuttling of MRTF-A/SRF (Serum Response Factor) that is associated with the abolition of nuclear translocation in response to serum stimulation (Ho, *et al*., 2013). In addition, the defective nuclear lamina present in HGPS cells has impaired dynamic active and passive transport of proteins between the cytoplasm and the nucleus (Ferri, Storti, and Bizzarri, 2017). Thus, lamin A is important for correct nuclear pore importation dynamics, and it facilitates the nuclear-cytoplasmic shuttling of transcription factors.

1.2.1.4 Genome Organisation

The nucleus is organised in a non-random fashion, the centromeres of chromosomes can be found in the same location across differentiated cells types, such as in the Purkinje cells (Manuelidis, 1984). The location of genes at the periphery of the nucleus is associated with transcriptional repression, and lamin A is suggested to take an active role in this process (Gonzalez-Suarez and Gonzalo, 2010). Chromosomes rich in actively expressed genes tend to be located towards the centre of the nucleus and gene poor chromosomes located at the nuclear periphery; internal lamin structures associate with condensed chromatin to regulate localisation independently from the nuclear membrane (Bridger, *et al*., 1993; Croft, *et al*., 1999). Lamin A binds directly to DNA and histones through its rod and terminal domain, and can associate with regions of the DNA containing Lamin-associated domains (LADs) through its LEM domain and NET interactions (Glass, et al., 1993; Taniura, et al., 1995; Stierlé, et al., 2003; Guelen, et al., 2008).

Chromosome Territories

Physical organisation is highly conserved and chromosome domains, known as chromosome territories, are located in close proximity to regulatory bodies. Highly expressed genes are found located towards the periphery of these territories (Kurz, *et al*., 1996; Boyle, *et al*., 2001; Mahy, *et al*., 2002; Chambeyron and Bickmore, 2004). Lamina located at the nuclear periphery and in internal lamin structures act as a scaffold, providing structural support to chromosome territories (Bridger, *et al*., 1993; Ma, Siegel, and Berezney, 1999). On myoblast differentiation, chromosomes rearrange these territories to adapt gene expression; relocating muscle-specific differentially expressed genes into active regions and repressing non-muscle-specific genes (Moen, *et al*., 2004).

Lamin-associated domains (LADs) and Topologically-associated domains (TADs)

LADs are enriched in heterochromatin and display low gene activity, demonstrating a repressive state (Guelen, *et al*., 2008). TADs are stable, well conserved chromatin interaction domains of a high-frequency that correlate with constraining the spread of heterochromatin, and are suggested to be involved in establishing higher order genome structures (Dixon, *et al*., 2012). Lamin A binds to DNA through defined regions of LADs and TADs to regulate genome organisation (Briand and Collas, 2018). Through redistributing and adjusting lamin A and LADs interactions, it has been discovered that these interactions are coupled with differentiation, linking lamin A with developmentally regulated gene-expression (Rønningen, *et al*., 2015).

LEM Domain

The LAP2β, emerin, and MAN1 proteins contain the LEM domain, a HLH fold roughly 40 residues long, and through this can bind to BAF, a DNA-bridging protein, and lamin A (Lee, *et al*., 2001; Shumaker, *et al.*, 2001; Cai, *et al*., 2001; Solovei, *et al*., 2013). LEM domain proteins and BAF dimers can compact and de-condense associated chromatin, silencing gene expression (Zheng, *et al*., 2000; Segura-Totten, *et al*., 2002; Capanni, *et al*., 2010).

Nuclear Envelope Transmembrane Proteins

The inner nuclear membrane also contains other nuclear envelope transmembrane proteins (NETs). NETs have been identified that are upregulated or downregulated during myoblast differentiation, these proteins actively promote or inhibit differentiation, respectively (Schirmer, *et al*., 2003; Chen, *et al*., 2006). These NETs regulate chromosome positioning, tethering genes to repress their expression and regulating tissue-specific gene expression (Zuleger, *et al*., 2013). NET39, Tmem38A, and WFS1 are strongly upregulated in skeletal and cardiac tissue during myogenesis, and are regulators of muscle regeneration (Liu, *et al*., 2009; Robson, *et al*., 2016). These three NETs are responsible for 37% of gene expression changes observed during myogenesis (Robson, *et al*., 2016). These interactions, between lamin A, NETs, and chromatin, are transcriptionally repressive and through chromatin organisation, enable the nuclear lamina to regulate gene expression.

Promoter Regulation

Experiments utilising the lac operator reporter arrays demonstrated a 2-3 fold reduction in gene expression after gene tethering to the nuclear lamina (Reddy, *et al*., 2008). Lamin A associates with the promoters of muscle-specific genes such as *MyoD*, *Myogenin*, and muscle creatine kinases in myoblasts, and dissociates from these promoters upon myoblast differentiation (Athar and Parnaik, 2015). Lamin A/C is required for the localisation of chromatin to the nuclear periphery in differentiated muscle cells (Solovei, *et al*., 2013).

In *C. elegans* an EDMD point mutation in *Lmna* prevents muscle-specific reorganisation of heterochromatin and leads to decreased muscle function in larvae and adult worms (Mattout, *et al*., 2011). In patients suffering with EDMD, caused by a mutation in *Lmna*, muscle fibres, fibroblasts, and cardiomyopathic hearts demonstrated abnormal distribution of chromosomes and levels of gene expression (Sewry, *et al*., 2001; Mewborn, *et al*., 2010). Fibroblasts from patients affected by HGPS have altered DNA-Lamin interactions, loss of chromosome domain spatial organisation, and loss of peripheral heterochromatin localisation (Goldman, *et al*., 2004; McCord, *et al*., 2013). In

addition, genome organisation is altered in primary laminopathy and X-EDMD human dermal fibroblasts; chromosomes are abnormally positioned in the nucleus, pRb is aberrantly localised, and incidences of apoptosis are increased (Meaburn, e*t al*., 2007). Furthermore, HGPS fibroblasts treated with farnesyltransferase inhibitor, to prevent the accumulation of farnesylated progerin, demonstrated restored nuclear chromosome positions (Mehta, *et al*., 2011; Bikkul, *et al*., 2018). Finally, during myoblast differentiation it has been observed that loss of *LBR* or *Lmna* results in an increase or decrease, respectively, of muscle-specific gene expression (Solovei, *et al*., 2013).

Therefore, these functions by lamin A act to ensure that chromatin is correctly organised at the nuclear periphery and that muscle-specific gene expression is coordinated, which is required during myoblast development.

1.2.2 Mechanical Stress Hypothesis

The following roles for lamin A can be grouped into the 'Mechanical Stress Hypothesis'.

1.2.2.1 Nuclear Fragility – LINC Complex

In addition to nuclear pores, the inner and outer nuclear membranes are also connected through LINC (Linker of Nucleoskeleton and Cytoskeleton) complexes. Consisting of Sad1 and UNC-84 (SUN) domain proteins and Klarsicht, ANC-1, and Syne Homology (KASH) domain nesprin proteins, which are located in the inner nuclear membrane and in the outer nuclear membrane, respectively (Crisp, *et al*., 2006). There are several different SUN proteins in mammalian cells and their C-terminal domain, which encompasses the SUN domain, is located within the perinuclear space (Malone, *et al*., 1999; Hodzic, *et al*., 2004; Crisp, *et al*., 2006). In the cytoplasm, nesprin proteins bind to signalling molecules and cytoskeletal elements (Padmakumar, *et al*., 2005). This signal is passed to SUN proteins through interactions in the perinuclear space, through their KASH and SUN domains. SUN binds to the tail domain of lamin A, linking and anchoring the complex to the nucleus, and enabling signal transduction to the nucleus (Crisp, *et al*., 2006; Haque, *et al*., 2006). The LINC complex is crucial during the fusion of myoblasts in differentiation and in myonuclei positioning

(Zhou, *et al*., 2017; Stroud, *et al*., 2017). Mechanical stimulation deforms the nuclear envelope and the lamina, initiating adaptation of lamin A-dependant transcription factor regulation and chromosome positioning (Maniotis, Chen, and Ingber, 1997; Mazumder and Shivashankar, 2010). Thus, the LINC complex is a structural scaffold that also communicates mechanical signals across the nuclear membrane to elicit downstream mechanosensitive responses in the nucleus. Stem cell differentiation into stiffer tissues is enhanced through high levels of lamin A, which provide additional structural support (Swift, et al., 2013).

Reduced levels of lamin A in *Drosophila* leads to weakened structural integrity of the nuclear envelope, it becomes distorted and forms clusters of nuclear pore complexes (Lenz-Böhme, *et al*., 1997). Fibroblasts from patients affected by LGMD have defective organisation of the inner nuclear membrane and changes in nuclear shape (van Engelen, *et al*., 2005). Nuclear mechanics in fibroblasts from *Lmna* knockout mice have increased nuclear fragility and deformation, and altered mechanotransduction in response to mechanical strain (Lammerding, *et al*., 2004). Moreover, fibroblasts from patients suffering with X-EDMD demonstrate increased solubility of lamin A (Markiewicz, *et al*., 2002b). Lamin A ensures that the nucleus is structurally stable and that mechanosensitive responses are correct; in laminopathies, this stability and regulation may be lost.

1.2.2.2 Oxidative Stress

Lamin A correlates with the suppression of oxidative stress and Reactive Oxygen Species (ROS) (Lattanzi, *et al*., 2012). In response to hydrogen peroxide induced stress, there is an increase in the translocation of Ankyrin repeat protein 2 (Ankrd2) into the nucleus (Cenni, *et al*., 2011). In the nucleus, Ankrd2 phosphorylates Atk and inhibits myogenic differentiation in skeletal muscle (Cenni, *et al*., 2011). Hence, in response to stress stimuli, this response prevents myogenesis and enables the myoblasts to enter recovery or apoptotic pathways. In the nucleus, lamin A binds to Ankrd2 and forms a complex (Angori, *et al*., 2017).

EDMD2-lamin A overexpressing cell lines and myotubes from patients suffering from EDMD2 demonstrate incorrect localisation of Ankrd2 and increased sensitivity to oxidative stress (Angori, *et al*., 2017). Knockdown of lamin A in human fibroblasts increases levels of intracellular ROS, and patients suffering from Emery-Dreifuss muscular dystrophy have increased serum levels of ROS, measured through total antioxidant capacity and total oxidant status (Sieprath, *et al*., 2015; Niebroj-Dobosz, *et al*., 2017). Finally, fibroblasts from patients suffering with progeria have elevated levels of ROS and an increased sensitivity to oxidative stress (Richards, *et al*., 2011).

1.2.3 Lamin A and the Circadian Clock

Despite the identification of essential general and tissue-specific functions of lamin A, the field remains no closer to a clear understanding of how laminopathy patients progress from mutation to phenotype. The functions discussed above are mechanisms relevant to musculoskeletal development and maintenance, and mutation or knockout of *Lmna* prohibits or perturbs each of these functions and severely impacts muscle. The gene expression and mechanical stress hypotheses have overlapping functions. Sensitive transcription factor and chromatin regulation by lamin A, observed in functions of the gene expression hypothesis, can only occur if the lamina, inner nuclear membrane, and nuclear pores are structurally secure. Distorted nuclear membranes and nuclear pores, observed in *Lmna* knockout fibroblasts, will be unable to facilitate the regulatory associations of lamin A with chromatin, transcription factors, and other proteins (Lenz-Böhme, *et al*., 1997). Similarly, mechanosensitive pathways vital to the mechanical stress hypothesis require lamin A to regulate and elicit downstream mechanosensitive gene expression, through interactions with transcription factors. Therefore, these functions are important factors in the disease progression of tissue-specific phenotypes seen across laminopathies. However, further research is required to understand exactly how these diseases are formed. The work in this thesis predicts that the molecular clock and lamin A are linked, and a functioning circadian clock is essential for lamin A to undertake all of these regulatory roles. Furthermore, it is predicted that the loss of lamin A, through

mutation or knockout, impairs the circadian clock, affecting both lamin A and many other cell-specific functions.

1.3 Circadian Rhythms

1.3.1 The Circadian clock

During the fourth century BC a description of the leaves of the tamarind tree that rhythmically open and close by the Greek Androsthenes marked the first account of circadian rhythms (Moore-Ede, *et al.,* 1982). Since this first description, oscillations in behaviour and physiological processes in all phyla of eukaryotes have been reported. Halberg named these 'circadian rhythms', originating from a Latin phrase that roughly translates to 'about a day' (Halberg, 1959). Circadian rhythms are defined as biological rhythms with a free-running period that is approximately equivalent to one rotation of the earth (Pittendrigh, 1960). A 'free running' rhythm is the rhythm observed once external stimuli are removed, meaning the oscillating pattern is able to continue in the absence of environmental cues. External cues set oscillating rhythms and these are known as external time givers or 'zeitgebers'. Examples of zeitgebers include temperature and light, which tend to oscillate with 24-hour pattern. The 'free-running' nature of circadian rhythms demonstrates that they are not simply responses to the diurnal cycle but rather are generated and maintained by an internal clock, which is 'set' by these zeitgebers. In the 1960s Aschoff placed volunteers into constant darkness – removing them from the zeitgeber light, through utilising military war bunkers from World War II. Volunteers who stayed for 3-4 weeks revealed rhythms in their sleep-wake cycle, urine excretion, and body temperature (Aschoff, 1969).

Circadian rhythms provide organisms with a selective advantage, regulating physiology and behaviour to synchronise with the external environment. In humans, circadian rhythms are involved in regulating many processes such as sleep-wake cycle, body temperature, hormone secretion, immune activity, and cardiovascular activity (Borbély, 1982; Aschoff and Heise, 1972; Weitzman, 1976; Lévi, *et al*., 1991). The circadian clock enables gene and protein expression to peak and trough

once every 24 hours. Accordingly, this allows the clock to control the timing of physiological processes and thus, provide temporal homeostasis. The research in this thesis focuses on the importance of circadian rhythms for effective development, maintenance, and mechanosensitive pathways within skeletal muscle.

1.3.2 Circadian Genes

In 1971, Konopka and Benzer began searching for 'clock genes' by carrying out reverse genetic systematic screens in *Drosophila melanogaster. D. melanogaster* mutants were created using ethyl methane sulfonate and three rhythm mutants were identified: short-period, long-period, and arrhythmic (Konopka and Benzer, 1971). All three mutants were located at the same locus on chromosome X and in the same functional gene: the *period* (*per*) locus (Konopka and Benzer, 1971). This was a revolutionary moment in the circadian biology field. Previously, it was believed that no single gene mutation could affect oscillating processes within an organism, due to the complex nature of circadian rhythms. Hence, this experiment paved the way for future work in the circadian biology field and there was a race to identify further 'clock genes' in *Drosophila* and in other organisms. Circadian genes were successfully identified in Chlamydomonas in 1971 and in Neurospora Crassa in 1973 (Bruce, 1972; Feldman and Hoyle, 1973). Next, the focus in circadian biology research turned to deciphering the molecular clock mechanism in mammals.

1.3.3 Mammalian Circadian Genes

In 1994, Vitaterna *et al.* performed mutagenesis experiments on mice to screen for clock mutants. They successfully identified *Clock*, a single gene located on mouse chromosome 5 and syntenic to human chromosome 4 (Vitaterna, 1994). On mutating *Clock*, both the periodicity and persistence of circadian rhythms were affected (Vitaterna, *et al*., 1994; King, *et al*., 1997). From these findings, it was concluded that Clock protein was a component of the core molecular clock in mammals. Positional cloning of *Clock* found it to be roughly 100 000 base pairs in length, span 24 exons, and

encode a transcription factor belonging to the basic helix-loop-helix (bHLH)-*Period-Arnt-Single-Minded* (PAS) (bHLH-PAS) family (King, *et al*., 1997).

Using the *Drosophila* period gene, studies were carried out to identify mammalian orthologs and lead to the discovery of *mPer1*, *mPer2*, and *mPer3*, proteins with a PAS and protein dimerisation domain (Sun, *et al*., 1997; Tei, *et al*., 1997; Albrecht, *et al*., 1997; Zylka, *et al*., 1998). The interactions of mPER complexes are important for nuclear localisation (Zylka, *et al*., 1998). A two-hybrid screen for proteins that interact with Clock identified *Bmal1* (Brain and Muscle ARNT-Like 1), *in situ* hybridisation displayed co-expression of *Bmal1* with *Clock* and *mPer1* in the mouse brain (Gekakis, *et al*., 1998). In 1999 and 2000, the CRY1 and CRY2 proteins, members of the Cryptochrome (Cry) and photolyases family, were identified. Mice null for CRY1 and CRY2 or BMAL1 proteins display a complete loss of free-running rhythmicity (Van der Horst, *et al*., 1999; Bunger, *et al*., 2000).

1.3.3.1 Transcriptional Translational Feedback Loop (TFFL)

The generation of circadian oscillations results from auto-regulatory interlocked feedback/feedforward transcriptional translational loops, these can be observed across different phylogeny including: cyanobacteria, fungi, and plants (Ishiura, *et al*., 1998; Crosthwaite, Dunlap, and Loros, 1997; Wang and Tobin, 1998). To begin deciphering the molecular interactions of mammalian clock proteins, a CACGTG E box sequence located in the promoter of *Per1* was firstly identified; experiments demonstrated that CLOCK and BMAL1 heterodimers positively regulate *Per1* through this E box (Gekakis, *et al.*, 1998). CLOCK and BMAL1 upregulate *Per1*, *Per2*, *Cry1*, and *Cry2* expression, and constitute the positive elements of the primary feedback loop – in accordance with their roles in *Drosophila*. The negative part of the feedback loop is established by PER:CRY heterodimers. Once their concentration reaches a critical level – during the evening, they are translocated into the nucleus, and directly interact with BMAL1:CLOCK complexes. This prevents their transcription and 'feeds-back' to complete the molecular loop (Griffin, *et al*., 1999; Kume, *et al*., 1999; Sato, *et al*., 2006). CLOCK, BMAL1, PER, and CRY are the integral 'core clock proteins' in the

transcriptional translational feedback loop, shown in Figure 1.4. These proteins regulate the expression of other genes and as a result, produce rhythmic expression of downstream genes across the genome; representing the output of the molecular clock. This is fine-tuned in a tissue-specific manner, ensuring that output genes are expressed at the time of day when and where they are physiologically required. The timing of downstream gene up- or down-regulation depends on the clock protein implementing the regulation. For example, in the liver, the BMAL1:CLOCK heterodimer specifically binds to several thousand sites in the genome to upregulate gene expression, which peak at midday (King, *et al*., 1997; Kume, *et al*., 1999; Rey, 2011; Takahashi, 2015).

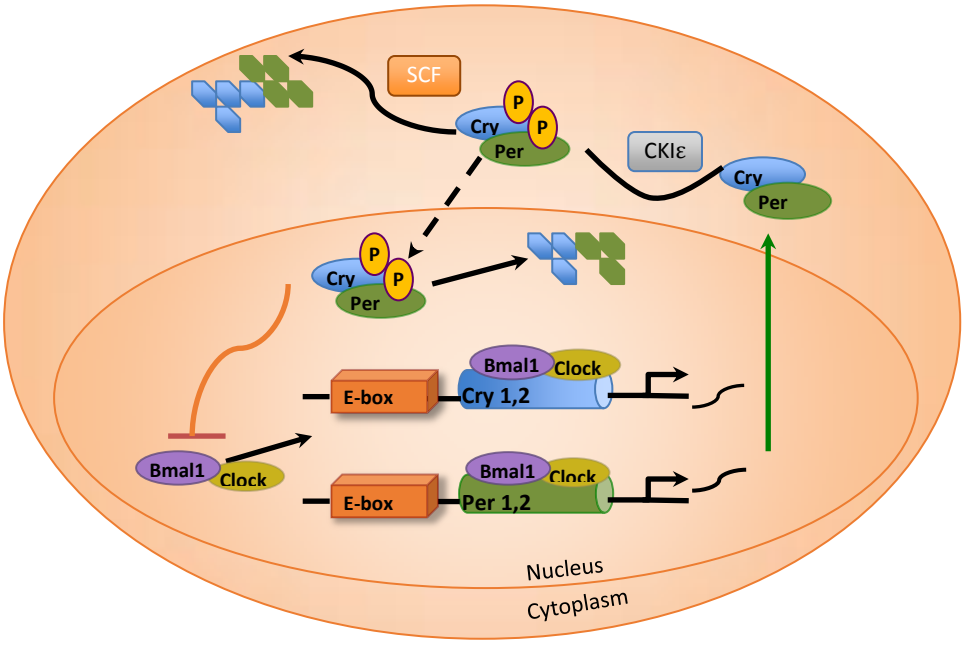

Figure 1.4. Schematic diagram of the molecular interactions between the core clock components involved in the interlocked feedforward/feedback loop.

1.3.3.2 Auxiliary Loops

Phosphatases and kinases act to ensure that the molecular loop takes roughly 24 hours to complete, and that the interactions and localisation of core clock proteins are correct. These are known as the stabilising loops and ensure that the molecular clock is robust; they provide extra temporal regulation on core clock genes and proteins. During the night, the PER and CRY proteins are

phosphorylated and targeted for ubiquitination by E3 ligases, such as $SCF^{\beta\text{-}TrCP1}$ and SCF^{Fbxl3}, and are degraded by ubiquitin-dependant pathways (Busino, *et al*., 2007; Siepka, *et al*., 2007; Reischl, *et al*., 2007). The rate at which PER:CRY is degraded or translocated to the nucleus is controlled by casein kinases CKIε and CKIδ, through phosphorylation of PER at multiple sites. Their own activity is regulated by phosphatases PP1 and PP5 (Lowrey, *et al*., 2000). CKIε and CKIδ phosphorylate PER during the night, resulting in its degradation (Keesler, *et al*., 2000; Akashi, *et al*., 2002; Eide, *et al*., 2005). CKIε is also able to phosphorylate CRY when both CRY and CKIε are bound to PER in a multimeric complex (Eide, *et al*., 2002). PP1 and PP5 dephosphorylate CKIε and CKIδ respectively, activating them to phosphorylate Per3 and inducing translocation to the nucleus (Takano, *et al*., 2000; Akashi, *et al*., 2002). PP5 is regulated by CRY, on receiving blue-light signals during the subjective night, CRY inhibits the phosphatase activity of PP5 and prevents PER phosphorylation (Zhao and Sancar, 1997; Partch, *et al*., 2006). Rhythmic degradation of PER is an important feature of a functioning molecular clock as it eases the repression of *Clock* and *Bmal1* expression. Additionally, further regulation of the circadian clock mechanism is provided by REV-ERBα and RORα, they compete to bind to ROR elements in the *Bmal1* promoter to repress and activate its transcription, respectively (Preitner, *et al*., 2002; Sato, *et al*., 2004).

The mitogen-activated protein (MAP) kinase pathway is an important regulator of the circadian clock mechanism through resetting the circadian clock in response to photic input during the subjective night (Obrietan, Impey, and Storm, 1998). MAPK peaks during the subjective day; however, photic stimuli during the subjective night results in prolonged MAPK cascade activation and leads to the expression of clock genes, such as *Per1* (Treisman, 1996; Butcher, *et al*., 2005). In accordance, this phase shifts the clock mechanism and entrains the molecular clock to the external cue (Goldsmith and Bell-Pedersen, 2013).

1.3.4 Mammalian Circadian Rhythms

In humans, circadian rhythms are important in temporal regulation of the sleep-wake cycle, body temperature, hormone secretion, immune activity, and cardiovascular activity (Borbély, 1982; Aschoff and Heise, 1972; Weitzman, 1976; Lévi, *et al.*, 1991). In addition, circadian rhythms affect many other physiological functions including locomotor activity, water, and food intake, the oestrous cycle, oxygen utilisation, and adrenal corticosterone production (Stephan and Zucker, 1972; Fitzgerald and Zucker, 1976; Bellisle and Le Magnen, 1981; Moore and Eichler, 1972). Multicellular organisms contain multiple circadian oscillators, as nearly every cell contains an autonomous circadian molecular clock. Pittendrigh first proposed that an organism contains a light sensitive oscillator that acts as a 'pacemaker' for the rest of clocks in the body, and scientists began to investigate areas of the brain that may be a suitable candidate (Pittendrigh, 1960). Research experiments began by creating lesions in the rodent brain and observing the effect, if any, on wheel running behaviour. They discovered that the suprachiasmatic nucleus (SCN), located above the optic chiasma in the anterior hypothalamus, was important for rhythmic locomotor activity and corticosterone secretion (Moore and Eichler, 1972; Stephan and Zucker, 1972).

1.3.5 The SCN

The molecular and physiological behaviour of the SCN follows a circadian rhythm, including the expression of clock genes, proteins, and glucose uptake (Schwartz and Gainer, 1977; Sun, *et al*., 1997). To prevent cells within a multicellular organism being on different circadian times to each other, they are organised into a hierarchical system. In mammals, the SCN is the 'master' internal clock and acts as the 'pacemaker', its neurons are autonomous, self-sustained circadian oscillators (Welsh, *et al*., 1995). The SCN is responsible for receiving retinal projections, via the retinohypothalamic tract (RHT), and for photic entrainment to the zeitgeber light (Rusak and Boulos, 1981). As well as photic projections along the RHT, photic signals are also indirectly projected from the intergeniculate leaflet (IGL) to the SCN via the Geniculo Hypothalamic tract (GHT) (Pickard, 1985;

Janik and Mrosovsky, 1994). The IGL sends a signal to the SCN through neuropeptide Y (NPY) and gamma-aminobutyric acid (GABA) release; this is delayed in comparison to the photic signal received from the RHT – providing additional information to the SCN (Moore and Card, 1994; Harrington, Nance, and Rusak, 1985). The IGL also receives information from non-photic signals via the dorsal raphe nucleus; thus, signals from the IGL are integrating both photic and non-photic signals (Meyer-Bernstein and Morin, 1996). Electrical stimulation of the GHT or the addition of NPY to the SCN induces phase-dependant phase shifts (Rusak, Meijer, and Harrington, 1989; Albers and Ferris, 1984). Furthermore, activity-induced phase shifts can be blocked through the application of NPY antiserum (Biello, Janik, and Mrosovsky, 1994). Finally, a third projection to the SCN is serotonergic projection via the midbrain raphe nucleus (MR) ending in neurons containing vasoactive intestinal peptide (VIP); there are rhythmic levels of VIP in the SCN, which peak during the night (Bosler and Beaudet, 1985; Shinohara, *et al*., 1993). The GHT and MR are necessary for entrainment to stimuli such as motor activity and light pulses; however, they are not a necessity for circadian periodicity of the SCN (Edelstein and Amir, 1999; Harrington and Rusak, 1986; Pickard, Ralph, and Menaker, 1987).

1.3.6 The Timekeeper

In order for the hierarchical system to work and the 'pacemaker' function of the SCN to be effective, the SCN is required to send 'time-keeping signals' to the peripheral clocks of the rest of the brain and body. The SCN undergoes this synchronisation by sending signals via neuronal and humoral pathways. Anterograde tracing of the SCN revealed a number of efferents terminating at a range of other sites in the brain, enabling the SCN to project signals directly to these areas (Watts, Swanson, and Sanchez-Watts, 1987). Other SCN output signals include: vasopressin, melatonin, prokineticin 2 (PK2), TGFα, and cardiolipin-like cytokine, and rhythmic levels of corticosterone release are controlled by vasopressin projected from the SCN to the hypothalamus (Kalsbeek, *et al*., 1992).

Locomotor activity is regulated by the molecular clock to oscillate with a circadian rhythm. It is proposed that the precise regulation of locomotor activity occurs through the action of numerous

secreted output factors. One of these factors includes the SCN rhythmic release of PK2 to the main projection targets of the brain; a high level of PK2 during the subjective day inhibits wheel-running activity in rodents (Cheng, *et al*., 2002). Furthermore, cardiolipin-like cytokine (CLC) is important for shaping rhythms in locomotor activity. CLC is synthesised and released rhythmically from SCN neurons, binding to receptors around the third ventricle and inhibiting locomotor activity (Kraves and Weitz, 2006). These examples demonstrate how the SCN, as the time-keeping pacemaker, can regulate behavioural and physiological processes through the rhythmic release of various output signals.

Early experiments identified oscillating transcripts of the core clock genes in tissues located across the rest of the body, such as in the liver and skeletal muscle (Zylka, *et al*., 1998). Within each cell-type, circadian rhythms are fine-tuned to upregulate tissue-specific genes and are physiologically central to the maintenance of many tissues. Peripheral clocks are important in many physiological processes; dysfunction of lipid and glucose metabolism, and diabetes mellitus occur when local clocks are perturbed and desynchronised (Lamia, Storch, and Weitz, 2008; Gale, *et al*., 2011).

1.3.7 Circadian Rhythms and Muscle

Many studies have identified oscillating core clock gene transcripts in muscle cells and roughly 7% of the skeletal muscle transcriptome has been shown to oscillate with a circadian rhythm (Zylka, *et al*., 1998; Yamazaki, *et al*., 2000; Miller, *et al*., 2007; McCarthy, *et al*., 2007). *MyoD*, a skeletal muscle-specific bHLH transcription factor important in regulating myogenesis and differentiation, is regulated by the circadian clock and is specifically upregulated by BMAL1:CLOCK (Andrews, *et al*., 2010). In addition, the myogenic regulatory factor *Myogenin* oscillates with a circadian rhythm in mouse muscle samples (Shavlakadze, *et al*., 2013). Undoubtedly, human and mouse muscle cells have a functioning circadian clock that regulates muscle-specific gene expression.

Studies have demonstrated that forced or voluntary scheduled exercise regimes can be used to entrain and enhance re-entrainment of circadian rhythms in mice, observed through their sleep-wake and drinking rhythms (Edgar and Dement, 1991; Marchant and Mistlberger, 1996; Yamanaka, *et al*., 2008). Studies in humans have also demonstrated that a night-time pulse of exercise was able to shift and delay the circadian clock, recorded through the plasma levels of two robust circadian oscillating hormones, thyrotropin and melatonin (Van Reeth, *et al*., 1994; Buxton, *et al*., 1997; Barger, *et al*., 2004). Resistance exercise regimes have also proven effective in entraining circadian rhythms (Zambon, *et al*., 2003). Furthermore, recent experiments in *Drosophila* have demonstrated that diurnal cycles of mechanical stimuli, vibration, and silence, are sufficient to entrain the circadian clock through daily locomotor activity (Simoni, *et al*., 2014). This research demonstrates how exercise can be used to entrain circadian rhythms in humans and reveals temporal feedback from behavioural outputs to the SCN, shown in Figure 1.5. Potential therapies may use time-scheduled exercise to reset circadian rhythms in individuals with jet lag, working night shifts or suffering from various diseases that affect their circadian rhythm.

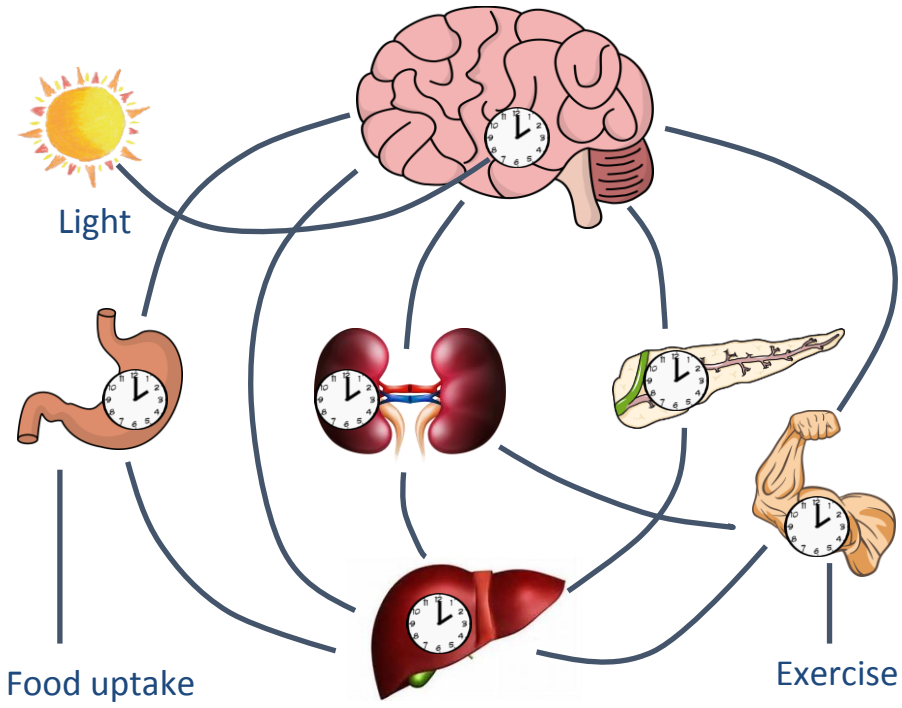

Figure 1.5. Diagram of the hierarchical structure of circadian rhythm synchronisation incorporating entrainment of peripheral clocks and the SCN by food uptake and exercise.

1.3.8 Muscle and Clock mutant mice

Clock mutant mice have been used to observe how the loss of functioning circadian rhythms affects skeletal muscle gene expression, development, and function.

1.3.8.1 *Clock* $^{\Delta 19/\Delta 19}$

Microarray analysis from skeletal muscle in *Clock* $^{\Delta 19/\Delta 19}$ mice demonstrated that 30% of transcripts no longer oscillate or had a phase shift in expression, 35% had a change in expression level, and 79% were significantly downregulated. Many of these downregulated genes are muscle-specific genes important in muscle structure, such as the genes for titin and myosin heavy chain IIx (McCarthy, *et al*., 2007). Skeletal muscle from *Clock* $^{\Delta 19/\Delta 19}$ mice have abolished circadian *MyoD* expression, altered expression of *MyoD* target genes, disrupted myofilament architecture, and demonstrated a 30% reduction in normalised maximal force (Andrews, *et al*., 2010).

1.3.8.2 *Bmal1* $^{-/-}$

Bmal1 $^{-/-}$ mice exhibit age-related pathologies: growth retardation, disrupted and reduced locomotor activity, significantly reduced body weight due to fat loss and sarcopenia, hair-loss, and decreased longevity (Kondratov, *et al*., 2006). To observe whether muscle-specific rescue of *Bmal1* restored the locomotor activity of these mice, *Bmal1* knockout mice were rescued with a *Bmal1* BAC transgene containing a human alpha actin-1 (*Acta1*) promoter, to rescue *Bmal1* expression in skeletal muscle only (McDearmon, *et al*., 2006). This *Bmal1* muscle-specific expression in *Bmal1* knockout mice resulted in increased locomotor activity, although remaining non-circadian in behaviour, body weight was no longer significantly lower and strikingly, their longevity was restored (McDearmon, *et al*., 2006).

1.3.8.3 *Per* $^{-/-}$

Mice with mutations in *Per2* also have poor locomotor performance, in light: dark conditions they demonstrate short period locomotor activity but completely lose circadian rhythms under dark: dark

and free-running conditions (Bae, *et al*., 2006; Zheng, *et al*., 2001). Mice with homozygous *Per1* mutations entrained locomotor activity to light: dark conditions but had significantly shorter periodicity in locomotor activity in dark: dark conditions (Zheng, *et al*., 2001). In addition, *mPer1* and *mPer2* double mutants also exhibit normal periodicity under light: dark conditions but lose rhythms in locomotor activity under dark: dark conditions (Zheng, *et al*., 2001). Rhythms could not be restored in response to a light pulse (Zheng, *et al*., 2001).

1.3.8.4 *Cry* $^{-/-}$

Cry1 knockout mice exhibit accelerated periodicity in locomotor activity under free-running conditions, and *Cry2* knockout mice exhibit delayed periodicity in locomotor activity under free-running conditions (van der Horst, *et al*., 1999). *Cry1* and *Cry2* double-knockout mice exhibit a complete loss of locomotor activity under free-running rhythm conditions (van der Horst, 1999).

The research in this thesis focuses on the potential involvement of the circadian clock in regulating lamin A, and its importance in muscle maintenance. Accordingly, studies will begin to investigate whether the molecular clock and lamin A in musculoskeletal tissues are part of a feedback regulatory mechanism, and whether the manipulation of lamin A in muscle myoblasts directly disrupts core clock gene expression.

1.4 Mechanical Stimulation

1.4.1 Mechanotransduction

The human body is subjected to mechanical forces ranging from sources such as gravity, ubiquitous force acting on the entire body, to tensile muscular force, which acts onto bone (Kohrt, Barry, and Schwartz, 2009). The detection and response to physical forces is essential to all cells, mechanotransduction refers to the process whereby cells 'convert' mechanical stimuli into biological signals. This enables cells to 'sense' their surroundings, provoking a cellular response to adapt their structure or functions accordingly. Many physiological functions such as embryonic development,

hearing, touch-sensitivity, and muscular stretch depend on mechanotransduction (Ingber, 2006). Tissues such as bone and blood vessels have been shown to undergo remodelling in response to mechanical loading and shear stress, respectively (Burr, 2002; Langille, 1996). Stem cells receive biophysical cues, such as substrate stiffness, which dictate differentiation during regeneration and development (Yim and Sheetz, 2012). Furthermore, mechanical stimulation impacts osteoblasts and myoblasts, triggering osteogenesis and myogenesis, respectively (Grossi, *et al*., 2007; Papachroni, *et al*., 2009). The research in this thesis will discuss the potential role of lamin A and circadian rhythms, in cells of the musculoskeletal system, for generating correct responses to mechanical stimulation.

1.4.2 Responding to Mechanical Stretch

Several molecules are proposed to act as biological mechanosensors: stretch-activated ion channels, transmembrane adhesion receptors, sarcomeric proteins (such as titin and myosin), and cell surface receptors. Integrin is a transmembrane receptor, consisting of α and β subunits, and connects the extracellular matrix (ECM) to the cytoskeleton to transmit signals such as mechanical stimulation (Burridge and Chrzanowska-Wodnicka, 1996). In response to ECM proteins binding to the receptor, integrin aggregates and triggers the accumulation of vinculin, α-actinin, talin, focal adhesion kinase (FAK), filamentous actin, and downstream signal transduction molecules, such as MEK, ERK, and RhoA, to form a plaque (Grinnell and Geiger, 1986; Burridge and Mangeat, 1984; Hanks, *et al*., 1992; Lewis and Schwartz, 1995; Miyamoto, *et al*., 1995). In response to these signals, cytoskeletal proteins reorganise and assemble actin filaments, anchor the cytoplasmic tails of integrin receptors, and form focal complexes. Focal complexes can mature to form more stable focal adhesions (FA), serving as a continuous connection between the ECM and the cytosol (Abercrombie and Dunn, 1975; Sastry and Burridge, 2000). Lamin A ensures that these FAs are stable; lamin A knockdown significantly decreases the size of FA contacts, leading to increased cell motility and more pronounced stress fibres (Corne, *et al*., 2017). Mechanical stimulation of cells may also result in an integrin-independent increase in tyrosine phosphorylated FAK (Hamasaki, *et al*., 1995). When cells

receive a mechanical signal, inducing cytoplasmic mechanotransduction pathways, the signal is propagated through the cell and cytoskeleton to the nucleus by the LINC complex. This facilitates the activation of nuclear mechanotransduction pathways and cascades – a pathway that is reliant upon the nuclear lamina and lamin A.

1.4.3 The Response in the Nucleus: Signal Cascades

Once the signal of mechanical stimulation passes successfully from the extracellular environment to the nucleus, specific signalling pathways such as MAPK, NF-$_K$B, MRTF-A/SRF, and TGF-β are activated (Goodyear, *et al*., 1996; Ho, *et al*., 2005;).

The MAPK signalling cascade involves three protein kinases; MAPKKK activation activates MAPKK by phosphorylation and consequently, activates MAPK by dual phosphorylation (Lange-Carter, *et al*., 1993). These kinases up-regulate other components of the cascade including extracellular regulated kinases (ERK) 1 and 2, c-Jun NH2-terminal kinases (JNK), p38 MAPK, and ERK5/MAPKK, these are all up-regulated in response to mechanical stimulation (Goodyear, *et al*., 1996). Once activated, these signals modulate downstream gene expression through chromatin remodelling or by regulating the activity of transcription factors (Plotnikov, *et al*., 2011). During skeletal muscle contraction, JNK activation increases the expression of transcription factors *c-jun* and *c-fos* (Aronson, Dufresne and Goodyear, 1997). These are both regulators of cell proliferation, musculoskeletal-specific gene expression, DNA repair, apoptosis, and inflammation (Kovary and Bravo, 1991; Bishopric, Jayasena, and Webster, 1992; Xanthoudakis, *et al*., 1992; Kumari and Alvarez-Gonzalez, 2000; Morse, *et al*., 2003).

NF-$_K$B consists of a family of five members, which interact to form active homo- and heterodimeric complexes: p50 (NF-$_K$B1), p52 (NF-$_K$B2), p65 (RelA), RelB, and c-Rel, and are up-regulated in muscle and cardiac tissue following contraction (Ho, *et al*., 2005; Balan and Locke, 2011; Thanos and Maniatis, 1995). Upon activation, the NF-$_K$B family regulates the transcription of over 150 genes, important for inflammation, immunity, cell-adhesion, and cell-survival regulation (Pahl, 1999).

Accordingly, the activation of NF-$_{K}$B serves to protect the muscle from oxidative stress, induce a brief pro-inflammatory response, and prevent apoptosis.

MRTF-A and SRF are members of the Myocardin related transcription factors and MADS-box families, respectively. They interact to form a transcription complex and upregulate the transcription of many genes, including muscle-specific and growth-inducible genes (Wang, *et al*., 2001). In response to mechanical stimulation, Rho-actin-dependant signalling exposes a nuclear localisation signal in MRTF-A; once in the nucleus, it interacts with SRF and upregulates target gene expression (Miralles, *et al*., 2003; Hirano and Matsuura, 2011). The MRTF transcription factors are upregulated in response to muscle injury and regeneration, and are essential for skeletal muscle development and maintenance (Mokalled, *et al*., 2012; Cenik, *et al*., 2016).

TGF-β is a transcription factor important in skeletal muscle development and regeneration. It inhibits muscle differentiation and represses muscle-specific proteins, such as MyoD and Myogenin, coordinating the onset of muscle regeneration (Liu, *et al*., 2001). It is also acts as a chemotactic factor and stimulates immune-response signalling cascades, such as the Smad pathways (Reibman, *et al*., 1991; Li, *et al*., 2006).

1.4.4 Mechanotransduction in Muscle

Recognising and responding to mechanical stimuli is essential for the development and function of the musculoskeletal system. Astronauts suffer from muscle atrophy, a reduction in muscle mass and strength, as a result of mechanical unloading from the force of gravity (Vandenburgh, *et al*., 1999). In skeletal muscle, the sarcolemma membrane surrounds the functional unit of myofibrils, called the sarcomere. Between sarcomere units lies costameres, identified as clusters of vinculin (Pardo, Siliciano, and Craig, 1983). Other FA proteins, such as talin, and complexes such as dystrophin-glycoprotein and vinculin-talin-integrin are also located in these costameres (Belkin, Zhidkova, and Koteliansky, 1986; Ervasti and Campbell, 1993; Mondello, *et al*., 1996). Costameres are areas of

stable focal adhesion, ensuring constant organisation of the myofibrils and the transmission of force in lateral and longitudinal directions (Danowski, *et al*., 1992; Bloch and Gonzalez-Serratos, 2003).

These mechano-sensing connections enable muscle fibres to sense and respond to their surroundings. Receiving signals of mechanical stimulation triggers essential signal cascades for muscle cells, such as MAPK (Goodyear, *et al*., 1996). Mechanical stimulation of human muscle samples upregulates the expression of ERK1/2, JNK, and p38, with the highest upregulation observed in ERK1/2 expression (Widegren, *et al*., 1998). Mechanotransduction in humans is required for the development and maintenance of muscle cells (Arvind and Huang, 2017).

1.4.5 Lamin A and Mechanotransduction

Physical stress upregulates levels of lamin A, altering nuclear properties and gene expression, and making it an important 'mechanostat' factor in mechanotransduction (Swift, *et al*., 2013). Tissues of soft stiffness, such as brain and fat, experience little mechanical load, whilst stiffer tissues of the musculoskeletal system, such as bone and muscle, experience higher mechanical load. There is a correlation between higher levels of lamin A in musculoskeletal tissues that have a stiffer microenvironment (Swift, *et al*., 2013). Lamin A has an important role in muscle maintenance; it acts to alter the biophysical properties in cells residing within these tissues and is involved in MSC cell differentiation and migration (Chen, *et al*., 2018). Lamin A ensures effective transduction of mechanical signals to the nucleus, correct muscle-specific gene responses, and structural stability of the nucleus.

Lamin A regulates the transcription of mechanosensitive genes; knockout or mutation of lamin A in human and mouse musculoskeletal cells alters their response to mechanical stimulation (Osmanagic-Myers, Dechat, and Foisner, 2015). Undifferentiated skeletal muscle C2C12 cells transfected with wild type or autosomal dominant lamin A EDMD mutations demonstrate an increase in expression of MAPK signal cascade genes and enhanced nuclear translocation of activated ERK and JNK (Muchir, *et al*., 2007). A mouse model of the same EDMD mutation identified increased expression and nuclear

translocation of MAPK signal cascade genes in mouse hearts (Muchir, *et al*., 2007). In addition, embryonic fibroblasts from *Lmna*-deficient mice show attenuated NF-κB-regulated transcription in response to mechanical stimulation – despite an increase in the transcription factor bound to DNA (Lammerding, *et al*., 2004). Embryonic fibroblasts from lamin A knockout and DCM mice have impaired nuclear-cytoplasmic shuttling of mechanosensitive MRTF-A/SRF (Ho, *et al*., 2013). Finally, embryonic fibroblasts from *Lmna* knockout mice have altered TFG-β signalling and increased levels proliferation (Van Berlo, *et al*., 2005). These data support a role for lamin A in coordinating the transcription of musculoskeletal mechanosensitive pathways in response to mechanical stimulation in human and mice.

1.5 Circadian Dynamics - The missing link

The focus of this research is to investigate a potential link between circadian rhythms and lamin A. The function of lamin A in cells of the musculoskeletal system has been the focus of recent research and debate since the discovery that some muscular dystrophies are caused by mutations in *Lmna*; however, it remains unknown how mutations in *Lmna* lead to the observed tissue-specific pathogenesis. Currently, as outlined previously, two hypotheses form the basis of this research: the gene expression hypothesis and the mechanical stress hypothesis. The research in this thesis predicts that the missing link in this research is circadian dynamics, and the temporal regulation of tissue-specific gene expression, genome organisation, and mechano-sensitive signalling pathways.

Recent work identified that the nuclear lamina temporally regulates the expression of circadian genes through interactions with chromatin (Zhao, *et al*., 2015). Driven by poly [ADP-ribose] polymerase 1 (PARP1) and CCCTC-binding factor (CTCF), circadian genes are repressed at the nuclear periphery and released for active expression in a circadian manner, when temporally required (Zhao, *et al*., 2015). Furthermore, chromosome conformation capture (Hi-C) and circular chromosome conformation capture (4C) techniques have identified circadian rhythmicity in DNA looping and chromatin promoter-enhancing interactions (Kim, *et al*., 2018; Mermet, *et al*., 2018). This provides a

mechanism by which lamin A is suggested to be involved in controlling and regulating the circadian timing system, and highlights a mechanism whereby it may regulate further genes in a circadian manner. Functioning circadian rhythms are vital in muscle development and maintenance. In laminopathy patients, this mechanism of circadian clock regulation by lamin A may be lost and may contribute to the phenotype of musculoskeletal pathologies (Briand and Collasa, 2018).

This work supports the hypothesis that lamin A and a subset of circadian genes are bi-directionally regulated. This research predicts that the circadian clock upregulates lamin A expression, and lamin A exerts feedback to negatively regulate the expression of one or more core clock genes.

1.6 Circadian Dynamics and Lamin A

1.6.1 Circadian Dynamics: Gene Expression Hypothesis

The "gene expression" hypothesis surrounds the research that lamin A regulates muscle-specific transcription factors, muscle-specific chromosome organisation, and progression through the cell cycle. In laminopathy patients, this hypothesis predicts tissue-specific regulation is lost, having direct consequences on muscle development and maintenance. A missing factor to consider in this hypothesis is the regulation of these regulatory pathways by the circadian clock. Muscle-specific transcription factors that are regulated by lamin A, such as *MyoD* and *Myogenin,* are also subject to circadian regulation (Andrews, *et al*., 2010; Shavlakadze, *et al*., 2013). In addition, 3D nuclear architecture and chromosomal organisation oscillates with a circadian rhythm, facilitating the daily relocation of genes to repressive and active states, many of which may be muscle-specific (Aguilar-Arnal, *et al*., 2013; Chen, *et al*., 2015a; Kim, *et al*., 2018; Mermet, *et al*., 2018). Lastly, the circadian clock regulates or 'gates' entry to phases of the cell cycle. Entry into G2/M is controlled by BMAL1:CLOCK regulation of WEE1 kinase, and entry into G1 is controlled by BMAL1 regulation of $p21^{WAF1/CIP1}$ (Matsuo, *et al*., 2003; Gréchez-Cassiau, *et al*., 2008). Therefore, the gene expression and transcription factor regulation important for the gene expression hypothesis are also processes that are subject to circadian clock control.

1.6.2 Circadian Dynamics: Mechanical Stress Hypothesis

The mechanical stress hypothesis suggests that musculoskeletal cells are subject to periodic levels of mechanical stress, and lamin A-dependant mechanical pathways are essential in mounting protective adaptive responses. The nuclear lamina structurally supports the nucleus and regulates mechanosensitive pathways; the circadian clock is also central to mechanosensitive-signalling pathways in musculoskeletal cells. Transcription factors such as MAPK, NF-κB, SRF, and TGF-β are all also under circadian clock control (Obrietan, Impey, and Storm, 1998; Spengler, *et al*., 2012; Gerber, *et al*., 2013; Kon, *et al*., 2008; Yang, *et al*., 2017). In addition, lamin A is involved in protective responses to oxidative stress and the suppression of ROS, which increases in response to exercise (Lattanzi, *et al*., 2012; He, *et al*., 2016). Circadian rhythms are responsible for orchestrating protective responses to oxidative stress; peroxiredoxin oscillates with a circadian rhythm and is involved in peripheral clock synchronisation through corticosterone entrainment (Kil, *et al*., 2012; Rhee, 2016). Additionally, the accumulation of ROS resets the circadian clock through a hydrogen peroxide responsive circadian pathway (Tamaru, *et al*., 2013; Schippers, *et al*., 2013). Therefore, the pathways of the mechanical stress hypothesis are regulated by both lamin A and the circadian clock.

1.6.3 Circadian lamin A Dynamics: Research Focus

This research predicts that lamin A and the circadian clock are part of a feedback regulatory pathway important for the correct development and maintenance of musculoskeletal tissues. Research has shown that muscles from clock gene and *Lmna* mutant mice are reduced, weak, and respond incorrectly to mechanical stimulation. This research aims to uncover a temporal feedback relationship between lamin A and the circadian clock, and determine whether the musculoskeletal core clock is mechanosensitive. Future research has the potential to discover new circadian and mechanical pathways within muscle cells that can be manipulated. This may provide future avenues for novel therapeutic and pharmacological strategies to enhance tissue-specific cell differentiation and reverse tissue deterioration in disease.

1.7 Hypothesis and Aims

1.7.1 Hypothesis

The hypothesis of this research is that lamin A and the circadian clock bi-directionally regulate one another; that lamin A is under direct circadian clock control in musculoskeletal tissues, and that lamin A feeds back to regulate and manipulate the clock. Furthermore, the circadian clock in muscle cells will be mechanosensitive and that this is transduced to the clock by a lamin A-regulated signal.

1.7.2 Aims

- Identify whether lamin A is under clock control, focusing on muscle cells.
- Determine whether circadian clock genes are responsive to lamin A manipulation, through utilising knockdown and overexpression experiments.
- Determine whether circadian clock genes are mechanosensitive in muscle cells and investigate whether this response is mediated by lamin A.
- Create mathematical models of potential lamin A and circadian gene interactions to enhance mechanistic studies and assist experimental laboratory studies.

2. Methods

2.1 Cell Culture

2.1.1 Cell Passage

Undifferentiated murine embryonic myoblasts (C2C12; Yaffe and Saxel, 1977), wild-type (WT) Mouse Embryonic Fibroblasts (MEF), *Cry*$^{-/-}$ MEFs (kind gift from Gilbert van der Horst; Yagita, *et al*., 2001), and NIH/3T3 mouse embryonic fibroblast cells (Jainchill, *et al*., 1969) were used in all cell culture experiments. These were cultured in growth media: Dulbecco's Modified Eagle's Medium (DMEM; Sigma) high glucose supplemented with 10% (v/v) Foetal Bovine Serum (FBS; Sigma), 2nM L-Glutamine (L-Glu) (Sigma), 0.1mg/mL Penicillin/Streptomycin (Pen/Strep) (Sigma), and maintained in incubators at 37°C, 5% CO_2, and atmospheric oxygen (21.6%). Cells were passaged using 1% trypsin (Sigma) and were not used in experiments if they exceeded passage 15.

2.1.2 Primary Cell Culture and Tissue Collections

2.1.2.1 Myoblast Isolation

Muscle was stripped from the hind legs of Per2::Luc mice (Jackson Laboratories), shortly after they were culled using an increasing concentration of CO_2. The muscle was minced to produce a slurry and incubated at 37°C for 1 hour in F12C media (Sigma) supplemented with 2nM L-Glutamine, 1.5 U/mL collagenase D (Sigma), and 2.4U/mL Dispase II (Sigma). Digests were centrifuged at 300 g for 5 minutes to pellet the cells and re-suspended in F12 supplemented with 10% FBS, 5% horse serum, 2nM L-Glutamine, 0.1mg/mL Pen/Strep, and 2.5 ng/mL FGF (Peprotec). The cells were plated in a laminin coated flask and maintained in incubators at 37°C, 5% CO_2, and atmospheric oxygen (21.6%). Primary myoblasts were passaged using 0.025% Trypsin (Sigma) and maintained for up to 3 weeks in culture.

2.1.2.2 Tissue Dissections

Tissues were collected from C57BL/6J mice (Wild Type, WT; Jackson laboratories). The dark: dark circadian time-course utilised constant dark housing conditions for 5 days prior to sample collection. Samples were collected every 4 hours between CT2 to CT22 hours, and red light was used until the mice were culled and their heads removed. Gastrocnemius muscles were collected, stored in RNA later (Biorad), and frozen at −80°C.

2.1.2.3 Muscle homogenisation

Muscle was homogenised in 2 mL microcentrifuge tubes (Thermo Fisher Scientific) with MP Biomedicals™ Lysing Matrix D (Thermo Fisher Scientific) homogenising beads with the addition of 1 mL Purezol (Biorad). The tubes were homogenised on FastPrep-24™ Classic Grinder (MP Bio) for five cycles of 6.5 m/s for 25 seconds or until no visible muscle was left remaining in the tube, with 5 minutes rest on ice between cycles. Once homogenisation was complete, the Purezol containing the homogenised muscle sample was transferred to a new tube, and RNA and protein isolation completed (section 2.4.1 and section 2.5.1, respectively).

2.2 Cell Cycle FACS Analysis

2.2.1 Time-course FACS Collections

C2C12 myoblasts were grown in 12-well plates until 80% confluent, they were synchronised by serum shock with 50% horse serum for 2 hours. After 24 hours, the cells were collected every 4 hours through incubation with trypsin, centrifuged at 500 g, the pellet was washed in Phosphate Buffered Saline (PBS), and the cells were fixed in 70% cold ethanol for 30 minutes at 4°C. After two PBS washes, the cells were centrifuged at 850 g for 5 minutes and the supernatant was discarded. The cells were then treated with 5µg ribonuclease in PBS for 30 minutes at 37°C, prior to the addition of 10µg of Propidium Iodide to label the DNA. Samples were left on ice until analysis.

2.2.2 FACS Analysis

Using a BD Accuri C6 Flow Cytometer (BD Biosciences), the side scatter and forward scatter were measured to select single cells. Next, the pulse area vs. pulse height was measured to exclude cell doublets, and PI emission and forward scatter were measured to identify labelled cells. Each plot was gated to identify single and labelled cells, and dead cells and debris were removed; these gates are combined and applied to the PI plot. Finally, cell count is plotted against PI to create a plot of cells that have levels of DNA respective to G1, S or G2/M phases; as shown in Figure 2.1, these phases reflect a single set of chromosomes, actively replicating chromosomes or a full set of replicated chromosomes that are ready for mitosis, respectively.

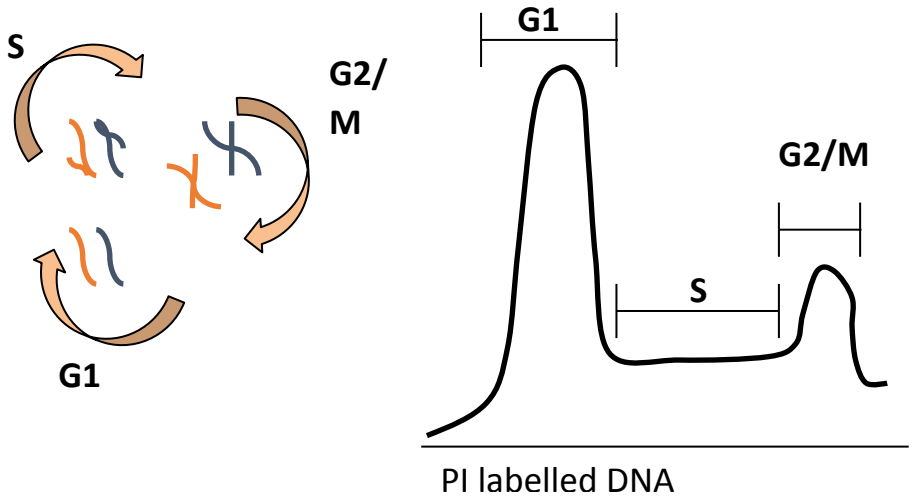

Figure 2.1. The stages in the cell cycle of chromosome replication and the correlation with FACS cell cycle analysis peaks. The first peak, G1 phase, represents a cell containing a single copy of each chromosome. The second peak, G2/M phase, represents a cell containing fully replicated sister chromatids. The area between these two peaks is S phase, and represents a cell that has actively replicating chromosomes that are not yet fully replicated to sister chromatids.

2.3 Immunocytochemistry

2.3.1 Immunocytochemistry sample preparation

C2C12 myoblasts or Per2::Luc primary myoblasts were grown in ibidi (Thistle Scientific) μ-slide 8 well chambers, until 80% confluence, and then synchronised by serum shock with 50% horse serum for 2 hours. After 24 hours, sample collection began with cells being harvested every 4 hours. This involved removal of the media and incubation of the cells in 4% paraformaldehyde (PFA) (Sigma) for 15 minutes at room temperature. Following this, the cells were incubated in 0.05% Triton X100 at 4°C for 5 minutes to fix and permeabilise the cells. The cells were stored within the chambers in PBS (Sigma) at 4°C before staining the following day. To stain cell layers, they were first blocked with 1% Goat serum (Sigma) in PBS for 45 minutes at room temperature. Next, they were incubated in a 1:1000 dilution of rabbit polyclonal anti-lamin A antibody (Sigma; L1293), diluted in PBS containing 1% goat serum overnight at 4°C. Unbound primary antibody was then washed from the cells with 3x 5-minute PBS washes before the addition of R532 goat anti-rabbit secondary (Invitrogen), diluted 1:200 in 1% goat serum for one hour. Unbound secondary antibody was washed from the cells with 3x 5-minute PBS washes and then 1:2000 dilution of 4',6-diamidino-2-phenylindole (DAPI) (Sigma) in PBS, was added for 5 minutes. Finally, the cells were then given 3x 5-minute PBS washes.

2.3.2 Immunocytochemistry imaging and quantification

Fixed C2C12 myoblasts or Per2::Luc myoblasts were imaged on a Nikon TE2000 microscope. DAPI images were converted to binary and used as a mask to outline the nucleus on Fiji (Fiji Is Just Image J) software, version 2.0. The integrated density of lamin A was measured and normalised to background levels. Nuclei with an area lower than 2000 or higher than 8000 were excluded- to account for mislabelled or merged nuclei. Any nuclei not selected under these criteria were manually added. A minimum of 150 and 50 cells were measured per image, for C2C12 cells and Per2::Luc cells respectively. Measurements for integrated density were averaged across at least 6 images and this

was repeated 3 times. Values shown relative to the mean integrated density for the first image in the 24-hour sample.

2.4 Gene Expression Analysis

2.4.1 RNA Extraction

All RNA was extracted from Purezol (Biorad) collections; Chloroform was added at a ratio of 0.2:1 to each sample, samples were centrifuged at 12000 g for 15 minutes, and the RNA-containing aqueous phase was removed. An equal volume of isopropanol was added and the samples were incubated for 10 minutes at room temperature. Precipitated total RNA was pelleted by centrifugation for 10 minutes at 12000 g, the pellet was washed in 75% ethanol before being dissolved in RNAse-free water and stored at -80°C until required in downstream applications. A Nanodrop 2000 (Thermo Scientific) was used to determine the concentration of RNA in each sample.

2.4.2 cDNA Synthesis

cDNA was synthesised from RNA using High-Capacity cDNA Reverse Transcriptase kit (Applied Biosystems). A single reaction contained; 2.0µL of 10X RT Buffer, 0.8µL 25X dNTP Mix (100mM), 2.0µL 10X RT Random Primers, 1µL MultiScribe™ Reverse Transcriptase, and 14.2µL of 1µg RNA and Nuclease-free H_2O. These were placed into a thermocycler to perform reverse transcription at the following conditions; 25°C for 10 minutes, 37°C for 2 hours, and 85°C for 5 minutes. cDNA was stored at -20°C until required for further analysis.

2.4.3 qRT-PCT

Quantitative real-time PCR (qRT-PCR) was carried out using a CFX Connect Real-Time System (BioRad). Each qRT-PCR reaction consisted of 5µL Sybr Green (Eurogentec), 1.5µL RNAse-free water, 0.25µL of each 1µM Primer – forward and reverse, and 3µL cDNA. Primer sequences used in this thesis are shown in Table 2.1. The reaction protocol consisted of 95°C for 3 min, followed by 40 amplification cycles of 95°C for 10 seconds, and 60°C for 30 seconds. Data were analysed using the

Pfaffl method for relative quantification (Pfaffl, 2001) and genes were normalised to the house-keeping gene *β-Actin*. A literature review identified *β-Actin* has been used as a house-keeper in studies investigating the response of cells to lamin A knockdown with siRNA, lamin A overexpression, and mechanical strain (Muchir, Wu, and Worman, 2009; Cesarini, *et al*., 2015; Boguslavsky, Stewart, and Worman, 2006; Zuo, *et al*., 2012; Kumar, *et al*., 2004; Chang, *et al*., 2016).

2.4.4 Primer Sequences

Table 2.1. Primer Sequences used in all studies.

Primer Name	Sequence (5'-3')
Actin F	CTGCCTGACGGCGAGG
Actin R	GGAAAAGAGCCTCAGGGCAT
Clock F	ATGGTGTTTACCGTAAGCTGTAG
Clock R	CTCGCGTTACCAGGAAGCAT
Bmal1 F	TGACCCTCATGGAAGGTTAGAA
Bmal1 R	GGACATTGCATTGCATGTTGG
Per1 F	CGGATTGTCTATATTTCGGAGCA
Per1 R	TGGGCAGTCGAGATGGTGTA
Per2 F	GAAAGCTGTCACCACCATAGAA
Per2 R	AACTCGCACTTCCTTTTCAGG
CRY1 F	CACTGGTTCCGAAAGGGACTC
CRY1 R	CTGAAGCAAAAATCGCCACCT
Rev-erbα F	TACATTGGCTCTAGTGGCTCC
Rev-erbα R	CAGTAGGTGATGGTGGGAAGTA
Lmna F	ACCCCGCTGAGTACAACCT
Lmna R	TTCGAGTGACTGTGACACTGG

2.4.5 Primer Efficiencies

Efficiencies were calculated by completing qRT-PCR reactions for each primer set with a cDNA sample at 1:1, 1:2, 1:4, 1:8, 1:16, and 1:32 dilutions. The log of the sample cDNA dilution was plotted against the Ct value (a set threshold value that the reaction exponentially increases to when the SYBR green is detected), and the slope of the line of best fit is calculated, shown in Figure 2.3. As described by Pfaffl, once the slope of the line has been determined, the efficiency of the primer in one cycle of the exponential phase is calculated through the equation $E = 10^{[-1/\text{slope}]}$ (Pfaffl, 2001). An output efficiency of 2 is equivalent to 100% efficiency; an output of 1.9 and 2.1 represents 90% and 110%, respectively.

Once the primer efficiencies have been calculated, they need to be incorporated into the qRT-PCR calculations. The expression of a gene of interest in a sample is calculated as a ratio of a control sample normalised to a reference gene, shown in Figure 2.2. E(target) is the primer efficiency of target primer; E(ref) is the primer efficiency of the reference gene primer, or housekeeping gene; ΔCt target is the Ct deviation of the sample subtracted from the control sample from the gene of interest; ΔCt ref is the Ct deviation of the sample subtracted from the control sample for the reference gene. Therefore, the calculation of the Pfaffl Ratio requires the individual q-RT-PCR primer efficiencies and the Ct deviation (ΔCt) for the gene of interest and reference gene in the control and sample of interest.

$$\text{Ratio} = \frac{E_{(\text{target})}^{\Delta\text{Ct target (control - sample)}}}{E_{(\text{ref})}^{\Delta\text{Ct ref (control- sample)}}}$$

Figure 2.2. The Pfaffl Equation used to calculate gene ratio changes between a control and a sample, normalised to a reference gene (Pfaffl, 2001)**.**

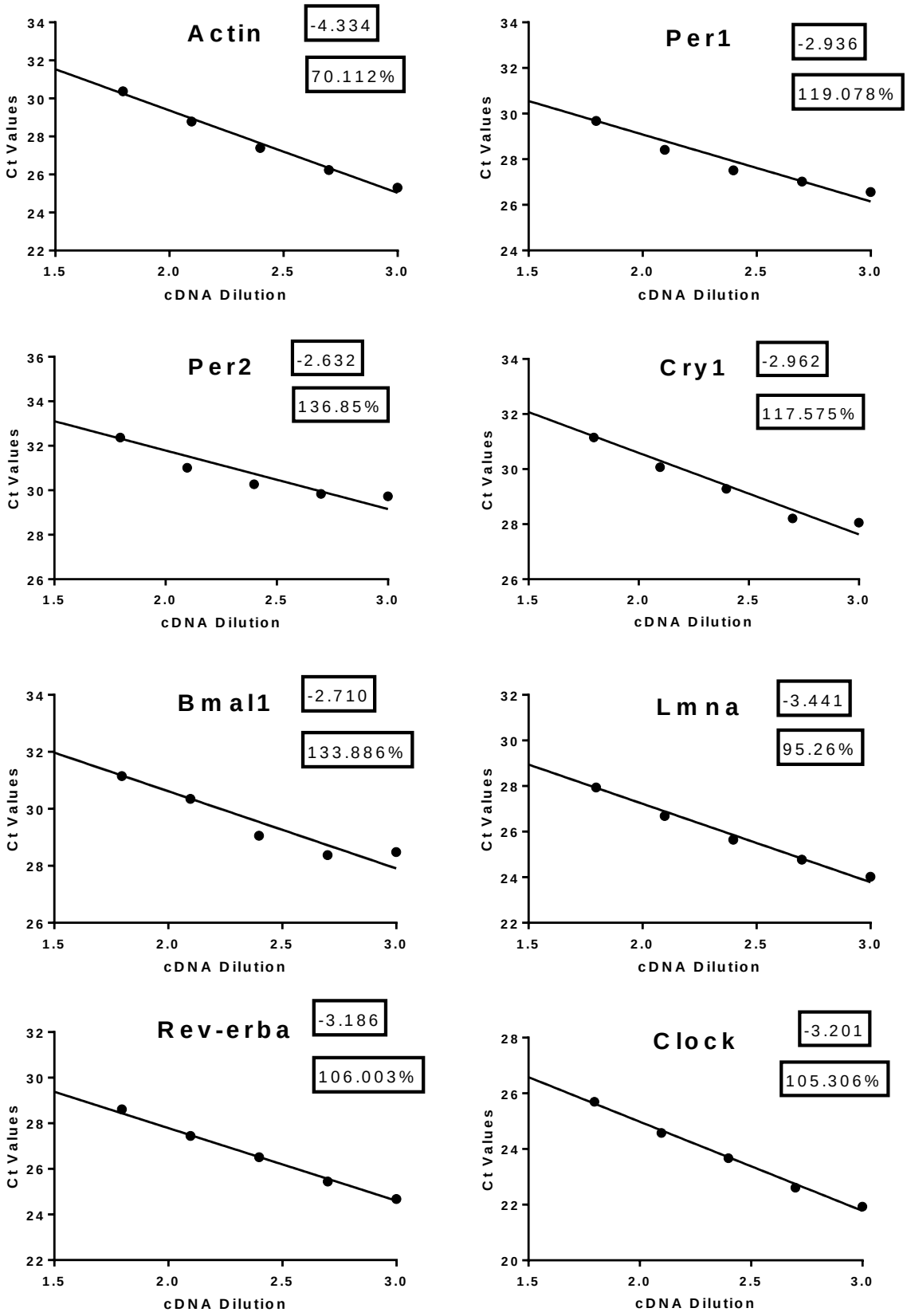

Figure 2.3 qRT-PCR of serial diluted cDNA with primer pairs to determine Primer Efficiency. The Ct value was plotted against the cDNA dilution and the slope of the line was used to determine the primer efficiency. The slope and respective primer efficiency are displayed with each graph (Pfaffl, 2001).

2.5 Protein Analysis

2.5.1 Cell culture protein sample preparation

Protein lysates in the organic phase from samples collected in Purezol (Biorad) were precipitated in ice-cold acetone and centrifuged at 12000 g. The resultant pellet was washed in T-PER™ Tissue Protein Extraction Reagent (Pierce), and resuspended in T-PER lysis buffer and 4x Laemmli Sample buffer (BioRad). Prepared protein samples were boiled for 5 minutes at 95°C, centrifuged for 5 min at 10000 g, and stored at -20°C until required for further analysis.

2.5.2 Tissue Protein Extraction

Tissue samples were snap frozen in liquid nitrogen and homogenised in an Eppendorf with an Eppendorf micropestle (Sigma). 4x Laemmli and T-Per lysis buffer were added, and the homogenised powder was re-suspended. Samples were frozen at -20°C until required.

2.5.3 Western Blotting

2.5.3.1 SDS-PAGE Electrophoresis

20µL of each sample protein and 3µL of Precision Plus Protein™ Dual Colour Standards Ladder (BioRad) were loaded onto a 10% polyacrylamide gel (1mm thick). Proteins were separated by electrophoresis in 1x electrophoresis buffer (0.025M Tris, 0.0192M Glycine, 0.01% (w/v) Sodium dodecyl sulfate (SDS), pH 9.2), initially at 80V and increasing to 100V and 120V as the proteins progressed through the gel. Electrophoresis was stopped once the loading dye reached the bottom of the gel.

2.5.3.2 Protein Transfer

Following separation by electrophoresis, proteins were transferred onto a nitrocellulose membrane (Millipore) using the wet transfer method, shown in the schematic in Figure 2.4.

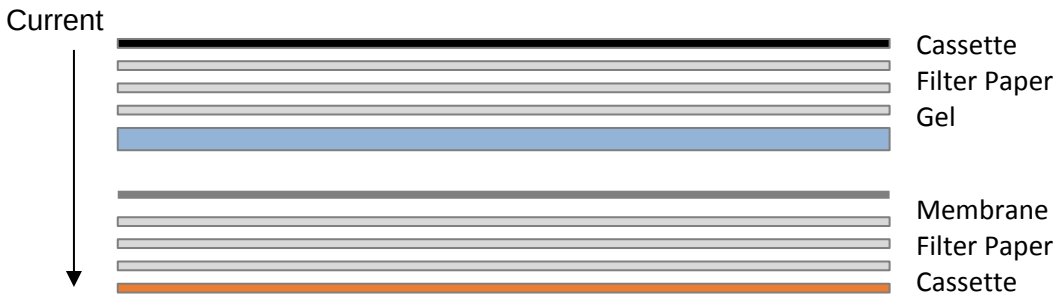

Figure 2.4. Assembly order of transfer sandwich components required for the Western blot wet transfer method. The gel is placed next to the membrane and sandwiched between filter paper, sponges, and the transfer cassette. All air bubbles are removed and the cassette is placed in the transfer apparatus with transfer buffer. The electrodes are placed on top of the sandwich and the gel is nearest the black electrode.

The nitrocellulose membrane and gel were sandwiched between six pieces of 3mm Whatman paper (three on each side). This assembly was then placed into a cassette, soaked in transfer buffer (1% electrophoresis buffer (pH 9.2), 20% methanol (v/v)), and the proteins were blotted onto the membrane using a current of 200mA for 90 minutes at room temperature.

2.5.3.3 Antibody Protein detection

The membrane was sequentially washed three times for 5 minutes each in Blot Rinse Buffer/Tween (100 mM Tris pH 7.4, 100 mM NaCl, 50 mM EDTA (pH 7.8), 0.1% (v/v) Tween 20), blocked for 1 hour at room temperature in 5% dried skimmed milk powder/PBS, and probed with primary antibodies against β-ACTIN and LMNA (1:2000, in PBS containing 5% dried skimmed milk powder) for either 1 hour at room temperature or overnight at 4°C with agitation.

Secondary fluorescence IRDye® antibodies for Goat anti-Rabbit 800CW and Goat anti-Mouse 680RD diluted in 5% milk (1:20000; Licor) were incubated at room temperature for an hour. After washing the membranes three times for 5 minutes in Blot Rinse Buffer/Tween, blots were imaged using a LI-COR Odyssey. The intensity of LMNA protein bands were normalised to β-ACTIN bands and quantified using the densitometry analysis tool on Image Studio Lite software (Version 5.2).

2.6 Genetic Techniques

2.6.1 siRNA

2.6.1.1 Transient 48-hour siRNA transfection

C2C12 myoblasts were seeded into a 12-well plate and grown until 60% confluency. siRNA complexes were formed by the addition of 1.6µL Dharmafect and 5nM validated lamin A siRNA or scrambled control siRNA per 12-well reaction, to serum and antibiotic-free media, and incubated at room temperature for 20 minutes. The media containing siRNA complexes was added to C2C12 myoblasts with fresh growth media containing antibiotics. The cells were incubated for 48 hours, collected in 200µL Purezol (Biorad), and stored at -20°C before subsequent RNA and protein analysis.

2.6.1.2 siRNA time-course

C2C12 myoblasts were seeded into 12-well plates and grown until 60% confluency. Cells were transfected with 5nM validated lamin A siRNA or scrambled control complexes as described above. After 24 hours, they were synchronised by the addition of 100 nM Dexamethasone (Dex) to the media for 45 minutes and after 24 hours, collections were completed every 4 hours for 24 hours. Samples were collected in 200µL Purezol (Biorad) and stored at -20°C before further processing.

2.6.2 Plasmid Transfections

2.6.2.1 Plasmid Preparation

Plasmids stubs were stored at 4°C and glycerol stocks at -80°C until they were streaked out onto LB agar plates with the relevant antibiotic and left at 37°C overnight. Single colonies were picked and grown in starter cultures of 5mL LB Broth, containing the relevant antibiotic. After 8 hours, 100uL of starter culture was added to 100mL of LB Broth, containing the relevant antibiotic, to grow a larger culture. The larger culture was spun down at 6000 g for 15 minutes and the pellet stored at -20°C until required for further processing. A Maxi prep for Plasmid Purification (Qiagen) was completed

on the frozen pellets following manufacturer's instructions and DNA was eluted into 500uL of water.

DNA plasmid concentration was calculated using a Nanodrop spectrophotometer.

Table 2.2. Plasmids used in gain-of function studies.

Plasmid	Supplier and catalogue number/reference	Relevant antibiotic and Concentration
pLPC-LaminA	Gerardo Ferbeyre. Addgene; 69059. (Moiseeva, *et al*., 2015).	Ampicillin 100ug/mL
pcDNA3	Invitrogen, Laboratory Stock	N/A
Emerin pEGFP-N2 (588)	Eric Schirmer. Addgene; 61985 (Zuleger, *et al*., 2011).	Kanamycin 100ug/mL
pmaxGFP™	Amaxa. Laboratory stock	Kanamycin 100ug/mL
Bmal1::Luc	Kind gift from Prof. Qing Jun Meng. (Meng, *et al*., 2008)	Hygromycin 400ug/mL
Per2::Luc	Kind gift from Prof. Qing Jun Meng. (Meng, *et al*., 2008)	N/A
Bmal1	Kind gift from Dr. Kazuhiro Yagita (Kyoto Prefectural University of Medicine, Japan).	N/A
Clock	Kind gift from Dr. Kazuhiro Yagita (Kyoto Prefectural University of Medicine, Japan).	N/A
Cry1	Kind gift from Dr. Kazuhiro Yagita (Kyoto Prefectural University of Medicine, Japan).	N/A

2.6.2.2 Transient 48-hour plasmid transfection

C2C12 myoblasts were seeded into 12-well plates and grown to 60% confluency. For each well of a 12-well plate 1ug of lamin A or pcDNA3 plasmid was added to 5µL PolyFect (Qiagen), mixed in serum-free medium, and incubated for 10 minutes at room temperature to allow complex formation. C2C12 myoblasts were changed to fresh growth medium containing antibiotics before the addition of serum-free medium containing the plasmid complexes. Cells were incubated for 48 hours, collected in Purezol (Biorad) and stored at -80°C before subsequent RNA and protein analysis.

2.6.2.3 Plasmid time-course

C2C12 myoblasts were seeded into 12-well plates, grown until 60% confluency, and transfected with 1µg of lamin A or pcDNA3 plasmid complexes as described above. After 24 hours they were synchronised by the addition of 100nM Dexamethasone to the media and after a 24 hours, samples were collected every 4 hours for another 24 hours. Samples were collected in 200µL Purezol (Biorad) and stored at -20°C until analysis.

2.6.2.4 Stable Bmal1::Luc Plasmid transfection

2.6.2.4.1 Kill curve

To generate stable cell lines of C2C12 myoblasts transfected with Bmal1::Luc (Luciferase Reporter) plasmid a plasmid containing Hygromycin resistance cassette was used (Meng, *et al*., 2008). Firstly, the minimum concentration of Hygromycin (Santa Cruz) antibiotic required to kill C2C12 myoblasts within 5 days was ascertained. C2C12 cells were seeded into 6-well plates and grown to 50% confluency and then treated with 0µg/mL, 50µg/mL, 100µg/mL, 200µg/mL, 400µg/mL or 1mg/mL of Hygromycin. After 5 days, 400µg/mL and 1mg/mL had killed all of the cells in the well whereas cells still survived at the lower concentrations of Hygromycin (Figure 4.16). Consequently, 400µg/mL was used in subsequent stable transfection experiments.

2.6.2.4.2 Stable Transfection

C2C12 myoblasts were seeded into a 6-well plate and grown to 60% confluency. Transfection complexes were set up by the addition of 1µg Bmal1::Luc plasmid and 10µL of PolyFect to serum and antibiotic-free media, and after 10 minutes incubation at room temperature these were added to the C2C12 myoblasts. After 48 hours, 400µg/mL of Hygromycin was added to the transfected cells. The Bmal1::Luc myoblasts were maintained in 200µg/mL of Hygromycin, passaged twice and used immediately for experiments or frozen in 10% DMSO in FBS.

2.6.3 LumiCycle

2.6.3.1 LumiCycle recording

Bmal1::Luc myoblasts were seeded in 35mm dishes and allowed to reach 90-100% confluency. They were then exposed to 100nM Dexamethasone for 45 minutes to synchronise the cells and after 24 hours, the media was changed to LumiCycle media, (phenol-red free DMEM supplemented with: 20% FBS, 10mM HEPES (Sigma), 1mM Sodium Pyruvate (Sigma), 2nM L-Glutamine, and 100nM Luciferin (Promega). Dishes were sealed with vacuum greased cover slips and placed into the carousel unit of a 32 channel LumiCycle recording apparatus (Actimetrics). The LumiCycle channels facilitated high-throughput photon counting of the 32 samples to read the Luciferase signal and traces were analysed using LumiCycle Analysis software (Acimetrics).

2.6.3.2 LumiCycle lamin A siRNA transfection

C2C12 myoblasts stably transfected with Bmal1::Luc plasmid, were seeded into 35mm dishes and grown to 60% confluency. siRNA complexes were formed by the addition of 5nM validated lamin A siRNA or scrambled control to 3.2µL Dharmafect, to serum and antibiotic-free media, for each 35mm dish reaction, and were incubated at room temperature for 20 minutes. Fresh media containing antibiotics was added to the cells, before the addition of the siRNA complexes. After 24 hours, the cells were treated with 100nM Dexamethasone to synchronise the cells. After another 24 hours, the

media was changed to LumiCycle media, the dishes sealed with vacuum greased coverslips, and the cells were placed in the LumiCycle.

2.6.3.3 LumiCycle lamin A plasmid transfection

C2C12 myoblasts with stable Bmal1::Luc transfection, were seeded into 35mm dishes and grown to 60% confluency. The relevant volume of lamin A or pcDNA3 plasmid that constitutes 1.5µg and 10µL PolyFect (Qiagen) – per 12-well, were mixed in serum-free medium and incubated for 10 minutes at room temperature to allow complex formation. The myoblasts were changed to fresh growth medium with antibiotics before the addition of the serum-free medium containing the plasmid complexes. After 24 hours, the myoblasts were treated with 100nM of Dexamethasone to synchronise the cells. After a further 24 hours, the media was changed to LumiCycle media, the dishes sealed with vacuum greased cover slips, and placed in the LumiCycle.

2.6.4 Luciferase Reporter Transfections

2.6.4.1 Luciferase Reporter transfections: lamin A increasing concentration

NIH-3T3 cells were seeded into 12-well plates and grown to 60% confluency. Transfection complexes contained 500ng Per2::Luc (Luciferase Reporter) or Bmal1::Luc, alongside increasing concentrations of lamin A plasmid. Each complex contained 2.5µL PolyFect per well and concentrations of lamin A plasmid were 50ng, 100ng, 200ng, or 500ng. pcDNA3 was added where necessary to ensure that the same levels of total plasmid was transfected into cells and β-Galactosidase reporter plasmid was transfected as a control to determine transfection efficiency. After 48 hours, the 3T3 cells were collected in Dual Assay Reporter Lysis buffer (Applied Biosystems), frozen at -80°C, and subsequently analysed using the Chemiluminescent Reporter Gene Assay System for the Combined Detection of Firefly Luciferase and β-Galactosidase, Dual-Light System (Applied Biosystems) following the manufacturer's protocol. Luminescence for the Luciferase and β-Galactosidase reporter enzyme reactions was measured using a GloMax®-Multi Detection System (Promega).

2.6.4.2 Luciferase Reporter transfections: lamin A, Bmal1 and Clock

3T3 cells were seeded into 12-well plates and grown to 60% confluency. Transfection complexes contained 500ng Per2::Luc-Luciferase Reporter, alongside combinations of Bmal1, Clock, and lamin A plasmid. Each complex contained 2.5µL PolyFect per well and Bmal1 and Clock plasmid was used at 200ng:200ng with or without lamin A plasmid at 500ng. pcDNA3 was added where necessary to ensure that the same levels of total plasmid were transfected into cells. In addition, β-Galactosidase reporter plasmid was co-transfected as a control to determine transfection efficiency. After 48 hours, the 3T3 cells were collected in Dual Assay Reporter Lysis buffer (Applied Biosystems), frozen at -80°C, and subsequently analysed using the Chemiluminescent Reporter Gene Assay System for the Combined Detection of Firefly Luciferase and β-Galactosidase, Dual-Light System (Applied Biosystems) following the manufacturer's protocol. Luminescence for the Luciferase and β-Galactosidase reporter enzyme reactions was measured using a GloMax®-Multi Detection System (Promega).

2.6.4.3 Luciferase Reporter transfections: lamin A and Cry1

3T3 cells were seeded into 12-well plates and grown to 60% confluency. Transfection complexes contained 500ng Bmal1::Luc, alongside combinations of Cry1 and lamin A plasmid. Each complex contained 2.5µL PolyFect per well and Cry1 was transfected at 200ng with or without lamin A at 500ng. pcDNA3 was added where necessary to ensure that the same levels of total plasmid were transfected into cells and β-Galactosidase reporter plasmid was transfected as a control for transfection efficiency. After 48 hours, the cells were collected in Dual Assay Reporter Lysis buffer (Applied Biosystems), frozen at -80°C, and subsequently analysed using the Chemiluminescent Reporter Gene Assay System for the Combined Detection of Firefly Luciferase and β-Galactosidase, Dual-Light System (Applied Biosystems) following the manufacturer's protocol. Luminescence for the Luciferase and β-Galactosidase reporter enzyme reactions was measured using a GloMax®-Multi Detection System (Promega).

2.6.4.4 Luciferase Reporter transfections: Calculations

The luminescence values for both Luciferase and β-Galactosidase reporter enzyme reactions were normalised to background levels through subtracting luminescence levels measured from empty wells on the 96-well plate. The luminescence values from the Luciferase reporter could then be normalised to the β-Galactosidase reporter plasmid, which accounts for differing transfection efficiencies or cell numbers. The mean luminescence values for each replicate condition could then be calculated.

2.7 Mechanical *in vitro* loading

2.7.1 Myoblast BioFlex Strain

C2C12 or primary Per2::Luc myoblasts were seeded onto BioFlex culture plates coated with laminin (Flexcell International) and allowed to reach 70-80% confluency. Laminin coated plates were chosen as it is an excellent substrate for the short-term and long-term maintenance of myogenic cell cultures (Penton, *et al*., 2016; Soriano-Arroquia, *et al*., 2017). The BioFlex plates were then subject to equibiaxial 6.66% strain at a frequency of 1Hz applied via the computer-controlled Flexcell® FX-5000™ Tension System, for 24 hours. 6.66% strain was chosen as similar percentages have been applied to myoblasts in recent studies (Zhan, *et al*., 2006; Nakai, *et al*., 2010; Chen, *et al*., 2013; Chang, *et al*., 2016). The Flexcell system generates strain on the Bioflex membranes through applying a vacuum underneath the membrane to stretch it over the underlying loading posts, as shown in Figure 2.5. Samples were collected in 300µL of Purezol and stored at -20°C until required for downstream analysis.

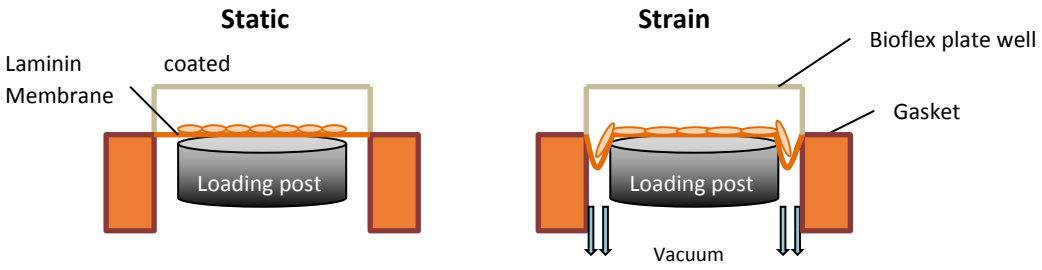

Figure 2.5. Schematic diagram depicting Flexcell vacuum induced strain of BioFlex membrane.

2.7.2 Differentiated myotube BioFlex Strain

C2C12 or primary Per2::Luc myoblasts were seeded onto BioFlex culture plates coated with laminin (Flexcell International). Once they were 60% confluent, the media was changed to low serum differentiation media (DMEM; 2% horse serum; 2nM L-Glu, 0.1mg/mL Pen/Strep). After 10 days differentiation, C2C12 and Per2::Luc myotubes were synchronised by serum shock with 50% horse serum for 2 hours. The BioFlex plates were then subject to equibiaxial strain applied via the Flexcell® FX-5000™ Tension System, for 24 hours. Samples were collected in 300µL of Purezol and stored at -20°C until required for downstream analysis.

2.7.3 siRNA BioFlex Strain

C2C12 myoblasts were seeded onto BioFlex culture plates coated with laminin (Flexcell International). Once they were 60% confluent the media was changed and siRNA complexes added. These complexes were formed by the addition of 3.2µL Dharmafect and 5nM validated lamin A siRNA or scrambled control per well to serum and antibiotic-free media, and incubating at room temperature for 20 minutes. After 24 hours, C2C12 cells were synchronised by serum shock with 50% horse serum for 2 hours. The BioFlex plates were then subject to equibiaxial 6.66% stretch at a frequency of 1Hz, applied via the computer-controlled Flexcell® FX-5000™ Tension System, for 24-hours. Samples were collected in 300µL of Purezol and stored at -20°C until required for downstream analysis.

2.8 Mechanical *in vivo* loading

2.8.1 *In vivo* loading

Male and female WT mice were anesthetised with isoflurane throughout the loading procedure and the right tibia was positioned vertically between custom-made cups (Figure 2.6 A.). A servo-hydraulic materials testing machine (model HC10; Dartec) applied axial compressive loads through the knee

joint. The upper cup was attached to the actuator and applied the load to the knee; the lower cup was linked to the load cell and monitored the loads (Poulet, *et al*., 2011).

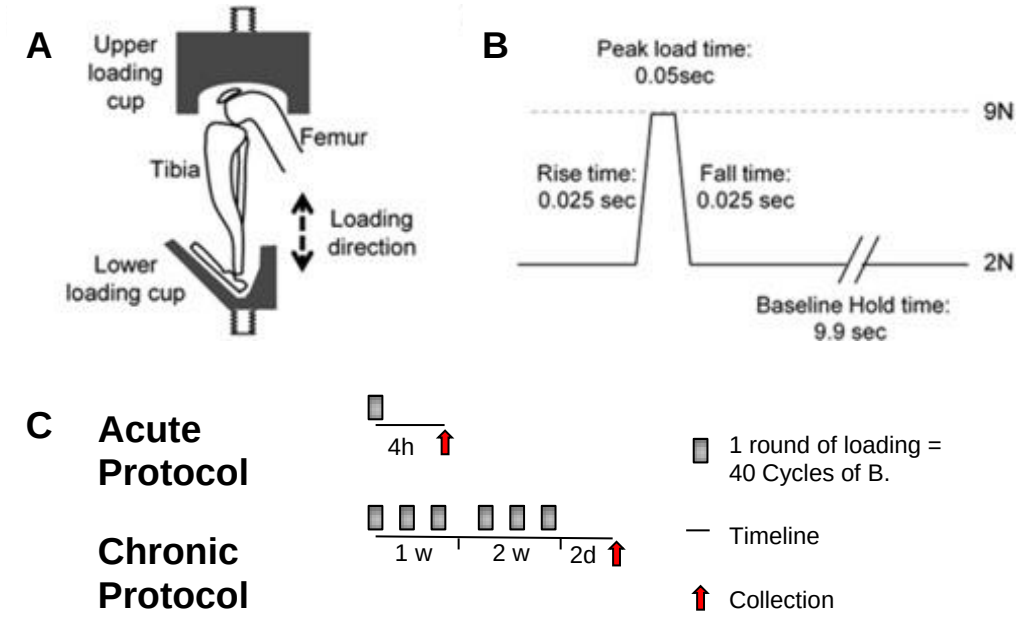

Figure 2.6. Schematic diagram of loading model, the loading cycle, and outline of the acute and chronic loading protocols. (Adapted from Poulet, *et al*., 2011).

Both acute and chronic protocols used a pattern of loading depicted in Figure 2.6 B. Peak loads of 9N were applied for 0.05 seconds, with a rise and fall time of 0.025 seconds, and a baseline hold of 2N load for 9.9 seconds (Poulet, *et al*., 2011). The baseline hold ensures the tibia remains in position. The loading pattern was repeated forty times to the right knee in each loading episode, and the left knee was used as a non-loaded control. This loading regime was chosen because the experiments were conducted as part of an ongoing study by Blandine Poulet; this is a standard protocol used in the field and will allow the group to compare data between studies (Poulet, *et al*., 2011). Loading was completed by Blandine Poulet.

Mice received either the acute or chronic protocol of loading. Mice in the acute protocol (n = 5) were loaded and after 4 hours after one regime, were collected 4 hours after this loading pattern

completed; mice in the chronic protocol (n = 5) were loaded with this loading pattern three times a week for two weeks and were collected two days later (Figure 2.6 C.). These two loading protocols enable the comparison of acute and chronic loading episodes on the circadian clock.

2.8.2 Muscle Analysis

Mice were culled by cervical dislocation, Quadricep and Gastrocnemius muscle were quickly dissected, snap frozen in liquid nitrogen and stored at -80°C. Muscle was homogenised following the muscle homogenisation protocol (2.1.2.3). RNA was isolated from Purezol containing the homogenised muscle samples, cDNA was synthesised and qRT-PCR analysis completed to quantify clock gene expression.

2.9 Statistical Tests

2.9.1 Unpaired t-test

An unpaired t-test was used in studies to test the null hypothesis that the means related to two independent samples, from an approximately normal distribution, are equal (GraphPad Prism 6).

2.9.2 One-way ANOVA

A one-way Analysis of Variance (ANOVA) was used in studies to test the null hypothesis that the means related to three or more independent samples, from an approximately normal distribution, are equal (GraphPad Prism 6). In these samples, multiple t-tests are not appropriate as multiple comparisons increase the chances of finding a statistically significant difference by chance.

2.9.3 Two-way ANOVA

A two-way Analysis of Variance (ANOVA) was used to compare the mean differences between two groups that consist of independent variables and are measured with a dependent variable (time). The two-way ANOVA tests were used in studies comparing two groups over a circadian time-course, such as lamin A knockdown and control over 24 hours (GraphPad Prism 6).

2.9.4 Cosinor Periodogram circadian analysis

To determine circadian rhythmicity and its significance, cosinor periodogram analysis software was used in studies to determine the significance of the oscillation (p value), acrophase, amplitude, mesor, and robustness; software available from the Refinetti Circadian Rhythm Laboratory (www.circadian.org/softwar.html) (Refinetti, 2016). The acrophase is the time at which the peak of a rhythm occurs, represented as the phase angle of the peak of a cosine wave fitted to the raw data of a rhythm over a time series (Refinetti, Lissen, and Halberg, 2007). The amplitude is the difference between the peak (or trough) value and the mean value of a wave. The mesor is a circadian rhythm adjusted mean based on the parameters of a cosine function fitted to the raw data of a rhythm, it is an estimate of the central tendency of the distribution of values in an oscillating variable and the average value around which the variable oscillates (Refinetti, Lissen, and Halberg, 2007). The robustness refers to the strength and endurance of a rhythm, measuring the signal-to-noise ratio and the stationarity of a rhythm (a stationary oscillation is an oscillation with parameters that remain constant over time) (Refinetti, Lissen, and Halberg, 2007).

3 Lamin A Oscillates with a Circadian Rhythm at the mRNA and protein level in skeletal muscle

3.1 Introduction

3.1.1 Studying Circadian Rhythms

Circadian dynamics in mammals have evolved to ensure that physiological, metabolic, and behavioural processes are fine-tuned to occur at appropriate times in accordance with daily environmental changes. These are not passive responses but allow mammals to adapt and anticipate daily changes, ensuring they are not wasting any energy. Circadian oscillations in the expression of tissue-specific genes can be seen across many different cell types. Studies have shown that the circadian clock is important in the development and maintenance of many different tissues, such as muscle (Dierickx, Van Laake, and Geijsen, 2018). In skeletal muscle, 7% of the transcriptome oscillates with a circadian rhythm and clock deficient mice, such as in *Clock* $^{\Delta 19/\Delta 19}$ and *Bmal1* $^{-/-}$ mice, exhibit severe muscle developmental and functional defects (Miller, *et al*., 2007; McCarthy, *et al*., 2007; Kondratov, *et al.*, 2006). Consequently, functioning circadian rhythms are vital for the development and maintenance of muscle. The aim of this research was to further investigate circadian rhythms in skeletal muscle cells, focusing on a potential involvement of the intermediate nuclear filament protein lamin A.

Cell lines grown in culture exhibit a circadian rhythm, despite no longer being maintained within an organism and a time-synchronised hierarchical system. Accordingly, the clocks in these cells will be 'set' to different times. To study circadian rhythms cell culture, these cellular clocks needs to be synchronised, enabling the investigation of molecular core clock dynamics and downstream rhythmic gene expression (Balsalobre, Damiola, and Schibler, 1998). Experiments have demonstrated that cells can be synchronised through several different methods, including exposure to glucocorticoids, forskolin, butyryl cAMP, heat shock, temperature cycling, and serum shock

(Balsalobre, *et al*., 2000; Balsalobre, Marcacci, and Schibler, 2000; Burh, Yoo, and Takahashi, 2010; Balsalobre, Damiola, and Schibler, 1998). Serum shock synchronises the circadian clock by up-regulating the expression of *Per1*, *Per2*, and *c-fos* (Balsalobre, Damiola, and Schibler, 1998). The glucocorticoid Dexamethasone (Dex) synchronises the circadian clock by up-regulating the expression of *Per1* alone (Balsalobre, *et al*., 2000). The up-regulation of *Per1* and *Per2* clock genes, regardless of what stage in the transcriptional translation feedback loop (TTFL) the cells were previously, shifts the clock in these cells through the up-regulation of the negative arm of the TTFL. This synchronisation is due to subsequent repression of the positive arm of the molecular clock. Cells exposed to any of these synchronisation techniques become 'set' to the same time as they all experience up-regulation of the same phase in the core clock cycle. The discovery of synchronisation methods facilitated molecular biology research of the core molecular clockwork mechanisms. In addition, it advanced studies investigating the role of the clock within specific cell types, including musculoskeletal cells.

3.2 Lamin A

3.2.1 A Temporal Role of lamin A

Lamin A performs many roles within the nucleus including structural support, chromatin organisation, transcription regulation, cell cycle regulation, and mechanotransduction (Lenz-Böhme, *et al*., 1997; Croft, *et al*., 1999; Ozaki, *et al*., 1994; González, *et al*., 2008; Swift, et al., 2013). Circadian oscillations of lamin A could therefore deliver higher levels of protection and regulation to the nucleus at a certain time of day. It was predicted that fine-tuning the levels of lamin A during the day, as musculoskeletal cells are exposed to varying levels of mechanical load, would provide physiological benefits to musculoskeletal cells. Temporal control of lamin A would refine the levels of mechanotransduction pathway regulation, muscle-specific gene regulation, and structural support to the nucleus (Swift, *et al*., 2013).

3.2.2 Circadian Regulation in the Nucleus

This research hypothesised that the circadian clock regulates the nuclear lamina. This is supported by the work of Lin and colleagues who discovered that lamin B1, LBR, and MAN1 mRNA and protein levels oscillate over a 24-hour period in the mouse liver (Lin, *et al*., 2014). In addition, recent data have identified a link between the nuclear lamina and circadian dynamics in genome organisation (Zhao, *et al*., 2015). This work recognised that the clock can dynamically regulate proteins located within the nucleus, and this was demonstrated at both the gene expression and protein level. Furthermore, this work directly corroborates a relationship between the nuclear lamina and circadian clock machinery, warranting further study. Due to the different regulatory roles played by lamin A within the musculoskeletal nucleus, deciphering its own regulation by the circadian clockwork will provide interesting functional consequences. Research has shown that circadian rhythms regulate tissue-specific gene expression and cell cycle progression in muscle cells (Miller, *et al*., 2007; McCarthy, *et al*., 2007; Gréchez-Cassiau, *et al*., 2007). If lamin A is a clock-controlled gene, it may be an important factor in orchestrating these circadian processes in muscle cells.

3.3 Hypothesis and Aims

3.3.1 Hypothesis

It was hypothesised that lamin A is regulated by the circadian molecular clock in musculoskeletal tissues. To test this hypothesis, a study was designed to determine whether lamin A mRNA and protein oscillates with a circadian rhythm in muscle cells, muscle tissue, and MEFs. Lamin A levels at the mRNA and protein level were detected by qRT-PCR, western blotting, and immunocytochemistry.

3.3.2 Aims

- Investigate whether lamin A mRNA expression and protein oscillates in C2C12 myoblasts over a circadian time-course.
- Establish whether lamin A oscillations are responsive to cell-cycle changes.
- Investigate whether lamin A mRNA expression and protein oscillate in differentiated C2C12 and primary myotubes over a circadian time-course.
- Observe whether lamin A mRNA expression oscillates in 'free-running' cycles, by tissue samples collected from mice housed in dark: dark conditions.
- Determine whether lamin A mRNA expression oscillates over a circadian time-course in WT mouse embryonic fibroblasts (MEFs) and determine whether this oscillation is lost upon Cry 1 and 2 double knockout in MEFs.

3.4 Results

3.4.1 C2C12 undifferentiated skeletal muscle myoblasts have oscillatory lamin A mRNA expression and protein levels

3.4.1.1 C2C12 myoblasts synchronised with Dexamethasone demonstrate low amplitude oscillations in lamin A mRNA expression and protein levels

To begin investigating whether skeletal muscle cells exhibit oscillatory expression in *Lmna* mRNA and protein levels, a circadian time-course of undifferentiated muscle C2C12 myoblasts (immortalised mouse-derived skeletal muscle cells) was collected (Yaffe and Saxel, 1977). C2C12 myoblasts were synchronised by treatment with 100nM Dexamethasone and collected every 4 hours for 28 hours starting 24 hours after synchronisation. Samples were analysed by qRT-PCR and western blotting (Figure 3.1 and Figure 3.2). *Lmna* mRNA expression, normalised to that of *β-Actin*, was found to oscillate over the 24-hour time-course with a low amplitude and with 85.5% robustness (robustness equates to how uniform the oscillations are) (Table 3.1, Cosinor Periodogram amplitude analysis: 0.4292, and robustness analysis). *Lmna* mRNA expression was in phase with the core clock genes of the negative arm (*Per1*, *Per2*, and *Cry1*) and they had similar acrophase values (the phase of the peak of the cosine wave fitted to the expression pattern) (Figure 3.1; Table 3.1, Cosinor Periodogram Acrophase analysis: *Lmna* -238°, and *Per1*, *Per2* and *Cry1*: -335°, -241° and -273°). *Lmna* expression peaked at 36 hours, and *Per2*, *Per1*, and *Cry1* expression peaked at the 40- and 44-hour time-points. *Rev-erbα* was anti-phase to *Bmal1* at the 36-hour time-point, when *Lmna* was at peak expression, and *Bmal1* expression was at a trough (Figure 3.1). *Bmal1* is part of the positive arm of the core clock, and the positive and negative core clock genes are expressed in opposite phases. Hence, *Lmna* expression was antiphase to *Bmal1* expression and expressed in phase with the negative arm of the clock.

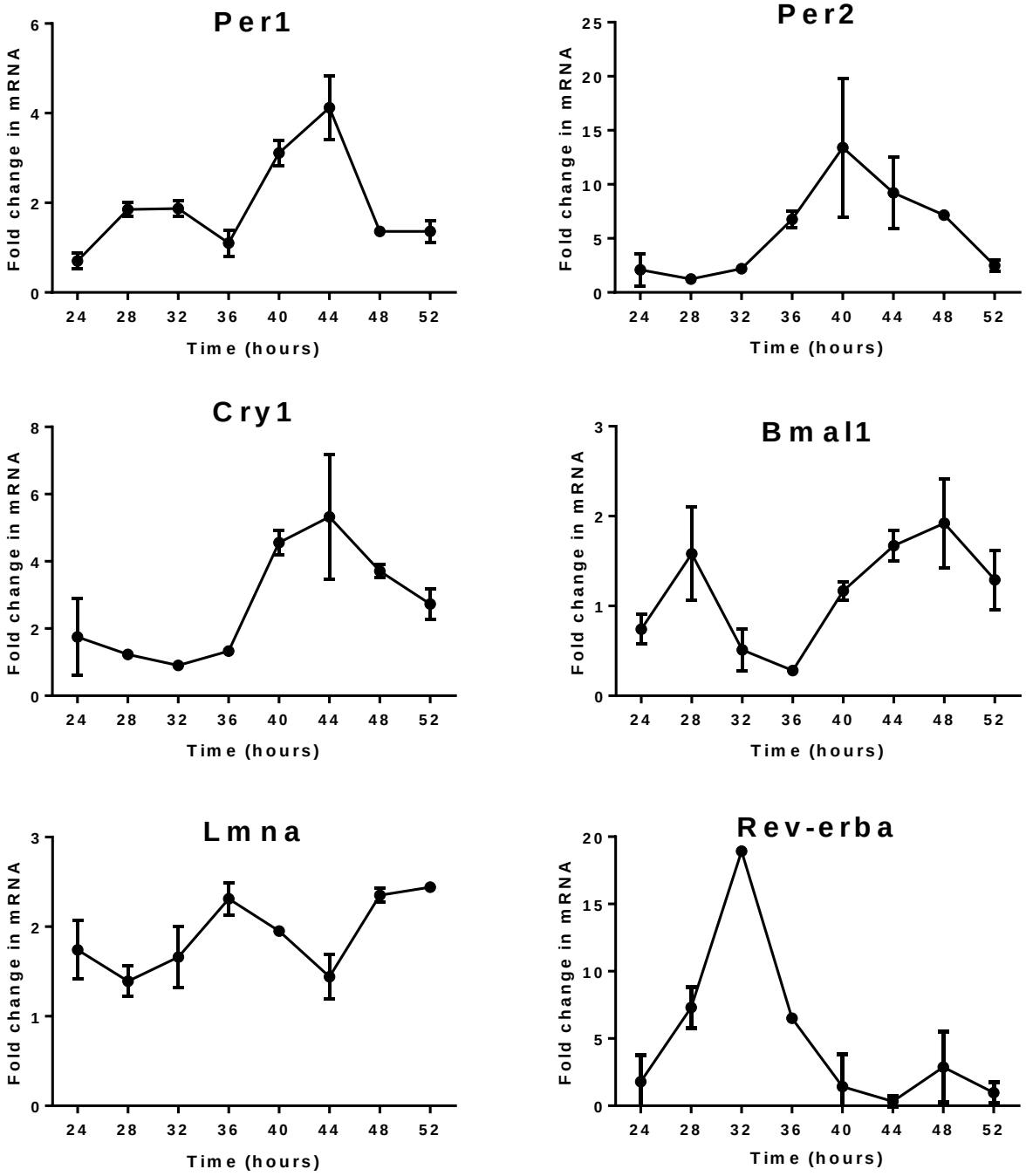

Figure 3.1. Circadian time-course of gene expression in Dexamethasone synchronised C2C12 myoblasts, demonstrate oscillation in *Lmna* expression. Myoblasts were synchronised by the addition of 100 nM Dexamethasone to the media (DMEM supplemented with 10% FBS, 2nM L-Glu, 0.1mg/mL P/S). After 24 hours, myoblasts were collected every 4 hours for 28 hours in Purezol, expression of circadian genes were measured using qRT-PCR, analysed using the Pfaffl method (Pfaffl, 2001), normalised to *β-Actin* and shown relative to the 24-hour time point. *n*=3 and data were presented as mean± s.e.m.

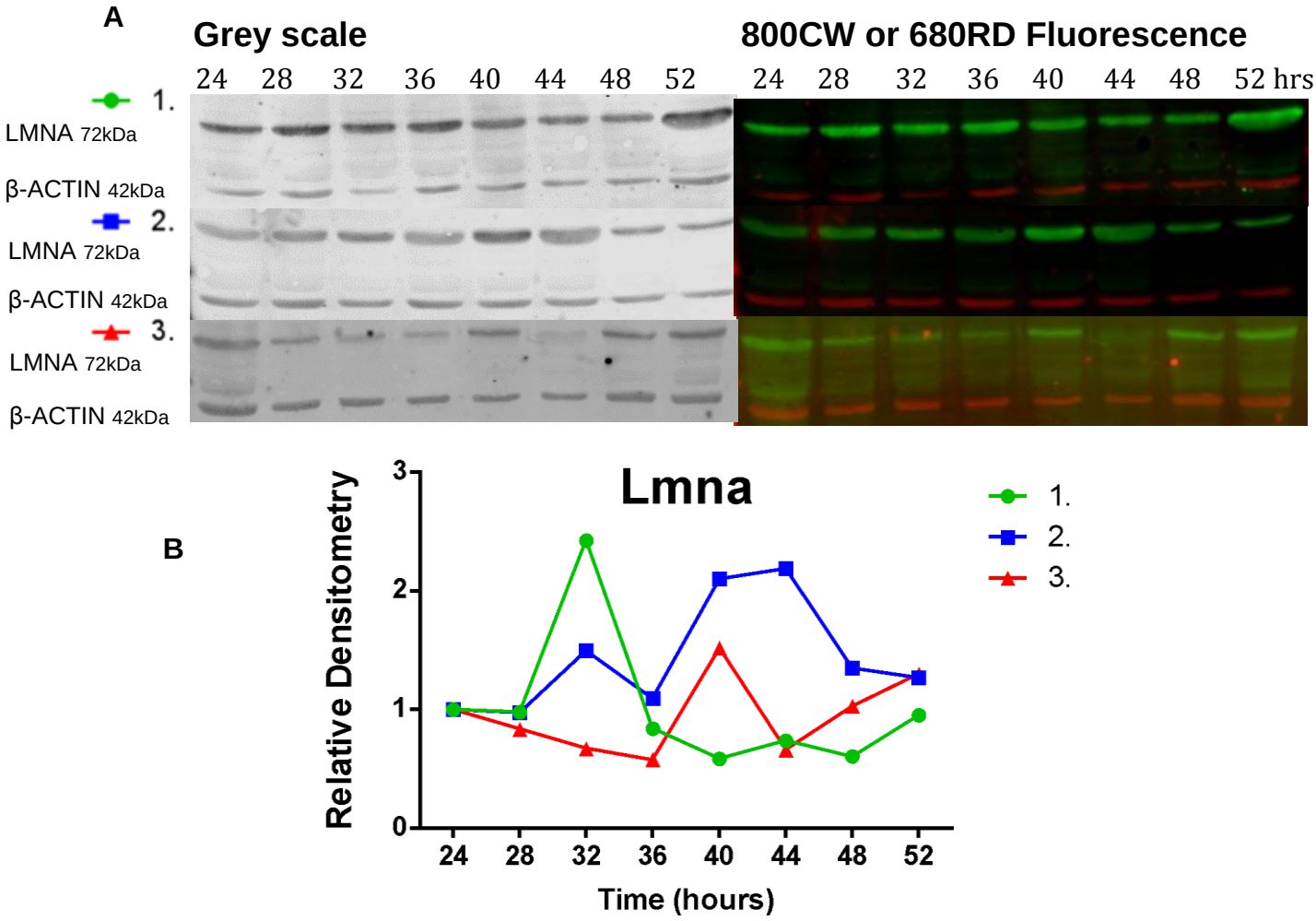

Figure 3.2. Representative Western blot images and protein densitometry traces of circadian time-course in Dexamethasone synchronised C2C12 myoblasts, demonstrates oscillatory LMNA. (A) Protein samples were ran on 10% acrylamide gels, transferred, and incubated with primary antibodies for anti-mouse Lmna (Sigma; 1:2000) and anti-rabbit β-Actin (Sigma; 1:2000) followed by secondary IRDye® antibodies for goat anti-rabbit 800CW and goat anti-mouse 680RD (Licor; 1:20000). (B) Densitometry values were calculated using the analysis software provided by Image Studio Lite Version 5.2. LMNA bands were normalised to β-ACTIN. Data were expressed as % change relative to the first time-point, n=3.

Table 3.1. Dexamethasone synchronised qRT-PCR Cosinor Periodogram circadian analysis (Refinetti, 2016).

	Lamin	*Per1*	*Per2*	*Bmal1*	*Cry1*	*Rev-erbα*
Period (h)	20.0	20.0	26.0	23.0	26.0	22.5
p value	0.0548	0.1828	0.0032*	0.0029*	0.0113*	0.0333*
Acrophase (°)	-238	-335	-241	-353	-273	-128
Amplitude	0.4292	1.3399	5.5655	0.8435	2.1864	8.1033
Mesor	1.7857	2.264	6.2408	1.1705	2.7633	6.2537
Robustness (%)	85.5	67.8	91.2	96.1	84.0	82.2

Table 3.2. Dexamethasone synchronised LMNA western blot Cosinor Periodogram circadian analysis (Refinetti, 2016).

	1.	**2.**	**3.**
Period (h)	26.0	20.0	26.0
p value	0.2461	0.1531	0.3026
Acrophase (°)	-52	-47	-253
Amplitude	0.8988	0.5907	0.5008
Mesor	1.2163	1.6002	1.0622
Robustness (%)	75.4	84.4	69.7

The relative density of LMNA protein for the three circadian time-course replicates oscillated with a low amplitude (Table 3.2, Cosinor Periodogram Amplitude analysis: 0.8988, 0.5907, and 0.5008). These LMNA protein traces do not to appear to be well synchronised within the replicates, one trace peaked at 32 hours and two traces peaked at 40 hours (Figure 3.2; Table 3.2, Cosinor Periodogram Acrophase analysis: -52°, -47°, -253°).

3.4.1.2 C2C12 myoblasts synchronised by serum shock demonstrate high amplitude oscillations in lamin A mRNA expression and low amplitude protein oscillations

In order to observe potential oscillatory patterns in *Lmna* mRNA expression and lamin A protein levels from C2C12 myoblasts synchronised using a different method, serum shock treated C2C12 myoblasts were also collected in a circadian time-course. The myoblasts were shocked by the addition of 50% horse serum for 2 hours, returned to normal supplemented DMEM, and after 24 hours, were collected every 4 hours for 28 hours. Samples were analysed by qRT-PCR and western blotting. The *Lmna* mRNA expression, normalised to *β-Actin*, oscillated with a two-fold higher amplitude in comparison to the traces observed in the Dexamethasone synchronised circadian time-course (Figure 3.3; Table 3.3, Cosinor Periodogram Amplitude analysis: 1.0558). The oscillatory expression of the negative arm core clock genes themselves appeared to be less synchronised to each other, but the phase of their peaks remained similar (Figure 3.3; Table 3.3, Cosinor Periodogram Acrophase analysis: *Per1*, *Per2*, and *Cry1*: -175°, -177°, and -162°). *Lmna* expression peaked at 32 and 48 hours, demonstrating similarities to the expression peaks for the negative arm core clock genes: *Per1*, *Per2,* and *Cry1*, which peaked at 32 and 44-48 hours. Acrophase analysis of *Lmna* expression fits a cosine peak angle at phase -145°, similar to the negative arm core clock genes (Table 3.3, Cosinor Periodogram Acrophase analysis).

Rev-erbα expression was antiphase to *Bmal1* expression, *Bmal1* was at peak expression at the 40-hour time-point, when *Lmna* expression was at its trough (Figure 3.3). Again, this demonstrates that *Lmna* expression is antiphase to *Bmal1* expression and is in phase with the negative arm core clock genes.

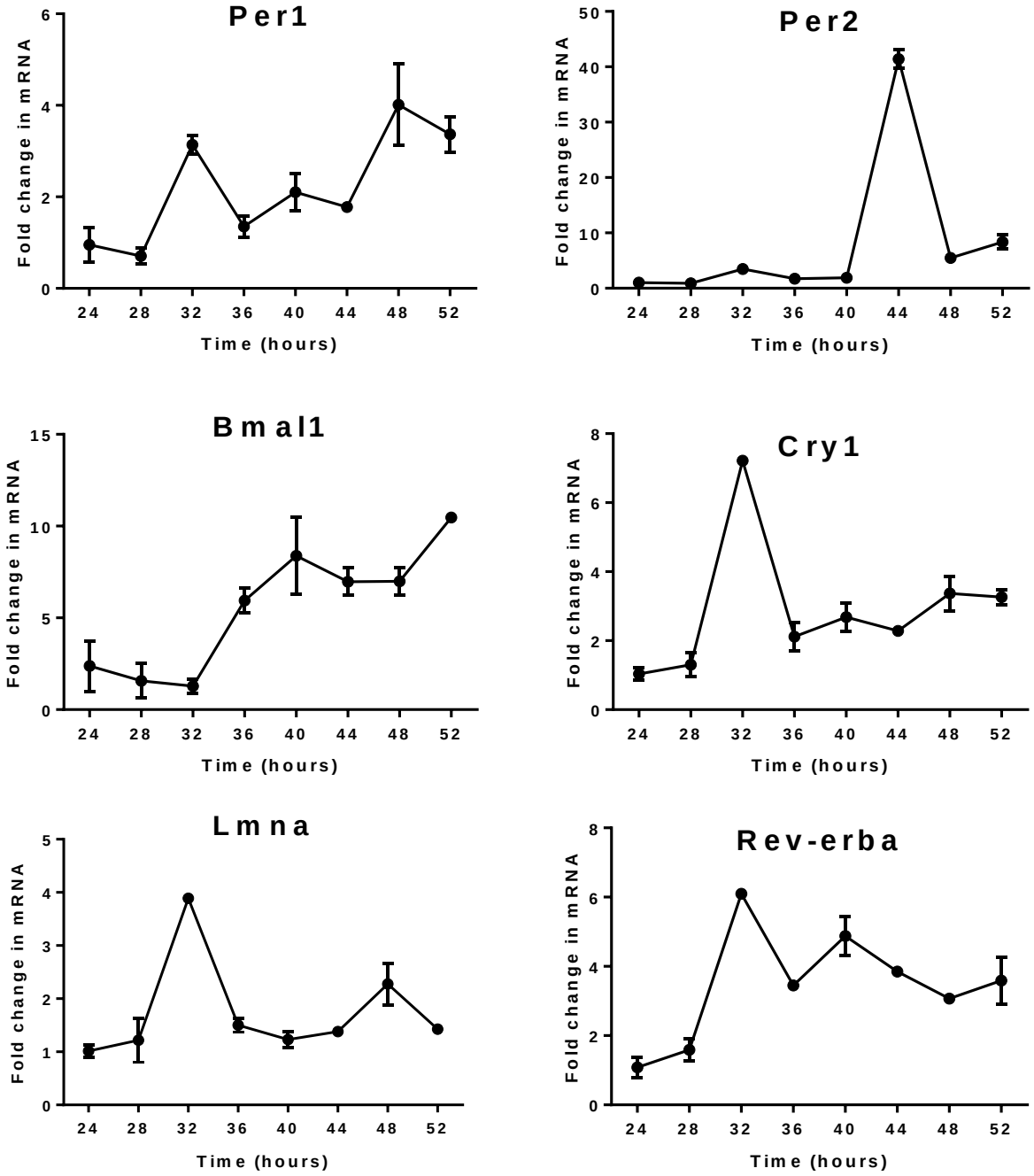

Figure 3.3. Circadian time-course of gene expression in serum shock synchronised C2C12 myoblasts, demonstrate oscillation in *Lmna* expression. Myoblasts were synchronised by changing the media to 50% horse serum for 2 hours (DMEM supplemented with 50% HS, 2nM L-Glu, 0.1mg/mL P/S), they were then returned to normal DMEM media (DMEM supplemented with 10% FBS, 1% L-Glu, 1% P/S). After 24 hours, myoblasts were collected every 4 hours for 28 hours in Purezol, expression of circadian genes were measured using qRT-PCR, analysed using the Pfaffl method (Pfaffl, 2001), normalised to *β-Actin* and shown relative to the 24-hour time point. *n*=3 and data were presented as mean± s.e.m.

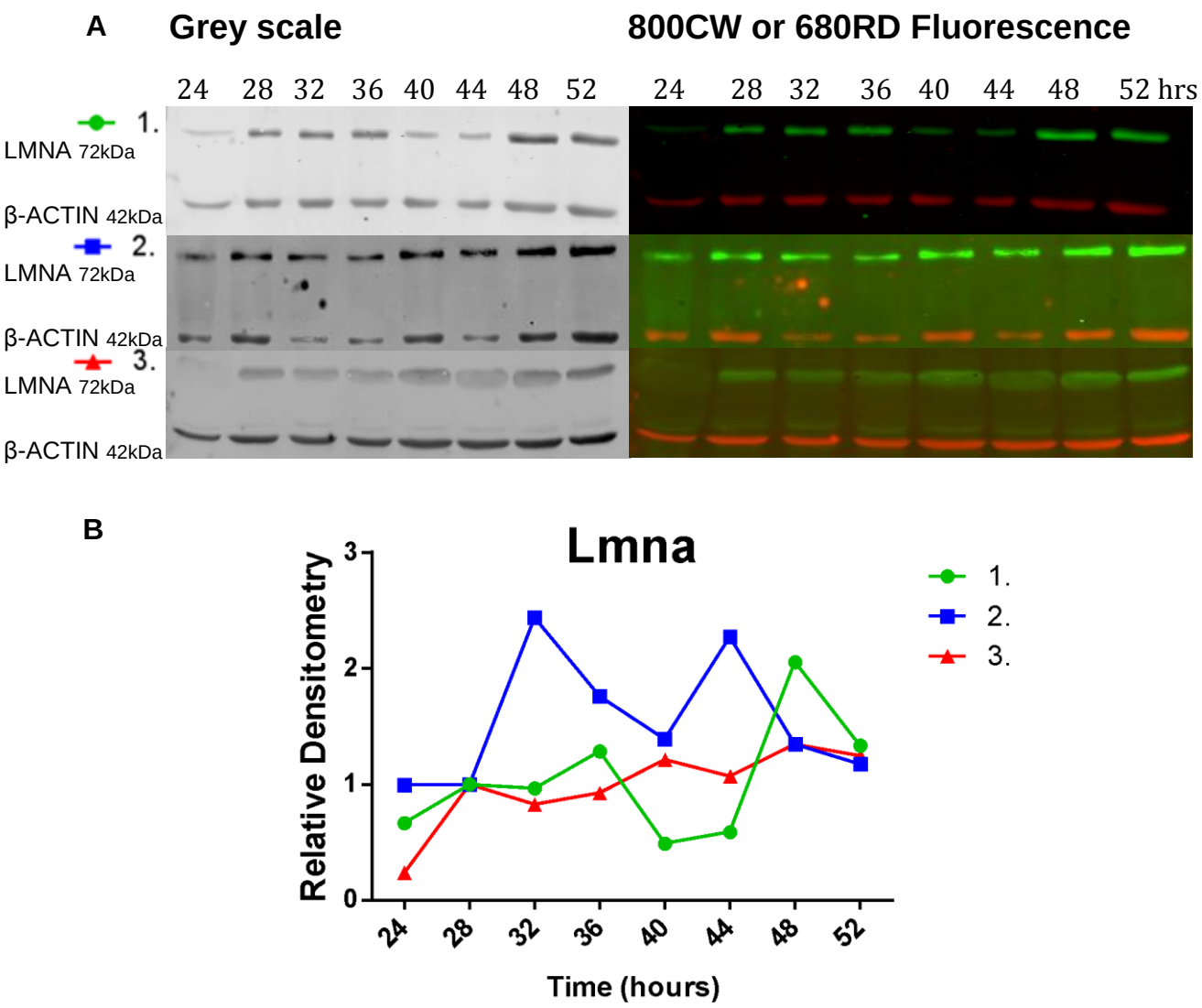

Figure 3.4. Representative Western blot images and protein densitometry traces of circadian time-course in serum shock synchronised C2C12 myoblasts, demonstrates rhythmic LMNA. (A) Protein samples were ran on 10% acrylamide gels, transferred, and incubated with primary antibodies for anti-mouse Lmna (Sigma; 1:2000) and anti-rabbit β-Actin (Sigma; 1:2000) followed by secondary IRDye® antibodies for goat anti-rabbit 800CW and goat anti-mouse 680RD (Licor; 1:20000). (B) Densitometry values were calculated using the analysis software provided by Image Studio Lite Version 5.2. LMNA bands were normalised to β-ACTIN. Data were expressed as % change relative to the first time-point, n=3.

Table 3.3. Serum shock synchronised qRT-PCR Cosinor Periodogram circadian analysis (Refinetti, 2016).

	Lamin	***Per1***	***Per2***	***Bmal1***	***Cry1***	***Rev-erbα***
Period (h)	20.0	22.1	20.0	26.0	20.0	20.0
p value	0.1729	0.6499	0.4946	0.0185*	0.5152	0.3435
Acrophase (°)	-145	-175	-177	-249	-162	-291
Amplitude	1.0558	0.743	0.9239	3.7569	2.2152	0.6982
Mesor	1.8689	1.5935	1.802	4.8224	2.8711	3.7670
Robustness (%)	58.4	35.0	50.5	87.1	48.5	65.6

Table 3.4. Serum shock synchronised LMNA western blot Cosinor Periodogram circadian analysis (Refinetti, 2016).

	1.	**2.**	**3.**
Period (h)	20.3	20.0	26.0
p value	0.3511	0.2448	0.3266
Acrophase (°)	-222	-251	-276
Amplitude	0.3306	0.6647	0.1959
Mesor	0.8628	1.5173	1.0698
Robustness (%)	64.9	75.6	67.3

The LMNA protein relative density oscillated with a low amplitude (Table 3.4, Cosinor Periodogram Amplitude analysis: 0.3306, 0.6647, and 0.1959). Relative density LMNA traces peaked at 32-36 and 44-48 hours, these traces appear to be more synchronised than the Dexamethasone protein samples, as the fitted acrophase cosine peak expression values were very similar (Figure 3.4; Table 3.4, Cosinor Periodogram Acrophase analysis: -222°, -251°, and -276°).

3.4.1.3 C2C12 myoblast LMNA rhythmicity can be detected by immunocytochemistry

To investigate whether oscillations in LMNA protein localisation within the cell can be observed, a circadian time-course of synchronised C2C12 myoblasts was collected for immunocytochemistry analysis. C2C12 myoblasts were grown in ibidi 15µ-Slide 8 well chambers (Thistle Scientific), synchronised with serum shock and after 24 hours, fixed with PFA every 4 hours. Myoblasts were stained with anti-lamin A (1:5000; Sigma), anti-rabbit secondary (1:200; Invitrogen), counterstained with DAPI (1:2000; Sigma), and imaged on the Nikon Eclipse TE2000 (Figure 3.5). Primary negative controls were used to ensure there was no non-specific antibody binding (Figure 3.6). Analysis was completed on Fiji, and DAPI was used as a mask to outline and measure LMNA fluorescence intensity in the nucleus. Integrated density values were used to ensure that the volume of the nucleus was not skewing the data sets. Larger nuclei would have higher LMNA fluorescence due to having a higher proportion of LMNA protein present. All integrated density values were normalised to the mean integrated density of the first image in the 24-hour time-point. Integrated density data demonstrated an oscillation in LMNA integrated fluorescence over the 24-hour period, with a peak in integrated density at 32-hours and a trough at 44-hours (Figure 3.7). Cosinor Periodogram analysis identified a period of 20-hours, acrophase of -246°, 74.9% robustness but a low amplitude of 0.2969 (Table 3.5).

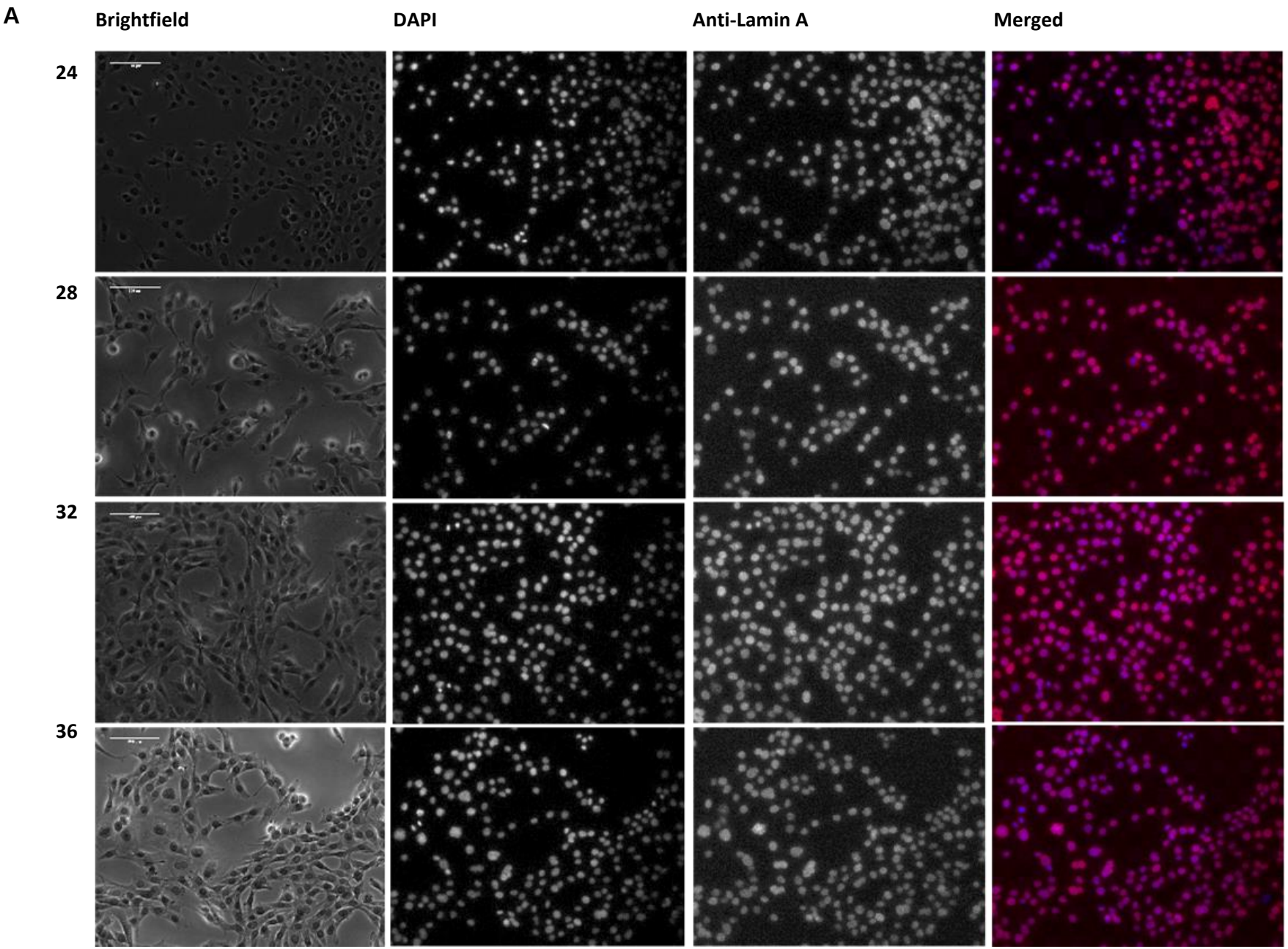
A
Brightfield
DAPI
Anti-Lamin A
Merged
24
28
32
36

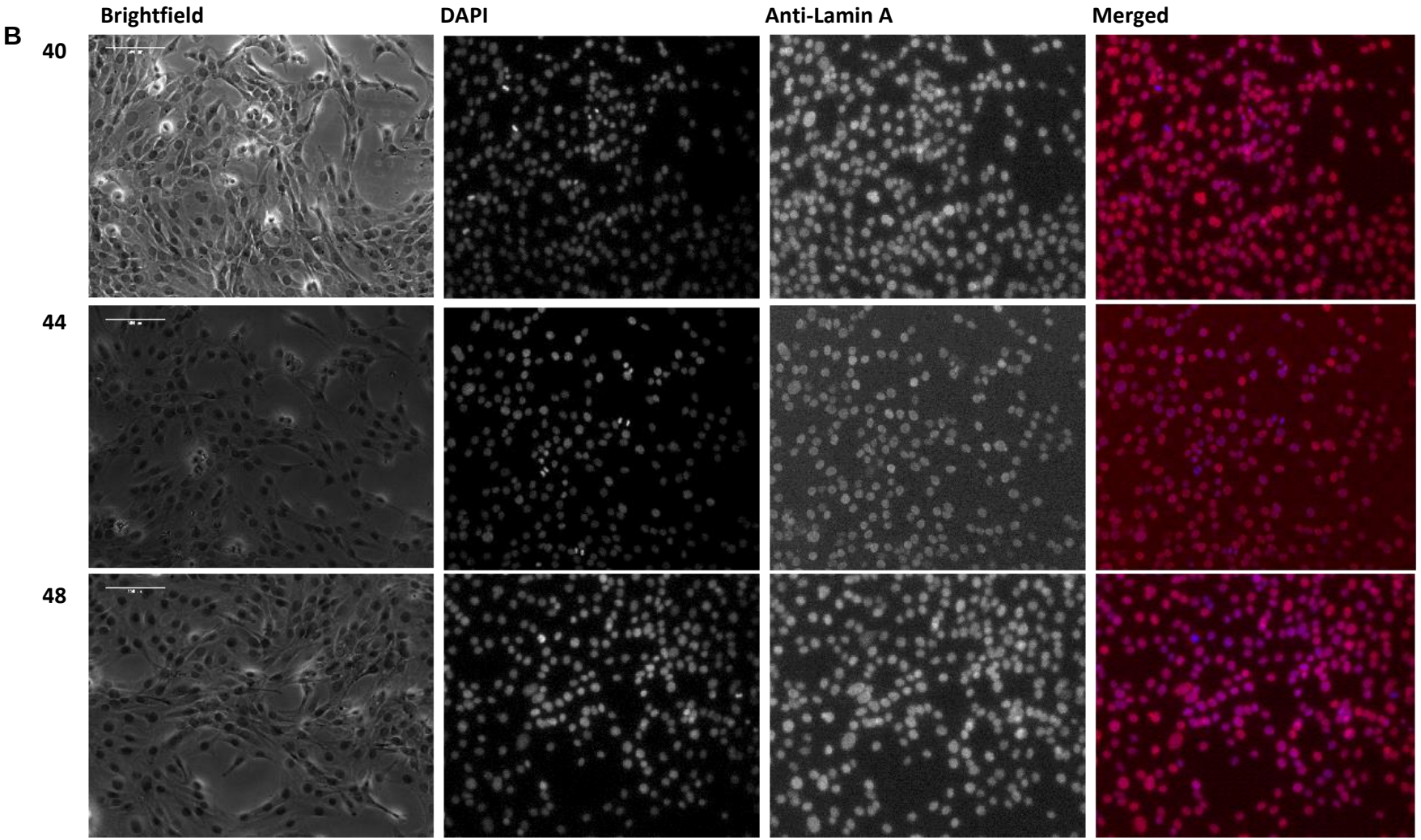

Figure 3.5. Representative images of circadian time-course immunocytochemistry in serum shock synchronised C2C12 myoblasts, fixed every 4 hours between A. 24-36 and B. 40-48 hours. Images of Brightfield, DAPI counterstain, Anti-lamin A, and DAPI and Anti-lamin A merged, in C2C12 myoblasts stained with anti-lamin A (1:5000), anti-rabbit (1:200), and counterstained with DAPI (1:2000) and images were collected on the Nikon Eclipse TE2000 at 20x.

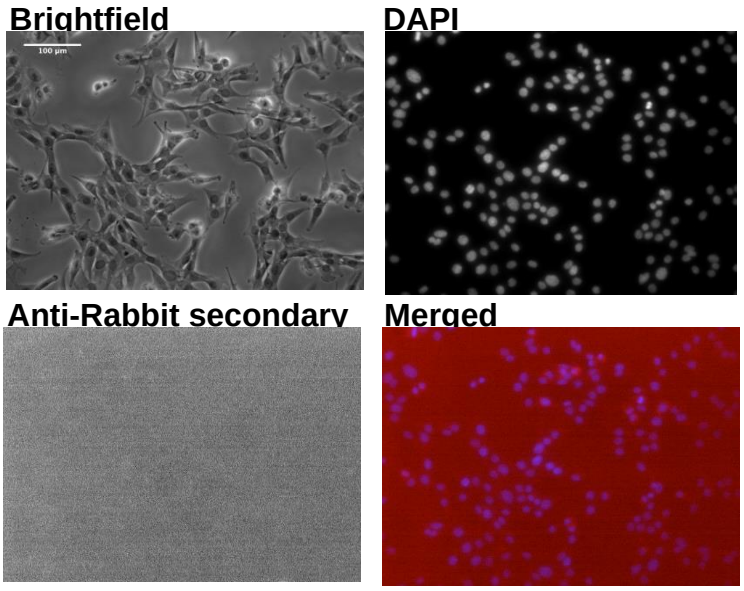

Figure 3.6. Representative imagines of C2C12 myoblast primary negative control. Representative images of fixed, primary negative C2C12 myoblasts stained with anti-rabbit (1:200) and DAPI (1:2000). Images represent Brightfield, DAPI counterstain, anti-rabbit (with no primary lamin A to bind), and DAPI and anti-rabbit merged, images were collected on the Nikon Eclipse TE2000 at 20x.

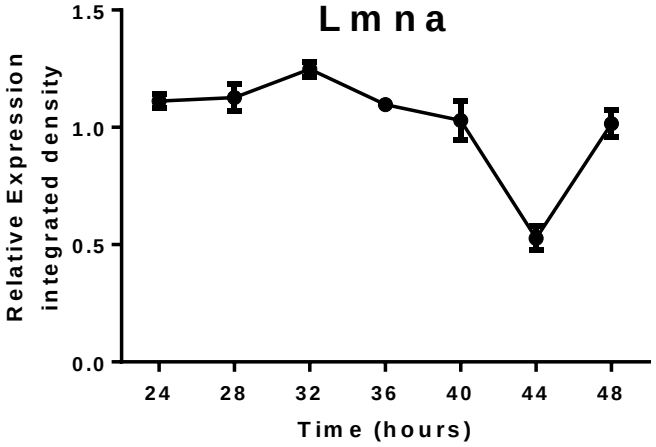

Figure 3.7. Relative Integrated Density of circadian time-course immunocytochemistry in serum shock synchronised C2C12 myoblasts, demonstrates oscillation in LMNA fluorescence. Values are normalised to the mean relative density of the first image in the 24-hour data set. Data plotted as mean± s.e.m.

Table 3.5. Immunocytochemistry Cosinor Periodogram circadian analysis (Refinetti, 2016).

Period (h)	20.0
p value	0.2508
Acrophase (°)	-246
Amplitude	0.2969
Mesor	0.9833
Robustness (%)	74.9

3.4.2 Oscillations in lamin A mRNA expression and protein are not due to changes in the cell cycle

3.4.2.1 Dexamethasone synchronised C2C12 myoblasts do not show oscillations in cell cycle progression

Lamin A and the circadian clock both have a role in regulating cell cycle gating. Hence, changes in the levels of *Lmna* mRNA and protein may be due to oscillations in synchronised cell cycle progression. In order to determine whether lamin A oscillations are due to changes in the cell cycle, FACS analysis was completed on C2C12 myoblasts synchronised by Dexamethasone, collected in a circadian time-course every 6 hours for 24 hours, and labelled with Propidium Iodide (PI). FACS analysis demonstrated that the levels of G2/M are constant with approximately 20% of cells residing in this stage of the cell cycle across the time-course (Figure 3.8 and Figure 3.9). Cosinor Periodogram circadian analysis identified no oscillatory pattern in G2/M levels; G2/M percentages had a small amplitude of 1.39 around a large mesor (the average value across the distribution of variables in a cycle, also known as the rhythm adjusted mean) of 23.8, and a robustness of 39.8% (Table 3.6). At this stage in the cell cycle, cells are rapidly growing in preparation for mitosis, and are actively undergoing mitosis. Large changes in the percentage of cells residing within this stage across the time-course would result in large changes in *Lmna* mRNA and protein production. In contrast, FACS circadian time-course data from Dexamethasone synchronised C2C12 myoblasts shows relatively constant levels of cells residing in G2/M and thus, the cell cycle cannot be attributed to the oscillatory changes observed in lamin A.

Table 3.6. Dexamethasone synchronised FACS Cosinor Periodogram analysis (Refinetti, 2016).

	Dexamethasone
Period (h)	20.0
p value	0.6026
Acrophase (°)	-353
Amplitude	1.391
Mesor	23.8026
Robustness (%)	39.8

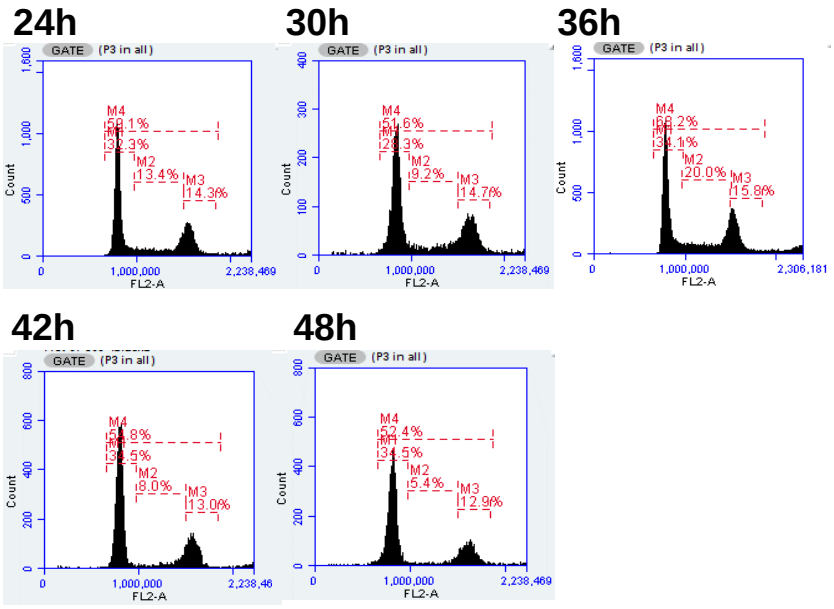

Figure 3.8. Representative traces of circadian time-course FACS Cell Cycle analysis in Dexamethasone synchronised C2C12 myoblasts, showing consistent percentages across 24 hours. Myoblasts were synchronised by the addition of 100 nM Dexamethasone to the media (DMEM supplemented with 10% FBS, 2nM L-Glu, 0.1mg/mL P/S). After 24 hours, myoblasts were collected every 6 hours for 24 hours for FACS analysis and the DNA was labelled with 100 ug/mL Propidium Iodide. Myoblasts were then analysed on the BD Accuri C6 Flow Cytometer and sorted to observe the percentage of cells within a sample that are residing in G1, S, and G2/M phase of the cell cycle- based on DNA content, roughly 20,000 cells were counted on the FACS machine for each replicate.

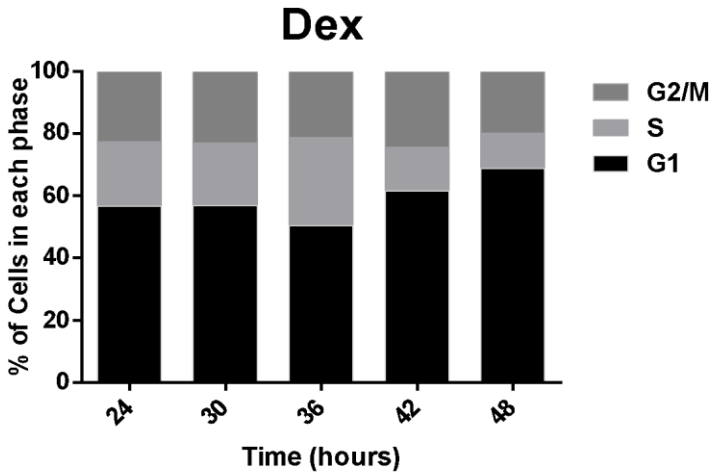

Figure 3.9. Circadian time-course FACS analysis in Dexamethasone synchronised C2C12 myoblasts, showing consistent percentages in each phase across 24 hours. Myoblasts were synchronised with Dexamethasone and collected, after 24 hours, every 6 hours for 24 hours. The percentage of cells in G1, S, and G2/M was calculated by averaging data from three replicates for each time-point.

3.4.2.2 Serum shock synchronised C2C12 myoblasts do not show large oscillations in cell cycle progression

To rule-out changes in the cell cycle being responsible for the oscillations in *Lmna* mRNA and protein observed in the C2C12 myoblast circadian time-course synchronised by serum shock, myoblasts were also collected for FACS analysis. Myoblasts were synchronised by the addition of 50% horse serum for 2 hours, returned to normal supplemented DMEM, and after 24 hours, were collected every 6 hours for 24 hours. Myoblasts were labelled with PI and analysed by FACS analysis. Across the circadian time-course, there was little change in number of cells residing in G2/M phase, with typically 10-30% residing at this stage of the cycle (Figure 3.10 and Figure 3.11). Cosinor Periodogram circadian analysis identified no oscillatory pattern in G2/M levels; G2/M percentages had low amplitude of 4.87 around a large mesor of 26.2, and a robustness of 54.4% (Table 3.7). As with the Dexamethasone circadian time-course, this ensures that the observed oscillations in lamin A mRNA and protein are not due to circadian oscillations in cell cycle progression.

Table 3.7. Serum shock synchronised FACS Cosinor Periodogram circadian analysis (Refinetti, 2016).

	Serum shock
Period (h)	20.0
p value	0.4561
Acrophase (°)	-6
Amplitude	4.8696
Mesor	26.2016
Robustness (%)	54.4

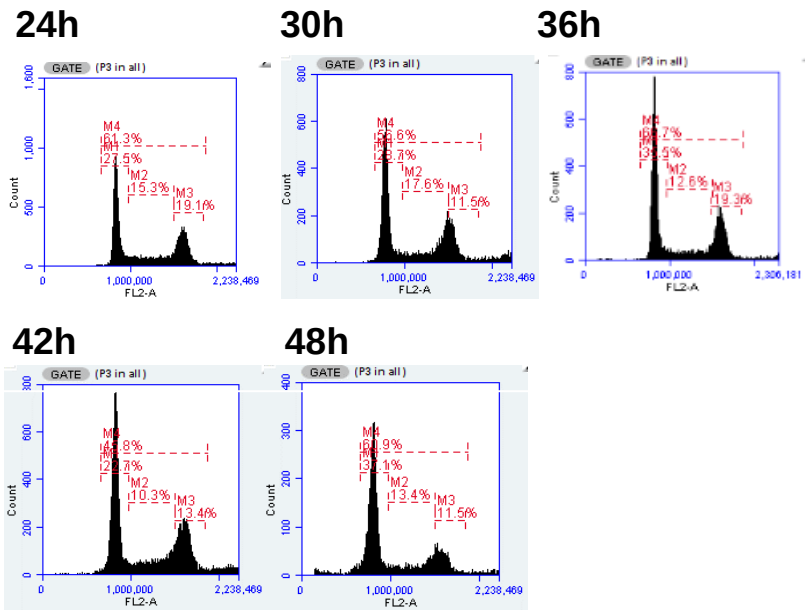

Figure 3.10. Representative traces of circadian time-course FACs Cell Cycle analysis in serum shock synchronised C2C12 myoblasts, showing consistent percentages across 24 hours. Myoblasts were synchronised by changing the media to 50% horse serum for 2 hours (DMEM supplemented with 50% HS, 1% L-Glu, 1% P/S), they were then returned to normal DMEM media (DMEM supplemented with 10% FBS, 2nM L-Glu, 0.1mg/mL P/S). After 24 hours, myoblasts were collected every 6 hours for 24 hours for FACS analysis and the DNA was labelled with 100 ug/mL Propidium Iodide. Myoblasts were then analysed on the BD Accuri C6 Flow Cytometer and sorted to observe the percentage of cells within a sample that are in G1, S, and G2/M phase of the cell cycle- based on DNA content.

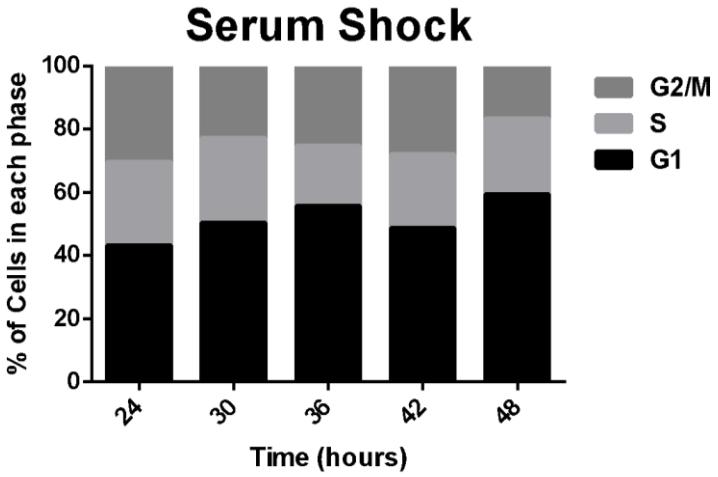

Figure 3.11. Circadian time-course FACS analysis in serum shock synchronised C2C12 myoblasts, showing consistent percentages in each phase across 24 hours. Myoblasts were synchronised by serum shock and collected, after 24 hours, every 6 hours for 24 hours. The percentage of cells in G1, S, and G2/M was calculated by averaging data from three replicates for each time-point.

3.4.3 Differentiated myotubes exhibit oscillations in lamin A mRNA expression and protein levels

3.4.3.1 C2C12 myotubes oscillate with a circadian rhythm in lamin A mRNA and protein

Next, it was investigated whether circadian oscillations in *Lmna* mRNA expression and protein levels continue upon the differentiation of myoblasts into myotubes. A circadian time-course of synchronised differentiated myotubes was collected. After 12 days of differentiation in 2% horse serum differentiation media (DMEM supplemented with 2% HS, 2nM L-Glu, 0.1mg/mL P/S), myotubes were synchronised by serum shock with 50% horse serum for 2 hours. 24 hours after returning to differentiation DMEM, samples were collected every 6 hours for 48 hours. This technique was shown in myoblasts to produce clear oscillations in lamin A mRNA (see Figure 3.3). Samples were analysed by qRT-PCR and western blotting, and both mRNA and protein data were normalised to β-Actin. Circadian time-course data demonstrated clear oscillations in *Lmna* expression with peak expression at 36 and 54 hours (Figure 3.12). Cosinor Periodogram analysis identified an amplitude of 0.4049, oscillating around a mesor of 1.4621, and 84.2% robustness (Table 3.6). Similar to the observations in myoblasts, *Lmna* expression in myotubes was in phase with the negative arm core clock genes *Per1* and *Cry1* (Table 3.6, Cosinor Periodogram Acrophase analysis: *Lmna*, *Per1*, and *Cry*: -177°, -178°, and -43°). The expression of *Per2* appeared to be out of synchronisation with the other negative arm core clock genes, and *Bmal1* expression was only slightly anti-phase; however, the expression of *Rev-erbα* remained antiphase to *Bmal1* expression (Table 3.6 Cosinor Periodogram Acrophase analysis: *Per2*, *Bmal1*, and *Rev-erbα*: -299°, -339°, and -259°).

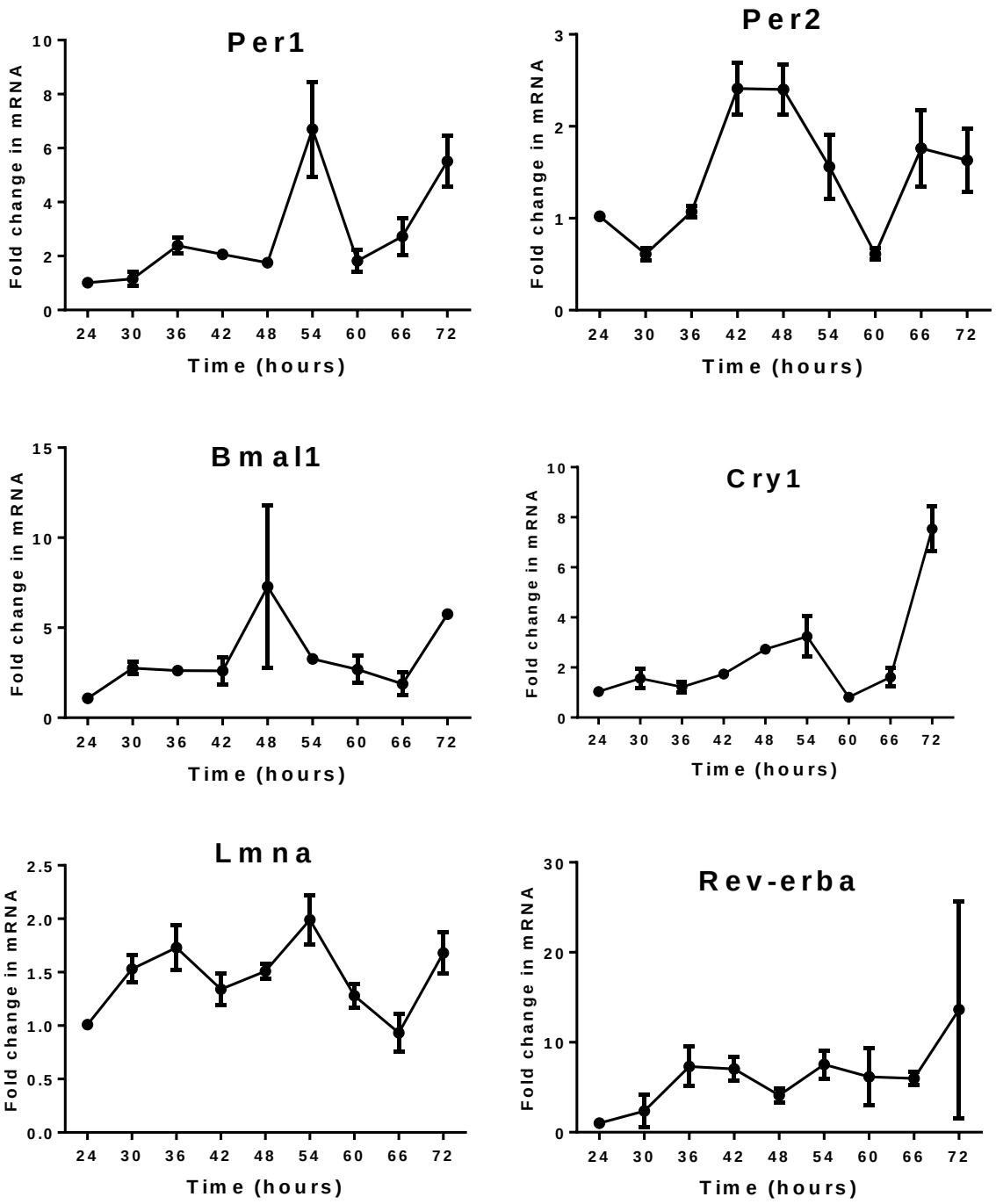

Figure 3.12. Circadian time-course of gene expression in serum shock synchronised C2C12 myotubes, demonstrate circadian oscillations in *Lmna* expression. Myoblasts were differentiated through changing to 2% horse serum differentiation media (DMEM supplemented with 2% horse serum, 2nM L-Glu, 0.1mg/mL P/S) for 12 days, and were synchronised by serum shock with 50% horse serum media for 2 hours, they were then returned to differentiation media. After 24 hours, myotubes were collected every 6 hours for 48 hours in Purezol, expression of circadian genes were measured using qRT-PCR, analysed using the Pfaffl method (Pfaffl, 2001), normalised to *β-Actin* and shown relative to the 24 hour time point. *n*=3 and data were presented as mean± s.e.m.

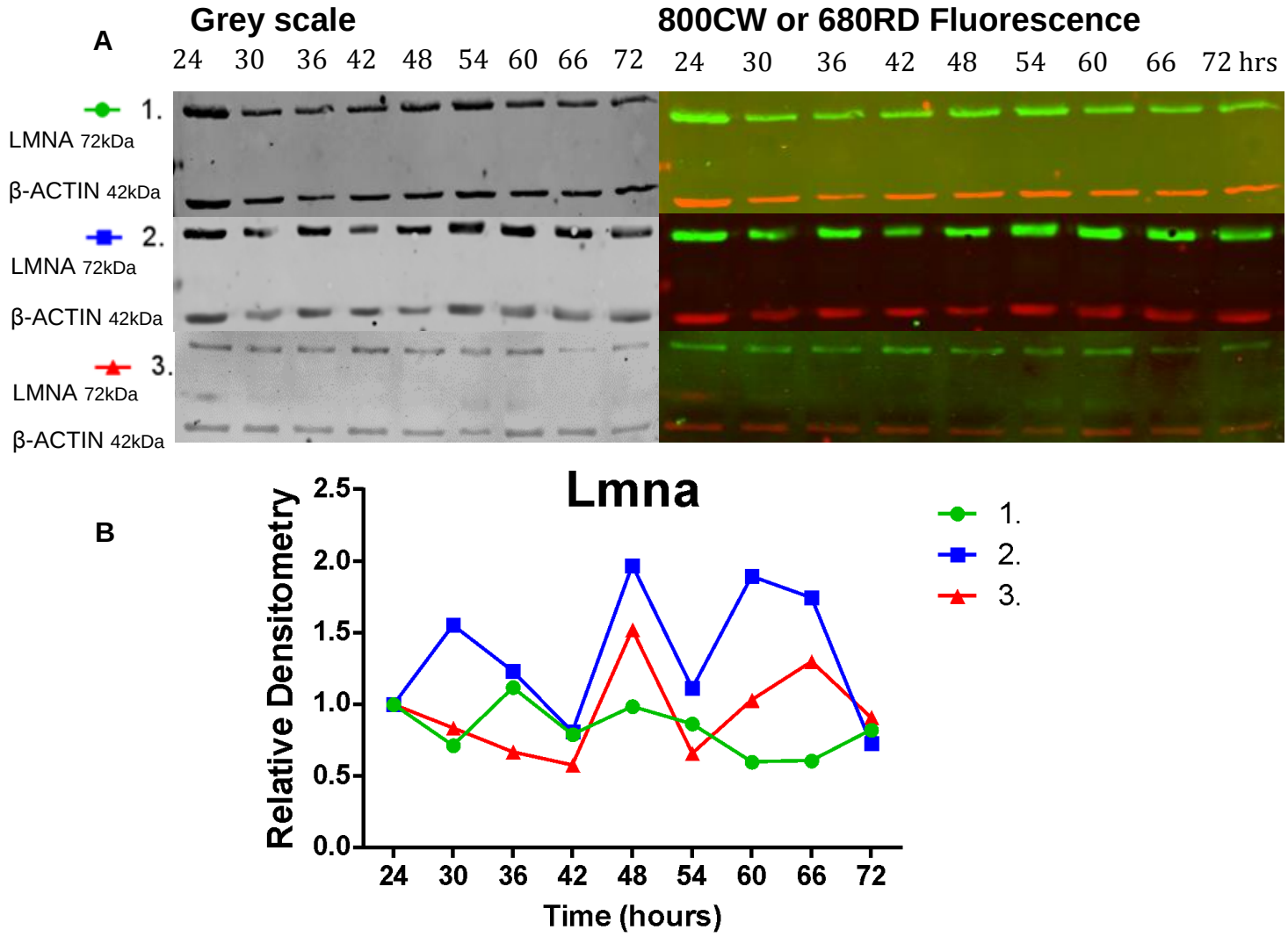

Figure 3.13. Representative Western blot images and protein densitometry traces of circadian time-course in serum shock synchronised C2C12 myotubes, demonstrates oscillations in LMNA. (A) Protein samples were ran on 10% acrylamide gels, transferred, and incubated with primary antibodies for anti-mouse Lmna (Sigma; 1:2000) and anti-rabbit β-Actin (Sigma; 1:2000) followed by secondary IRDye® antibodies for goat anti-rabbit 800CW and goat anti-mouse 680RD (Licor; 1:20000). (B) Densitometry values were calculated using the analysis software provided by Image Studio Lite Version 5.2. LMNA bands were normalised to β-ACTIN. Data were expressed as % change relative to the first time-point, n=3.

Table 3.8. C2C12 Myotubes qRT-PCR Cosinor Periodogram circadian analysis (Refinetti, 2016).

	Lamin	*Per1*	*Per2*	*Bmal1*	*Cry1*	*Rev-erbα*
Period (h)	20.3	20.0	26.0	25.6	23.6	20.0
p value	0.0046*	0.7555	0.0149*	0.2134	0.0450*	0.1756
Acrophase (°)	-177	-178	-299	-339	-43	-259
Amplitude	0.4049	2.4314	1.0303	1.9702	1.1916	2.6832
Mesor	1.4621	3.5909	1.6829	3.8753	2.1648	5.9570
Robustness (%)	84.2	82.1	93.8	64.3	87.3	82.5

Table 3.9. C2C12 Myotubes LMNA western blot Cosinor Periodogram circadian analysis (Refinetti, 2016).

	1.	**2.**	**3.**
Period (h)	26.0	20.0	20.0
p value	0.0378*	0.1874	0.1283
Acrophase (°)	-325	-184	-103
Amplitude	0.1943	0.5271	0.3973
Mesor	0.7672	1.2825	1.0623
Robustness (%)	88.6	81.4	87.3

The relative densitometry LMNA protein traces from a circadian time-course of C2C12 myotubes showed less distinct oscillatory patterns and had low amplitude values of 0.1943, 0.5271, and 0.3973 for each trace, respectively (Table 3.7, Cosinor Periodogram amplitude analysis). However, the protein levels peaked at both 30- and 48- hour time-points, and the second and third replicate traces were in better synchronisation (Figure 3.13; Table 3.7, Cosinor Periodogram acrophase analysis traces 1, 2, and 3: -325°, -184°, and -103°). In addition, all three LMNA traces had a robustness higher than 80% (Table 3.7, Cosinor Periodogram robustness analysis: 88.6%, 81.4%, and 87.3%).

3.4.3.2 Primary myotubes isolated from Per2::Luc mice demonstrate oscillations in *Lmna* mRNA expression

To investigate whether primary myoblasts also express *Lmna* in a circadian manner, myoblasts were isolated from the muscle tissue of Per2::Luc mice by digestion with collagenase and dispase (Figure 3.14). Once isolated, they were differentiated for 12 days in 2% horse serum DMEM media prior to synchronisation and collection. The myotubes were synchronised by serum shock through the addition of 50% horse serum for 2 hours, and returned to normal supplemented differentiation DMEM before collection every 6 hours for 48 hours.

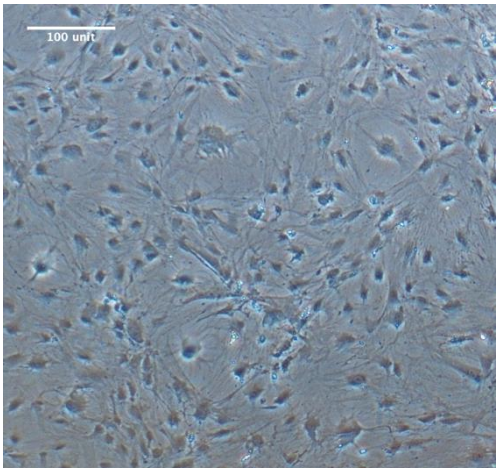

Figure 3.14. Primary myotubes isolated from Per2::Luc mice and differentiated for 7 days. Image taken on Nikon Eclipse TS100 microscope at x20.

Time-course samples were analysed by qRT-PCR and normalised to *β-Actin*. Consistent with previous data, *Lmna* expression demonstrated oscillations that were 81% robust, and in phase with *Per1*, *Per2*, *Cry1*, and *Rev-erbα* expression (Figure 3.15; Table 3.8, Cosinor Periodogram robustness analysis and acrophase analysis, *Lmna*, *Per1*, *Per2*, *Cry1*, and *Rev-erbα*: -261°, -264°, -312°, -333°, and -227°). Expression peaked at 42-48 and 72 hours, and was anti-phase in relationship with *Bmal1* expression (Table 3.8, Cosinor Periodogram acrophase analysis, *Bmal1*: -163°).

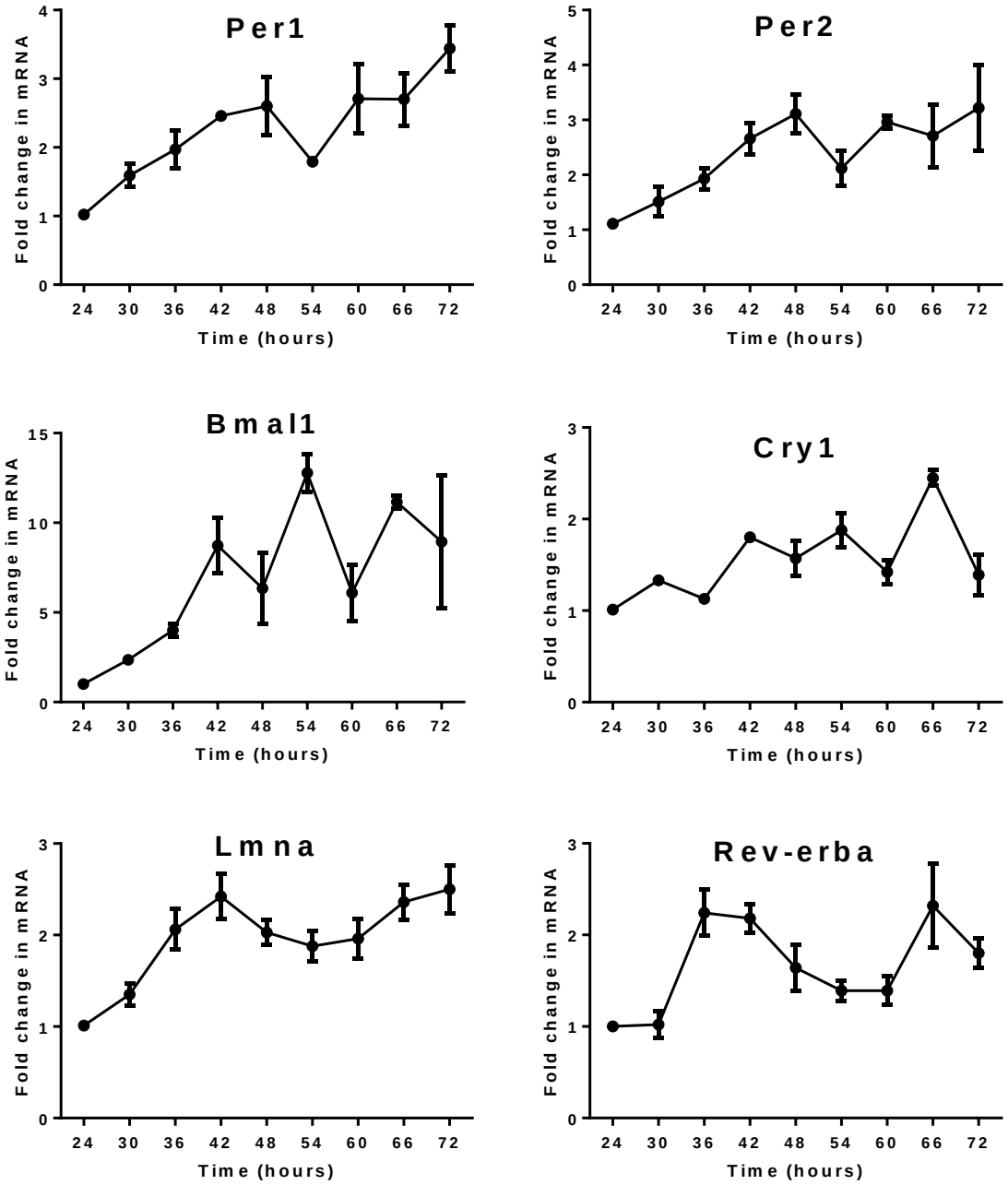

Figure 3.15. Circadian time-course of gene expression in serum shock synchronised Per2::Luc primary myotubes, demonstrate oscillations in *Lmna* expression. Per2::Luc primary myoblasts were differentiated through the addition of 2% horse serum media (DMEM supplemented with 2% horse serum, 2nM L-Glu, 0.1mg/mL P/S) for 12 days. Myotubes were synchronised by 50% horse serum media for 2 hours (DMEM supplemented with 50% HS, 2nM L-Glu, 0.1mg/mL P/S), and returned to differentiation DMEM media. After 24 hours, myotubes were collected every 6 hours for 48 hours in Purezol, circadian genes were measured using qRT-PCR, analysed using the Pfaffl method (Pfaffl, 2001), normalised to *β-Actin* and shown relative to the 24-hour time point. *n*=3 and data were presented as mean± s.e.m.

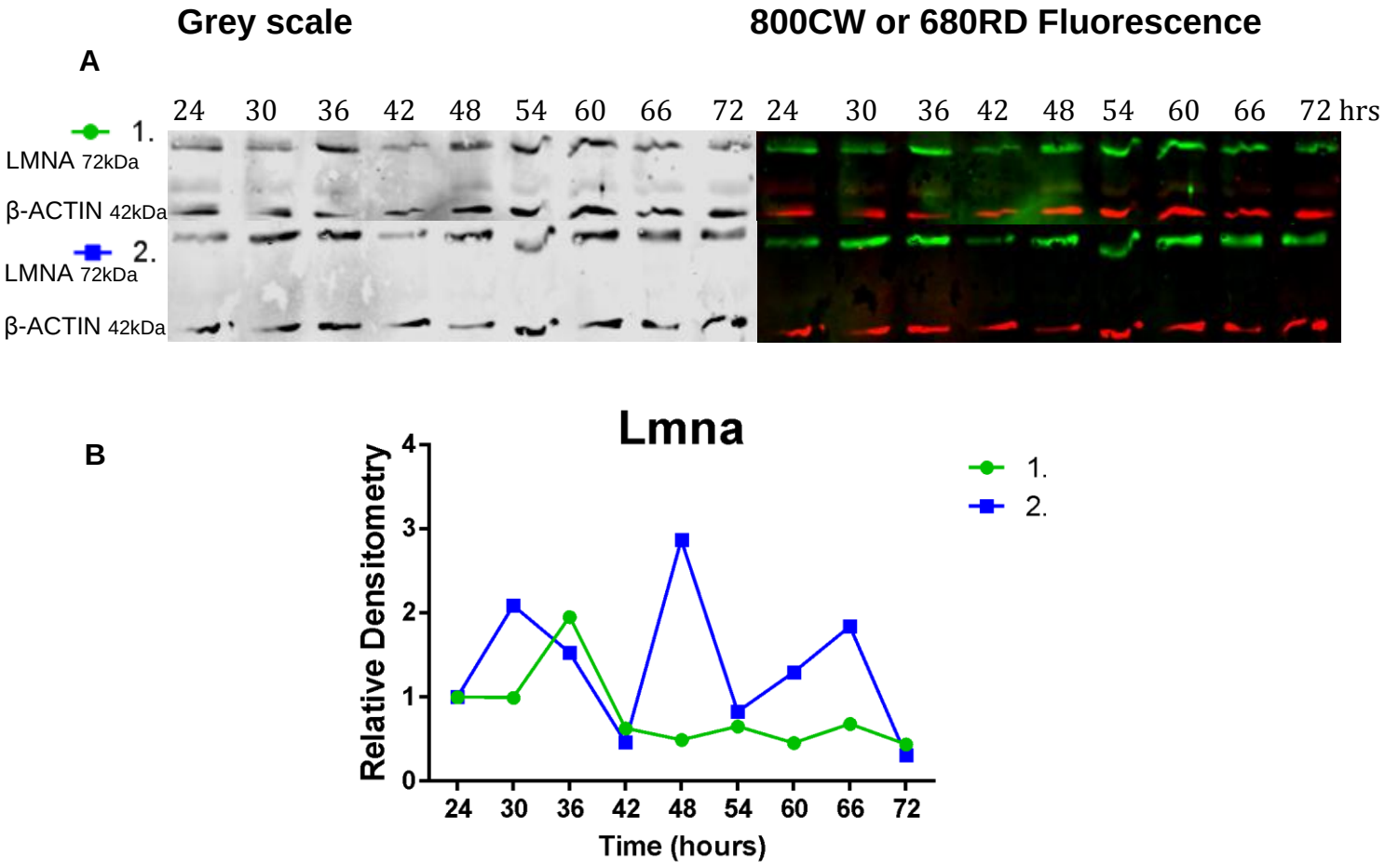

Figure 3.16. Representative Western blot images and protein densitometry traces of circadian time-course in serum shock synchronised Per2::Luc primary myotubes, demonstrates oscillations in LMNA. (A) Protein samples were ran on 10% acrylamide gels, transferred, and incubated with primary antibodies for anti-mouse Lmna (Sigma; 1:2000) and anti-rabbit β-Actin (Sigma; 1:2000) followed by secondary IRDye® antibodies for goat anti-rabbit 800CW and goat anti-mouse 680RD (Licor; 1:20000). (B) Densitometry values were calculated using the analysis software provided by Image Studio Lite Version 5.2. LMNA bands were normalised to β-ACTIN. Data were expressed as % change relative to the first time-point, n=3.

Table 3.10. Per2::Luc myotubes qRT-PCR Cosinor Periodogram circadian analysis (Refinetti, 2016).

	Lamin	***Per1***	***Per2***	***Bmal1***	***Cry1***	***Rev-erbα***
Period (h)	24.9	26.0	20.0	26.0	26.0	26.0
p value	0.0377*	0.5321	0.2123	0.2596	0.5191	0.0069*
Acrophase (°)	-261	-264	-312	-163	-333	-227
Amplitude	0.3916	0.4020	0.4557	3.6804	0.2356	0.6247
Mesor	2.0140	2.5245	2.5618	4.5544	1.5626	1.6709
Robustness (%)	81.0	74.5	64.4	74.1	38.7	81.7

Table 3.11. Per2::Luc myotubes LMNA Western blot Cosinor Periodogram circadian analysis (Refinetti, 2016).

	1.	**2.**
Period (h)	25.9	20.0
p value	0.2016	0.1802
Acrophase (°)	-133	-188
Amplitude	0.7352	1.074
Mesor	0.945	1.5418
Robustness (%)	79.9	82.1

The relative densitometry LMNA protein traces from Per2::Luc primary differentiated myotubes circadian time-course samples showed amplitude values of 0.7352 and 1.074 for each trace, respectively (Table 3.9, Cosinor Periodogram amplitude analysis). The LMNA traces were well synchronised and had a robustness of 79.9% and 82.1% (Figure 3.16; Table 3.9, Cosinor Periodogram robustness analysis and acrophase analysis traces 1 and 2: -133° and -188°).

3.4.3.3 Primary myoblast LMNA rhythmicity can be detected by immunocytochemistry

To investigate whether rhythmic LMNA integrated density fluorescence can be observed in primary myoblasts, myoblasts isolated from Per2::Luc mice were collected in a circadian time-course and analysed by immunocytochemistry. Primary myoblasts were grown in ibidi 15µ-Slide 8 well chambers (Thistle Scientific), synchronised with serum shock by 50% horse serum, and after 24 hours, fixed with PFA every 4 hours. Myoblasts were stained with anti-lamin A (1:5000; Sigma), anti-rabbit secondary (1:200; Invitrogen), counterstained with DAPI (1:2000; Sigma), and imaged on the Nikon Eclipse TE2000 (Figure 3.17). Primary negative controls were used to ensure there was no non-specific antibody binding (Figure 3.18). Analysis was completed on ImageJ, and DAPI was used as a mask to outline and measure LMNA fluorescence intensity in the nucleus. Integrated density values showed an oscillation in LMNA fluorescence over 24 hours although Cosinor Periodogram analysis demonstrated a low robustness and amplitude values (Figure 19; Table 3.10, Cosinor Periodogram robustness analysis: 55.8%, and amplitude analysis: 0.2149).

A

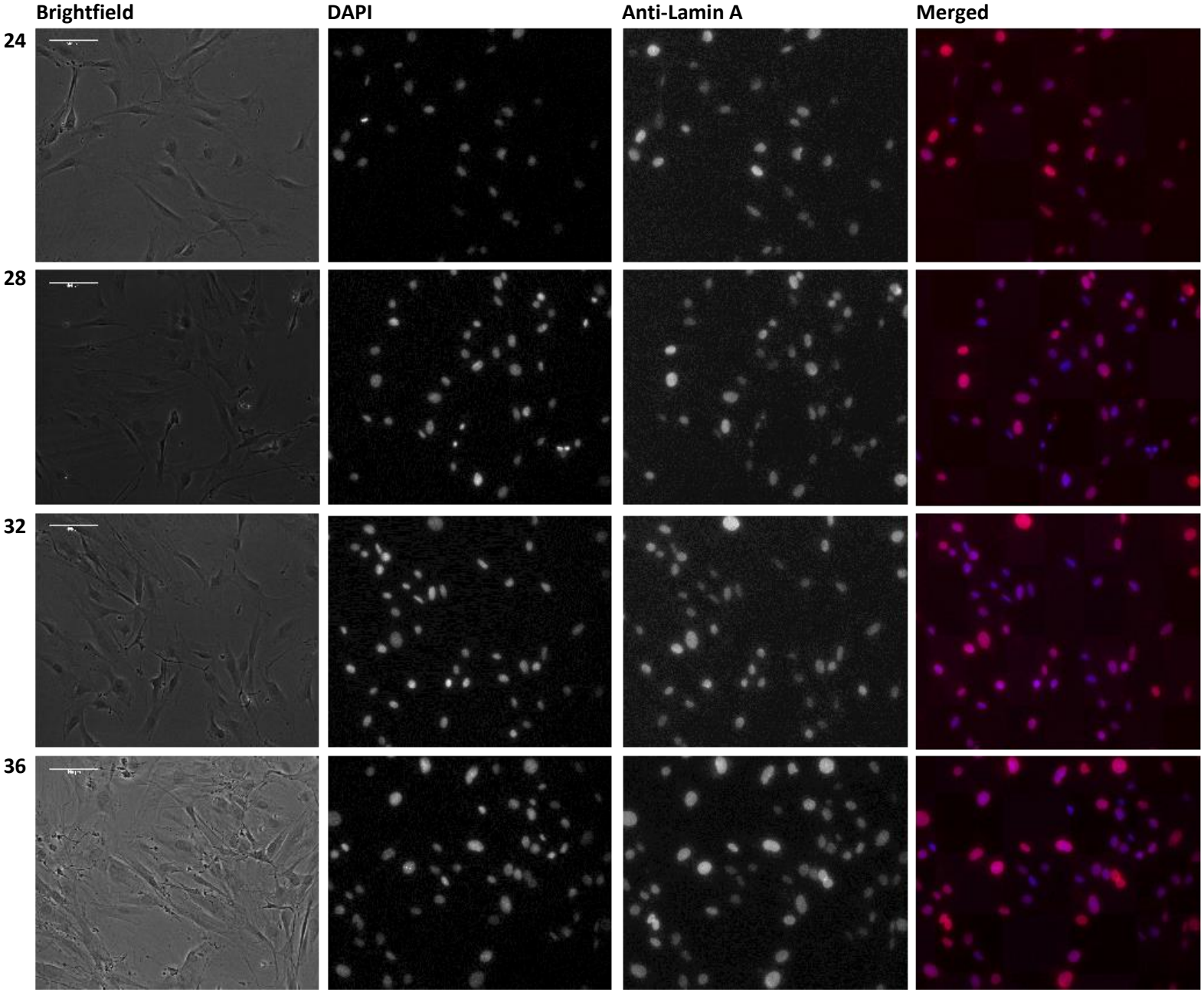

B

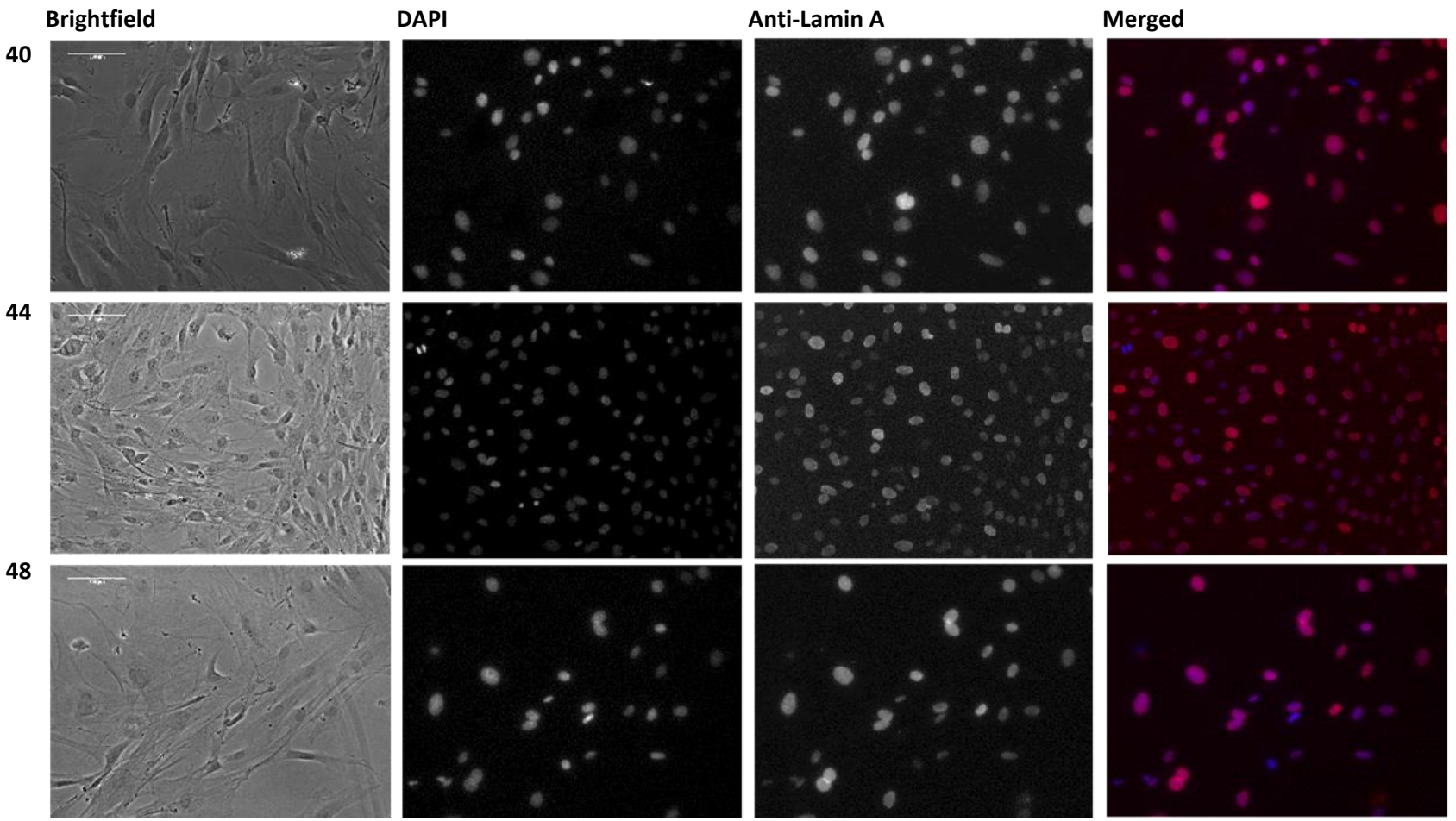

Figure 3.17. Representative images of circadian time-course immunocytochemistry in serum shock synchronised Per2::Luc primary myoblasts fixed every 4 hours between A. 24-36 and B. 40-48 hours. Representative images of PFA fixed Per2::Luc Brightfield, DAPI counterstain, Anti-lamin A, and DAPI and Anti-lamin A merged images. Cells were stained with anti-lamin A (1:5000; Sigma), anti-rabbit (1:200; Invitrogen), counterstained with DAPI (1:2000; Sigma) and images were collected on the Nikon Eclipse TE2000 at 20x**.**

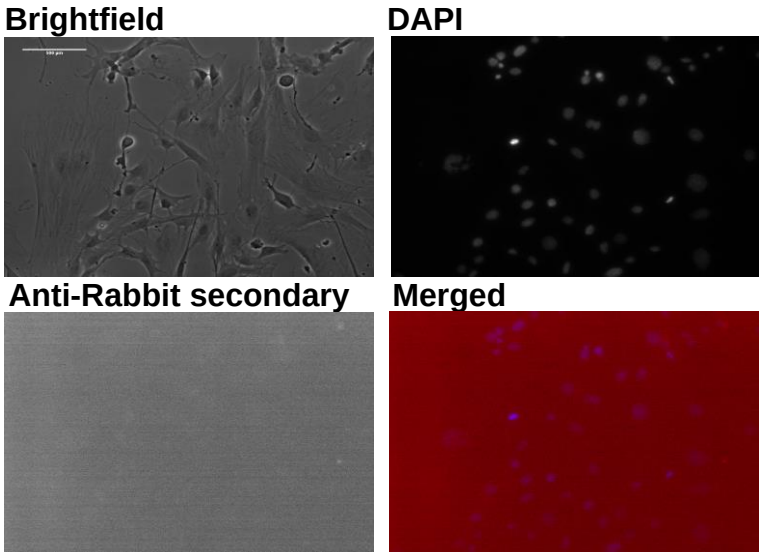

Figure 3.18. Representative Images of Primary Per2::Luc myoblasts primary negative control. Representative images of fixed, primary negative Per2::Luc myoblasts stained with anti-rabbit (1:200) and DAPI (1:2000). Images represent Brightfield, DAPI counterstain, anti-rabbit (with no primary lamin A to bind), and DAPI and anti-rabbit merged, images were collected on the Nikon Eclipse TE2000 at 20x.

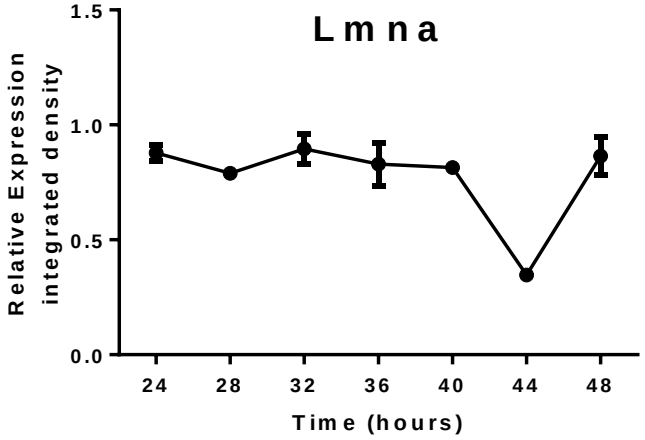

Figure 3.19. Relative Integrated Density of circadian time-course immunocytochemistry in serum shock synchronised Primary myoblasts, demonstrates oscillation in LMNA fluorescence. Values are normalised to the mean relative density of the first image in the 24-hour data set. Data plotted as mean± s.e.m.

Table 3.12. Primary myoblast immunocytochemistry Cosinor Periodogram analysis (Refinetti, 2016).

Period (h)	20.0
p value	0.4419
Acrophase (°)	-243
Amplitude	0.2149
Mesor	0.7502
Robustness (%)	55.8

3.4.4 Murine muscle samples exhibit free-running circadian oscillations in lamin A mRNA

3.4.4.1 Time-course data from Dark: Dark murine Gastrocnemius samples have circadian oscillations in lamin A mRNA expression

Mice housed in dark: dark conditions are removed from the zeitgeber light. Consequently, they have no time-keeping signals acting to entrain their circadian clocks with the environment and their clocks oscillate with 'free-running' rhythms, as the TTFL will continue to cycle. This can be observed in the expression of core clock genes themselves and through the 'output' of the clock, the downstream regulation that orchestrates behaviour and physiology. Here, the aim was to investigate whether *Lmna* expression continues to oscillate upon the removal of these external time-cues and 'free-run' with the core clock genes. Mice were housed in dark: dark conditions for 5 days prior to Gastrocnemius muscle sample collection at CT 2, 6, 10, 14, 18, and 22. Samples were analysed by qRT-PCR and normalised to *β-Actin*. *Lmna* expression peaked at CT 10 and slowly continued to increase up to CT 22, although Cosinor Periodogram analysis identified only 50.6% robustness (Figure 3.13; Table 3.10). Consistently, the *Lmna* expression pattern is in phase with the expression of the negative core clock genes *Per1*, *Per2*, and *Cry1* (Table 3.10, Cosinor Periodogram acrophase analysis *Lmna*, *Per1*, *Per2* and *Cry*: -302°, -249°, -246°, and -292°).

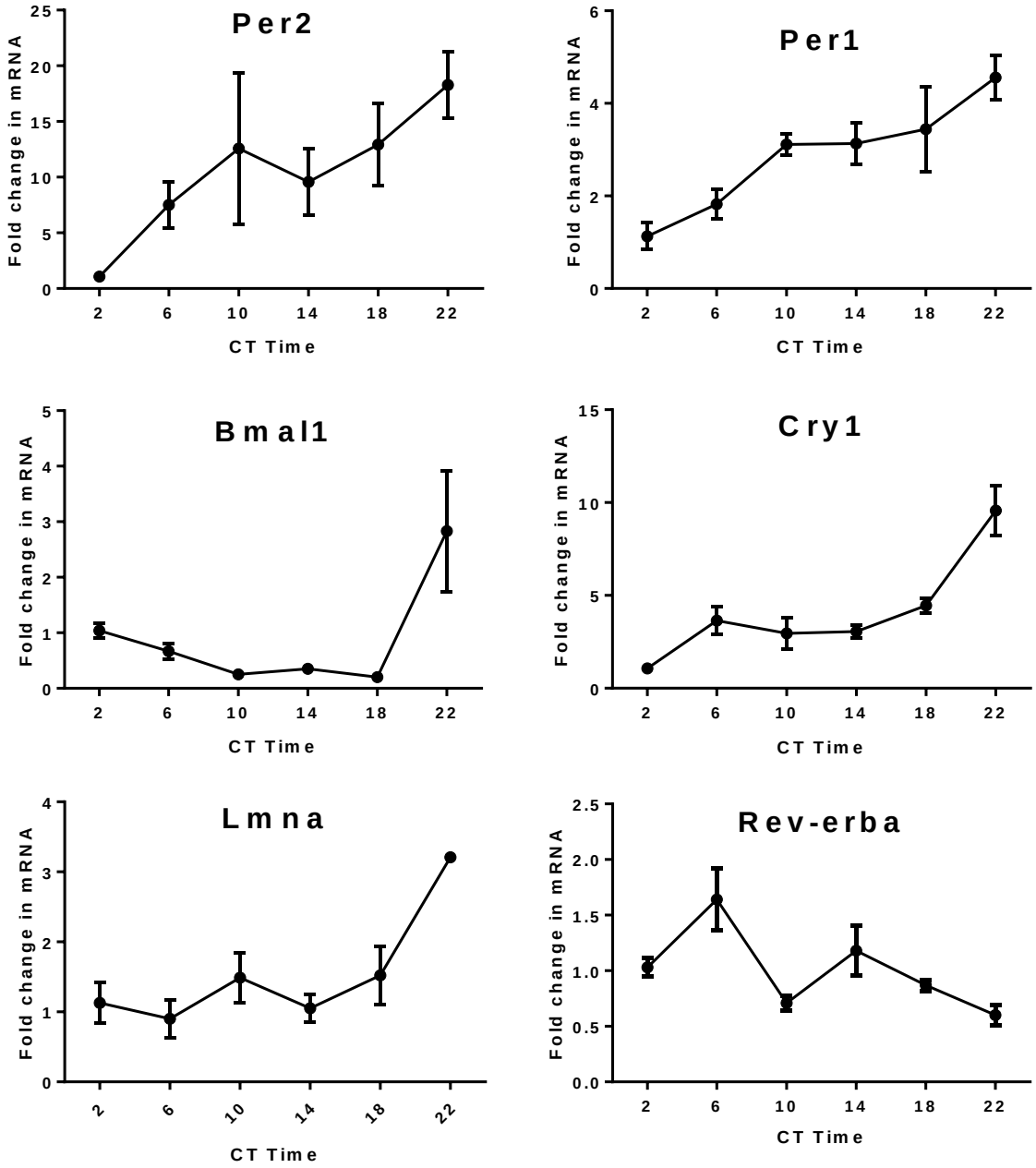

Figure 3.20. Circadian time-course of gene expression in Gastrocnemius muscle from wild-type C57/BL6 mice collected in dark: dark conditions, demonstrate oscillations in *Lmna* expression. Mice were housed in constant dark conditions for 5 days prior to sample collection and all collections were completed in red light conditions until the mice had been culled and their heads removed. Gastrocnemius muscle was dissected and RNA-later added to preserve the muscle prior to RNA extraction and processing. The expression of circadian genes was measured using qRT-PCR, analysed using the Pfaffl method (Pfaffl, 2001), normalised to *β-Actin* and shown relative to the 24-hour time point. *n*=3 and data were presented as mean± s.e.m.

Table 3.13. Gastrocnemius time-course qRT-PCR Cosinor Periodogram circadian analysis (Refinetti, 2016).

	Lamin	*Per1*	*Per2*	*Bmal1*	*Cry1*	*Rev-erbα*
Period (h)	26.0	26.0	26.0	26.0	26.0	26.0
p value	0.3477	0.2254	0.2656	0.2797	0.1361	0.6566
Acrophase (°)	-302	-249	-246	-347	-292	-84
Amplitude	0.7841	1.1963	5.2474	1.4035	3.5539	0.2876
Mesor	1.5983	2.8514	7.8024	1.2168	5.534	1.0275
Robustness (%)	50.6	63.0	73.4	72.0	86.5	34.4

3.4.5 Mouse Embryonic Fibroblast (MEF) cells exhibit low amplitude oscillations in lamin A mRNA that are lost when the circadian clock is abolished

3.4.5.1 Circadian time-course data demonstrates that WT MEFs reveal lamin A oscillations that are lost upon double knockout of Cry1 and Cry2

Cry1 and Cry2 are critical components forming part of the negative arm of the core circadian clock. To investigate whether molecular disruption of the circadian clock led to changes in lamin A oscillation, Cry1/Cry2 knockout MEFs were used. First, WT MEF cells were studied to determine whether they produce oscillations in lamin A mRNA expression. Next, whether these oscillations are lost upon double knockout of Cry 1 and 2 was determined. Circadian time-courses were collected for both cell types. Cells were synchronised by serum shock and after 24 hours, collected every 4 hours for 24 hours. The time-course samples were analysed by qRT-PCR and normalised to *β-Actin*. *Lmna* expression in the WT MEF time-course showed an oscillatory pattern of expression with a trough at 28 hours and a peak at 40 hours, Cosinor Periodogram analysis identified 84.1% robustness in the oscillation (Figure 3.21; Table 3.11 Cosinor Periodogram robustness analysis). Consistent with previous circadian time-course data, *Lmna* expression was in phase with *Per2* and antiphase to *Bmal1* expression (Table 3.11 Cosinor Periodogram acrophase analysis, *Lmna*, *Per2*, and *Bmal1*: -215°, -282°, and -79°). In the *Cry1* and *Cry2* double knockout time-course, *Lmna* expression lost this oscillatory behaviour, expression fluctuated around fold change of 3, and the Cosinor Periodogram robustness analysis decreased to 45.3% (Figure 3.21; Table 3.11). In addition, *Bmal1* expression and *Per2* expression were decreased and increased respectively, in comparison to expression from the WT MEF time-course (Figure 3.21). Interestingly, *Lmna* expression follows *Per2* expression upon double knock out of *Cry1* and *Cry2*, increasing from 1-1.4 fold change to 3-4 fold change (Figure 3.21). This supports earlier findings that *Lmna* expression is in-phase and linked to the expression of the clock genes in the negative arm: *Per2* and *Cry1*.

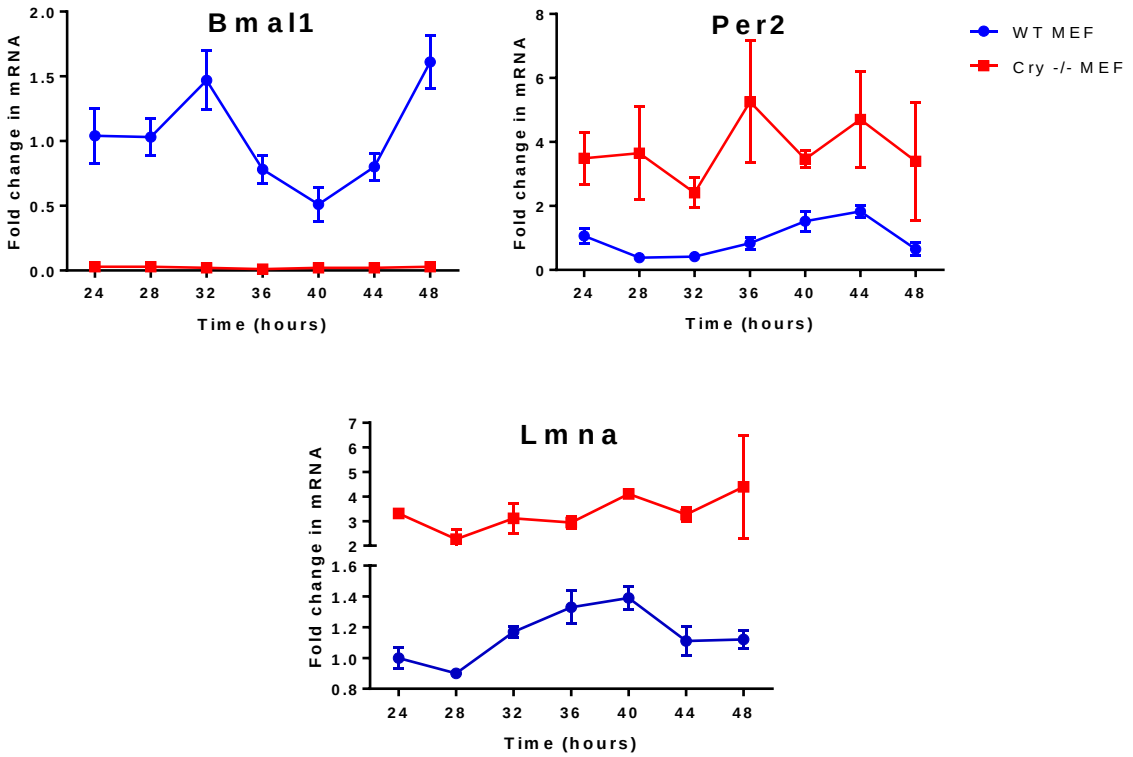

Figure 3.21. Circadian time-course of gene expression in serum shock synchronised WT and Cry1 and 2 knockout MEFs, demonstrate oscillations in *Lmna* expression in WT MEFs that is lost with Cry double knockout. Cells were synchronised by changing the media to 50% horse serum for 2 hours (DMEM supplemented with 50% HS, 2nM L-Glu, 0.1mg/mL P/S), they were then returned to normal DMEM media. After 24 hours, cells were collected every 4 hours for 24 hours in Purezol, circadian genes were measured using qRT-PCR, analysed using the Pfaffl method (Pfaffl, 2001), normalised to *β-Actin* and shown relative to the 24-hour time point. n=3 and data were presented as mean± s.e.m.

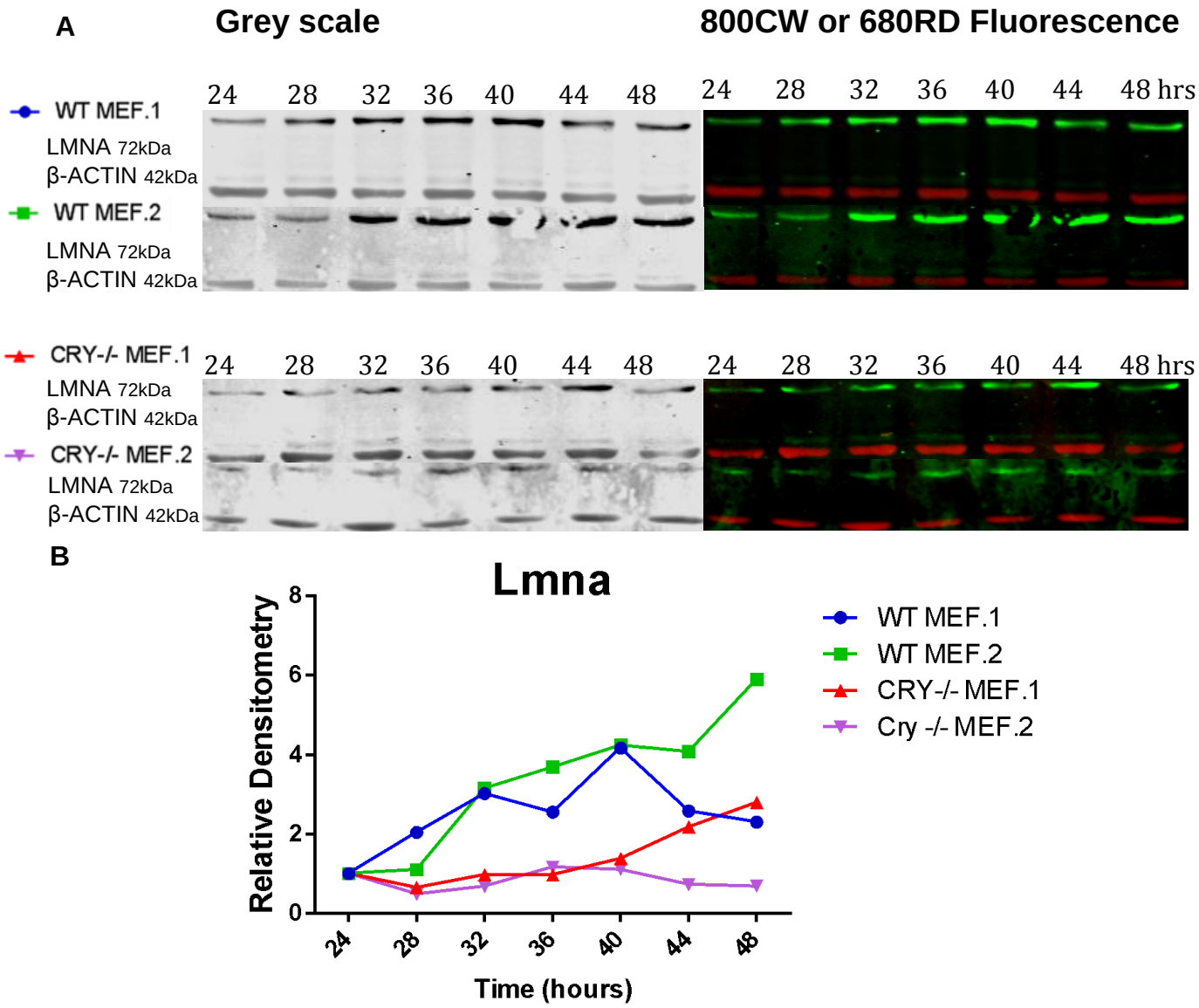

Figure 3.22. Representative Western blot images and protein densitometry traces of circadian time-course in serum shock synchronised WT and CRY1 and 2 -/- MEF cells, demonstrates oscillations in LMNA in WT MEFs that is lost on Cry double knockout. (A) Protein samples were ran on 10% acrylamide gels, transferred, and incubated with primary antibodies for anti-mouse Lmna (Sigma; 1:2000) and anti-rabbit β-Actin (Sigma; 1:2000) followed by secondary IRDye® antibodies for goat anti-rabbit 800CW and goat anti-mouse 680RD (Licor; 1:20000). (B) Densitometry values were calculated using the analysis software provided by Image Studio Lite Version 5.2. LMNA bands were normalised to β-ACTIN. Data were expressed as % change relative to the first time-point, n=3.

Table 3.14. WT and double CRY-/- MEF qRT-PCR Cosinor Periodogram circadian analysis (Refinetti, 2016).

		Lamin	*Per2*	*Bmal1*
WT MEF	Period (h)	24.4	22.7	20.0
	p value	0.0270*	0.0084*	0.0489*
	Acrophase (°)	-215	-282	-79
	Amplitude	0.2053	0.7534	0.5440
	Mesor	1.1668	0.9532	1.1366
	Robustness (%)	84.1	91.9	86.6
CRY $^{-/-}$ MEF	Period (h)	26.0	23.5	26.0
	p value	0.2994	0.5646	0.1923
	Acrophase (°)	-272	-253	-19
	Amplitude	0.6503	0.6533	0.2685
	Mesor	3.328	3.8040	0.6096
	Robustness (%)	45.3	25.0	66.7

Table 3.15. WT and double CRY-/- MEF LMNA western blot Cosinor Periodogram circadian analysis (Refinetti, 2016).

		1.	2.
WT MEF	Period (h)	26.0	26.0
	p value	0.3255	0.0384*
	Acrophase (°)	-168	-167
	Amplitude	1.0965	1.6723
	Mesor	2.5304	2.5892
	Robustness (%)	67.4	96.0
CRY $^{-/-}$ MEF	Period (h)	26.0	20.0
	p value	0.1507	0.0533
	Acrophase (°)	-261	-336
	Amplitude	0.1517	0.1102
	Mesor	0.2584	0.2689
	Robustness (%)	61.2	85.8

WT MEF protein samples analysed by western blotting demonstrated oscillations in LMNA protein with the first trace more robust than the second, and high amplitudes of 1.0965 and 1.6723 respectively (Figure 3.22; Table 3.12 Cosinor Periodogram amplitude and robustness analysis: 67.4% and 96%). When CRY1 and CRY2 was knocked-out, circadian time-course data showed low amplitude oscillations in LMNA protein but robustness remained at 61.2% and 85.8% (Figure 3.22; Table 3.12 Cosinor Periodogram robustness analysis and amplitude analysis: 0.1517 and 0.1102).

3.5 Discussion

Despite recent interest and research aimed at deciphering a clearer role for lamin A in laminopathy disease pathogenesis, how the different roles performed by lamin A may contribute to the disease phenotype is still unknown. This research aims to understand more about the regulation of lamin A, specifically in muscle cells, and investigate a potential link with the circadian molecular clock. By advancing the awareness of lamin A dynamics in muscle cells, one of the tissues largely affected in laminopathies, the role and responsibilities of lamin A can be better understood and may contribute to understanding whether a temporal aspect of regulation is currently being overlooked. Hence, the focus of this chapter was to explore whether temporal dynamics are involved in lamin A regulation in muscle cells.

Consistent with previous studies determining whether a gene and protein of interest oscillate with circadian rhythm, experiments began by observing circadian time-course qRT-PCR and Western blot data to study lamin A (Rohman, *et al*., 2005; Lin, *et al*., 2014; Pekovic-Vaughan, *et al*., 2014; Yang, *et al*., 2017). In addition, immunocytochemistry and quantification of LMNA fluorescence was utilised to investigate whether rhythmic protein expression could be observed in synchronised samples around the clock, as completed by Pekovic-Vaughan and colleagues when studying NRF2 rhythmicity (Pekovic-Vaughan, *et al*., 2014).

These results demonstrate that muscle cells have a circadian rhythmicity in *Lmna* expression and, although slightly less clearly, protein levels. Experiments utilised C2C12 cell-line murine myoblasts and myotubes, primary muscle myoblasts and myotubes, and murine muscle samples to confidently conclude that lamin A oscillates with a circadian rhythm in musculoskeletal tissues. Therefore, lamin A may be a downstream clock controlled gene. In addition, a circadian rhythm in lamin A mRNA and protein levels was identified in mouse embryonic fibroblasts (MEF) cells, and a loss of the molecular clock in these MEF cells- through *Cry1* and *Cry2* double knockout, resulted in a loss of this oscillatory lamin A expression.

Post-transcriptional regulation is an important factor in determining protein rhythmicity and, regardless of whether there is rhythmic mRNA transcription, co-ordinating the regulation of processes such as splicing, polyadenylation, and translation may permit oscillations in protein levels (Kojima, Shingle, and Green, 2011). Proteomic data from mouse liver samples revealed 20% of soluble proteins in the liver oscillated with a circadian rhythm, despite half of these proteins having no rhythmicity in mRNA transcription (Reddy, *et al*., 2006). Accordingly, processes such as splicing, polyadenylation, and translation are themselves subject to circadian control and resultantly, are important factors to consider when observing protein temporal dynamics (McGlincy, *et al*., 2012; Kojima, Sher-Chen, and Green, 2012; Lipton, *et al*., 2015). Protein data in this chapter revealed peaks and troughs in oscillatory LMNA protein levels that are generally in the same phase as the mRNA expression data. Therefore, in musculoskeletal tissues, it is most likely that other post-transcriptional mechanisms do not play a significant role in regulating lamin A protein production and rhythm.

Although data demonstrated rhythmic oscillations in *Lmna* expression, in order to conclude that the core clock controls this regulation further experiments are necessary. Future work may include comparing *Lmna* and circadian clock gene time-course oscillations from C2C12 myoblasts and myotubes, primary myotubes, and muscle to genes that are known not to oscillate in musculoskeletal cells. These data can further identify *Lmna* oscillations as potentially clock-controlled, and rule-out all genes within the musculoskeletal cell or tissue oscillating over a circadian time-course. In addition, further future studies may include utilising ChIP-seq, core clock siRNA or the production of a Lmna::Luciferase reporter construct. ChIP-seq data can be used to observe whether BMAL1:CLOCK or PER:CRY protein heterodimers associate with the *Lmna* promoter to up- or down-regulate its expression, as used in other circadian studies (Rey, *et al*., 2011). Furthermore, once identified, site-directed mutagenesis experiments within the *Lmna* promoter can be incorporated to identify the precise region by which BMAL1:CLOCK or PER:CRY associate with the promoter and regulate *Lmna* expression. These experiments would be consistent with previous work identifying core clock protein regulation of downstream genes (Rohman, *et al*., 2005). Additionally,

experiments may be completed using a core clock siRNA to eliminate the TTFL of the core clock and prevent any downstream circadian gene regulation, as completed by Dong *et al.* in lung epithelial cells and fibroblasts (Dong, *et al*., 2016). Transfection of a core clock siRNA into C2C12 muscle cells, and subsequent circadian time-course collection and analysis, should prevent rhythmicity. If lamin A transcription is regulated by the clock, this will produce a flat-line in *Lmna* expression; similar to the loss of oscillatory expression observed on comparison of the WT and Cry double knockout MEF circadian time-course data (Figure 3.21). Finally, further experiments may include the production of a Lmna::luciferase construct, a luciferase reporter protein driven by the *Lmna* promoter, using cloning techniques and subsequent insertion into a plasmid containing a CMV promoter (Geusz, *et al*., 1997). This plasmid can then be transfected into C2C12 cells and after synchronisation, *Lmna* expression observed through real-time bioluminescence imaging in the LumiCycle. Furthermore, this technique can further be used for simultaneous transfection with a core clock gene siRNA and the newly created Lmna::Luc plasmid; this will provide real-time analysis of core clock abolishment on *Lmna* expression (Vollmers, Panda, and DiTacchio, 2008).

An increasing body of data have demonstrated that the circadian clock is coupled to the cell cycle, through regulating and gating cell cycle progression (Nagoshi, *et al*., 2004; Feillet, *et al*., 2014, Bieler, *et al.,* 2014; Matsu-Ura, *et al*., 2016), although some studies have demonstrated a lack of circadian clock and cell cycle coupling (Pendergast, *et al*., 2010; Yeom, *et al.*, 2010). Given that lamin A regulates the cell cycle, and its levels increase and decrease with progression through the cell cycle, the data may be a consequence of oscillations in cell cycle progression. To ensure that this was not the case, FACS cell cycle analysis was used to study circadian time-courses of C2C12 myoblasts, synchronised by serum shock and Dexamethasone, as used in other studies researching circadian clock and cell cycle coupling (Ünsal-Kaçmaz, *et al*., 2005; Kowalska, *et al*., 2013; Laranjeiro, *et al*., 2018). Accordingly, FACS analysis circadian time-course data demonstrated only slight variations in G2/M residing cells, suggesting that cell cycle changes as the cause of lamin A mRNA expression and protein level oscillations can be excluded.

qRT-PCR traces from some musculoskeletal circadian time-course data do not show clear anti-phase relationships between *Per1*, *Per2*, and *Cry1*, and *Bmal1* expression; hence, the TTFL and coordinated up- and down-regulation of core clock genes may appear to be less accurate. However, the data are from cell culture experiments and, although each cell has a functioning core circadian clock, these cells are removed from the whole organism and are consequently lacking systemic cues. A study generating and observing real-time bioluminescence imaging of primary rat-1 fibroblast cells transfected with *Bmal1* and *Dbp* luciferase reporter constructs successfully produced oscillating traces (Yagita, *et al*., 2010). However, like some of the data in this chapter, these traces are almost but not clearly anti-phase in relationship (Yagita, *et al*., 2010). Although *in vitro* techniques for analysing circadian rhythms are simplified and permit rapid, cheaper, and highly controlled experiments, this simplified nature is also a weakness. The oscillating core clock in these cells is driven by general methods of synchronisation, and this includes coordinating a cellular response from many different growth factors. *In vitro*, these cells are likely to be absent of other essential systemic signals that act to ensure that tissues are homogenous. Moreover, the circadian clock is extremely sensitive and the artificial environmental conditions of *in vitro* experiments may result in perturbations of circadian rhythms. For example, research with cultures of astrocytes from Per2::Luc mice and Per1::Luc rats demonstrated that the circadian clock in cultured cells can be affected by very small fluctuations in temperature (Prolo, Takahashi, and Herzog, 2005). In contrast, recent research comparing the response of primary fibroblasts to temperature cycles with expected *in vivo* traces from within the organism concluded that single cell oscillators behave similarly to systemic tissue oscillators (Abraham, *et al*., 2018). Hence, cell culture core clock studies are a useful and widely used tool; however, they may not completely mimic systemic oscillations *in vivo*.

In order to account for this, future studies can incorporate additional whole organism studies. Time-course muscle samples can be collected from animal models and studied to observe mRNA and protein levels through qRT-PCR and Western blot analysis, respectively; mice are a widely used and versatile animal model in circadian studies (Eckel-Mahan and Sassone-Corsie, 2015). Through

collecting Gastrocnemius muscle circadian time-course samples from mice housed in dark: dark conditions, this research aimed to begin incorporating *in vivo* research. Dark: dark housing eliminates external stimuli and leaves only the endogenous, free-running circadian clock; qRT-PCR data demonstrated rhythmic behaviour in *Lmna* expression under these conditions (Figure 3.13).

Future research to develop and expand the studies in this chapter may include comparing these dark: dark traces with light: dark traces. Moreover, animal models harbouring disruptions to the molecular clock, such as *Bmal1*$^{-/-}$ and *Clock*$^{\Delta 19/\Delta 19}$ mice, may be used to determine whether rhythmic *Lmna* mRNA expression and protein levels persist once the core clock is abolished (Ihara, *et al*., 2017; Kondratov, *et al.*, 2006). A study by McDearmon *et al.* demonstrated that restoring the circadian clock in the muscle only of *Bmal1*$^{-/-}$ mice, restored the body weight and activity in these mice (McDearmon, *et al*., 2006). Utilising this experimental design, it would be interesting to observe if *Lmna* rhythmic expression was restored in the muscle of these mice, whereby the only functioning circadian clocks in the mouse model are within the muscle. In addition, to develop resources at a more affordable cost, future work may be adapted to include circadian time-course data from animal models such as Zebrafish and *Drosophila*; these models have been shown to be suitable for circadian studies (Vatine, *et al*., 2011; Tataroglu and Emery, 2014).

Previous research that is contradictory to these results are studies conducted to observe oscillatory gene expression and protein levels in cells and tissues that failed to identify lamin A, such as circadian time-course proteomics data from mouse liver samples (Mauvoisin, *et al*., 2014; Wang, *et al*., 2018). However, these studies may not have identified cyclical expression of lamin A as the regulation of lamin A by the circadian clock may be in a tissue-specific manner. As a result, lamin A may not be oscillating with a circadian rhythm in these liver samples. Conversely, previous research articles have also investigated circadian dynamics in samples from muscle but failed to identify rhythmic oscillations in lamin A. In 2007, the skeletal muscle circadian transcriptome was identified and 215 transcripts were found to oscillate with a circadian rhythm (McCarthy, *et al*., 2007). The

Lmna transcript was not identified as having oscillatory expression over the 48 hour circadian time-course of muscle samples (McCarthy, *et al*., 2007). Additionally, Zhan *et al*. investigated transcriptional circadian oscillations across 12 mouse organs, including skeletal muscle, over time by RNA-seq, and the *Lmna* transcript was not identified (Zhang, *et al*., 2014). The lack of lamin A identification in these studies may be due to the microarray and RNA-seq approaches that are used not being sensitive enough to detect significant oscillation in the *Lmna* transcript when statistical tests have to incorporate multiple comparisons.

Conversely, these results are supported by previous research undertaken to study potential links between the nuclear envelope and circadian clock regulation. Lin *et al*. began observing whether proteins of the nuclear envelope oscillate with a circadian rhythm, and identified rhythmic mRNA and protein in MAN1, LBR and lamin B1 in human osteosarcoma U2OS cells; MAN1 contains the LEM domain and subsequently binds to lamin A/C through BAF (Lin, *et al*., 2014; Margalit, *et al*., 2005). In addition, recent research by Wang and colleagues completed proteomic circadian time-course screens in mouse liver samples and emerin was identified in a screen for proteins that form rhythmic nuclear complexes (Wang, *et al*., 2017a). In this regard, nuclear proteins can be subject to dynamic circadian clock control through regulation of their transcript and proteins levels, and by regulation of their complex formation and activity.

Furthermore, a recent study by Zhao and colleagues identified circadian oscillations in the nuclear lamina interaction and organisation of the genome; consequently, this regulates gene expression of respective genes re-located to or released from the nuclear periphery (Zhao, *et al*., 2015). In muscle cells, the nuclear lamina interacts with and represses muscle gene-specific promoters important for differentiation- such as MyoD and Myogenin, and releases these promoters upon induction of differentiation (Athar and Parnaik, 2015). Thus, this work demonstrates how the circadian core clock can regulate lamin A activity and supports the research hypothesis that this may be an important factor in muscle maintenance and development.

3.6 Conclusion

In conclusion, this research demonstrates a circadian rhythm in the expression of lamin A mRNA and protein in muscle myoblasts and myotubes. As the phenotype of muscle-wasting and muscular defects surrounding laminopathy patients are still misunderstood, these temporal dynamics may be an important missing factor. Further investigation into whether these oscillations are clock controlled may contribute to furthering the understanding of specific roles played by lamin A within the nucleus.

4 Lamin A regulates the expression of the core circadian clock genes

4.1 Introduction

4.1.1 The Molecular Clock Mechanism

Across many different tissues, the molecular clock temporally regulates downstream genes in a tissue-specific manner, enhancing gene expression in accordance with exact conditions required by each tissue respectively (Buhr and Takahashi, 2013). In skeletal muscle, the circadian clock is an important factor in regulating myogenesis and differentiation; the transcription factors *MyoD* and *Myogenin* are both regulated by the circadian clock (Andrews, *et al*., 2010; Shavlakadze, *et al*., 2013). The circadian molecular clock is composed of a transcriptional translational feedback loop (TTFL) of core clock proteins: BMAL1, CLOCK, PER1, PER2, and CRY1, with auxiliary or stabilising loops such as REV-ERBα and RORA (Buhr and Takahashi, 2013). The BMAL1:CLOCK heterodimer is the positive arm of the loop and upregulates the expression of *Per1*, *Per2*, and *Cry1* (Gekakis, *et al*., 1998; Kume, *et al*., 1999; Yoo, *et al*., 2005). The negative arm of the loop is formed of PER:CRY, which feeds-back to repress the expression of *Bmal1* and *Clock* – completing the loop (Griffin, et al., 1999; Kume, et al., 1999; Sato, et al., 2006). The auxiliary loops function as extra mechanisms of feedback regulation; they provide further co-ordination of the core clock proteins and ensure that the molecular clock remains at 24 hours (Cho, *et al*., 2012). An example of these robust mechanisms includes the casein kinases CKIε and CKIδ. During the night, CKIε and CKIδ phosphorylate PER which is targeted for degradation; during the day, CKIε and CKIδ phosphorylate PER:CRY and enable its translocation into the nucleus (Keesler, *et al*., 2000; Akashi, *et al*., 2002). CKIε and CKIδ themselves are regulated by Protein Phosphatases 5 and 1 (PP5 and PP1), safeguarding the levels of these CKI kinases to ensure that the initiation of translocation or degradation occurs at the correct time of day (Lowrey, *et al*., 2000). These fine-tuning mechanisms keep the molecular clock in synch in different tissues, ensuring

there is coordinated downstream clock-controlled gene regulation. Disrupted circadian rhythms within mice and humans are linked to premature ageing as well as diseases such as cancer, cardiovascular diseases, and diabetes (Dai, *et al*., 2011; Lamia, Storch, and Weitz, 2008; Gale, *et al*., 2011). In muscle, *Bmal*$^{-/-}$ and *Clock*$^{\Delta 19/\Delta 19}$ mutant mice exhibit defects in muscle development, maintenance, and function (Andrews, *et al*., 2010; Kondratov, *et al*., 2006). Therefore, these robust, extra mechanisms are an important 'fail-safe' in ensuring that these physiologically essential biological rhythms are synchronised with the external environment.

4.1.2 Bidirectional regulation of the Molecular Clock

Proteins within a mechanism that acts to regulate the circadian clock are often under circadian regulation themselves; this ensures that temporally, the regulation acting on the clock only occurs during correct periods of the circadian molecular cycle. In accordance, no repression or activation can occur out of synchronisation with the core clock. One example is the nuclear orphan receptors REV-ERBα and RORα; these two proteins act together, with opposing roles, to form a stabilising loop and ensure that *Bmal1* remains rhythmically expressed (Preitner, *et al*., 2002; Sato, *et al*., 2004). REV-ERBα and RORα repress and stimulate *Bmal1* expression, respectively. In this regard, *Bmal1* expression is at a trough when REV-ERBα is highly active, and is at its peak expression when RORα is active and when *Rev-erbα* expression is at a trough (Ueda, *et al*., 2002; Triqueneaux, *et al*., 2004; Sato, *et al*., 2004). As the BMAL1:CLOCK heterodimer drives the expression of these regulatory proteins, these two mechanisms of regulation bi-directionally regulate one another; *Rev-erbα* expression is stimulated by BMAL1:CLOCK and trans-repressed by PER:CRY (Preitner, *et al*., 2002). Although this feedback loop maintains rhythmic expression of *Bmal1*, this loop is not essential for appropriate driving of the core TTFL (Liu, *et al*., 2008). The research in this thesis focuses on whether nuclear proteins regulate molecular clock components and whether a bi-directional regulation loop may exist between lamin A and the core clock proteins.

4.2 Nuclear Lamina

4.2.1 A role for the Nuclear Lamina in Molecular Clock Regulation

The nuclear lamina is a structural meshwork formed by A- and B-type lamins and contains integral membrane proteins; it underlies the nuclear envelope and associates with chromatin and nuclear proteins (Foisner, 2001; Gruenbaum, *et al*., 2003). The integral membrane proteins at the nuclear lamina include emerin, LBR, LAP, MAN1, and nurim, and these proteins increase chromatin interactions, reinforce mechanical support, and regulate protein localisation and activity (Naetar, Ferraioli, and Foisner, 2017).

Within the nucleus, the nuclear lamina provides structural support and regulates processes such as DNA transcription, genome organisation, cell cycle progression, and mechanotransduction pathways (Lenz-Böhme, *et al*., 1997; Markiewicz, *et al*., 2002a; Ivorra, *et al*., 2006; Bridger, *et al*., 2007; Swift, *et al*., 2013). Research has identified that all of these nuclear processes are under regulation by the circadian clock and benefit from temporal optimisation (Yang, *et al*., 2017; Trott and Menet, 2018; Kim, *et al*., 2018; Gaucher, Montellier, and Sassone-Corsi, 2018). Moreover, these processes have the potential to be involved in mechanisms that provide feedback regulation to the molecular clock.

Recent research has identified a link between nuclear proteins and circadian clock regulation, the integral membrane proteins MAN1 and LBR, and lamin B1 oscillate with a circadian rhythm (Lin, *et al*., 2014). Hence, this research demonstrated that proteins within the nucleus can be subject to dynamic temporal regulation by the circadian clock; consistent with research in the previous chapter that identified circadian oscillations in lamin A mRNA and protein levels in musculoskeletal cells. In addition, MAN1 binds to the *Bmal1* promoter and up-regulates *Bmal1* expression, demonstrating bi-directional regulation between a nuclear integral membrane protein and a core clock protein (Lin, *et al*., 2014). Furthermore, recent studies have observed a relationship between the nuclear lamina and the circadian clock. Zhao *et al.* identified circadian timing in the formation of nuclear lamina interactions with the genome. Around the clock, multiple ADP-ribose polymerase 1 (PARP1) and the

transcription factor CTCF relocate genes to the nuclear periphery where they interact with the nuclear lamina through Lamina-Associated Domains (LADs) (Zhao, *et al*., 2015; Zullo, *et al*., 2012). Subsequently, genes relocated to the nuclear periphery become transcriptionally silenced. This highlights a mechanism of direct gene regulation by the nuclear lamina through chromatin interactions that incorporates dynamic, temporal regulation around the clock.

Indeed, research is beginning to define a relationship between the circadian molecular clock and processes within the nucleus – including those with direct interactions with the nuclear lamina. In this regard, the nuclear lamina and lamin A as a tool for regulating gene expression in a circadian manner warrants further investigation. As the previous chapter demonstrated circadian oscillations in the production of lamin A mRNA and protein levels in musculoskeletal cells, and as bi-directional feedback regulation is a common mechanism amongst circadian regulatory pathways, the next aim was to observe whether lamin A is capable of providing feedback regulation to the circadian clock. It was predicted that lamin A exerts time-of-day dependent feedback regulation on the core proteins of the circadian molecular clock.

4.3 Hypothesis and Aims

4.3.1 Hypothesis

Our hypothesis was that varying lamin A levels modulates the circadian molecular clockwork by feedback regulation on clock gene promoters. To this end, this chapter will utilise loss-of and gain-of lamin A function experiments (lamin A siRNA and lamin A plasmid overexpression to knockdown and overexpress lamin A, respectively) in a skeletal muscle myoblast cell line (C2C12 cells). Downstream experiments will involve gene/protein expression analysis using qRT-PCR and Western blotting as well as real-time bioluminescent imaging and dual-reporter luciferase assays to assess whether clock gene expression, rhythmicity, and promoter activity are altered in response to these lamin A protein manipulations.

4.3.2 Aims

- Investigate the effects of loss-of and gain-of lamin A function (lamin A knockdown and overexpression, respectively) on clock gene expression and temporal dynamics in C2C12 myoblast cells.
- Determine the effects of lamin A knockdown and overexpression in C2C12 myoblasts stably transfected with clock luciferase reporters using real-time bioluminescence imaging of circadian clock gene cycles.
- Establish the effects of lamin A protein overexpression, alone or synergistically with clock transcription factors, on clock promoter regulation using dual luciferase reporter assays.

4.4 Results

4.4.1 Lamin A knockdown in C2C12 myoblasts decreases clock gene expression

4.4.1.1 Lamin A knockdown in C2C12 myoblasts using targeted siRNA

To begin investigating whether lamin A is involved in regulation of the circadian molecular clock, validated *Lmna* siRNA was used to knockdown LMNA and the response in circadian clock gene expression was observed. C2C12 myoblasts were grown in 12-well plates and at 60% confluency, were transfected with 5nM validated lamin A siRNA or scrambled siRNA as a negative control (Qiagen) using Dharmafect reagent (Dharmacon). Samples were analysed for gene or protein expression by qRT-PCR and Western blotting respectively, both normalised to β-actin. A successful lamin A knockdown at the mRNA and protein level was demonstrated in C2C12 myoblast cells (Figure 4.1 and 4.2, unpaired t-test, p≤0.0001 and p≤0.01).

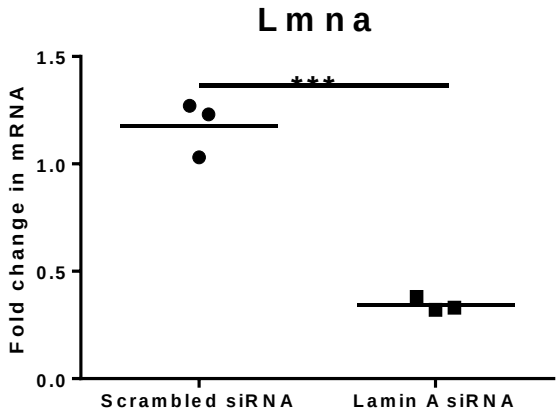

Figure 4.1. Lamin A knockdown in C2C12 myoblasts transfected with validated lamin A siRNA compared to scrambled control. C2C12 myoblasts were seeded into a 12-well plate and transfected at 60% confluency. Myoblasts were incubated for 48 hours before collection and RNA extraction. *Lmna* mRNA was analysed by qRT-PCR using the Pfaffl method and normalised to house-keeping gene *β-actin* (Pfaffl, 2001). Data were expressed as fold change relative to scrambled control which was expressed as 1 and presented as means (unpaired t-test, ***p≤0.0001, three independent experiments n=3).

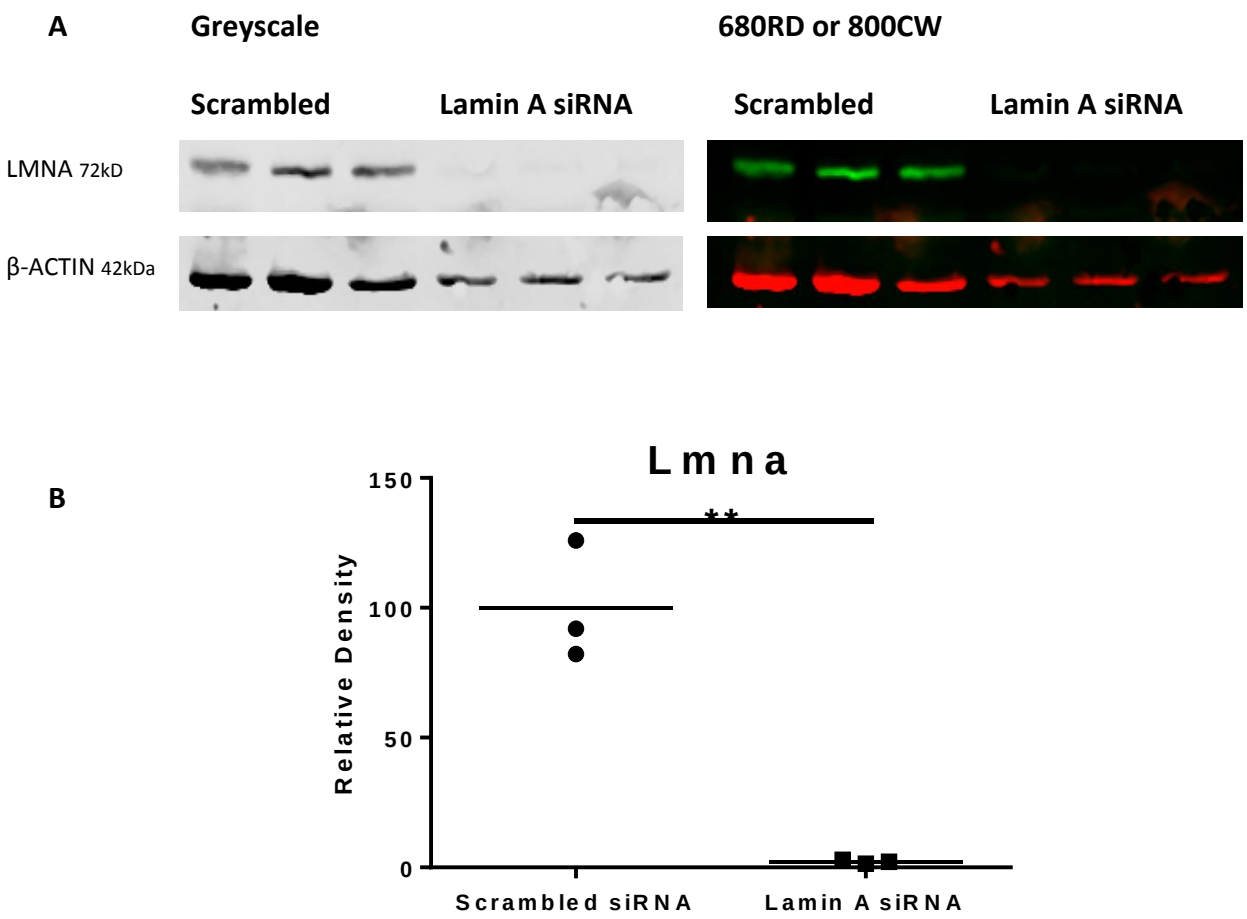

Figure 4.2. Representative Western blot images and protein densitometry analysis of lamin A protein expression in C2C12 myoblasts transfected with lamin A siRNA or scrambled control, demonstrates a knockdown of LMNA. (A) Protein samples were ran on 10% acrylamide gels, transferred, and incubated with primary antibodies for anti-mouse Lmna (Sigma; 1:2000) and anti-rabbit β-Actin (Sigma; 1:2000) followed by secondary IRDye® antibodies for goat anti-rabbit 800CW and goat anti-mouse 680RD (Licor; 1:20000). (B) Densitometry values were calculated using the analysis software provided by Image Studio Lite Version 5.2. LMNA bands were normalised to β-ACTIN. Data were expressed as % change relative to scrambled which was expressed as 100 and presented as means (unpaired t-test, **p≤0.01, three independent experiments n=3).

4.4.1.2 Lamin A knockdown in C2C12 myoblasts significantly decreases circadian gene expression

To investigate whether lamin A knockdown impacts on the expression of the circadian clock genes in C2C12 myoblasts, this study focused on the expression of the core clock genes belonging to the positive arm (*Bmal1*), negative arm (*Per1*, *Per2*, and *Cry1*), and the auxiliary loop (*Rev-erbα*). RNA samples were analysed by qRT-PCR for circadian clock genes and normalised to *β-Actin*. Lamin A knockdown led to a significant decrease in the expression of the circadian clock genes that were investigated; an unpaired t-test identified this decrease to be $p \leq 0.01$ for *Per1*, *Per2*, *Cry1*, and *Rev-erbα*, and $p \leq 0.05$ for *Bmal1* (Figure 4.3).

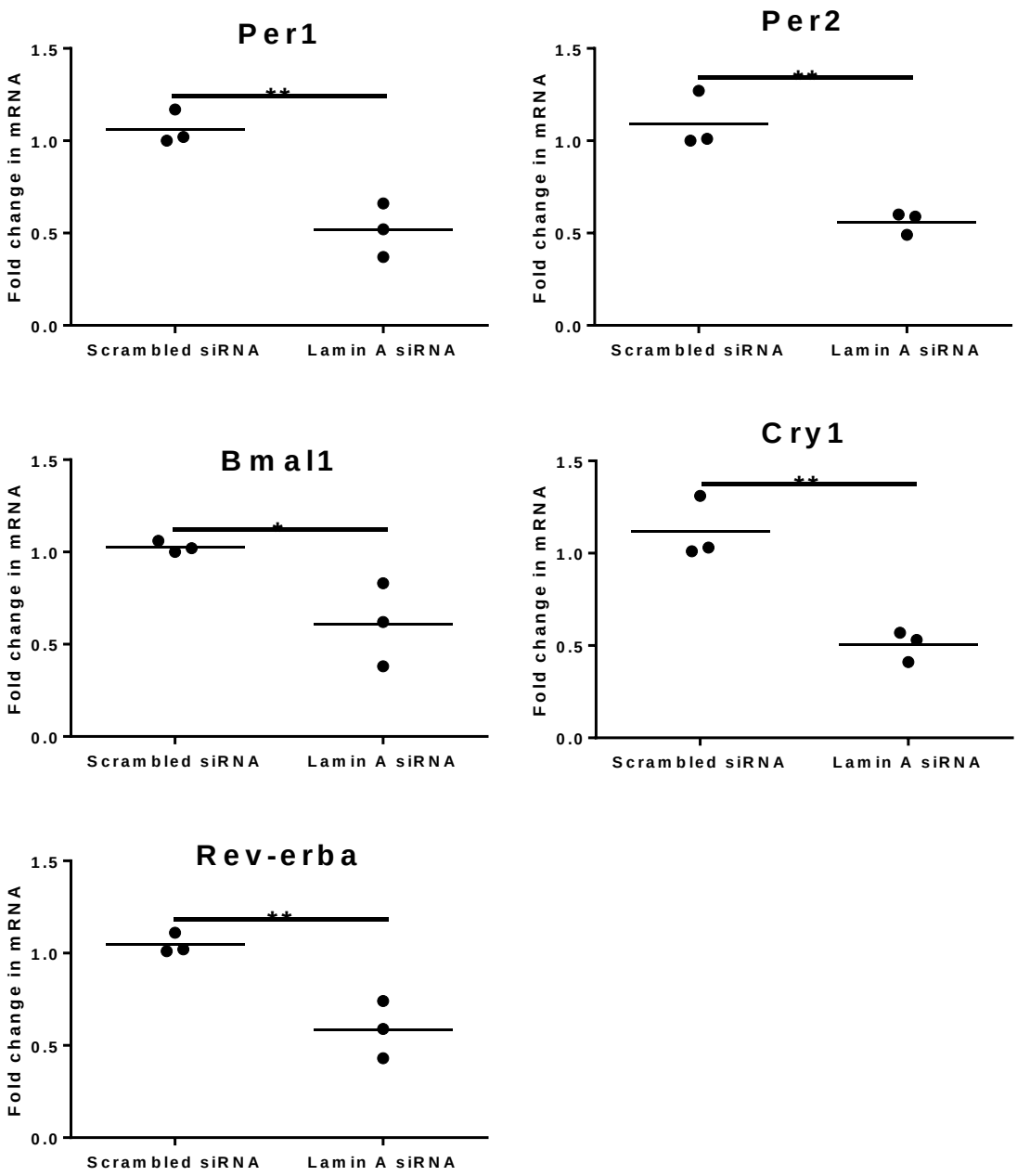

Figure 4.3. Circadian clock gene expression in C2C12 myoblasts transfected with lamin A siRNA compared to scrambled control. C2C12 myoblasts were seeded into a 12-well plate and at 60% confluency and transfected with 5nM lamin A siRNA or scrambled control. Myoblasts were incubated for 48 hours before collection and RNA extraction. Circadian clock gene mRNA was analysed by qRT-PCR using the Pfaffl method and normalised to *β-Actin* (Pfaffl, 2001). Data were expressed as fold change relative to scrambled which was expressed as 1 and presented as means (unpaired t-test, *p≤0.05, **p≤0.01, three independent experiments n=3).

4.4.1.3 Lamin A knockdown is sustained in C2C12 myoblasts after synchronisation for 48 hours

To further investigate the effect of lamin A knockdown on circadian clock gene cycles, the next aim was to collect a circadian time-course of C2C12 myoblasts transfected with validated lamin A siRNA or scrambled control, and clock-synchronised by 100nM Dexamethasone for 1 hour. Samples were collected every 4 hours for 24 hours over 7 time-points (starting from 24hrs after Dexamethasone synchronisation) and analysed for gene and protein expression by qRT-PCR and Western blotting, respectively, both normalised to β-Actin. Data demonstrated a sustained knockdown of lamin A over the duration of the circadian time-course in comparison to the scrambled control samples (Figures 4.4 and 4.5, two-way ANOVA: *p≤0.05, **p≤0.01, ***p≤0.001, and ****p≤0.0001).

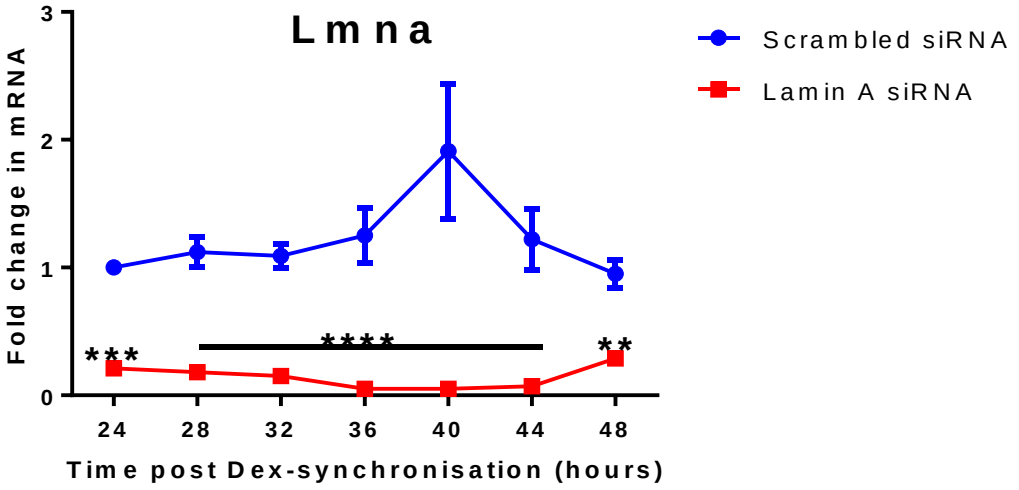

Figure 4.4. Circadian time-course of lamin A expression in Dexamethasone synchronised C2C12 myoblasts transfected with validated lamin A siRNA or scrambled control, demonstrates sustained knockdown of *Lmna* expression. C2C12 myoblasts seeded into 12-well plates, at 60% confluency, were transfected with 5nM lamin A siRNA or scrambled control. 24 hours after transfection, they were synchronised through the addition of 100nM Dexamethasone for 1 hour and after 24 hours, cells were collected every 4 hours for 24 hours (time-points 24-48hrs). *Lmna* expression was analysed by qRT-PCR using the Pfaffl method and normalised to *β-Actin* (Pfaffl, 2001). Data were expressed as fold change relative to scrambled control which was expressed as 1 and presented as means± s.e.m (two-way analysis of variance (ANOVA), **p≤0.01, ***p≤0.001, and ****p≤0.0001, three independent experiments n=3).

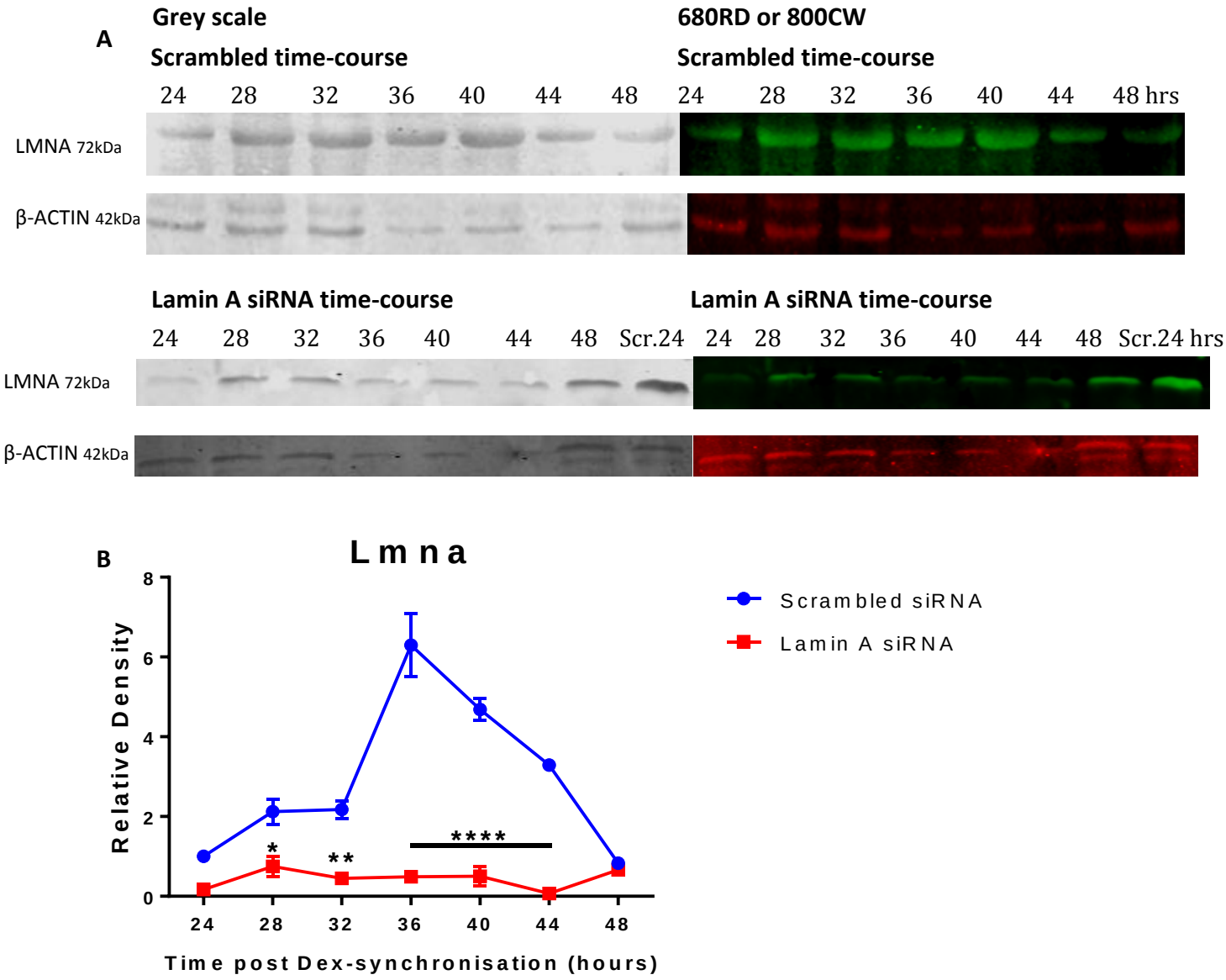

Figure 4.5. Representative Western blot images and protein densitometry analysis of circadian time-course in synchronised C2C12 myoblasts transfected with lamin A siRNA or scrambled control. (A) Protein samples were ran on 10% acrylamide gels, transferred and blotted against primary antibodies for anti-mouse Lmna (Sigma; 1:2000) and anti-rabbit β-Actin (Sigma; 1:2000) followed by secondary IRDye® antibodies for goat anti-rabbit 800CW and goat anti-mouse 680RD (Licor; 1:20000). (B) Densitometry values were calculated using the analysis software provided by Image Studio Lite Version 5.2. LMNA bands were normalised to β-ACTIN. Data were expressed as a fold change relative to scrambled which was expressed as 1 and presented as means± s.e.m (two-way ANOVA, *p≤0.05, **p≤0.01, ****p≤0.0001, n=3).

4.4.1.4 Time-course data from synchronised C2C12 myoblasts reveals that lamin A knockdown supresses rhythmic clock gene expression

Circadian time-course of synchronised C2C12 myoblast samples with a sustained knockdown of lamin A were further analysed by qRT-PCR for rhythmic clock gene expression and normalised to *β-Actin*. On comparison with scrambled control samples, circadian clock gene expression over 24 hours was supressed. There was a significant decrease in expression at the 44-hour time-point for *Per1*, *Bmal1*, and *Cry1*, as well as at 40 and 44-hour time-points for *Per2* (Figure 4.6, two-way ANOVA: $p \leq 0.001$, $p \leq 0.001$, and $p \leq 0.0001$, and $p \leq 0.05$ and $p \leq 0.001$). Interestingly, the rhythmic expression of the auxiliary gene *Rev-erbα* was not changed throughout the time-course, compared to the scrambled control (Figure 4.6).

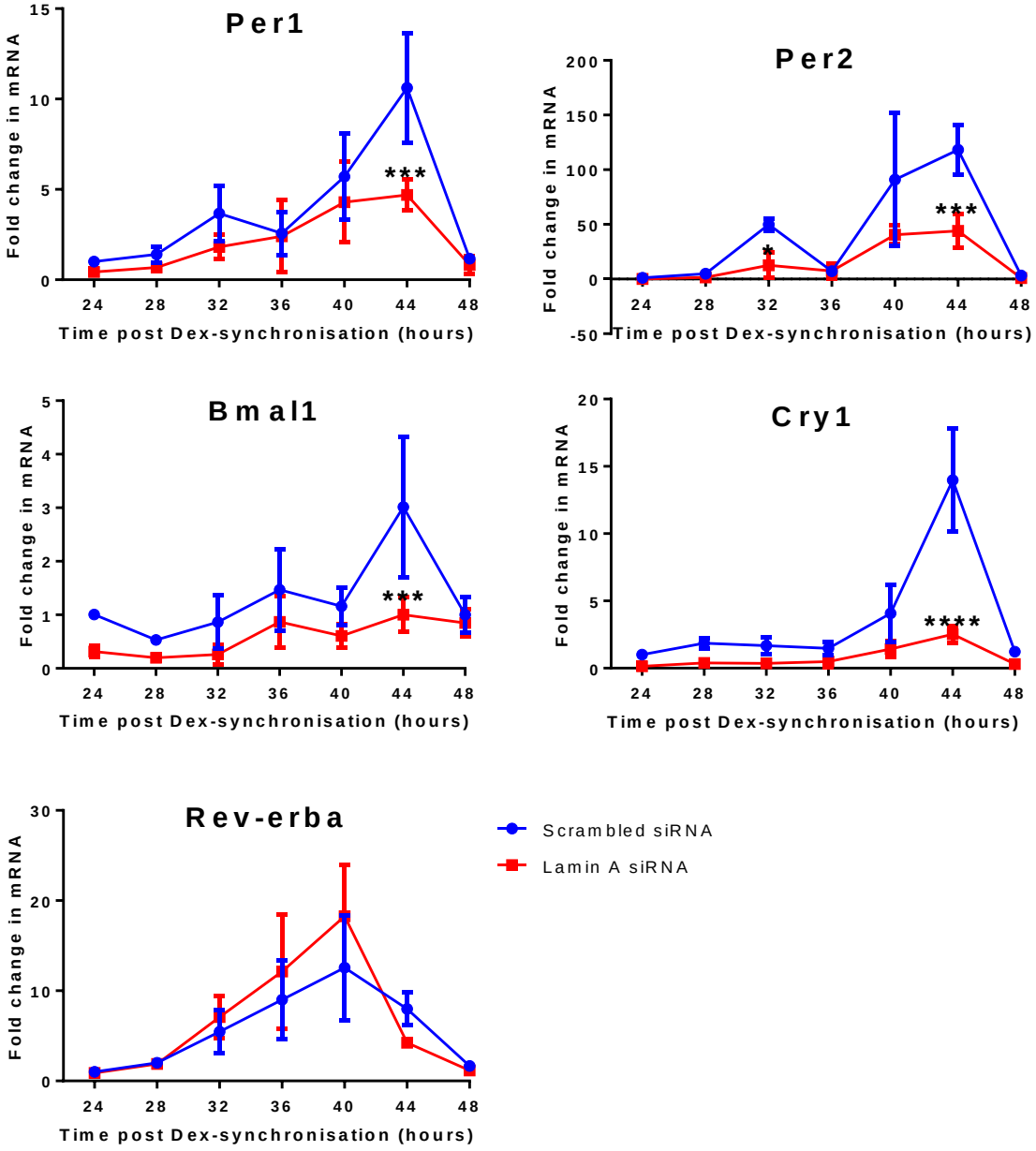

Figure 4.6. Circadian time-course of clock gene expression in Dexamethasone synchronised C2C12 myoblasts with a sustained knockdown of lamin A compared to scrambled control. C2C12 myoblasts seeded into a 12-well plate at 60% confluency were transfected with 5nM validated lamin A siRNA or scrambled control and incubated for 24 hours before synchronisation with 100nM Dexamethasone for 1 hour. 24 hours post-synchronisation, cells were collected every 4 hours for 24 hours for RNA extraction. Circadian clock gene mRNA was analysed by qRT-PCR using the Pfaffl method and normalised to *β-Actin* (Pfaffl, 2001). Data were expressed as a fold change relative to scrambled which was expressed as 1 and presented as means± s.e.m (two-way ANOVA, *p≤0.05, ***p≤0.001, ****p≤0.0001, three independent experiments n=3).

4.4.2 Emerin overexpression in myoblasts with lamin A knockdown increases clock gene expression

4.4.2.1 Simultaneous lamin A knockdown and overexpression of Lamin-binding partner Emerin

The lamin A binding partner emerin has an inter-relationship with lamin A; lamin A tethers emerin at the nuclear lamina and, through LEM and LADs domains, acts as a scaffold to regulate chromatin and transcription factor positioning and subsequent activity (Vaughan, *et al*., 2001; Wagner and Khrone, 2007; van Steensel and Belmont, 2017). In this regard, the next aim was to overexpress emerin in myoblasts knocked-down for lamin A, and to observe whether this rescues changes in clock gene expression. C2C12 myoblasts were neo-transfected with 5nM of validated lamin A siRNA and 1ug of either GFP only control or GFP emerin plasmid (Zuleger, *et al*., 2011). Cells were collected after 42-hour incubation and mRNA levels for *Lmna* and *Emd* were analysed by qRT-PCR and normalised to *β-Actin*. *Lmna* expression was significantly increased following emerin over-expression in myoblasts with a knockdown of lamin A (Figure 4.7, unpaired t-test, $p \leq 0.01$). The expression of *Emerin* was significantly increased in myoblasts with combined emerin over-expression and lamin A knockdown in comparison to myoblasts transfected with lamin A siRNA and GFP only control (Figure 4.7, unpaired t-test, $p \leq 0.05$).

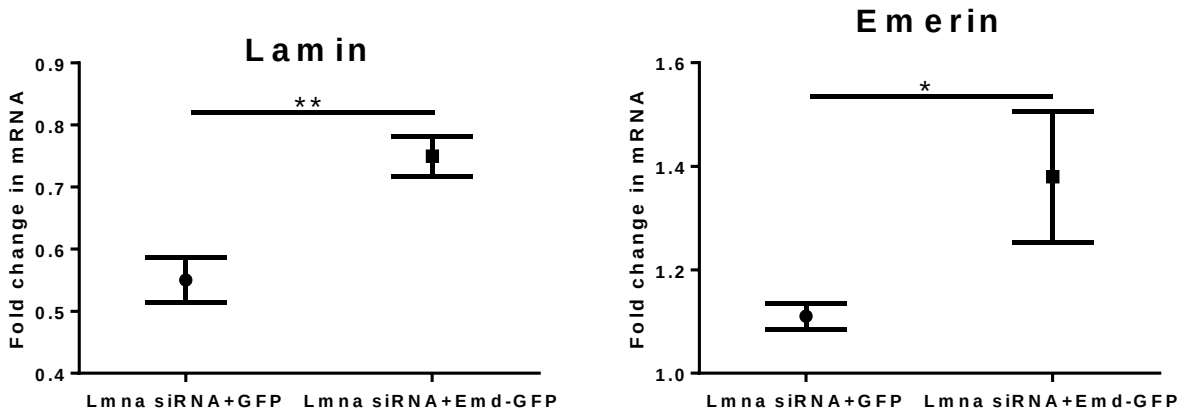

Figure 4.7. Simultaneous knockdown of lamin A expression and overexpression of emerin in C2C12 myoblasts. C2C12 myoblasts were neotransfected with 5nM lamin A siRNA together with 1ug emerin plasmid or GFP-only control plasmid. Cells were incubated for 42 hours before collection. *Lmna* and *Emd* mRNA was analysed by qRT-PCR using the Pfaffl method and normalised to *β-Actin* (Pfaffl, 2001). Data were expressed as a fold change relative to GFP control which was expressed as 1 and presented as means± s.e.m (unpaired t-test, *p≤0.05, **p≤0.01, n=3).

4.4.2.2 Emerin overexpression in C2C12 myoblasts with lamin A knockdown rescues clock gene expression

To investigate whether emerin overexpression can rescue clock gene expression, the next aim was to analyse clock gene expression in C2C12 myoblasts transfected with validated lamin A siRNA and 1µg of GFP only or emerin plasmids. Samples were analysed for gene expression by qRT-PCR and normalised to *β-Actin*. Myoblasts transfected with lamin A siRNA and emerin plasmid revealed a significant up-regulation in *Per1*, *Per2,* and *Rev-erbα* expression compared to myoblasts transfected with lamin A siRNA/GFP only control (Figure 4.8, unpaired t-test $p \leq 0.05$). Alternatively, there was no significant change in *Bmal1* or *Cry1* expression (Figure 4.8). This suggests that emerin has a positive effect on clock gene expression. However, the rescue in *Per1*, *Per2,* and *Rev-erbα* expression may be due to the increase in *Lmna* observed with overexpression of emerin. To determine whether emerin rescues circadian clock gene expression in the absence of *Lmna*, future work may include overexpressing emerin in *Lmna* mutant cells, such as DCM mutant mouse embryonic fibroblasts, and observing the response in circadian clock gene expression.

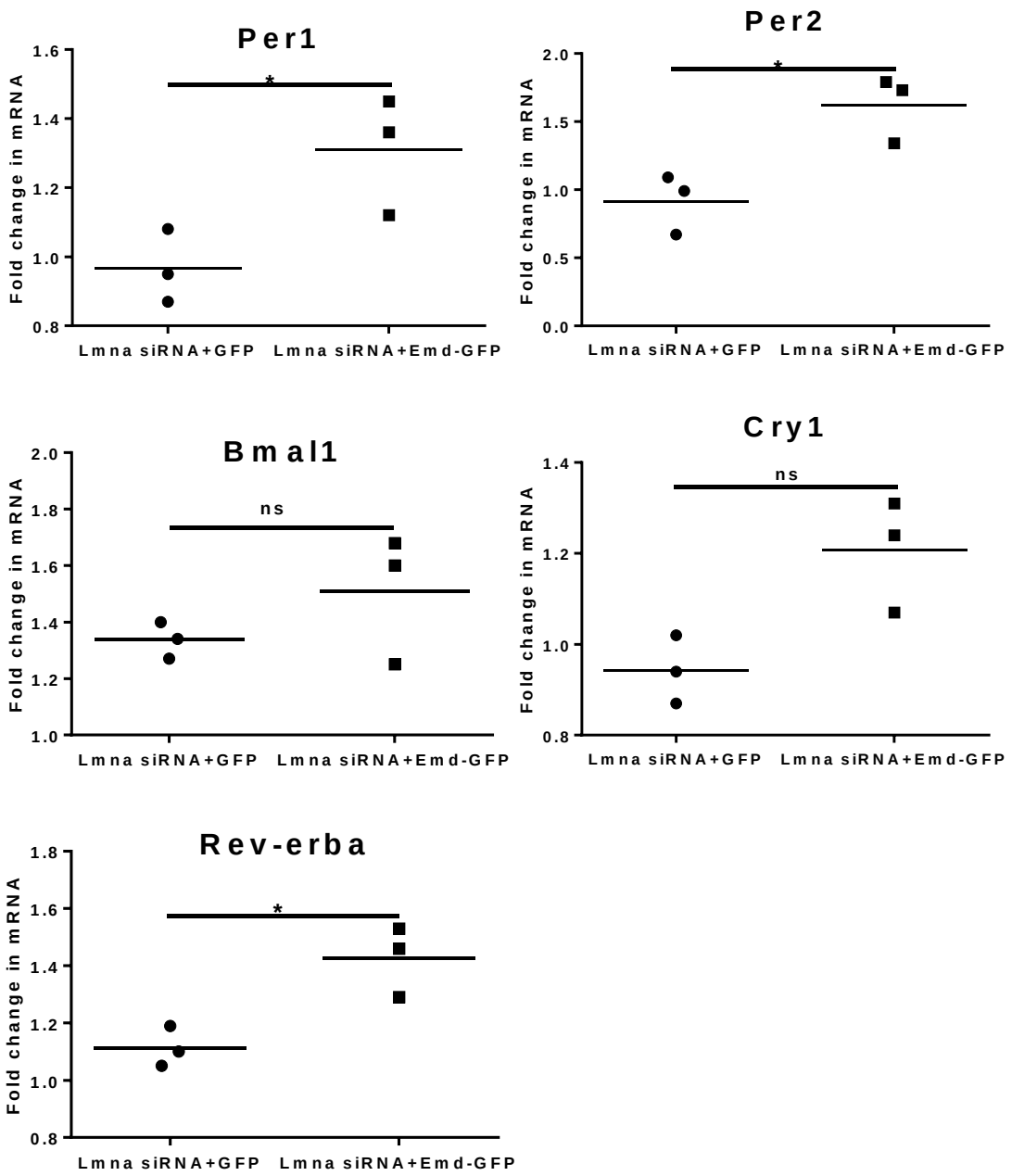

Figure 4.8. Circadian clock gene expression in C2C12 myoblasts transfected with lamin A siRNA and either emerin or GFP-only control plasmids. C2C12 myoblasts were neotransfected with 5nM lamin A siRNA and either 1ug emerin plasmid or GFP-only control and incubated for 42 hours before RNA extraction. Circadian clock gene expression was analysed by qRT-PCR using the Pfaffl method and normalised to *β-Actin* (Pfaffl, 2001). Data were expressed as a fold change relative to lamin A siRNA/GFP control which was expressed as 1 and presented as means (unpaired t-test, *p≤0.05, and ns =p>0.05, n=3).

4.4.3 Overexpression of lamin A in C2C12 myoblasts upregulates clock gene expression

4.4.3.1 Lamin A overexpression in C2C12 myoblasts

The next aim was to investigate the effect of lamin A overexpression on clock gene expression. C2C12 myoblasts were transfected with 1µg lamin A plasmid or pcDNA3 control using Polyfect reagent (Qiagen) (Moiseeva, *et al.*, 2015). Samples were analysed for gene and protein expression by qRT-PCR and Western blotting, respectively, both normalised to β-Actin. Data show a successful increase in lamin A mRNA and total LMNA protein levels in C2C12 myoblasts (Figure 4.9 and 4.10 and p≤0.001 and p≤0.05).

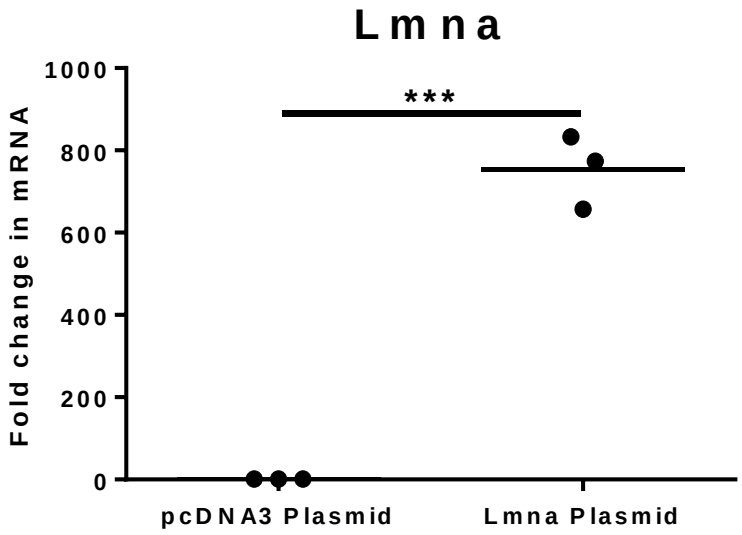

Figure 4.9. Lamin A overexpression in C2C12 myoblasts transfected with lamin A plasmid or pcDNA3 control. C2C12 myoblasts were transfected with 1µg lamin A plasmid or pcDNA3 control and incubated for 48 hours before RNA extraction. *Lmna* mRNA was analysed by qRT-PCR using the Pfaffl method and normalised to *β-Actin* (Pfaffl, 2001). Data were expressed as a fold change relative to pcDNA3 control which was expressed as 1 and presented as means (unpaired t-test, ***p≤0.001, three independent experiments n=3).

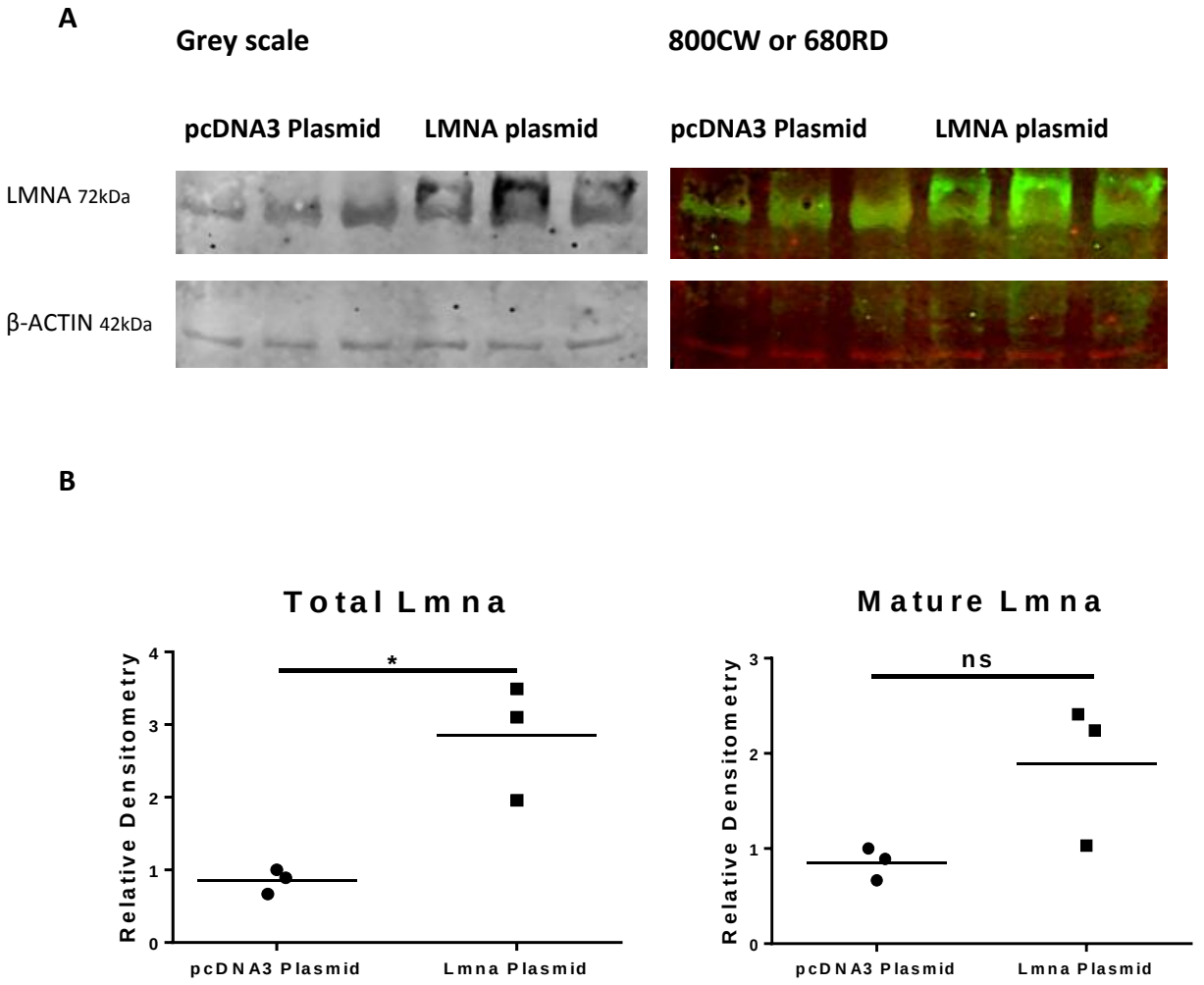

Figure 4.10. Representative Western blot images and protein densitometry analysis of C2C12 myoblasts transfected with lamin A plasmid or pcDNA3 control. (A) Protein samples were ran on 10% acrylamide gels, transferred, and incubated with primary antibodies for anti-mouse Lmna (Sigma;) and anti-rabbit β-Actin (Sigma; 1:2000) and followed by secondary IRDye® antibodies for goat anti-rabbit 800CW and goat anti-mouse 680RD (Licor; 1:20000) (B) Densitometry values were calculated using the analysis software provided by Image Studio Lite Version 5.2 and LMNA bands were normalised to β-ACTIN. Data were expressed as a fold change relative to pcDNA3 control which was expressed as 1 and presented as means (unpaired t-test, *p≤0.05, ns = p>0.05, n=3).

4.4.3.2 Lamin A overexpression in C2C12 myoblasts significantly up-regulates clock gene expression

To examine whether lamin A overexpression affects the expression of the core circadian clock genes, C2C12 myoblasts with lamin A overexpression were analysed by qRT-PCR to study clock gene mRNA and were normalised to *β-Actin*. Lamin A overexpression in C2C12 myoblasts significantly increased the expression of *Per1*, *Per2*, and *Bmal1*, and significantly decreased the expression of *Cry1* (Figure 4.11, unpaired t-test, $p \leq 0.05$, $p \leq 0.001$, and $p \leq 0.05$, and $p \leq 0.01$, respectively). An F-test of variance identified a significant change in the expression of *Rev-erbα* (Figure 4.11, $p \leq 0.05$).

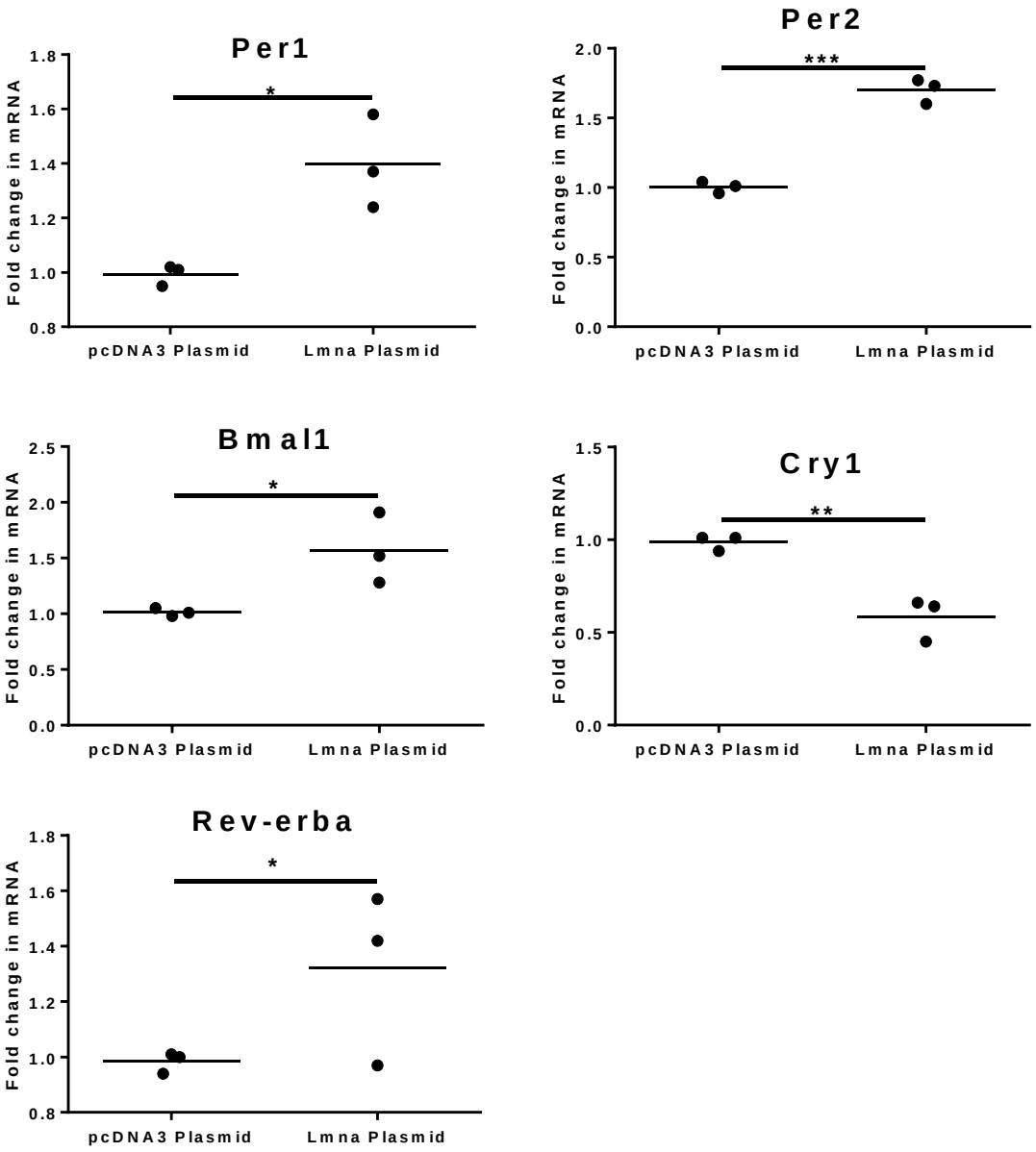

Figure 4.11. Circadian clock gene expression in C2C12 myoblasts transfected with lamin A plasmid or pcDNA3 control. C2C12 myoblasts were transfected with 1µg lamin A plasmid or pcDNA3 control and incubated for 48 hours before RNA extraction. Clock gene expression was analysed by qRT-PCR using the Pfaffl method and normalised to *β-Actin* (Pfaffl, 2001). Data were expressed as a fold change relative to pcDNA3 control which was expressed as 1 and presented as means (unpaired t-test, *p≤0.05, **p≤0.01, and ***p≤0.001, ns = p>0.05, three independent experiments n=3; *Rev-erbα* analysed by an F-test of variance, *p≤0.05).

4.4.3.3 Lamin A overexpression is sustained in C2C12 myoblasts after synchronisation for 48 hours

The next aim was to further investigate the effect of lamin A overexpression on circadian clock gene expression by collecting lamin A-overexpressing C2C12 myoblasts over a circadian time-course. C2C12 myoblasts were transfected with 1µg lamin A plasmid or pcDNA3 control and subsequently synchronised by 100nM Dexamethasone for 1 hour. Samples were collected every 4 hours for 24 hours over 7 circadian time points (24 hours-48 hours) and analysed for gene and protein expression by qRT-PCR and Western blotting, both normalised to β-Actin. Data demonstrated sustained overexpression of lamin A over the 24-hour time-course in comparison to the pcDNA3 control transfected samples (Figures 4.12 and 4.13, two-way ANOVA: p≤0.01, p≤0.001, and p≤0.0001).

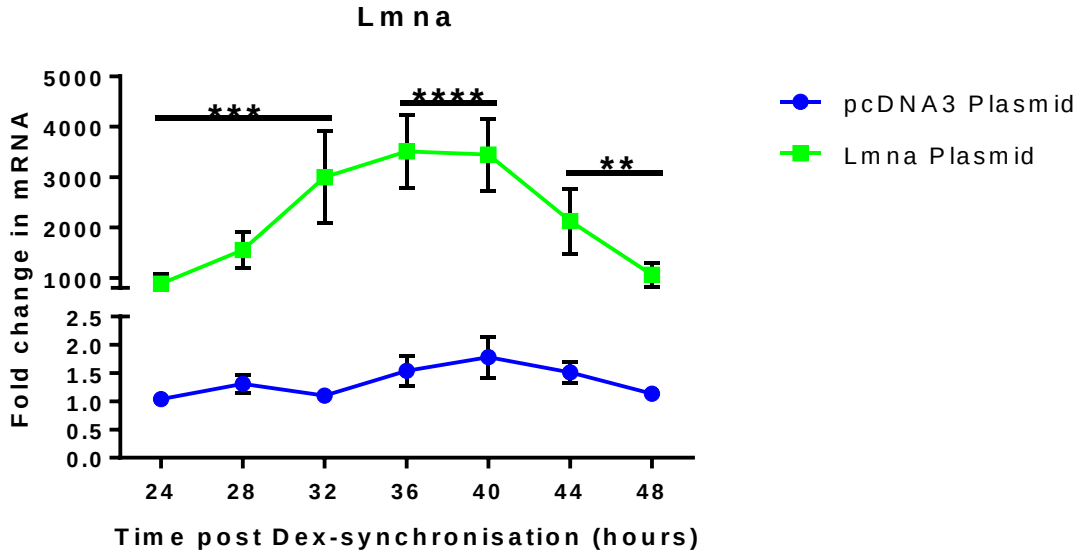

Figure 4.12. Circadian time-course of lamin A gene expression in Dexamethasone synchronised C2C12 myoblasts transfected with lamin A or pcDNA3 plasmids. C2C12 myoblasts were transfected with 1µg lamin A plasmid or pcDNA3 control and incubated for 24 hours before being synchronised with 100nM Dexamethasone for 1 hour. Twenty four hours post-synchronisation, cells were collected every 4 hours for 24 hours for RNA extraction. *Lmna* mRNA was analysed by qRT-PCR using the Pfaffl method and normalised to *β-Actin* (Pfaffl, 2001). Data were expressed as a fold change relative to pcDNA3 control which was expressed as 1 and presented as means± s.e.m (two-way ANOVA, **p≤0.01, ***p≤0.001, ****p≤0.0001, n=3).

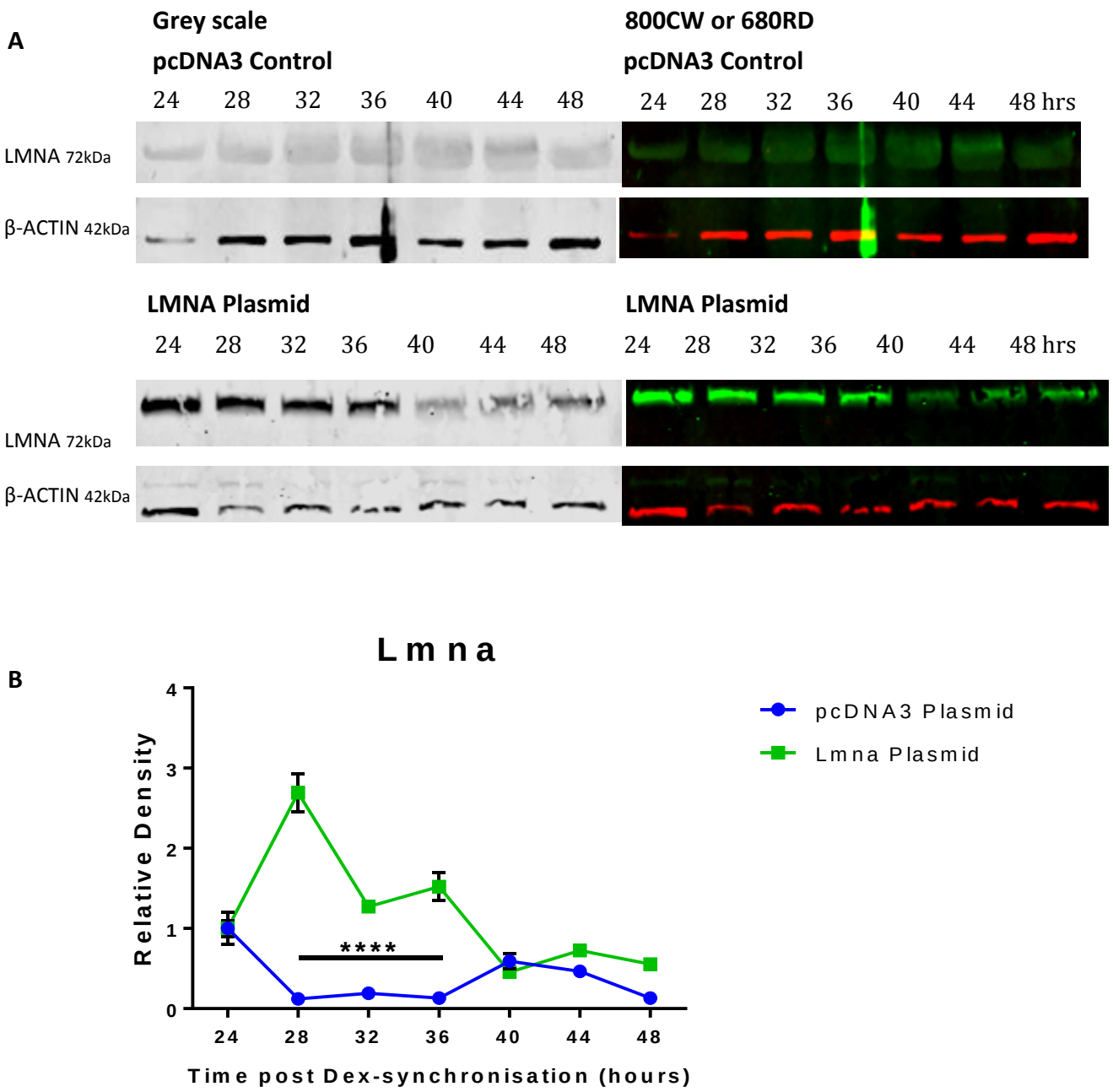

Figure 4.13. Representative Western blot images and protein densitometry analysis of circadian time-course in Dexamethasone synchronised C2C12 myoblasts transfected with lamin A or pcDNA3 plasmids. (A) Protein samples were ran on 10% acrylamide gels, transferred and primary antibodies incubated for anti-mouse Lmna (Sigma; 1:5000) and anti-rabbit β-Actin (Sigma; 1:2000), followed by secondary IRDye® antibodies for goat anti-rabbit 800CW and goat anti-mouse 680RD (Licor; 1:20000) (B) Densitometry values were calculated using the analysis software provided by Image Studio Lite Version 5.2. LMNA bands were normalised to β-ACTIN. Data were expressed as a fold change relative to pcDNA3 control which was expressed as 1 and presented as means± s.e.m (two-way ANOVA, ****p≤0.0001, n=3).

4.4.3.4 Circadian time-course of synchronised C2C12 myoblasts overexpressing lamin A demonstrates an upregulation of the core clock genes

The next aim was to investigate circadian clock gene expression in lamin A-overexpressing C2C12 myoblasts over a circadian time-course. qRT-PCR was used over a full circadian time-course (24-48hrs) to analyse the response of clock genes, and data were normalised to *β-Actin*. C2C12 myoblasts overexpressing lamin A demonstrated an up-regulated expression of *Per1* and *Bmal1* at the 36 and 44 hour time-points respectively, in comparison to pcDNA3 control transfected myoblasts (Figure 4.14, two-way ANOVA and $p \leq 0.05$ and $p \leq 0.01$). There was no significant change in *Per2*, *Cry1*, or *Rev-erbα* expression.

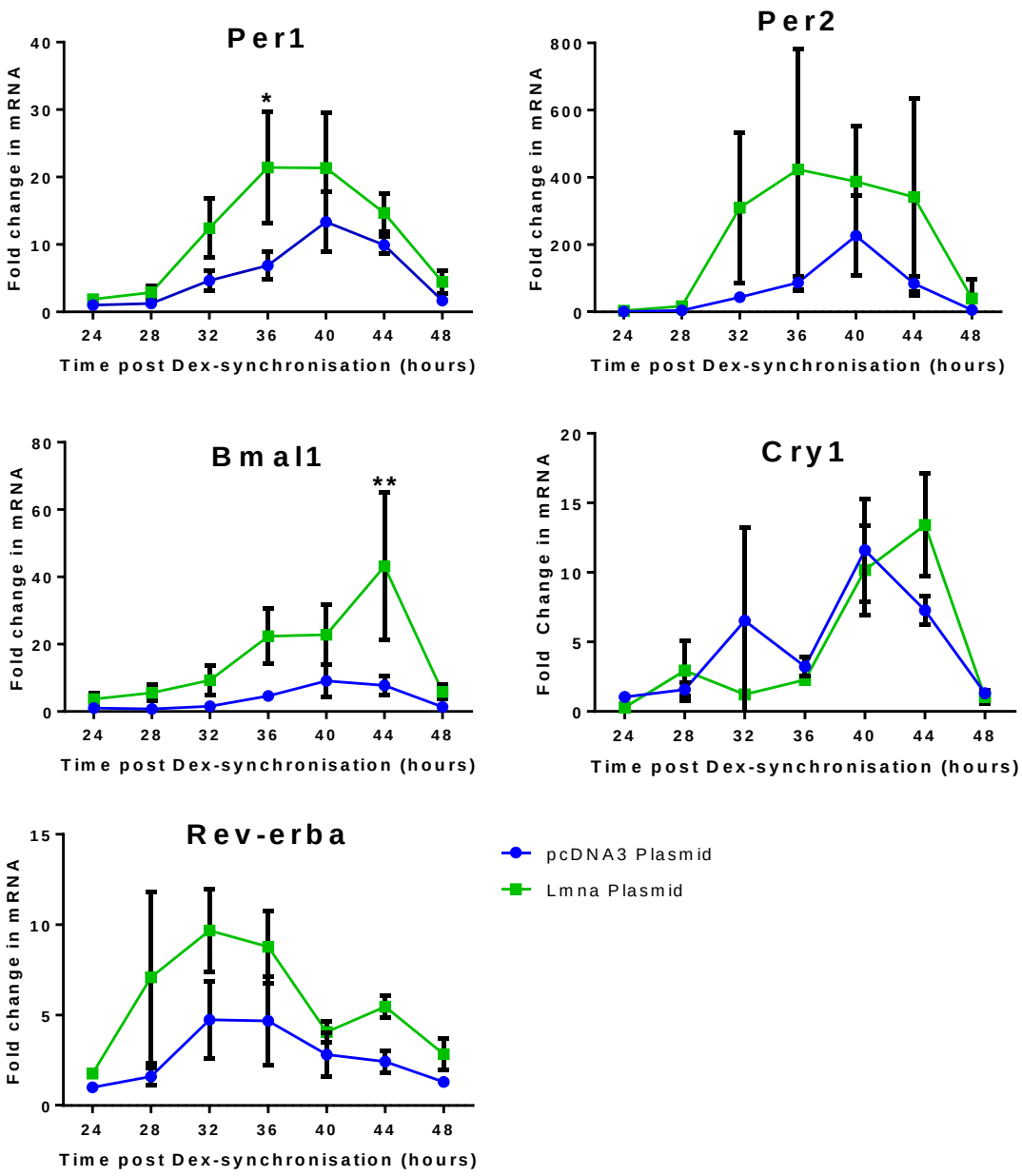

Figure 4.14. Circadian time-course of clock gene expression in Dexamethasone synchronised C2C12 myoblasts overexpressing lamin A. C2C12 myoblasts were transfected with 1µg of lamin A or pcDNA3 plasmid and incubated for 24 hours before synchronisation with 100nM Dexamethasone for 1 hour. Twenty four hours post-synchronisation, cells were collected every 4 hours for 24 hours for RNA extraction. Clock gene expression was analysed by qRT-PCR using the Pfaffl method and normalised to *β-Actin* (Pfaffl, 2001). Data were expressed as a fold change relative to pcDNA3 control which was expressed as 1 and presented as means± s.e.m (two-way ANOVA, *p≤0.05, **p≤0.01, three independent experiments n=3).

4.4.4 Real-time Bioluminescence imaging of Bmal1::Luc, lamin A up-regulates *Bmal1* gene expression

4.4.4.1 C2C12 myoblasts can be stably transfected with Bmal1::Luc plasmid

To dynamically visualise the expression of the core clock in C2C12 myoblasts, the next aim was to generate novel C2C12 myoblasts with a stable transfection of Bmal1::Luc reporter plasmid (Meng, *et al*., 2008). First, to identify a suitable concentration of selective antibiotic to use, C2C12 myoblasts seeded into a 6-well plate were treated with an increasing concentration of the antibiotic Hygromycin (Santa-Cruz) (Figure 4.15, 100µg, 200 µg, 400µg, and 1mg per mL concentrations). 400µg/mL of Hygromycin killed all myoblasts in the well within 5 days, and was chosen for stable transfection experiments. To set up stable transfections, C2C12 myoblasts were seeded into a 6-well plate and at 60% confluency were transfected with 1µg Bmal1::Luc plasmid. After 48 hours, myoblasts transfected with the plasmid were selected for by the addition of 400µg/mL Hygromycin, as the Bmal1::Luc plasmid contains a Hygromycin resistance gene. Once selected, cells with the stable Bmal1::Luc transfection were maintained in 200µg/mL of Hygromycin. To observe Bmal1::Luc expression in real-time, C2C12 myoblasts stably transfected with Bmal1::Luc were seeded into 35mm dishes and allowed to reach 90-100% confluency before they were synchronised with Dexamethasone or serum shock and placed into the LumiCycle. Real-time bioluminescent imaging permits the dynamic observation of *Bmal1* expression, and traces from myoblasts synchronised with Dexamethasone were in better synchronisation than those synchronised through serum shock (Figures 4.16 and 4.17).

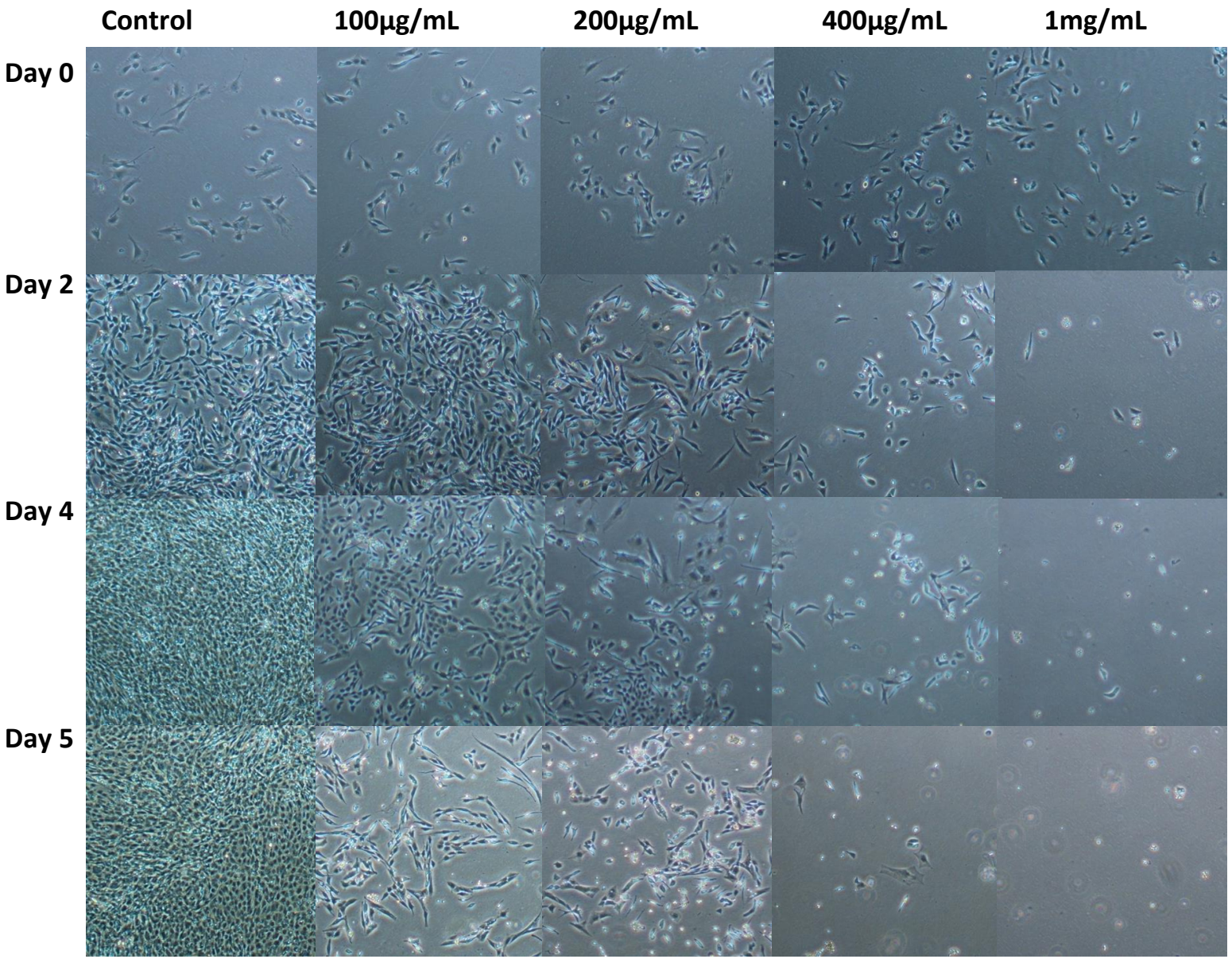

Figure 4.15. C2C12 cells left as a control or treated with an increasing concentration of Hygromycin (100µg/mL – 1mg/mL), and imaged between day 0 and day 5.

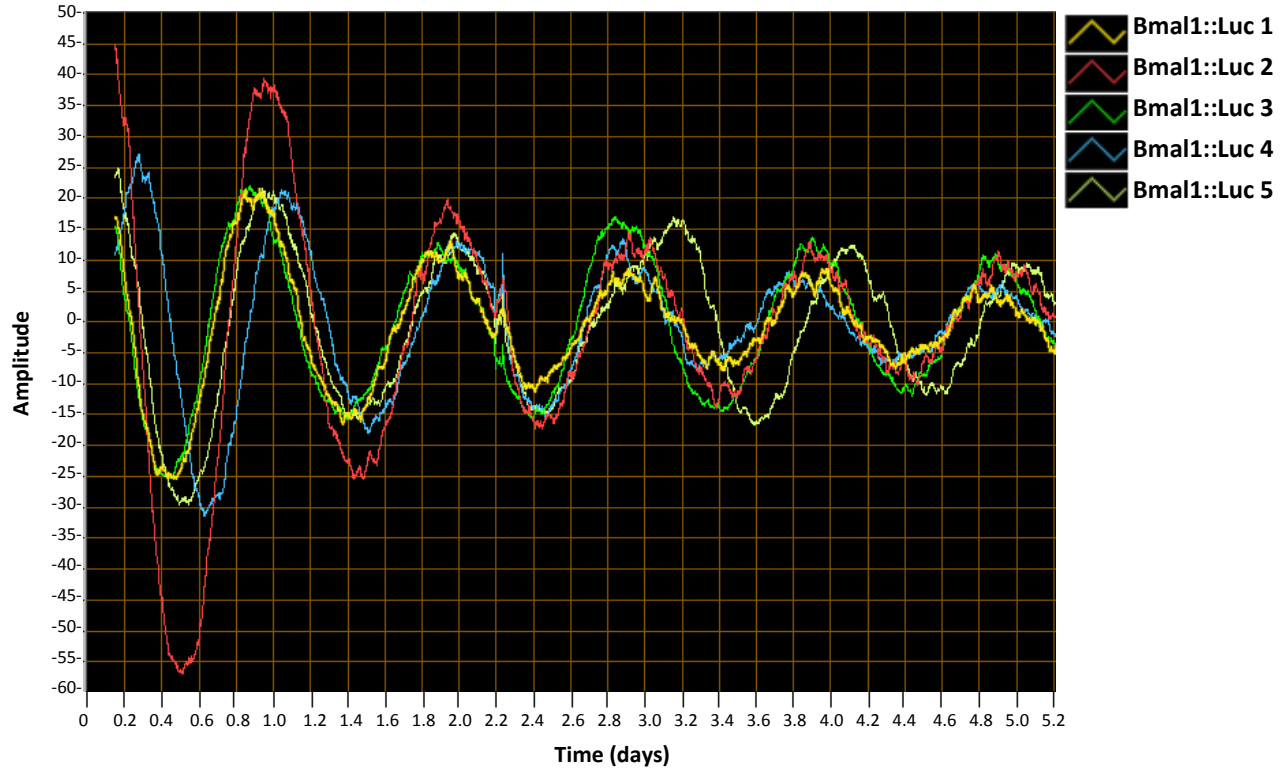

Figure 4.16. Real-time bioluminescent imaging of C2C12 myoblasts with stable transfection of Bmal1::Luc plasmid, synchronised with Dexamethasone and after two days – at time 2.2, resynchronised with Dexamethasone.

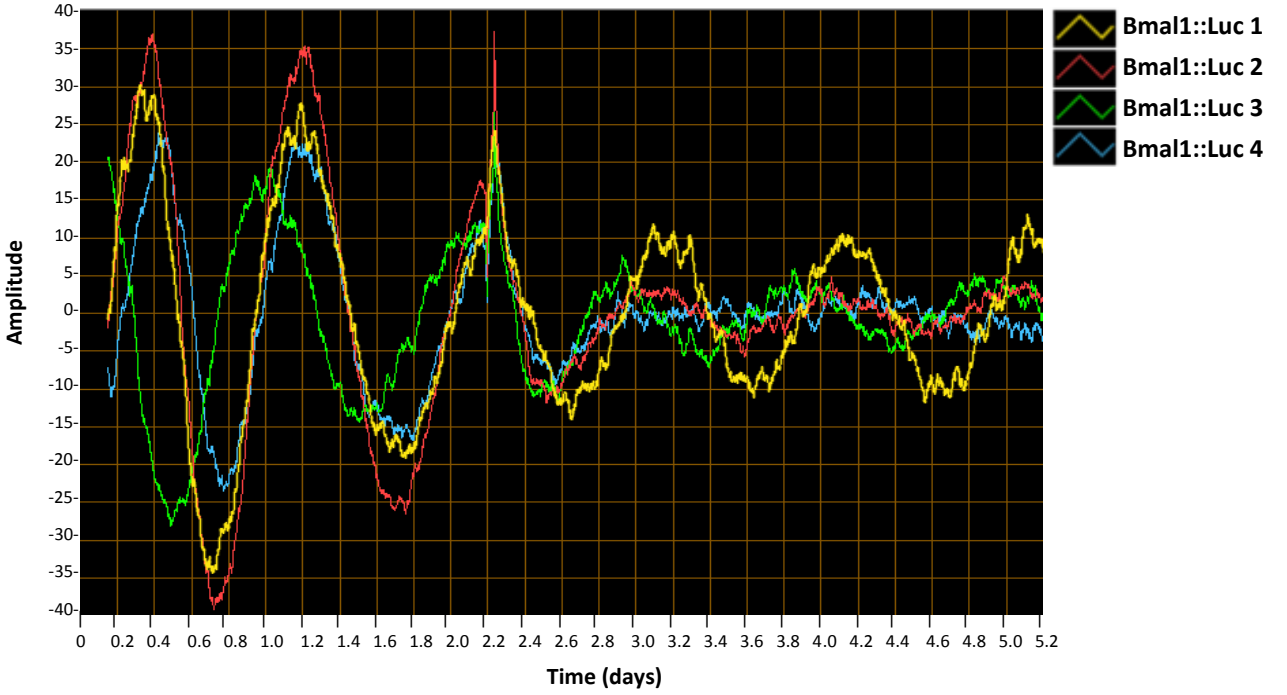

Figure 4.17. Real-time bioluminescent imaging of C2C12 myoblasts with stable transfection of Bmal1::Luc plasmid, synchronised with serum shock and after two days – at time 2.2, resynchronised with serum shock.

4.4.4.2 Knockdown of lamin A in C2C12 myoblasts stably transfected with Bmal1::Luc represses *Bmal1* expression

To investigate in real-time the effect of lamin A manipulation on the core clock gene *Bmal1* in muscle cells, the next aim was to knockdown lamin A in C2C12 myoblasts stably transfected with Bmal1::Luc plasmid and dynamically observe the response in the LumiCycle. Bmal1::Luc transfected C2C12 myoblasts were seeded into 35mm dishes and at 60% confluency were transfected with 5nm validated lamin A siRNA or scrambled control. After 24 hours they were synchronised with 100nM Dexamethasone and after a 45-minute incubation, the media was changed to LumiCycle media (Phenol red-free DMEM supplemented with 5% FBS, 10 mM Hepes (Sigma), 1 mM Sodium Pyruvate (Sigma), 2nM L-Glu, 0.1mg/mL P/S, and 100nM Luciferin (Promega)) and they were placed into the LumiCycle to record bioluminescence. Traces demonstrated that lamin A knockdown reduced the expression of *Bmal1*, a lower amplitude of expression can be observed in lamin A siRNA treated samples on comparison with scrambled control (Figure 4.18).

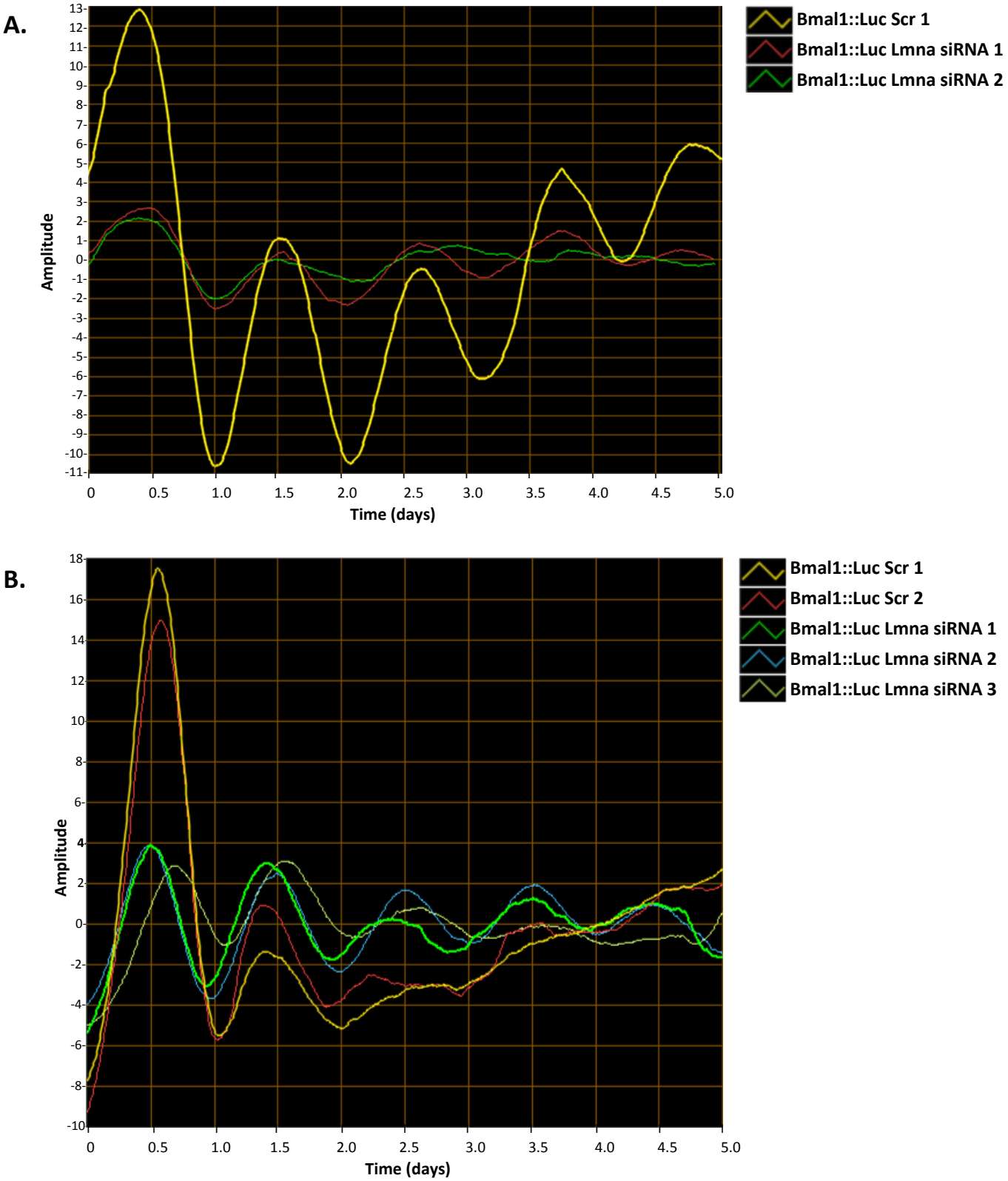

Figure 4.18. Real-time bioluminescent imaging of C2C12 cells with stable transfection of Bmal1::Luc plasmid and subsequent transfection with lamin A siRNA. 24 hours after transfection with 5nmol Lmna siRNA myoblasts were synchronised with 100nM Dexamethasone, after 45-minute incubation the media was changed to LumiCycle media and they were placed into the LumiCycle.

4.4.4.3 Overexpressing lamin A in C2C12 myoblasts stably transfected with Bmal1::Luc up-regulates *Bmal1* expression

To investigate in real-time the effect of lamin A overexpression on the core clock gene *Bmal1* in muscle cells, the next aim was to overexpress lamin A in C2C12 myoblasts stably transfected with Bmal1::Luc plasmid and dynamically observe the response in the LumiCycle. Bmal1::Luc transfected C2C12 myoblasts were seeded into 35mm dishes and at 60% confluency were transfected with 1µg lamin A plasmid or pcDNA3 control. After 24 hours incubation the cells were synchronised with 100nM Dexamethasone, and after a 45-minute incubation the media was changed to LumiCycle media and the myoblasts were placed into the LumiCycle. Traces demonstrated that lamin A overexpression up-regulates the expression of *Bmal1*, a higher amplitude of expression can be observed in lamin A transfected samples on comparison with pcDNA3 control (Figure 4.19).

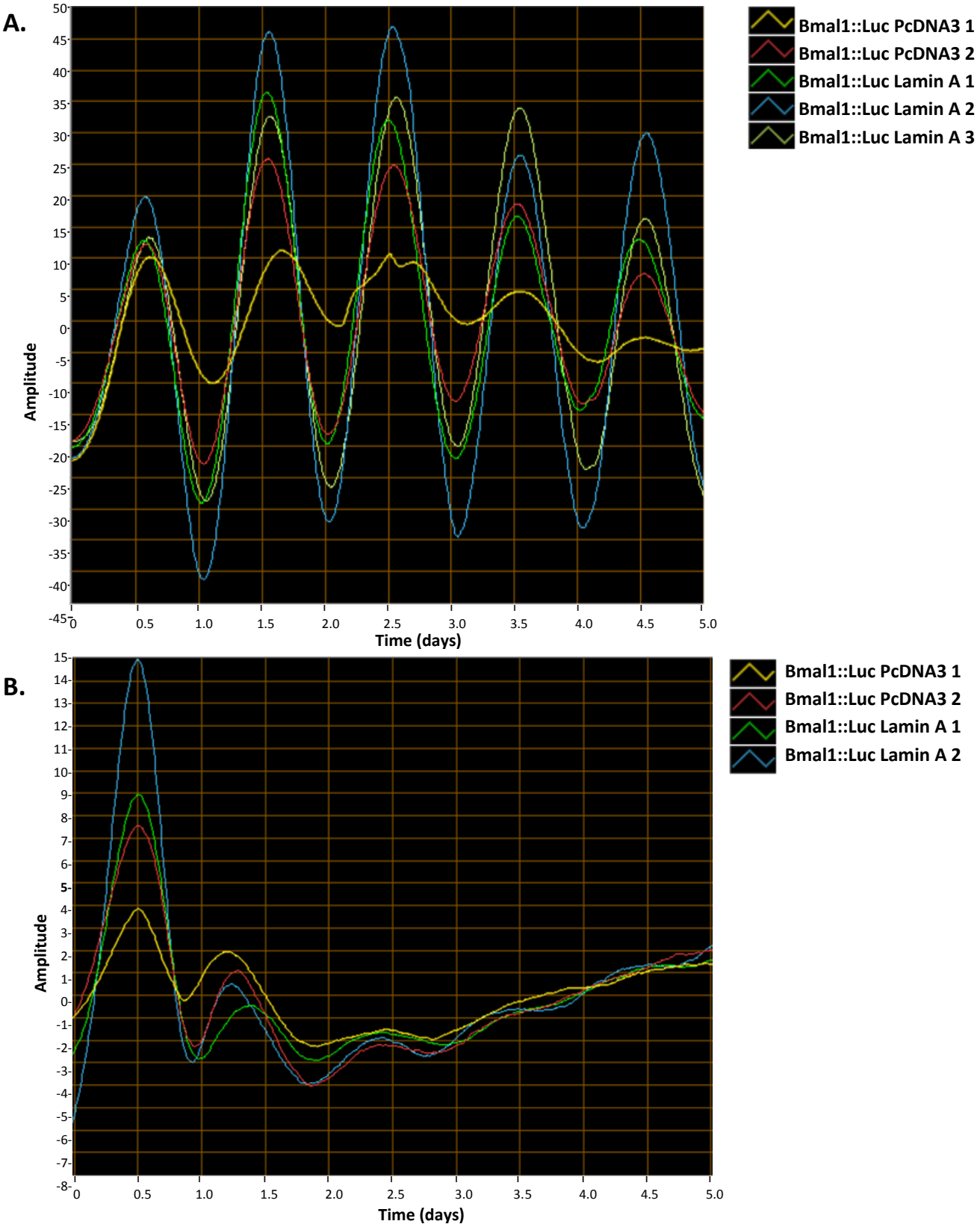

Figure 4.19. Real-time bioluminescent imaging of C2C12 myoblasts with stable transfection of Bmal1::Luc plasmid and subsequently transfected with lamin A plasmid. 24 hours after 1µg lamin A plasmid transfection the myoblasts were synchronised with 100nM Dexamethasone, after 45-minute incubation the media was changed to LumiCycle media and they were placed into the LumiCycle.

4.4.5 Luciferase Assays demonstrate Per2::Luc activity is decreased by lamin A

To investigate the relationship between lamin A and circadian clock gene expression using a different molecular technique, the next aim was to utilise reporter plasmids and observe the response of clock gene expression to different conditions involving lamin A. First, this study focused on observing the expression of *Per2*, part of the positive arm of the core clock. 3T3 cells were seeded into 12-well plates and at 50% confluency, transfected with 250 ng/mL of Per2::Luc plasmid and lamin A plasmid increasing in concentration from 0 to 500 ng per 2mL. Cells were incubated for 48 hours before collection in Dual Reporter Lysis solution and reporter activity was measured on a Luminometer following the Dual-Light® Luciferase & β-Galactosidase Reporter Gene Assay System kit protocol (Thermofisher Scientific). The reporter activity, and *Per2* expression, was decreased between the control and myoblasts transfected with 500 ng lamin A plasmid, and those transfected with 100 ng compared to 500 ng of lamin A plasmid (Figure 4.20; One-way ANOVA, $p \leq 0.01$ and $p \leq 0.05$).

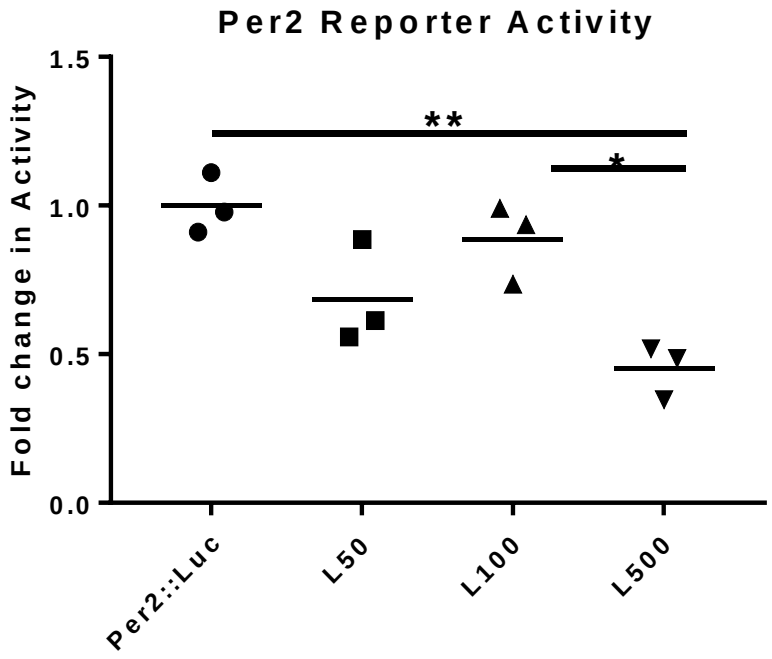

Figure 4.20. Dual luciferase reporter assay of 3T3 cells transfected with Per2::Luc reporter plasmid and an increasing concentration of lamin A plasmid. 3T3 cells were transfected with 250 ng/mL of Per2::Luc plasmid and an increasing concentration of lamin A plasmid- from 0 to 500ng per 2mL. Cells were incubated for 48 hours before collection in Dual Reporter Lysis solution and reporter activity was measured on a Luminometer following the Dual-Light® Luciferase & β-Galactosidase Reporter Gene Assay System kit protocol (Thermofisher Scientific). Data were expressed as a fold change relative to Per2::Luc only control which was expressed as 1 and presented as means (one-way analysis of variance (ANOVA), *p≤0.05, **p≤0.01, three independent experiments n=3).

4.4.6 Luciferase Assays demonstrate lamin A decreases the activity of Per2::Luc in the presence of BMAL1:CLOCK

To further investigate the downregulation of *Per* expression by lamin A, the next aim was to observe whether lamin A represses *Per* upregulation observed in response to the BMAL1:CLOCK heterodimer. In this regard, 3T3 cells were transfected at 50% confluency with 250 ng/mL Per2::Luc reporter plasmid and 250 ng/mL of Bmal1 and Clock plasmid, or 500 ng/mL of lamin A plasmid, or both in combination. Cells were incubated for 48 hours before collection in Dual Reporter Lysis solution and reporter activity was measured on a Luminometer following the Dual-Light® Luciferase & β-Galactosidase Reporter Gene Assay System kit protocol. There was an increase in *Per* expression with Bmal1 and Clock transfection and the expression of *Per* was decreased in lamin A transfected samples compared to Bmal1 and Clock transfected samples (Figure 4.21; One-way ANOVA, $p \leq 0.05$ and $p \leq 0.01$). The upregulation of *Per* in response to Bmal1 and Clock transfection was lost when myoblasts were transfected with Bmal1, Clock, and lamin A plasmid in combination (Figure 4.21).

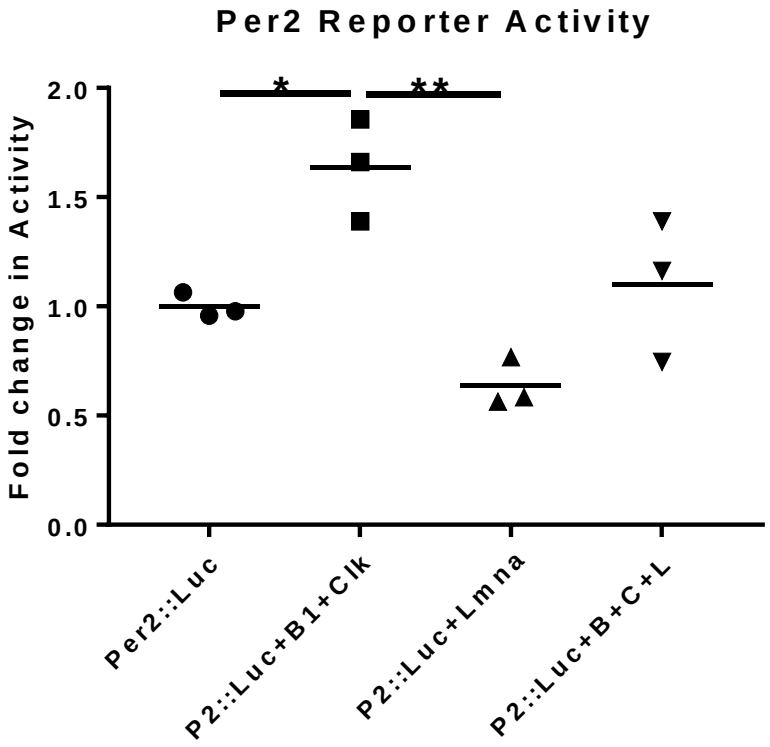

Figure 4.21. Dual luciferase reporter assay of 3T3 cells transfected with Per2::Luc reporter plasmid, Bmal1 and Clock, and lamin A plasmids. 3T3 cells were transfected with 250 ng/mL of Per2::Luc plasmid and 250 ng/mL of Bmal1 and Clock plasmid or 500 ng/mL of lamin A plasmid, or both. Cells were incubated for 48 hours before collection in Dual Reporter Lysis solution and reporter activity was measured on a Luminometer following the Dual-Light® Luciferase & β-Galactosidase Reporter Gene Assay System kit protocol (Thermofisher Scientific). Data were expressed as a fold change relative to Per2::Luc only control which was expressed as 1 and presented as means (one-way analysis of variance (ANOVA), *p≤0.05, **p≤0.01, three independent experiments n=3).

4.4.7 Luciferase Assays demonstrate lamin A increase does not change the activity of Bmal1::Luc

Next, a Bmal1::Luc reporter plasmid was used to observe the activity of *Bmal1*, part of the negative arm of the core clock, in response to different conditions involving lamin A. 3T3 cells at 50% confluency were transfected with 250ng/mL of Bmal1::Luc plasmid and lamin A plasmid increasing in concentration from 0 to 500 ng per 2mL. Cells were incubated for 48 hours before collection in Dual Reporter Lysis solution and reporter activity was measured on a Luminometer following the Dual-Light® Luciferase & β-Galactosidase Reporter Gene Assay System kit protocol. There was no change in *Bmal1* expression with increasing concentrations of lamin A (Figure 4.22).

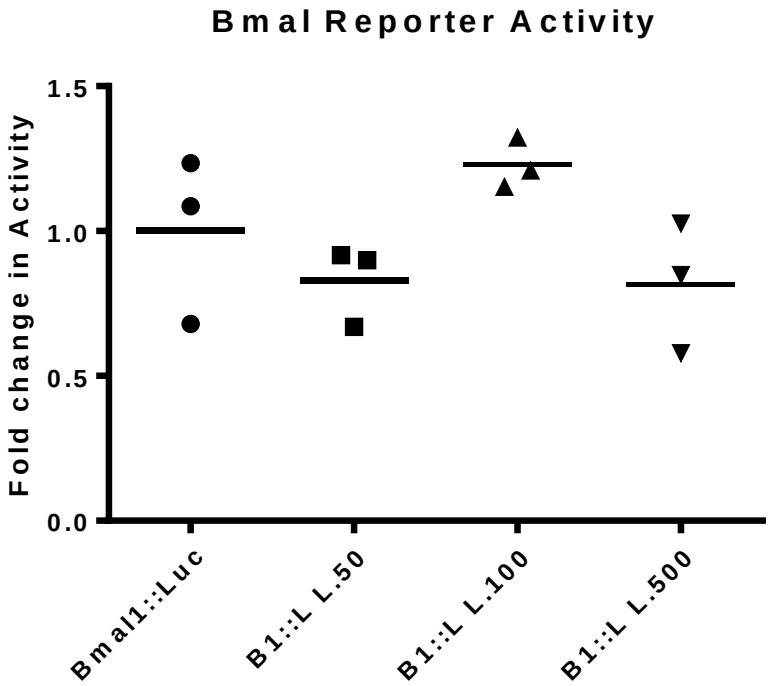

Figure 4.22. Dual luciferase reporter assay of 3T3 cells transfected with Bmal1::Luc reporter plasmid and an increasing concentration of lamin A plasmid. 3T3 cells were transfected with 250 ng/mL of Bmal1::Luc plasmid and an increasing concentration of lamin A plasmid- from 0 to 500 ng per 2mL. Cells were incubated for 48 hours before collection in Dual Reporter Lysis solution and reporter activity was measured on a Luminometer following the Dual-Light® Luciferase & β-Galactosidase Reporter Gene Assay System kit protocol (Thermofisher Scientific). Data were expressed as a fold change relative to Bmal1::Luc only control which was expressed as 1 and presented as means (one-way analysis of variance (ANOVA), three independent experiments n=3).

4.4.8 Luciferase Assays demonstrate lamin A does not alter the Cry1 repression of Bmal1::Luc

To further investigate whether *Bmal1* expression is responsive to lamin A, the next aim was to observe whether the repression of *Bmal1* expression observed in response to Cry1 is altered in the presence of lamin A. Cry1 is part of the negative arm of the core clock and naturally feeds-back to repress *Bmal1* expression. 3T3 cells were transfected at 50% confluency with 250 ng/mL Bmal1::Luc reporter plasmid and 250 ng/mL of Cry1 plasmid or 100 ng/mL of lamin A plasmid, or both in combination. Cells were incubated for 48 hours before collection in Dual Reporter Lysis solution and reporter activity was measured on a Luminometer following the Dual-Light® Luciferase & β-Galactosidase Reporter Gene Assay System kit protocol. There was a decrease in *Bmal1* expression with Cry1 transfection compared to both control and lamin A transfected cells (Figure 4.23; One-way ANOVA, $p \leq 0.05$). The expression of *Bmal1* remains decreased upon dual transfection with Cry1 and lamin A compared to cells transfected with either the control or lamin A alone (Figure 4.23; One-way ANOVA, $p \leq 0.05$).

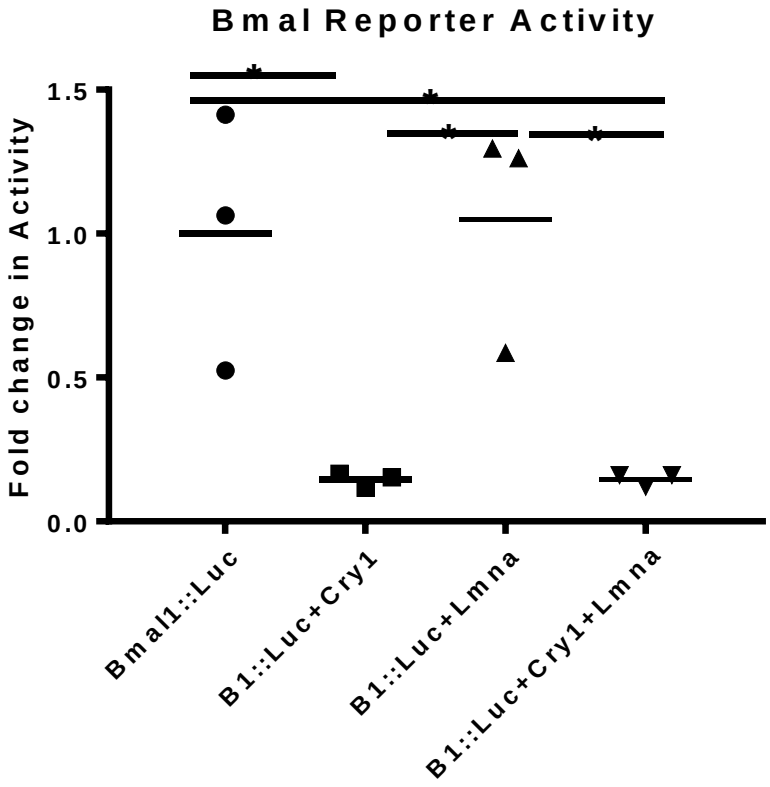

Figure 4.23. Dual luciferase reporter assay of 3T3 cells transfected with Bmal1::Luc reporter plasmid, Cry1, and lamin A plasmids. 3T3 cells were transfected with 250 ng/mL of Bmal1::Luc plasmid and 250 ng/mL of Cry1 plasmid or 100 ng/mL of lamin A plasmid, or both. Cells were incubated for 48 hours before collection in Dual Reporter Lysis solution. Reporter activity was measured on a Luminometer following the Dual-Light® Luciferase & β-Galactosidase Reporter Gene Assay System kit protocol (Thermofisher Scientific). Data were expressed as a fold change relative to Bmal1::Luc only control which was expressed as 1 and presented as means (one-way analysis of variance (ANOVA), *p≤0.05, three independent experiments n=3).

4.5 Discussion

Research in the previous chapter identified rhythmic oscillations in *Lmna* mRNA expression and protein levels, and that the expression of *Lmna* is in phase with the negative arm core clock genes. The next aim was to progress these studies and investigate a potential feedback relationship between lamin A and the circadian molecular clock. This is a common mechanism observed in other circadian clock controlled proteins that feedback to regulate the molecular clock itself, such as REV-ERBα and DEC1 (Guillaumond, *et al*., 2005; Nakashima, *et al*., 2008). These are known as stabilising or auxiliary loops and reinforce the molecular clock, increasing robustness. Recent research identified TGF-β as a clock-controlled gene up-regulated by BMAL1:CLOCK (Chen, *et al*., 2015b). Inhibition of TGF-β lengthened the molecular clock period, and decreased the amplitude and phase delayed *Per1* mRNA expression (Sloin, *et al*., 2018). Hence, TGF-β provides feedback regulation to the circadian clock through regulation of *Per1*. In addition, TGF-β inhibition disrupted the circadian rhythm of locomotor activity in Zebrafish larvae (Sloin, *et al*., 2018). Given the body of research recognising that some clock-controlled proteins provide feedback regulation to the molecular clock, it was predicted that lamin A also comprises a regulatory feedback loop. As discussed in the 'Gene Expression hypothesis', lamin A regulates gene expression through the regulation of transcription factor localisation, genome organisation, cell cycle control, and nuclear-cytoplasmic shuttling. These functions all represent plausible mechanisms that lamin A may use to regulate the core clock.

The experimental design of this chapter is consistent with previous studies investigating potential feedback regulation acting on the circadian clock. Proteins of interest are investigated through utilising overexpression, knockdown, and reporter assay experiments to observe whether the expression of core and auxiliary clock genes are altered (Akashi and Takumi, 2005; Nakashima, *et al*., 2008; Wang, *et al*., 2010; Shostak, *et al*., 2016). The molecular loop is a finely tuned orchestration of transcriptional regulation, protein production, protein localisation, and stability. Any proteins involved in providing fine-tuning, feedback regulation to the molecular clock must be present during

the correct periods of the cycle, in the correct location, and at the correct levels. Consequently, overexpression and knockdown experiments determine whether a protein of interest interacts with the core clock, as these genetic manipulations would result in abnormally high or low levels of this regulation. The effect of these manipulations on clock gene expression can then be monitored using qRT-PCR, Western blotting or reporter assays. Moreover, reporter assays may be used to observe clock gene activity in response to the deletion of segments of the protein of interest or of the clock gene promoters, to identify areas of potential interaction (Lin, *et al*., 2014). If these genetic manipulations disturb the sensitive cycling of the core clock and offset temporal cues in feedback pathways, this indicates that the protein of interest may be involved in regulating of one or more core clock genes.

The results in this chapter demonstrate a relationship between lamin A and the circadian clock. Lamin A knockdown in C2C12 myoblasts dampened the expression of the core and auxiliary clock genes: *Per1*, *Per2*, *Bmal1*, *Cry1*, and *Rev-erbα* (Figure 4.3, $p \leq 0.05$ and $p \leq 0.01$). Overexpression of lamin A increased the expression of *Per1*, *Per2*, and *Bmal1*, and decreased the expression of *Cry1* (Figure 4.11, $p \leq 0.05$, $p \leq 0.01$, and $p \leq 0.001$). These results were confirmed through real-time-bioluminescent imaging of lamin A manipulation in C2C12 myoblasts with a stable transfection of the Bmal1::Luc reporter plasmid (Figures 4.18 and 4.19). Hence, this enabled us to predict that lamin A feeds back to regulate the core clock through up-regulating the expression of *Per1, Per2*, and *Bmal1* and repressing the expression of *Cry1*. On lamin A knockout, lamin A repression of *Cry1* ceases but the other core clock genes are dampened due to loss of lamin A up-regulation. Accordingly, this would result in lower *Cry1* expression due to a lack of BMAL1:CLOCK positive up-regulation, despite the loss of *Cry1* repression. Overexpression of lamin A would increase *Cry1* repression, reducing the levels of *Cry1* expression, and would increase the expression of *Per1, Per2*, and *Bmal1*, as there would be higher levels of lamin A direct up-regulation.

Table 4.1. Lamin A manipulation in C2C12 myoblasts Experimental Data Summary. Table summarising significant gene changes in C2C12 myoblasts with lamin A siRNA knockdown or plasmid overexpression, *p≤0.05, **p≤0.01, ***p≤0.001, ****p≤0.0001.

Lamin A Manipulation	Circadian Clock response
C2C12 siRNA knockdown	Decrease in *Per1****, *Per2****, *Bmal1***, *Cry1****, and *Rev-erbα****
C2C12 siRNA knockdown time-course	Decrease in *Per1*****, *Per2*****, *Bmal1*****, and *Cry1******
C2C12 Lamin A overexpression	Increase *Per1***, *Per2*****, and *Bmal1***, Decrease *Cry1****
C2C12 Lamin A overexpression time-course	Increase in *Per1*** and *Bmal1****
Bmal1::Luc C2C12 lamin A siRNA	Decreased amplitude in *Bmal1* oscillation
Bmal1::Luc C2C12 lamin A overexpression	Increased amplitude in *Bmal1* oscillation

In contrast, Dual Reporter Assays of 3T3 cells transfected with Per2::Luc or Bmal1::Luc and expression plasmids for core clock genes and lamin A produced differing results to previous work. Transfection of 3T3 cells with Per2::Luc reporter plasmid and an increasing concentration of lamin A plasmid decreased *Per2* expression (Figure 4.20; One-way ANOVA, p≤0.01 and p≤0.05). Furthermore, 3T3 cells transfected with Per2::Luc, Bmal1, Clock, and lamin A plasmids lost the upregulation of Per2::Luc observed in response to transfection with Bmal1 and Clock alone – lamin A is preventing this upregulation (the positive arm proteins BMAL1:CLOCK act to upregulate Per) (Figure 4.21). Conversely, transfection of 3T3 cells with Bmal1::Luc reporter plasmid and an increasing concentration of lamin A plasmid demonstrated no change in *Bmal1* expression, and lamin A plasmid did not disturb Cry1 repression of *Bmal1* (Figure 4.22 and Figure 4.23). This Luciferase reporter data for Per2::Luc in response to lamin A supports the thesis hypothesis that lamin A interacts with the circadian clock but demonstrates an opposite relationship to previous results; overexpression of lamin A is no longer upregulating *Per1* or *Per2* expression (Figure 4.11). In addition, *Bmal1* expression is not increased in response to lamin A overexpression (Figure 4.11). It was predicted that these reporter assay results may be due to the section of the promoter sequence that is included in

the reporter plasmid constructs; these constructs do not include the entire promoter sequence. In particular, the section of the promoter through which lamin A interacts to regulate the expression of these core clock genes may not be included within these constructs. Hence, the same response in reporter activity would not be observed.

Table 4.2 Dual Reporter Assays of 3T3 cells Experimental Data Summary. Table summarising significant gene changes in Dual Report assays with Per2::Luc or Bmal1::Luc and expression plasmids for core clock genes and lamin A, **p≤0.01.

Lamin A Manipulation	Circadian Clock response
Per2::Luc Assay: Increasing Lmna	Lmna represses Per2**
Per2::Luc Assay: Lmna, Bmal1 + Clock	Lmna decreases Per2 upregulation by Bmal1:Clock
Bmal1::Luc Assay: Increasing Lmna	No Change
Bmal1::Luc Assay: Lmna, Cry1	Lmna no effect on Cry repression of *Bmal1*

This research is consistent with previous work that discovered proteins with feedback relationships to the molecular clock. Overexpression of Myc in U2OS cells dampens and attenuates the circadian clock through overexpressing *Rev-erbα* and repressing *Bmal1* expression (Altman, *et al*., 2015). Furthermore, Myc knockdown by siRNA increases the expression of core clock genes and the amplitude of oscillations, strengthening the circadian clock (Shostak, *et al*., 2016). Myc regulates cell cycle progression and proliferation with an inverse relationship to the core clock (Shostak, *et al*., 2016). Myc overexpression and repression promotes and reduces proliferation, respectively. This relationship with Myc and the molecular clock is opposite to the relationship observed with lamin A and the molecular clock. Moreover, Maged1 interaction with the clock was investigated through observing the response of the molecular clock to the loss of *Maged1* in knockout mice. qRT-PCR data demonstrated decreased expression of *Bmal1* and a short period phenotype, observed in the output of locomotor activity (Wang, *et al*., 2010). These genetic manipulations enable explorative studies into feedback relationship with the circadian clock.

Emerin is a lamin A binding partner and lamin A is important in ensuring correct localisation and function of emerin (Vaughan, *et al*., 2001). The impairment of MKL1 translocation in lamin $A^{-/-}$ MEFs was rescued by ectopic emerin transfection; it was hypothesised that emerin overexpression increased the levels of emerin correctly localised and available at the nuclear periphery (Ho, *et al.,* 2013). Given this previous research, the next aim investigated whether emerin overexpression could rescue clock gene expression in C2C12 myoblasts knocked-down for lamin A. The expression of core clock genes *Per1*, *Per2*, *Bmal1*, and *Rev-erbα* were upregulated with emerin overexpression, compared to C2C12 myoblasts with lamin A knockdown and overexpression of GFP only plasmid control (Figure 4.8). These data support emerin as an up-regulator of the core clock genes and *Rev-erbα*, not including *Cry1*, in myoblasts with lamin A knockdown. However, the increase in *Per1*, *Per2*, *Bmal1*, and *Rev-erbα* expression may be due to the increase in *Lmna* observed in response to overexpression of emerin.

This research is supported by previous studies alluding to the importance of circadian temporal dynamics within the nucleus. Lin *et al*. discovered circadian oscillations in MAN1, lamin B1, and LBR expression (Lin, *et al*., 2014). Thus, nuclear proteins can be subject to circadian clock control, as identified in the previous chapter for lamin A in musculoskeletal cells. Further experimentation identified MAN1 as regulator of *Bmal1*; through binding to the *Bmal1* promoter MAN1 up-regulates *Bmal1* expression (Lin, *et al*., 2014). Furthermore, recent work identified that the regulation of nuclear-cytoplasmic translocation is an important regulator of the circadian molecular clock. Transportin 1 (TNPO1), a nuclear import carrier, complexes with PER1 and acts to regulate its nuclear location; TNPO1 knockdown impairs the nuclear import rate of PER1 (Korge, *et al*., 2018). In response to redox stress, there is an increase in TNPO1 and PER1 complexes, and this may constitute a feedback pathway to the circadian clock in response to a change in redox states (Korge, *et al*., 2018). Importantly, this work supports the research in this chapter and reinforces nuclear protein involvement in providing feedback regulation to the molecular core clock through transcription regulation.

Recent research highlighted the importance of 3D genome organisation and temporal chromosome dynamics in functioning circadian rhythms. Circadian timing mechanisms were discovered in the recruitment of the genome, containing LAD domains, to the nuclear lamina by CTCF-PARP1 (Zhao, *et al*., 2015). At the nuclear periphery, genes become silenced and acquire the repressive H3K9me2 chromatin modifier. Time-course data revealed circadian oscillations in the relocation of genes to the nuclear lamina and H3K9me2 acquisition (Zhao, *et al*., 2015). The recruitment of genes to the nuclear periphery is already suggested to be important in developmental silencing of tissue-specific genes, such as silencing during muscle development (Solovei, *et al*., 2013). Research has also shown that functioning circadian rhythms are important in muscle development and maintenance; notably, clock gene mutant mice have impaired development, function, and activity (Kondratov, *et al*., 2006; Andrews, *et al*., 2010). Therefore, a functioning nuclear lamina and circadian clock are essential for correct development of muscle. Temporal localisation of genes to the nuclear lamina is one possible mechanism that links clock controlled gene expression with lamin A. The nuclear lamina regulates *Per1* expression through temporal localisation to and from the nuclear periphery in a circadian manner (Zhao, *et al*., 2015). This research is consistent with the findings in this chapter and supports a mechanism of feedback regulation by lamin A to the core clock.

4.6 Conclusion

To conclude, this research provides supportive data identifying a relationship between lamin A and the circadian clock. Manipulation of lamin A through overexpression and knockdown experiments disrupted core clock gene expression in C2C12 undifferentiated myoblasts, observed in both transient and circadian time-course samples. Future research may uncover the mechanism of regulation by lamin A to the circadian clock, and identify if the loss of circadian cycling in laminopathy patients contributes to tissue-specific defects.

5. A role for mechanobiology in regulating the circadian clock in musculoskeletal cells through lamin A associated mechanisms?

5.1 Introduction

5.1.1 The Suprachiasmatic Nucleus and Exercise

The development and homeostasis of muscle is reliant on functional circadian rhythms and exercise. The skeletal muscle transcriptome oscillates with a circadian rhythm; this includes genes that regulate myogenesis such as *MyoD* and *Myogenin* (McCarthy, *et al*., 2007; Andrews, *et al*., 2010; Shavlakadze, *et al*., 2013). The importance of functioning circadian rhythms in muscle can be demonstrated through mutating circadian genes and observing the response in musculoskeletal cells and in mouse models. C2C12 myoblasts with *Bmal1* knockout have suppressed expression of *MyoD*, *Myogenin*, and *Myf6*, and an impaired capacity to differentiate (Chatterjee, *et al*., 2013). This impairment in musculoskeletal tissues was also observed in primary myoblasts isolated from *Bmal1* knockout mice (Chatterjee, *et al*., 2013). Furthermore, in comparison to wild type mouse muscle, *Clock*$^{-/-}$ mice demonstrated altered transcription in 35% of the skeletal muscle transcriptome (McCarthy, *et al*., 2007). Moreover, exercise has the ability to feedback and modify circadian rhythms in mice (Edgar and Dement, 1991; Marchant and Mistlberger, 1996; Yamanaka, *et al*., 2008). Scheduled exercise in mice during the day and early during the dark phase dampened the oscillations of *Per1* and *Per2*, and *Per2* in the SCN, respectively (Maywood, *et al*., 1999; Schroeder, *et al*., 2012). Additionally, in humans, scheduled night-time exercise shifted and delayed the SCN circadian clock, observed through a shift in hormone oscillations such as melatonin (Barger, *et al*., 2004). Exercise also was also sufficient to accelerate the re-entrainment of the sleep-wake cycle to an 8-hour phase-advanced cycle; melatonin levels revealed that this re-entrainment was independent from the SCN (Yamanaka, *et al*., 2010). Hence, functioning circadian rhythms are

important in muscle development and maintenance, and muscular activity sends feedback information to the SCN as a time cue, or zeitgeber, to synchronise the circadian clock.

5.1.2 Skeletal muscle peripheral clock and exercise

Exercise synchronises the peripheral clocks, including those in skeletal muscle, independently from the SCN; however, the mechanism of how these signals are communicated remains unknown. The skeletal muscle circadian clock can be re-synchronised independently of the SCN by the zeitgeber exercise. Consequently, the peripheral clocks in skeletal muscle become synchronised to the behavioural activity of exercise. CLOCK protein in cardiac myocytes is localised at the Z-disk and in response to contractile activity, CLOCK protein production and its translocation into the nucleus is increased (Qi and Boateng, 2006). Furthermore, decreasing contractile activity significantly reduced the levels of CLOCK protein in the nucleus (Qi and Boateng, 2006). Exposure of Per2::Luc mice to 2 hours of voluntary or involuntary exercise for 4 weeks shifted the skeletal muscle clock, examined through real-time bioluminescent imaging of soleus, FDB, and EDL muscles (Wolff and Esser, 2012). Despite research identifying that the peripheral clocks in musculoskeletal tissues are synchronised by exercise, this mechanism of synchronisation has not been uncovered.

The ability of exercise to entrain circadian clocks within skeletal muscle ensures that muscle cells are synchronised to the correct time-of-day in accordance with environmental activities. The coupling of exercise with circadian rhythm temporal regulation is emerging as a vital role in the maintenance and health of skeletal muscle (Chatterjee and Ma, 2016). How circadian rhythms are regulated by mechanical stimulation and how circadian rhythms may be affected in chronic diseases of muscle is an exciting new area of research. Advances in this area may utilise exercise to manipulate and maintain effective circadian rhythms, and downstream clock-controlled regulation, with the aim of restoring temporal tissue-specific gene regulation and muscle health.

5.1.3 Mechanosensitive Lamins

Lamin A is mechanosensitive; cells that experience higher proportions of mechanical load, such as bone, have higher levels of lamin A (Swift, *et al*., 2013). Lamin A increases respectively with load to ensure that cells are protected against an increase in mechanical stimulation. Lamin A structurally protects the nucleus, preventing DNA damage, and can facilitate the regulation of mechanotransduction pathways and muscle-specific gene regulation through genome organisation and transcription factor regulation (Markiewicz, Ledran, and Hutchison, 2005; Mazumder and Shivashankar, 2010; Osmanagic-Myers, Dechat, and Foisner, 2015). Muscle cells experience mechanical strain in response to active/rest diurnal cycles. During behavioural exercise periods, the muscle is active and the cells are strained; this activity oscillates with a circadian rhythm. Previous research in this thesis demonstrated rhythmic oscillations in the levels of lamin A protein in musculoskeletal tissues, and a coupling of lamin A with the circadian clock through lamin A induced circadian gene upregulation (see Chapter 3, Figure 3.1 and Figure 3.3; Chapter 4, Figure 4.3 and Figure 4.11). As lamin A is mechanosensitive and relays mechanical stimulation signals to the nucleus to regulate mechanical signalling pathways, it was predicted that the relationship between lamin A and the circadian clock further includes regulation that communicates synchronising, time-keeping signals to the clock in response to exercise.

5.2 A non-invasive murine joint loading model

5.2.1 Benefits of an *in vivo* model

While *in vitro* and *ex vivo* experiments provide useful data, to understand the complexity of mechanobiology and the circadian clock, an *in vivo* model is required. Myoblasts or myotubes subject to mechanical stimulation *in vitro* will lack systemic signals, often important in circadian homeostasis. Hence, incorporating an *in vivo* model into this research facilitated more appropriate investigations into the effect of mechanical strain on circadian clock gene expression in specific muscles of interest. This research had the opportunity to collect muscle tissue from an *in vivo*

loading study and the aim was to determine whether, within the whole organism, the musculoskeletal circadian clock genes respond to acute and chronic loading regimes (undertaken to induce femorotibial joint osteoarthritis (OA)) through non-invasive loading in the knees of mice.

5.2.2 *in vivo* loading model

Non-invasive mechanical loading can be applied to the joint of a chosen animal model. This was first developed in rabbits as an *in vivo* model to produce and study OA in the joint, and was proposed as a less aggressive alternative to surgical models (Radin, *et al*., 1978). The model used in this *in vivo* study was first designed and described by Poulet *et al*. and samples were a kind gift from Blandine Poulet (Poulet, *et al*., 2011). The novel mechanism held the mouse tibia of the right knee in place with a baseline load of 2N. A force of 9N was applied to the tibia for 0.05 seconds, with a rise and fall time of 0.025 seconds, and the tibia was held at baseline load for 9.99 seconds in between peak loads (Figure 2.6). This was repeated for 40 cycles and produced no adverse side effects, mice walked normally on both their hind limbs immediately post-loading (Poulet, *et al*., 2011). Repetitive mechanical loading damages articular cartilage, modifies subchondral bone, and thickens epiphyseal trabecular bone, which are all characteristics of OA pathology (Poulet, *et al*., 2015).

5.3 Hypothesis and Aims

5.3.1 Hypothesis

The circadian clock in musculoskeletal tissues responds to *in vitro* and *in vivo* mechanical strain, investigated through utilising an *in vitro* cell culture loading device and an *in vivo* mechanical loading system, and lamin A is responsible for communicating this response.

5.3.2 Aims

- Determine whether circadian gene expression in musculoskeletal cells responds to *in vitro* cyclical strain.
- Observe whether the response in circadian clock gene expression to mechanical strain is altered following knockdown of lamin A.
- Utilise an *in vivo* loading model to determine whether the muscle circadian clock is responsive to loading, using two different loading protocol regimes.

5.4 Results

5.4.1 Clock genes in myoblasts are unchanged in response to *in vitro* strain

5.4.1.1 *In vitro* mechanical stimulation of C2C12 myoblasts does not lead to changes in *Lmna* expression

To investigate whether the circadian clock in undifferentiated myoblasts respond to mechanical stimulation, the cell culture-loading device the Flexcell machine (Flexcell International) was used. C2C12 myoblasts were seeded into Bioflex 6-well plates (Flexcell international), with wells containing a PDMS membrane coated with laminin, and at 60% confluency were loaded for 24 hours on the Flexcell machine at 6.66% strain and at a frequency of 1Hz, with no effect on myoblast viability (Figure 5.1). The myoblasts were collected straight after the loading period finished in Purezol (Biorad) and analysed by qRT-PCR and Western blotting, both normalised to β-Actin. Between static and loaded myoblasts, no change was identified in lamin A protein and a significant change in *Lmna* mRNA was identified (Figure 5.2 and Figure 5.3; F-test of variance, $p \leq 0.05$).

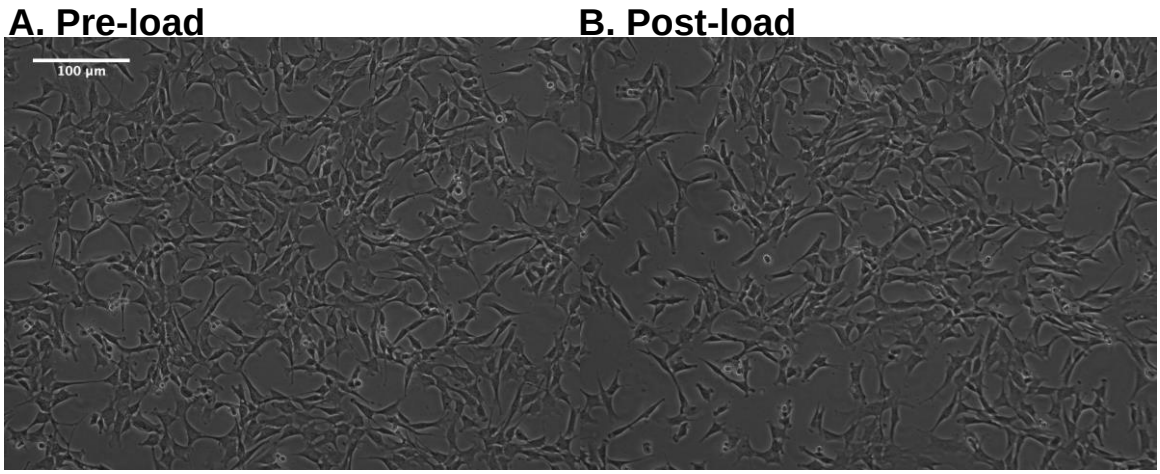

Figure 5.1. C2C12 myoblasts seeded onto laminin coated Bioflex plates loaded on the Flexcell machine, demonstrating loading has no effect on C2C12 viability. A. Myoblasts prior to loading grown in (DMEM supplemented with 10% FBS, 2nM L-Glu, 0.1mg/mL P/S). B. Myoblasts post 24 hours of 6.66% strain at a frequency of 1Hz.

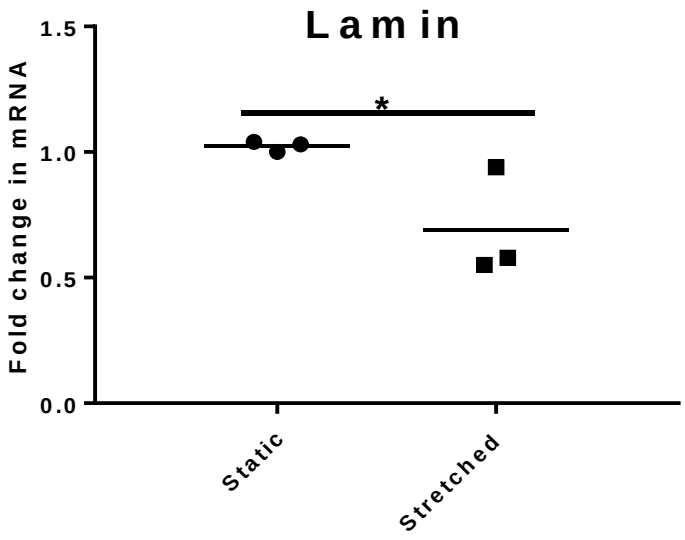

Figure 5.2. Lamin A gene expression in C2C12 myoblasts loaded on the Flexcell machine for 24 hours at 6.66% strain, demonstrate no change in *Lmna* expression compared to static control. C2C12 myoblasts were seeded onto Bioflex plates consisting of silicone wells coated with laminin. After 24 hours the chambers were loaded on the Flexcell machine for 24 hours at 6.66% strain before collection in Purezol. *Lmna* mRNA was analysed by qRT-PCR using the Pfaffl method and normalised to house-keeping gene *β-actin* (Pfaffl, 2001). Data were expressed as fold change relative to static control which was expressed as 1 and presented as means (F-test of variance, *p≤0.05, three independent experiments n=3).

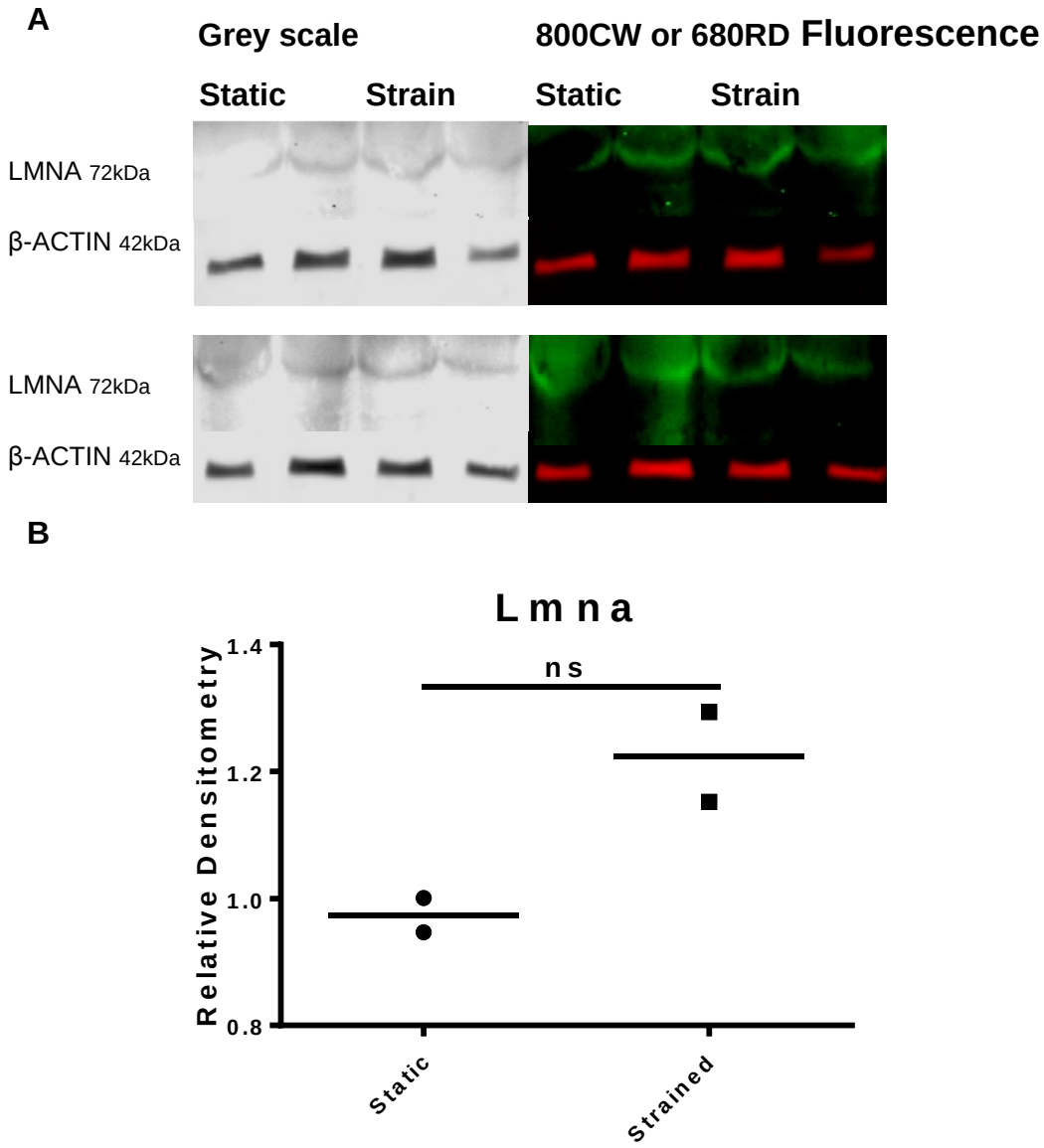

Figure 5.3. Representative Western blot images and densitometry analysis of lamin A protein expression in C2C12 myoblasts loaded on the Flexcell machine for 24 hours at 6.66% strain, demonstrates no change in LMNA. (A) Protein samples were ran on 10% acrylamide gels, transferred, and incubated with primary antibodies for anti-mouse Lmna (Sigma; 1:2000) and anti-rabbit β-Actin (Sigma; 1:2000) followed by secondary antibodies for goat anti-rabbit 800CW and goat anti-mouse 680RD (Licor; 1:20000). (B) Densitometry values were calculated using the analysis software provided by Image Studio Lite Version 5.2. LMNA bands were normalised to β-ACTIN. Data were expressed as % change relative to static which was expressed as 1 and presented as means (unpaired t-test, ns= $p>0.05$, two independent experiments n=2).

5.4.1.2 *In vitro* mechanical stimulation of C2C12 undifferentiated myoblasts does not lead to changes in clock gene expression

To determine whether the circadian clock in C2C12 myoblasts is responsive to 24 hours 6.66% strain on the Flexcell machine, qRT-PCR was used to analyse circadian clock gene expression between static and loaded C2C12 myoblast samples. Results were normalised to *β-Actin*. An F-test of variance identified a significant change in the expression of *Per1*, *Per2*, *Cry*, and *Bmal* between static and strained samples, and there was no change in the expression of *Rev-erbα* or *Clock* (Figure 5.4; unpaired t-test, $p \leq 0.05$, $p \leq 0.01$).

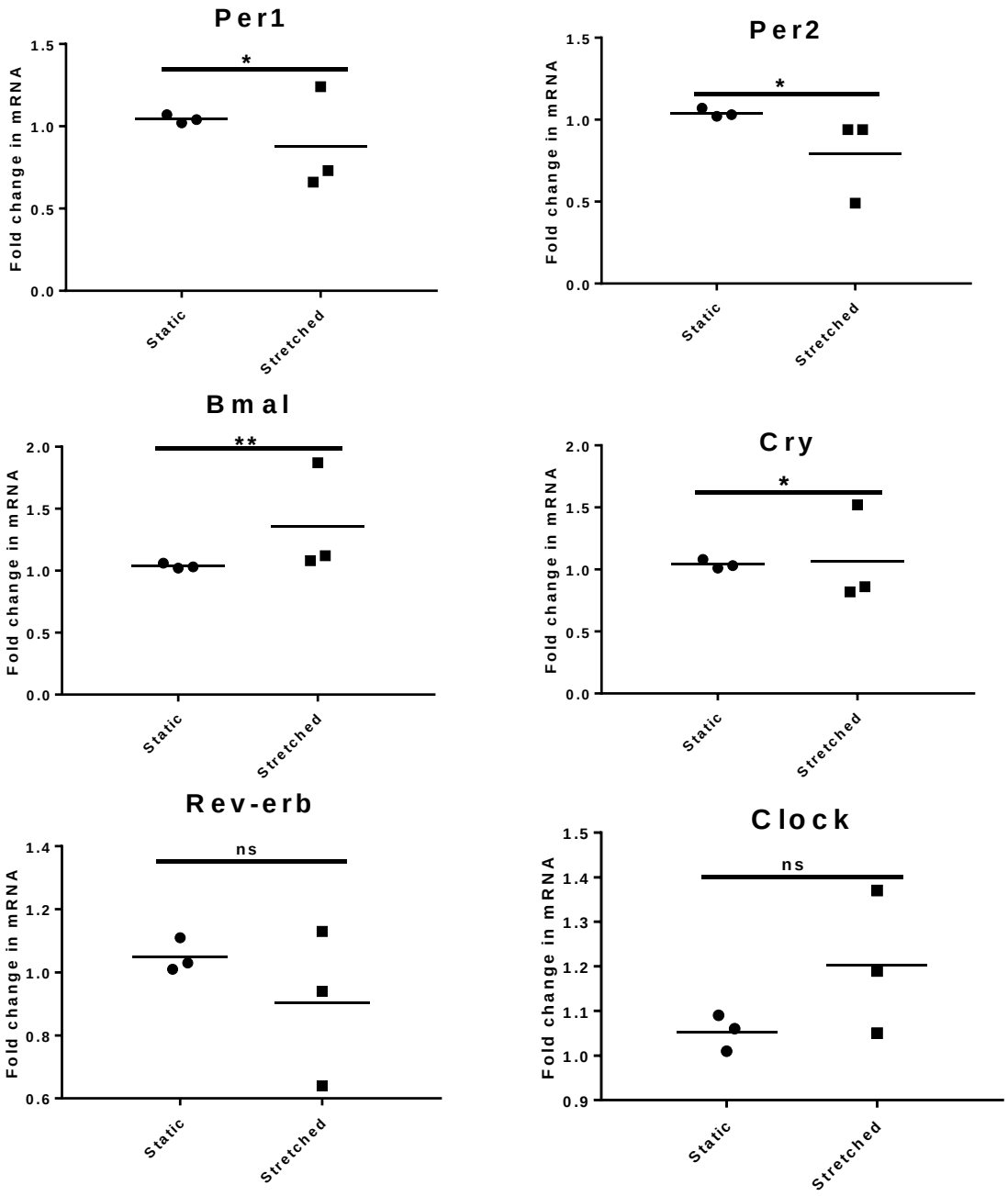

Figure 5.4. Circadian clock gene expression in C2C12 myoblasts loaded on the Flexcell machine for 24 hours at 6.66% strain, demonstrate no change in expression. C2C12 myoblasts were seeded onto Bioflex plates consisting of silicone wells coated with laminin. After 24 hours the chambers were loaded on the Flexcell machine for 24 hours before collection in Purezol. Circadian mRNA was analysed by qRT-PCR using the Pfaffl method and normalised to house-keeping gene *β-actin* (Pfaffl, 2001). Data were expressed as fold change relative to static control which was expressed as 1 and presented as means (F-test of variance, *p≤0.05, **p≤0.01, ns= p>0.05, three independent experiments n=3).

5.4.1.3 *In vitro* mechanical stimulation increases *Lmna* mRNA expression in primary myoblasts

To determine whether the circadian clock in undifferentiated primary muscle cells responds to mechanical strain Per2::Luc primary myoblasts were seeded into laminin coated Bioflex plates and, at 70% confluency, were loaded dynamically for 24 hours on the Flexcell machine at 6.66% strain with a frequency of 1Hz. There was no effect on primary myoblast viability (Figure 5.5). The myoblasts were collected straight after the loading period finished in Purezol and analysed by qRT-PCR and western blotting, both normalised to β-Actin. qRT-PCR data demonstrated an increase in lamin A mRNA expression in loaded myoblasts compared to static control (Figure 5.6; unpaired t-test, $p \leq 0.05$). Protein data demonstrated no change in lamin A levels (Figure 5.7).

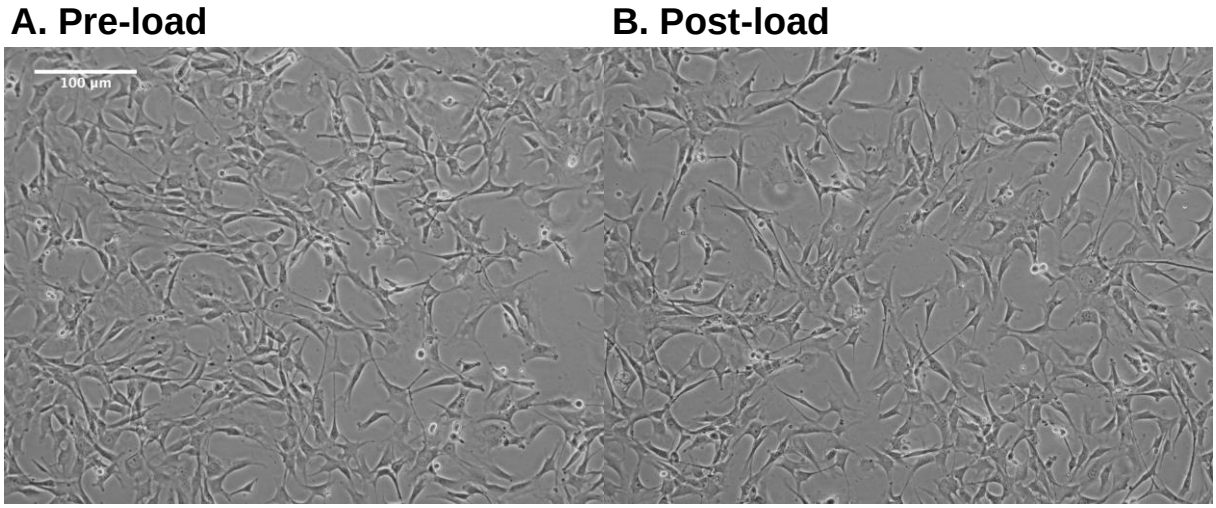

Figure 5.5. Per2::Luc primary myoblasts seeded onto laminin coated Bioflex plates loaded on the Flexcell machine demonstrate no change to primary myoblast viability. A. Myoblasts prior to loading. B. Myoblasts post 24 hours of load at 6.66% strain. Per2::Luc primary myoblasts were seeded onto Bioflex plates consisting of silicone wells coated with laminin in normal primary animal media (DMEM supplemented with 10% FBS, 5% HS, 2nM L-Glu, 0.1mg/mL P/S).

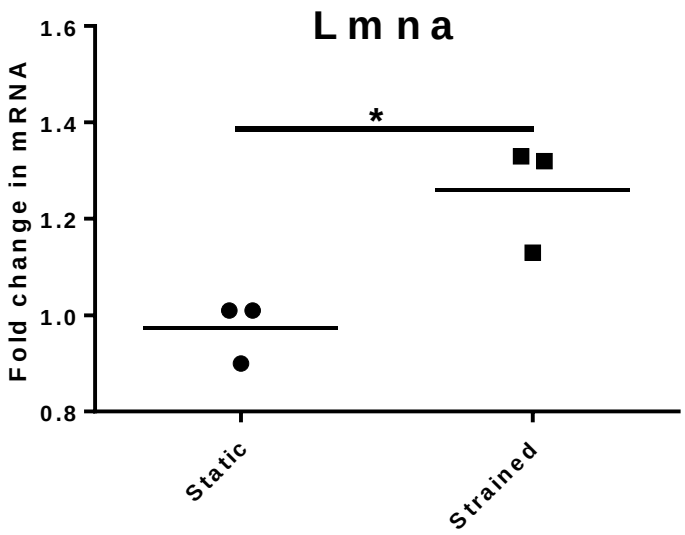

Figure 5.6. Lamin A gene expression in Per2::Luc primary myoblasts loaded on the Flexcell machine for 24 hours at 6.66% strain, demonstrate *Lmna* expression upregulation. Per2::Luc myoblasts were seeded onto laminin coated Bioflex plates, after 24 hours they were loaded on the Flexcell machine for 24 hours at 6.66% strain before collection in Purezol. *Lmna* mRNA was analysed by qRT-PCR using the Pfaffl method and normalised to house-keeping gene *β-actin* (Pfaffl, 2001). Data were expressed as fold change relative to static control which was expressed as 1 and presented as means (unpaired t-test, *p≤0.05, three independent experiments n=3).

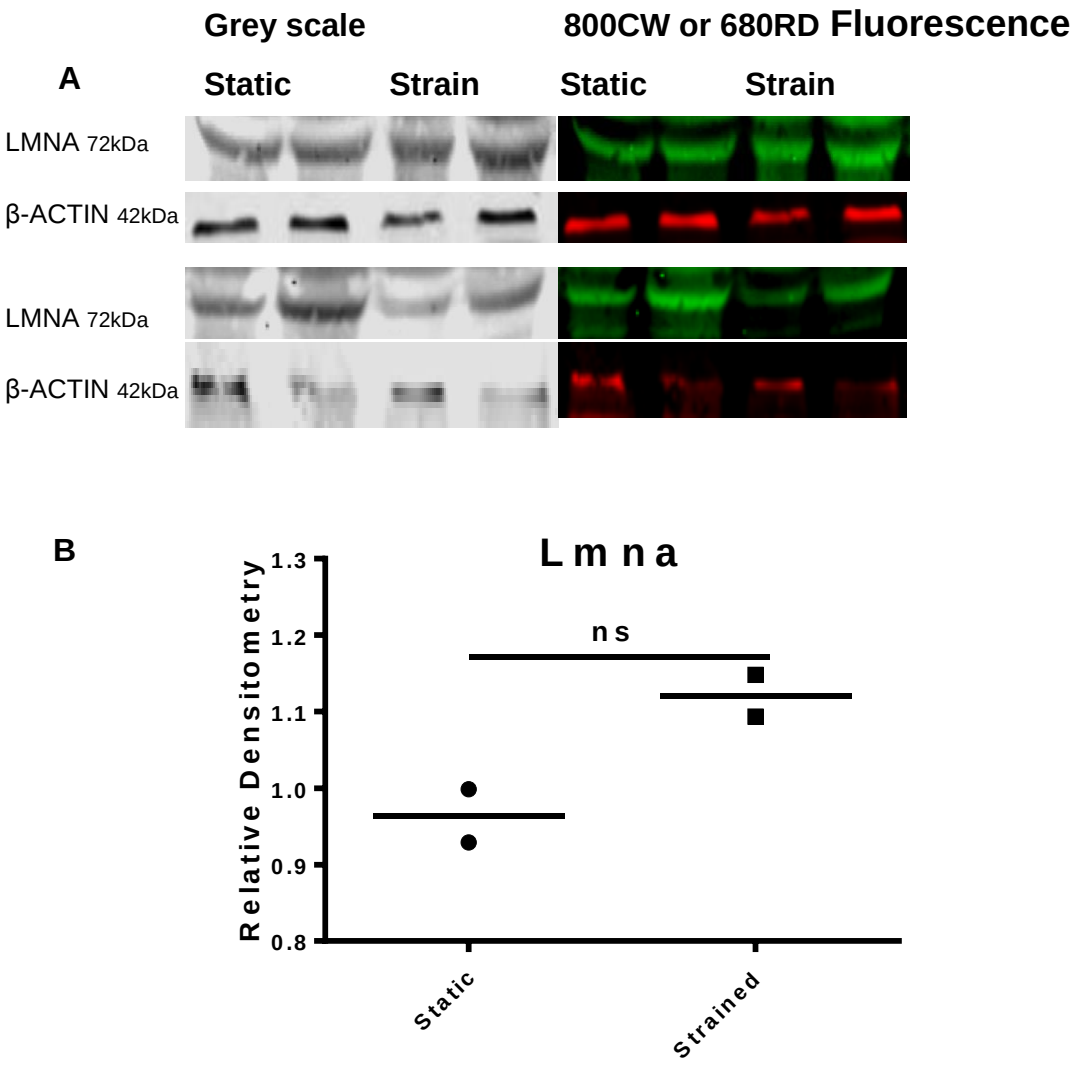

Figure 5.7. Representative Western blot images and densitometry analysis of lamin A protein expression in Per2::Luc primary myoblasts loaded for 24 hours on the Flexcell machine at 6.66% strain, demonstrates no change in LMNA. (A) Protein samples were ran on 10% acrylamide gels, transferred, and incubated with primary antibodies for anti-mouse Lmna (Sigma; 1:2000) and anti-rabbit β-Actin (Sigma; 1:2000) followed by secondary antibodies for goat anti-rabbit 800CW and goat anti-mouse 680RD (Licor; 1:20000). (B) Densitometry values were calculated using the analysis software provided by Image Studio Lite Version 5.2. LMNA bands were normalised to β-ACTIN. Data were expressed as % change relative to static which was expressed as 1 and presented as means (unpaired t-test, ns= $p>0.05$, two independent experiments n=2).

5.4.1.4 *In vitro* strain decreases *Cry1* mRNA expression in primary myoblasts

To determine whether the circadian clock in primary Per2::Luc myoblasts was responsive to *in vitro* strain on the Flexcell machine, qRT-PCR was used to analyse circadian clock gene expression between static and strained primary myoblast samples. Results were normalised to *β-Actin*. The loaded samples had a decrease in *Cry1* expression on comparison to the static samples (Figure 5.8; unpaired t-test, $p \leq 0.01$). An F-test of variance identified a significant change in the expression of *Bmal* and *Rev-erbα* (Figure 5.8; $p \leq 0.05$ and $p \leq 0.01$). There was no change in the expression of *Per1*, *Per2*, and *Clock* (Figure 5.8).

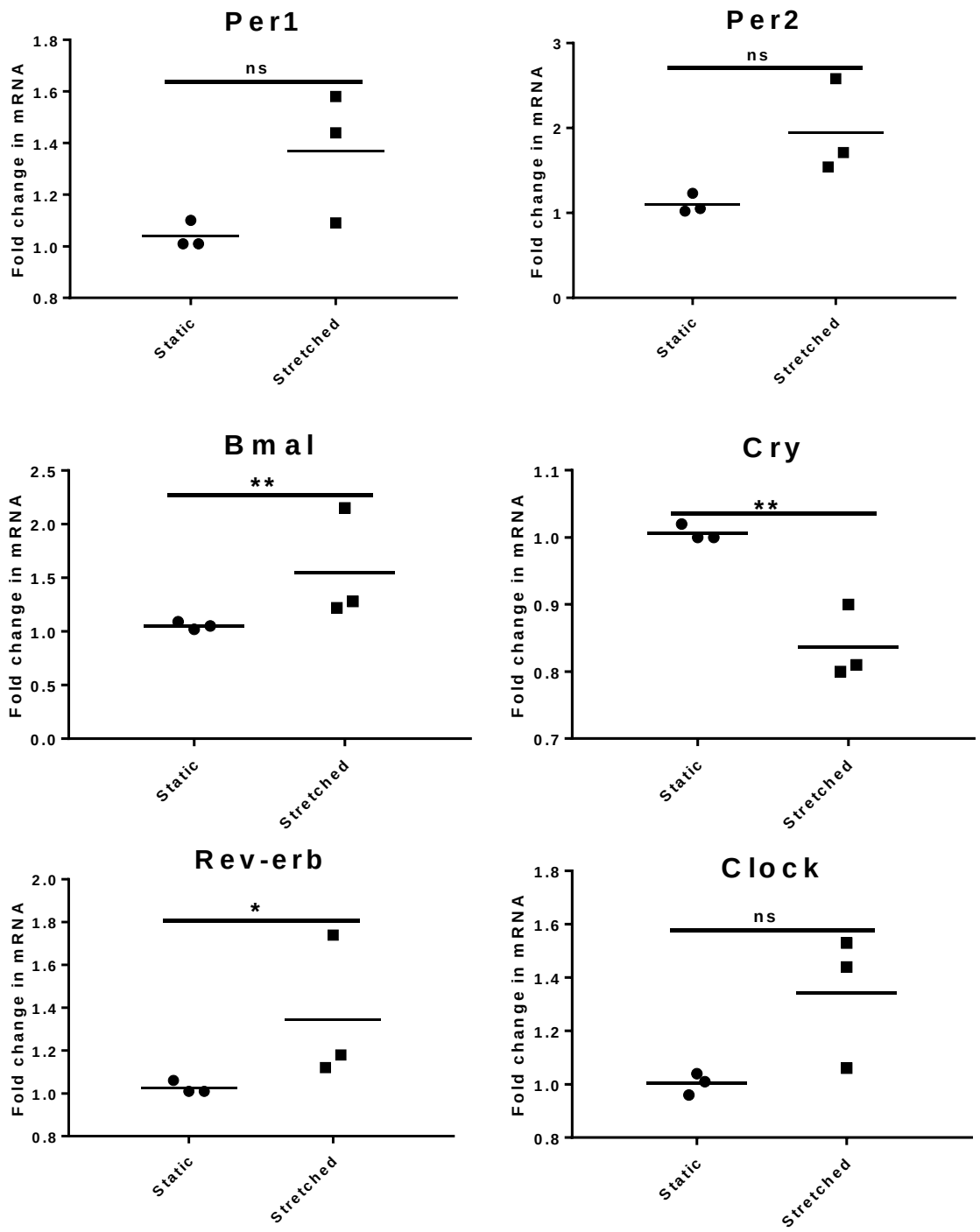

Figure 5.8. Circadian gene expression in primary myoblasts isolated from Per2::Luc mice and loaded for 24 hours on the Flexcell machine at 6.66% strain, demonstrate *Cry1* repression. Primary Per2::Luc myoblasts were seeded onto laminin coated Bioflex plates, after 24 hours, they were loaded on the Flexcell machine for 24 hours before collection in Purezol. Circadian mRNA was analysed by qRT-PCR using the Pfaffl method and normalised to house-keeping gene *β-actin* (Pfaffl, 2001). Data were expressed as fold change relative to static control which was expressed as 1 and presented as means (unpaired t-test, **p≤0.01, ns= p>0.05, three independent experiments n=3; *Bmal1* and *Rev-erbα* analysed by an F-test of variance, *p≤0.05, **p≤0.01).

5.4.1.5 Real-time Bioluminescent imaging confirms variable response of *Bmal1* to 24-hour *in vitro* strain

In order to dynamically visualise the effect of mechanical stimulation on the circadian clock in myoblasts, the next aim was to subject Bmal1::Luc C2C12 myoblasts to *in vitro* Flexcell strain and place them into the LumiCycle. The bioluminescence signal was read in real-time and allowed us to infer patterns of *Bmal1* expression. In comparison to the static control samples, the loaded samples show a variable response in *Bmal1* expression. The blue and purple loaded traces of *Bmal1* expression demonstrate dampened and increased amplitude oscillations, respectively (Figure 5.9).

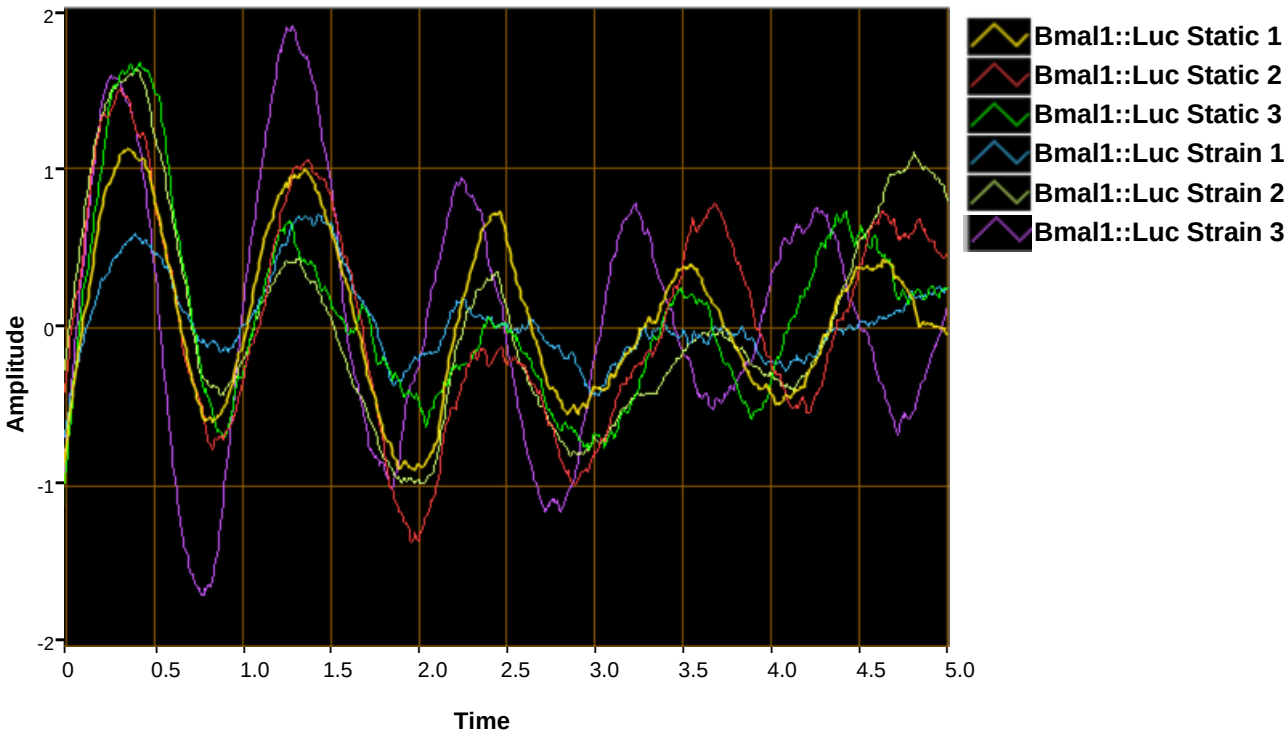

Figure 5.9 Real-time bioluminescent imaging of Bmal1::Luc myoblasts loaded on the Flexcell for 24 hours at 6.66% strain compared to the static control, demonstrate variable response to strain. Bmal1::Luc myoblasts were seeded into Bioflex plates coated with laminin, at 60% confluency they were subject to 6.66% strain for 24 hours on the Flexcell machine. The silicone membrane containing the Bmal1::Luc myoblasts was removed from the plate and placed into 35mm dishes suitable for the LumiCycle with LumiCycle media (Phenol red-free media supplemented with 5% FBS, 10 mM Hepes (Sigma), 1 mM Sodium Pyruvate (Sigma), 2nM L-Glu, 0.1mg/mL P/S, and 100nM Luciferin (Promega)).

5.4.2 Differentiated myotubes produce variable results when subject to *in vitro* strain

5.4.2.1 Differentiated C2C12 myotubes have no change in *Lmna* expression after *in vitro* strain

Next, it was investigated whether lamin A and the circadian clock in differentiated, synchronised C2C12 myotubes are responsive to mechanical strain. C2C12 myoblasts were seeded into Bioflex plates and at 50% confluency, were differentiated for 10 days through the addition of differentiation media. The myotubes were next synchronised by serum shock for 2 hours then subject to *in vitro* loading for 24 hours on the Flexcell machine (Figure 5.10). Myotubes were collected in Purezol immediately after the loading period and were analysed by qRT-PCR and western blotting, both normalised to β-actin. Gene expression and protein level analysis of lamin A demonstrated no change in lamin A expression or protein levels between static and loaded samples (Figure 5.11 and Figure 5.12).

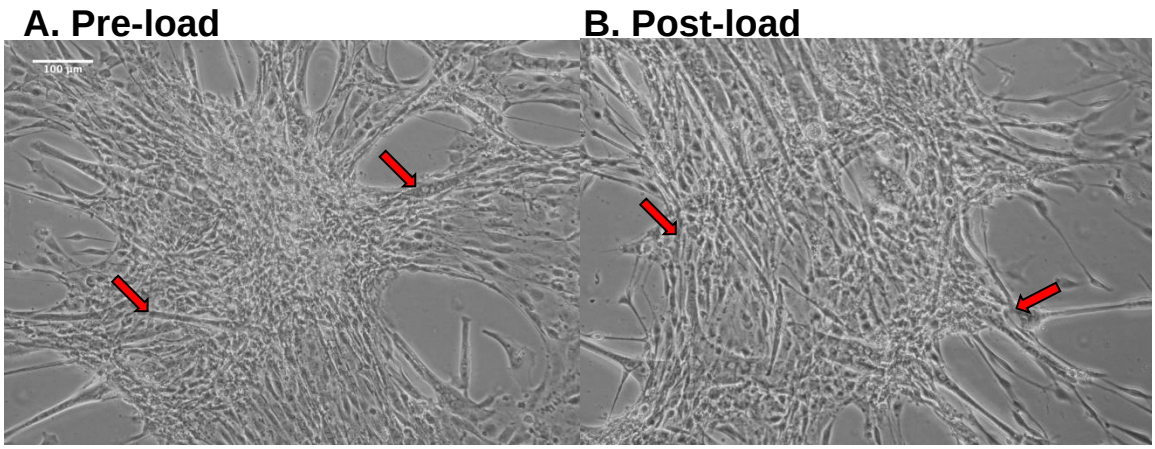

Figure 5.10. C2C12 myoblasts seeded onto Bioflex plates and differentiated into myotubes for 10 days, myotubes are highlight with red arrows, demonstrate no change in myotube viability. A. Prior to loading B. Post 24-hour loading at 6.66% strain on the Flexcell machine.

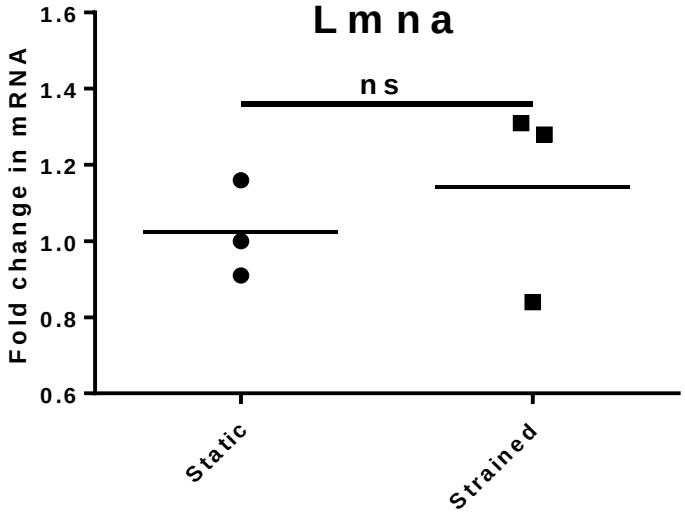

Figure 5.11. Lamin A gene expression in differentiated C2C12 myotubes loaded for 24 hours at 6.66% strain on the Flexcell machine demonstrate no change in *Lmna* expression. C2C12 myoblasts were seeded onto Bioflex plates consisting of silicone wells coated with laminin. They were differentiated into myotubes for 10 days in differentiation media, synchronised by serum shock for 2 hours, and after 24 hours, they were loaded on the Flexcell machine for 24 hours before collection in Purezol. *Lmna* mRNA was analysed by qRT-PCR using the Pfaffl method and normalised to house-keeping gene *β-actin* (Pfaffl, 2001). Data were expressed as fold change relative to static control which was expressed as 1 and presented as means (unpaired t-test, ns= $p>0.05$, three independent experiments n=3).

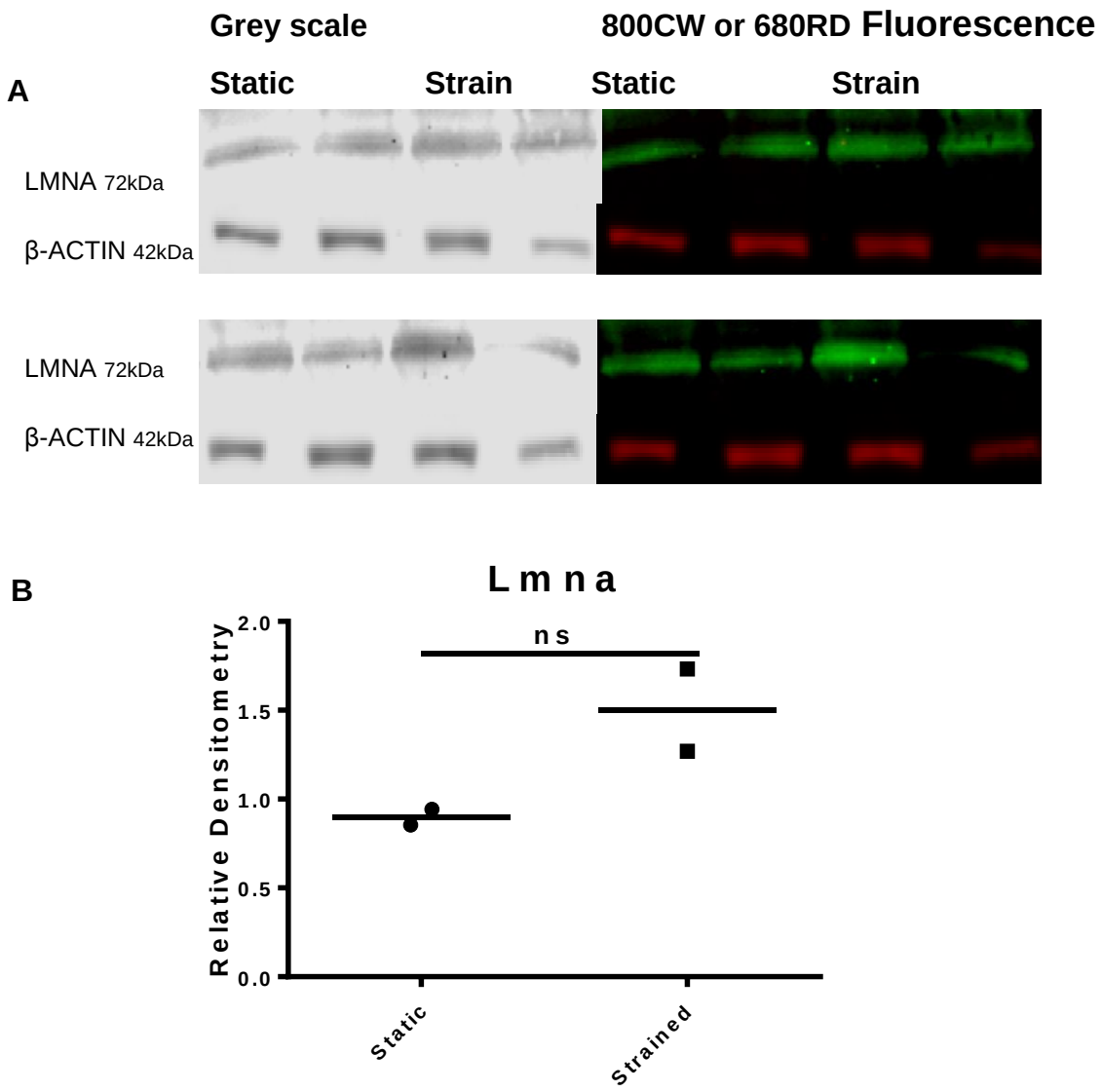

Figure 5.12. Representative Western blot images and densitometry analysis of lamin A protein expression in differentiated C2C12 myotubes loaded for 24 hours on the Flexcell machine, demonstrates no change in LMNA. (A) Protein samples were ran on 10% acrylamide gels, transferred, and incubated with primary antibodies for anti-mouse Lmna (Sigma; 1:2000) and anti-rabbit β-Actin (Sigma; 1:2000) followed by secondary antibodies for goat anti-rabbit 800CW and goat anti-mouse 680RD (Licor; 1:20000). (B) Densitometry values were calculated using the analysis software provided by Image Studio Lite Version 5.2. LMNA bands were normalised to β-ACTIN. Data were expressed as % change relative to static which was expressed as 1 and presented as means (unpaired t-test, ns= $p>0.05$, two independent experiments n=2).

5.4.2.2 Differentiated C2C12 myotubes have an increase in *Cry1* and *Bmal1* gene expression after *in vitro* strain

To investigate whether there was a response to 24-hour *in vitro* Flexcell strain observed in circadian clock gene expression, qRT-PCR was used to analyse circadian clock gene expression between static and loaded C2C12 myotube samples. Results were normalised to *β-Actin*. There was an increase in *Bmal1* and *Cry1* expression in loaded samples compared to static samples (Figure 5.13; unpaired t-test, $p \leq 0.01$). An F-test of variance identified a significant change in Per2 expression (Figure 5.13, $*p \leq 0.05$). There was no change in the expression of the remaining circadian genes (Figure 5.13).

These results demonstrated *Bmal1* and *Cry1* gene expression was responsive to mechanical stimulation in C2C12 myotubes, through subjecting them to 24-hour *in vitro* Flexcell strain. Unfortunately, this result was accompanied by no change in lamin A expression. Accordingly, this supports the hypothesis that circadian gene expression is responsive to mechanical strain; however, there is high variability and no significant change in the response of *Lmna* expression to mechanical strain in myotubes compared to static control samples.

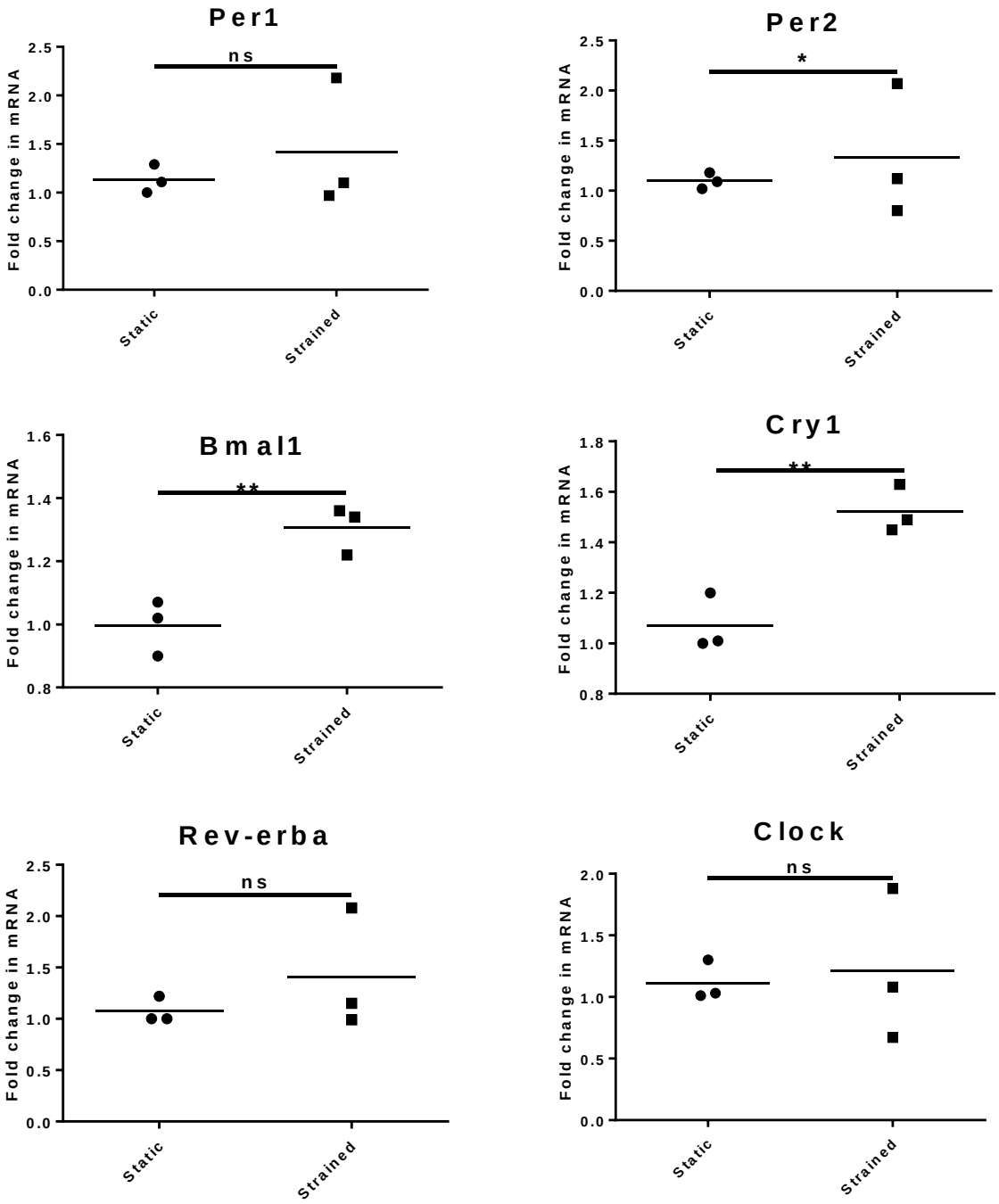

Figure 5.13. Circadian clock gene expression in C2C12 differentiated myotubes loaded at 6.66% strain on the Flexcell machine, demonstrates upregulation of *Bmal1* and *Cry1* expression. C2C12 myoblasts were seeded onto Bioflex plates consisting of silicone wells coated with laminin. They were differentiated in myotubes for 10 days in differentiation media, synchronised by serum shock for 2 hours, and after 24 hours, they were loaded on the Flexcell machine for 24 hours before collection in Purezol. Circadian mRNA was analysed by qRT-PCR using the Pfaffl method and normalised to house-keeping gene *β-actin* (Pfaffl, 2001). Data were expressed as fold change relative to static control which was expressed as 1 and presented as means (unpaired t-test, **p≤0.01, ns = P>0.05, three independent experiments n=3; *Per1* analysed by an F-test of variance, *p≤0.05).

5.4.2.3 Primary differentiated myotubes subject to *in vitro* strain have no change in *Lmna* expression

To investigate whether the circadian clock in differentiated primary muscle cells responded to mechanical stimulation, primary Per2::Luc myoblasts were seeded into Bioflex plates and at 50% confluency, were differentiated for 10 days through the addition of differentiation media. After 10 days differentiation, the myotubes were synchronised by serum shock for 2 hours and loaded for 24 hours on the Flexcell machine at 6.66% strain and at a frequency of 1Hz (Figure 5.14). Myotubes were collected straight after the loading period in Purezol, and analysed by qRT-PCR and western blotting. There was no change in the expression of *Lmna* in the primary myotubes (Figure 5.15). In contrast, there was an increase in the levels of lamin A protein (Figure 5.16; unpaired t-test, $p \leq 0.01$).

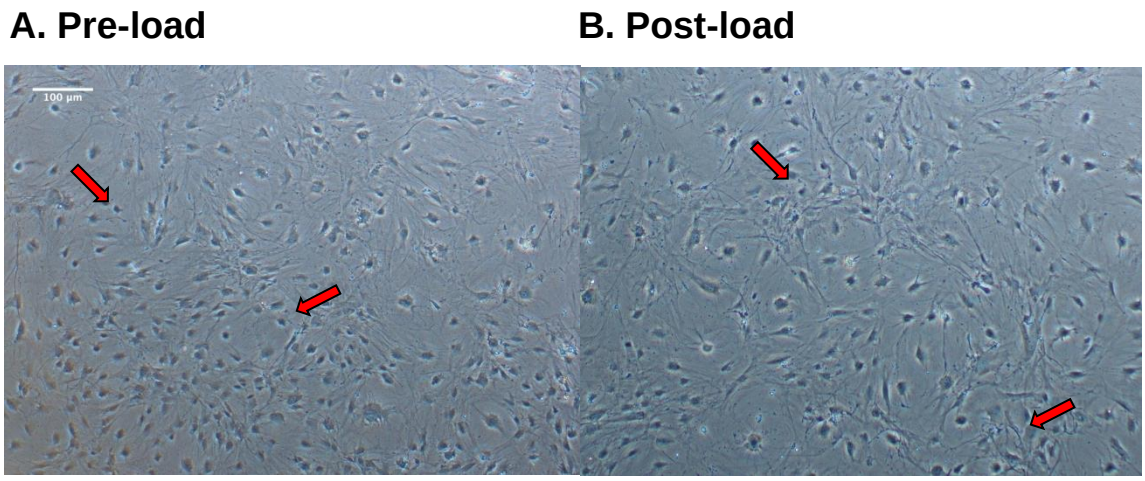

Figure 5.14. Primary myoblasts seeded onto Bioflex plates and differentiated into myotubes for 10 days, myotubes highlighted by red arrows and demonstrate no loss in viability. A. Prior to loading. B. Post 24-hour loading at 6.66% strain on the Flexcell machine.

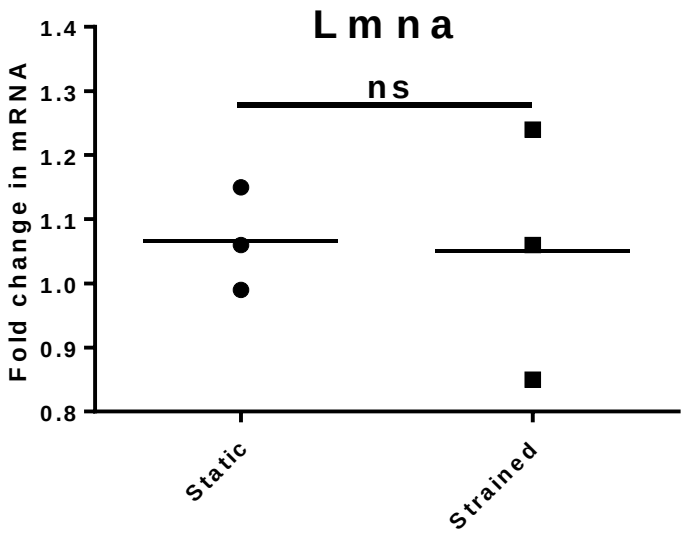

Figure 5.15. Lamin A gene expression in primary differentiated myotubes loaded for 24 hours on the Flexcell machine at 6.66% strain, demonstrate no change in *Lmna* expression. C2C12 myoblasts were seeded onto Bioflex plates consisting of silicone wells coated with laminin. They were differentiated in myotubes for 10 days in differentiation media, synchronised by serum shock for 2 hours, and after 24 hours, they were loaded on the Flexcell machine for 24 hours before collection in Purezol. *Lmna* mRNA was analysed by qRT-PCR using the Pfaffl method and normalised to house-keeping gene *β-actin* (Pfaffl, 2001). Data were expressed as fold change relative to static control which was expressed as 1 and presented as means (unpaired t-test, ns= $p>0.05$, three independent experiments n=3).

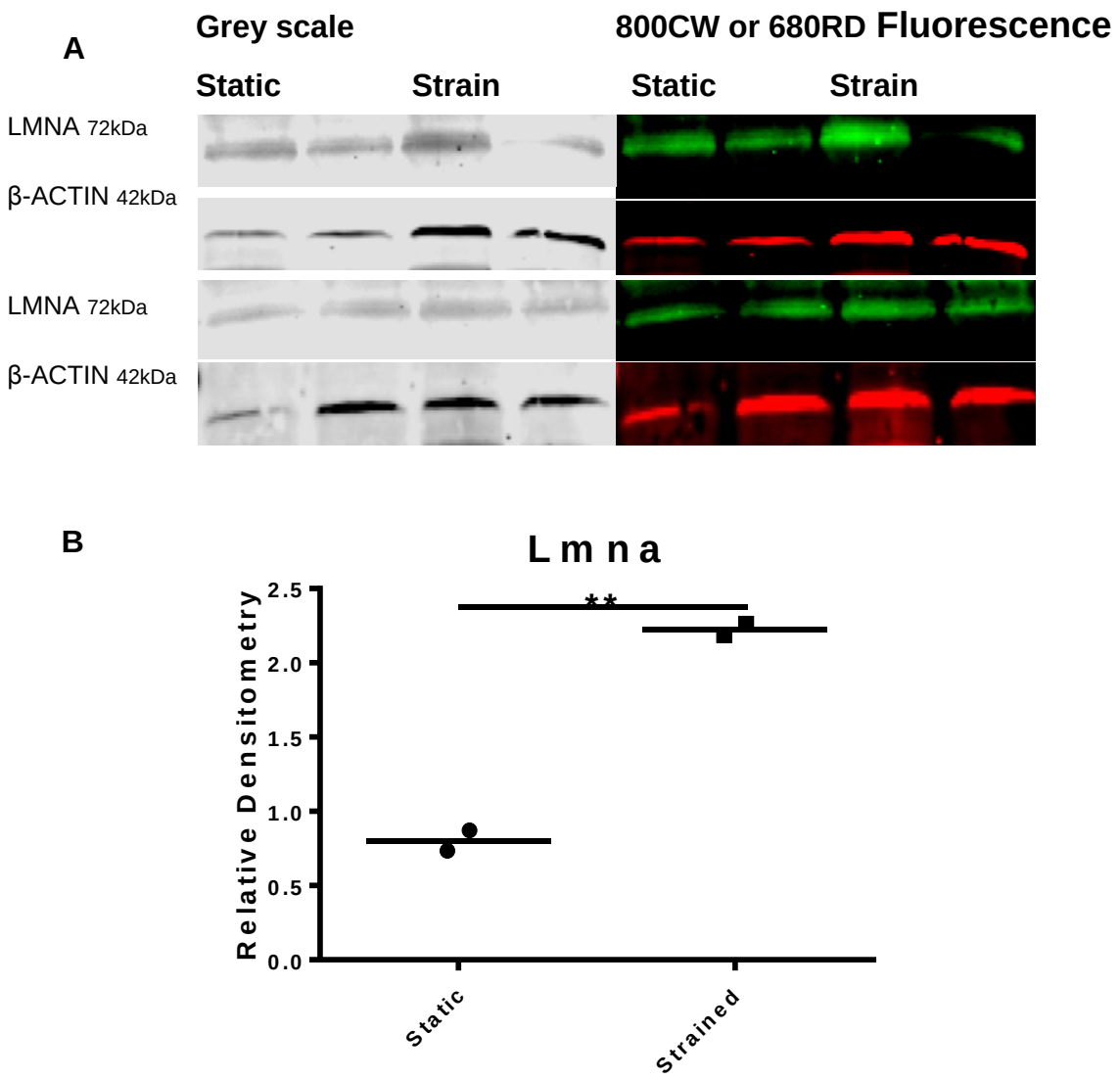

Figure 5.16. Representative Western blot images and densitometry analysis of lamin A protein expression in differentiated primary myotubes loaded for 24 hours on the Flexcell machine at 6.66% strain, demonstrates LMNA increase. (A) Protein samples were ran on 10% acrylamide gels, transferred, and incubated with primary antibodies for anti-mouse Lmna (Sigma; 1:2000) and anti-rabbit β-Actin (Sigma; 1:2000) followed by secondary antibodies for goat anti-rabbit 800CW and goat anti-mouse 680RD (Licor; 1:20000). (B) Densitometry values were calculated using the analysis software provided by Image Studio Lite Version 5.2. LMNA bands were normalised to β-ACTIN. Data were expressed as % change relative to static which was expressed as 1 and presented as means (unpaired t-test, **p≤0.01, two independent experiments n=2).

5.4.2.4 Primary differentiated myotubes have no alterations in circadian gene expression following *in vitro* strain

Next, it was investigated whether *in vitro* loading resulted in any changes to circadian clock gene expression in myotube samples, by using qRT-PCR to analyse circadian gene expression. An F-test of variance identified that loading induced a significant change in the levels of the circadian clock genes examined: *Per1*, *Per2*, *Bmal1*, *Cry1*, *Clock*, and *Rev-erbα* (Figure 5.17; F-test of variance, $p \leq 0.05$, $p \leq 0.01$, $p \leq 0.001$).

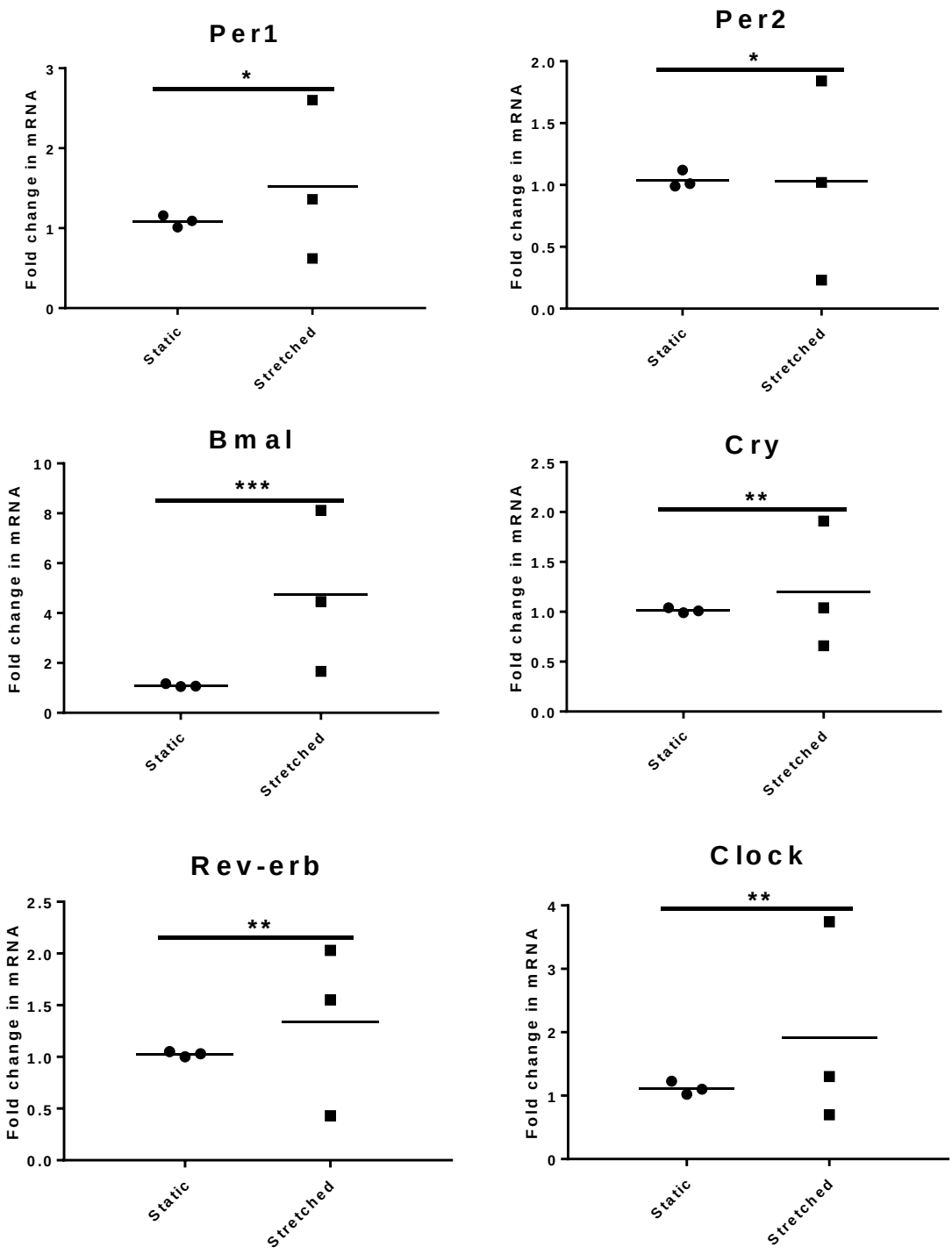

Figure 5.17. Circadian gene expression in Per2::Luc differentiated myotubes loaded for 24 hours on the Flexcell machine at 6.66% strain, demonstrate no change in expression. Primary Per2::Luc differentiated myotubes were synchronised by serum shock for 2 hours, after 24 hours, they were loaded on the Flexcell machine for 24 hours before collection in Purezol. Circadian mRNA was analysed by qRT-PCR using the Pfaffl method and normalised to house-keeping gene *β-actin* (Pfaffl, 2001). Data were expressed as fold change relative to static control which was expressed as 1 and presented as means (F-test of variance, *p≤0.05, **p≤0.01, ***p≤0.001, three independent experiments n=3).

5.4.4 Clock gene expression in C2C12 myoblasts with lamin A knockdown is not rescued by *in vitro* strain

5.4.4.1 Lamin A siRNA knockdown in C2C12 myoblasts, compared to scrambled control, for static and *in vitro* loaded myoblasts

To further the investigation into lamin A, the circadian clock, and mechanical strain, the next aim was to identify whether lamin A knockdown affects the mechanical response of circadian clock gene expression and observe whether strain rescues clock gene expression. C2C12 myoblasts seeded into laminin coated Bioflex plates, at 60% confluency, were transfected with 5 nmol validated lamin A siRNA or scrambled control. 24 hours after transfection, myoblasts were synchronised by 100 nM Dexamethasone, and after 24 hours, were subjected to 24 hours *in vitro* loaded on the Flexcell machine and collected immediately after loading. qRT-PCR and Western blotting was used to analyse *Lmna* expression and LMNA levels. The expression of lamin A was knocked-down in myoblasts treated with lamin A siRNA compared to scrambled control for both the static and the loaded samples (Figure 5.18; unpaired t-test, $p \leq 0.05$ and $p \leq 0.01$). A decrease in lamin A protein levels was also observed between static samples transfected with scrambled compared to samples transfected with lamin A siRNA (Figure 5.19; one-way ANOVA, $p \leq 0.05$). The protein levels for lamin A in the *in vitro* loaded samples remains low for both scrambled and lamin A siRNA transfected samples (Figure 5.19).

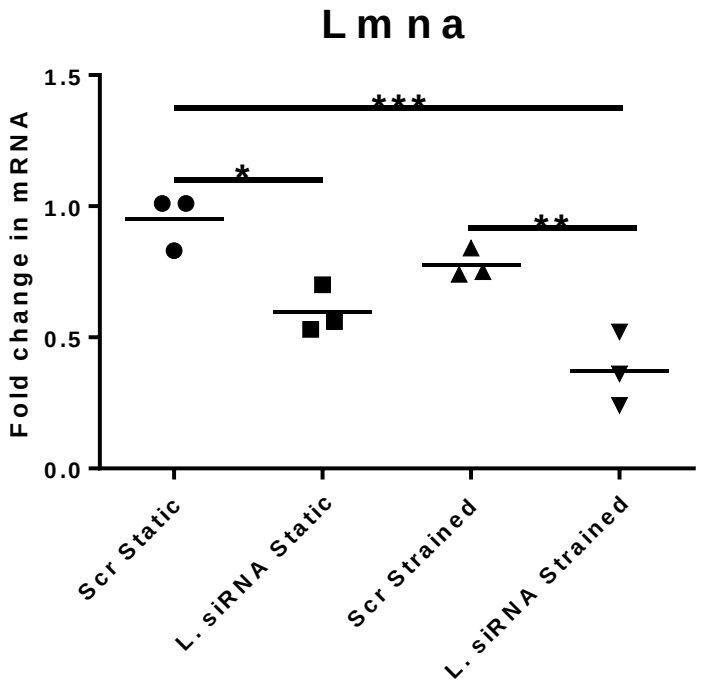

Figure 5.18. Lamin A gene expression in C2C12 myoblasts transfected with lamin A siRNA or scrambled control, and loaded on the Flexcell machine for 24 hours or left static as a control, demonstrate *Lmna* expression is decreased with lamin A siRNA transfection in static and strained samples. C2C12 myoblasts were seeded into laminin coated Bioflex plates, at 60% confluency, were transfected with 5 nmol lamin A siRNA or scrambled control. 24 hours after transfection myoblasts were synchronised with 100 nM Dexamethasone, and after 24 hours, were loaded for 24 hours on the Flexcell machine or left as static control. *Lmna* mRNA was analysed by qRT-PCR using the Pfaffl method and normalised to house-keeping gene *β-actin* (Pfaffl, 2001). Data were expressed as fold change relative to the static and scrambled control which was expressed as 1 and presented as means (one-way ANOVA, *p≤0.05, **p≤0.01, ***p≤0.001, three independent experiments n=3).

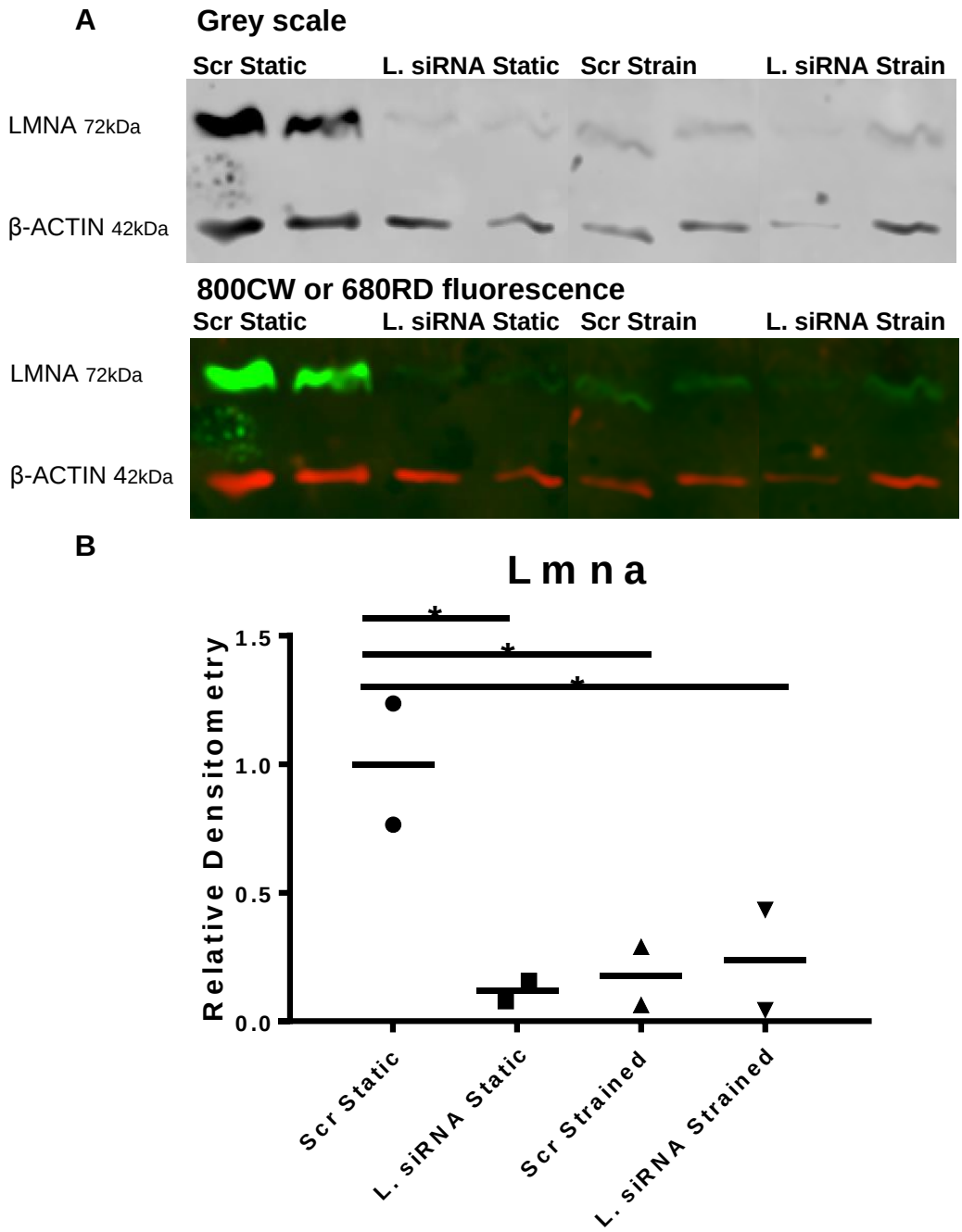

Figure 5.19. Representative Western blot images and densitometry analysis of lamin A protein expression in C2C12 myoblasts transfected with lamin A siRNA or scrambled control and either loaded on the Flexcell machine for 24 hours at 6.66% strain or left static as a control, LMNA protein decrease with lamin A siRNA transfection and strain. (A) Protein samples were ran on 10% acrylamide gels, transferred, and incubated with primary antibodies for anti-mouse Lmna (Sigma; 1:2000) and anti-rabbit β-Actin (Sigma; 1:2000) followed by secondary antibodies for goat anti-rabbit 800CW and goat anti-mouse 680RD (Licor; 1:20000). (B) Densitometry values were calculated using the analysis software provided by Image Studio Lite Version 5.2. LMNA bands were normalised to β-ACTIN. Data were expressed as % change relative to static which was expressed as 1 and presented as means (one-way ANOVA, *p≤0.05, ns= p>0.05, two independent experiments n=2).

5.4.4.2 The expression of *Per1* and *Per2* are repressed in C2C12 myoblasts with lamin A knockdown under both static and loaded conditions

The next aim was to determine whether there was an altered response to mechanical strain observed in circadian clock gene expression in C2C12 myoblasts transfected with validated lamin A siRNA, in comparison to static and scrambled control samples. qRT-PCR was used to examine the response of clock gene expression from the scrambled control or validated lamin A siRNA transfected samples. The expression of *Per1*, *Per2*, and *Rev-erba* was reduced in static samples with a knockdown of lamin A (Figure 5.20; one-way ANOVA, $p \leq 0.05$, $p \leq 0.01$). *Per1* and *Per2* expression was repressed in lamin A knockdown myoblasts subject to 24-hour strain on the Flexcell machine, compared to the scrambled control myoblast samples subject to Flexcell strain (Figure 5.20 one-way ANOVA, $p \leq 0.05$). This is consistent with previous data, in Chapter 4, observing the response in clock gene expression in C2C12 myoblasts to lamin A knockdown; the expression of *Per1*, *Per2*, and *Rev-erba* follows the expression pattern of *Lmna* (Figure 4.3).

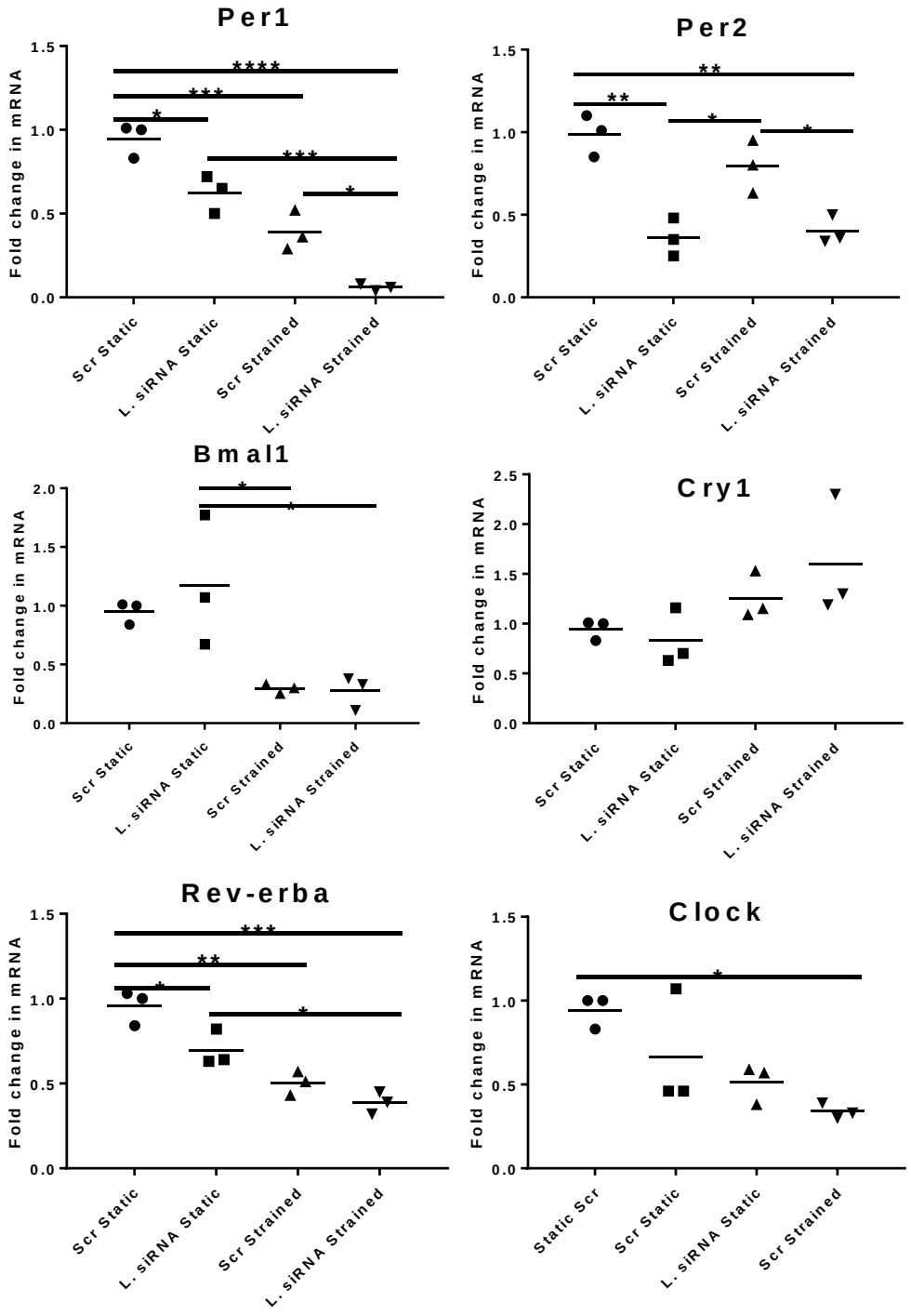

Figure 5.20. Circadian clock gene expression in C2C12 myoblasts transfected with lamin A siRNA or scrambled control and loaded for 24 hours on the Flexcell compared to static control. C2C12 myoblasts, at 60% confluency, were transfected with lamin A siRNA or scrambled control. 24 hours after transfection myoblasts were synchronised with 100 nM Dexamethasone, and after 24 hours, were loaded for 24 hours on the Flexcell machine or left as static control. Circadian mRNA was analysed by qRT-PCR using the Pfaffl method and normalised to house-keeping gene *β-actin* (Pfaffl, 2001). Data were expressed as fold change relative to static, scrambled control which was expressed as 1 and presented as means (one-way ANOVA, *p≤0.05, **p≤0.01, ***p≤0.001, ****p≤0.0001, three independent experiments n=3).

5.4.5 Acute *in vivo* loading in murine Gastrocnemius muscle upregulates *clock* expression

5.4.5.1 Acute Quadricep loading, no change in *Lmna*

In vitro Flexcell strain in primary and cell-line myoblasts demonstrated interesting results in the response of circadian clock gene expression. Accordingly, the next aim was to investigate these circadian gene responses to strain further and make use of the opportunity to collect samples from a study subjecting mice to an *in vivo* loading model to investigate OA in the knee. Wild-type mice undertook a loading regime performed on their right hind leg, and their left hind leg remained unloaded. To determine whether the expression of lamin A and circadian clock genes were responsive to an acute loading regime, muscle samples were collected from WT male mice 4 hours after one loading regime: 9N for 0.5 seconds with a 9.9 second break, repeated 40 times. Quadricep (Quad) and Gastrocnemius (Gas) muscle were collected, homogenised in Purezol, RNA extracted, and qRT-PCR analysis completed, data were normalised to *β-Actin*. It was predicted that during the loading of the right leg, the Quad muscle would be subject to strain. In Quad muscle, there was no change in lamin A expression between the loaded and unloaded leg (Figure 5.21).

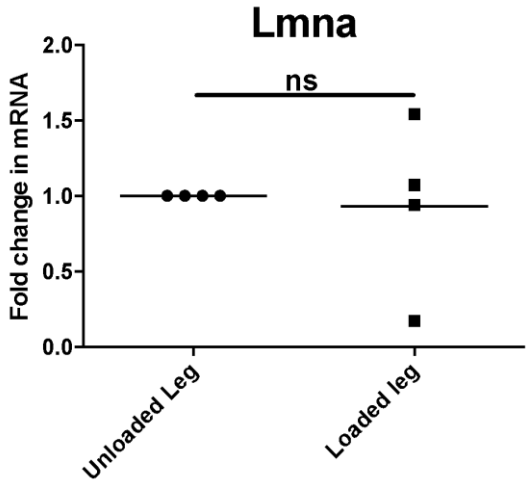

Figure 5.21. Lamin A gene expression in Quadricep samples from WT male mice subject to acute *in vivo* loading, no change in *Lmna* expression. *Lmna* mRNA was analysed by qRT-PCR using the Pfaffl method and normalised to house-keeping gene *β-actin* (Pfaffl, 2001). Data were expressed as fold change relative to unloaded leg which was expressed as 1 and presented as means (unpaired t-test, ns= p>0.05, n=4).

5.4.5.2 Acute Quadricep loading, no change in circadian gene expression

The next aim was to determine whether the circadian clock genes in Quad muscle are responsive to acute loading in wild-type mice. qRT-PCR analysis was used to compare circadian gene expression between the unloaded left leg and the loaded right leg, there was no change in the circadian genes examined (Figure 5.22). This is consistent with *Lmna* qRT-PCR data (Figure 5.21).

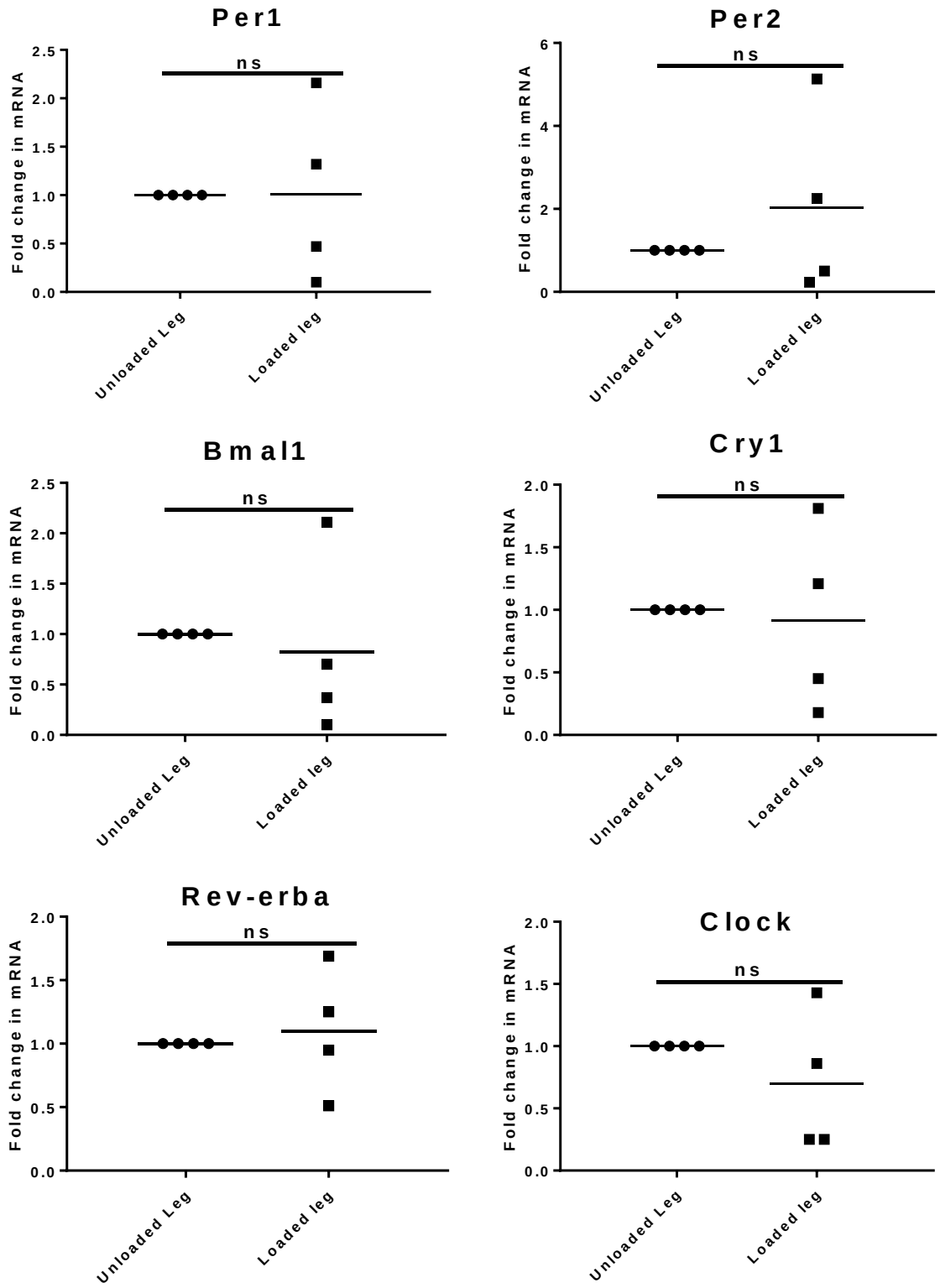

Figure 5.22. Circadian clock gene expression in Quadricep samples from WT male mice subject to acute *in vivo* loading, no change in expression. Circadian mRNA was analysed by qRT-PCR using the Pfaffl method and normalised to house-keeping gene *β-actin* (Pfaffl, 2001). Data were expressed as fold change relative to unloaded leg which was expressed as 1 and presented as means (unpaired t-test, ns= p>0.05, n=4).

5.4.5.3 Acute Gastrocnemius loading, no change in *Lmna*

Next, focus was turned to samples of Gas muscle. Gas muscle is located at the distal part on the plantar aspect of the hind leg and it was therefore predicted that on loading of the leg this muscle will be compressed. Gas was collected 4 hours after one acute loading regime. The muscle was homogenised in Purezol and qRT-PCR analysis completed to measure *Lmna* expression and compare muscle from the loaded, right leg with the unloaded, left leg. qRT-PCR analysis identified no change in *Lmna* expression between loaded and unloaded muscle (Figure 5.23).

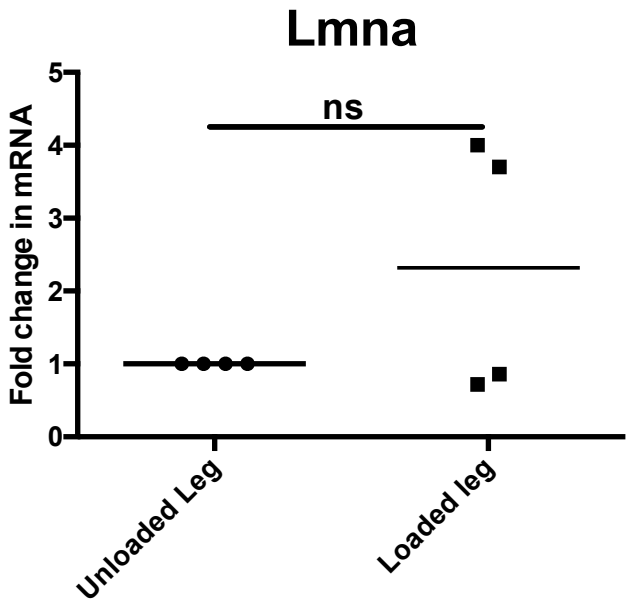

Figure 5.23. Lamin A gene expression in Gastrocnemius from WT male mice subject to acute *in vivo* loading, no change in *Lmna* expression. *Lmna* mRNA was analysed by qRT-PCR using the Pfaffl method and normalised to house-keeping gene *β-actin* (Pfaffl, 2001). Data were expressed as fold change relative to unloaded leg which was expressed as 1 and presented as means (unpaired t-test, ns= $p>0.05$, n=4).

5.4.5.4 Acute Gastrocnemius loading, *clock* upregulation

The next aim was to determine whether acute loading of Gas muscle elicited a response in circadian gene expression. qRT-PCR analysis identified significant increase in *Clock* expression in the loaded Gas compared to the unloaded Gas, and no change in the expression of the remaining circadian genes (Figure 5.24; unpaired t-test, $p \leq 0.05$).

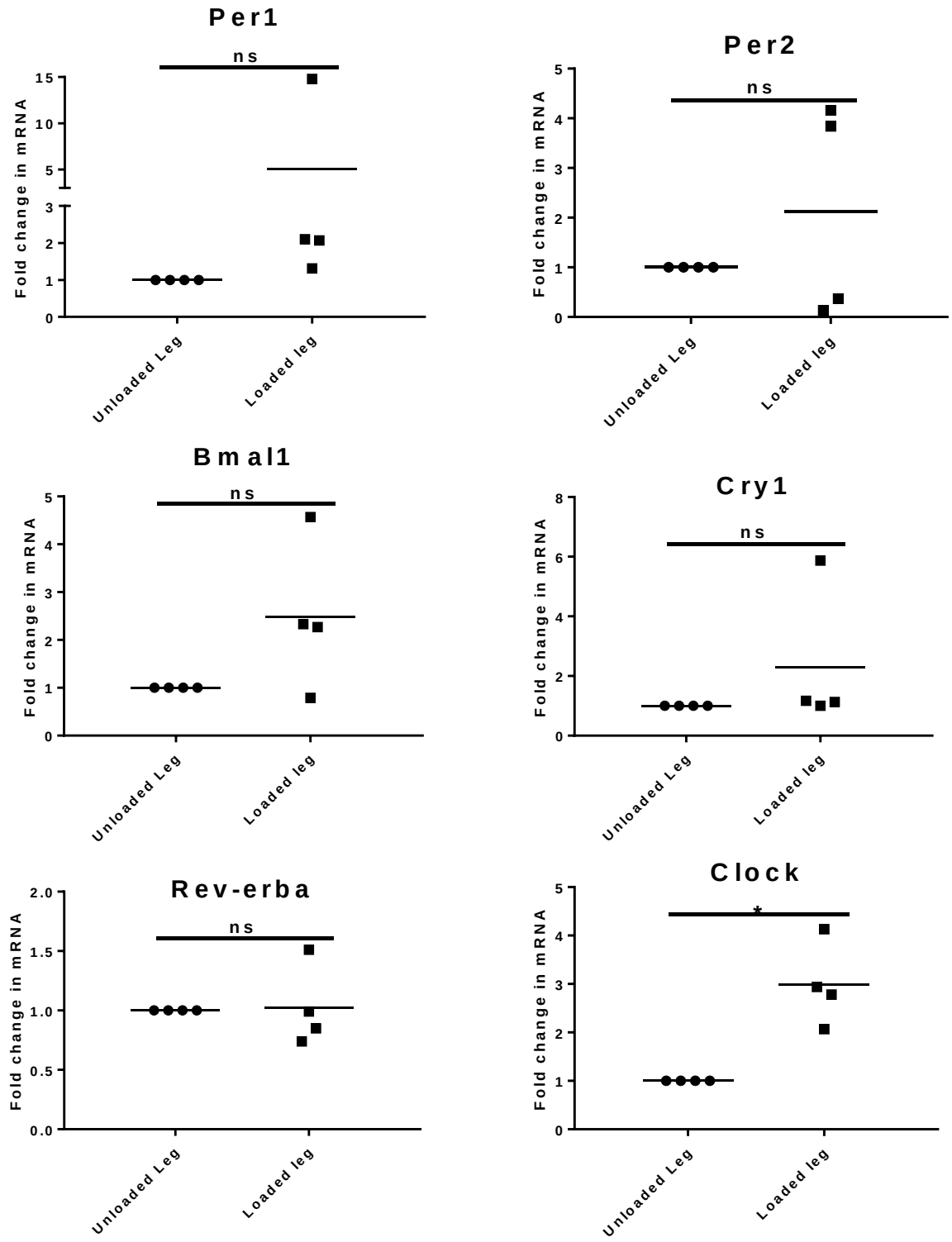

Figure 5.24. Circadian clock gene expression in Gastrocnemius samples from WT male mice subject to acute *in vivo* loading, demonstrate *Clock* gene upregulation. Circadian mRNA was analysed by qRT-PCR using the Pfaffl method and normalised to house-keeping gene *β-actin* (Pfaffl, 2001). Data were expressed as fold change relative to unloaded leg which was expressed as 1 and presented as means (unpaired t-test, *p≤0.05, ns= p>0.05, n=4).

5.4.6 Male murine Quadricep subject to *in vivo* chronic loading increases *clock* expression

To further investigate the circadian clock in response to mechanical strain, the next aim was to utilise studies following a chronic loading protocol. This protocol subjected mice to loading three times a week for two weeks, and tissue is collected two days after the last loading regime. Data from the acute study demonstrated an increase in *Clock* expression in Gas muscle tissue (Figure 5.25); the next aim was to investigate whether muscle subject to repeated loading regimes had a more consistent or heightened response in the expression of circadian genes and *Lmna*. In addition, tissue was collected from WT male and female mice involved in the chronic loading study, serving as a further comparison. Systemic signals across the body are different between male and females, and these signals, such as hormones, are important in clock regulation (Melancon, Lorrain, and Dionne, 2014; Santhi, *et al*., 2016). Hence, separating male and female groups allowed for these differences to be accounted for and enabled the investigation of whether the expression of circadian genes and *Lmna* in response to loading between male and female mice is altered.

Consistent with the acute protocol study, Quad and Gas muscle were collected from these mice. Muscle was homogenised in Purezol and qRT-PCR was used to analyse gene expression, normalised to *β-Actin*.

5.4.6.1 Male Quadricep chronic loading, no change in *Lmna*

To investigate the response of *Lmna* expression in male Quad muscle to loading regimes that follow the chronic loading protocol, qRT-PCR was used. Gene expression analysis identified no change in *Lmna* expression between loaded and unloaded muscle, normalised to *β-Actin* (Figure 5.25).

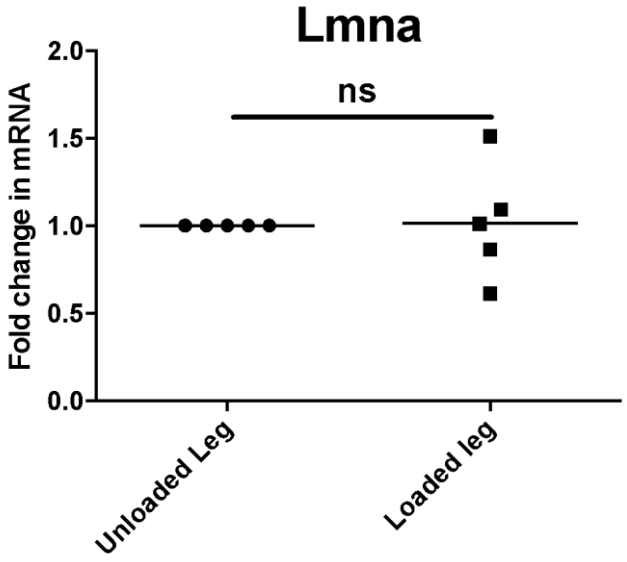

Figure 5.25. Lamin A gene expression in Quadricep from male WT mice subject to chronic *in vivo* loading protocol, no change in *Lmna* expression. *Lmna* mRNA was analysed by qRT-PCR using the Pfaffl method and normalised to house-keeping gene *β-actin* (Pfaffl, 2001). Data were expressed as fold change relative to unloaded leg which was expressed as 1 and presented as means (unpaired t-test, ns= $p>0.05$, n=5).

5.4.6.2 Male Quadricep chronic loading, *Clock* upregulation

Next, the response in circadian gene expression to loading following the chronic protocol in male Quad muscle was observed. qRT-PCR analysis identified a significant increase in *Clock* expression in the loaded leg compared to the unloaded leg (Figure 5.26; unpaired t-test, $p\leq0.05$). There was no change in the expression of the remaining circadian genes.

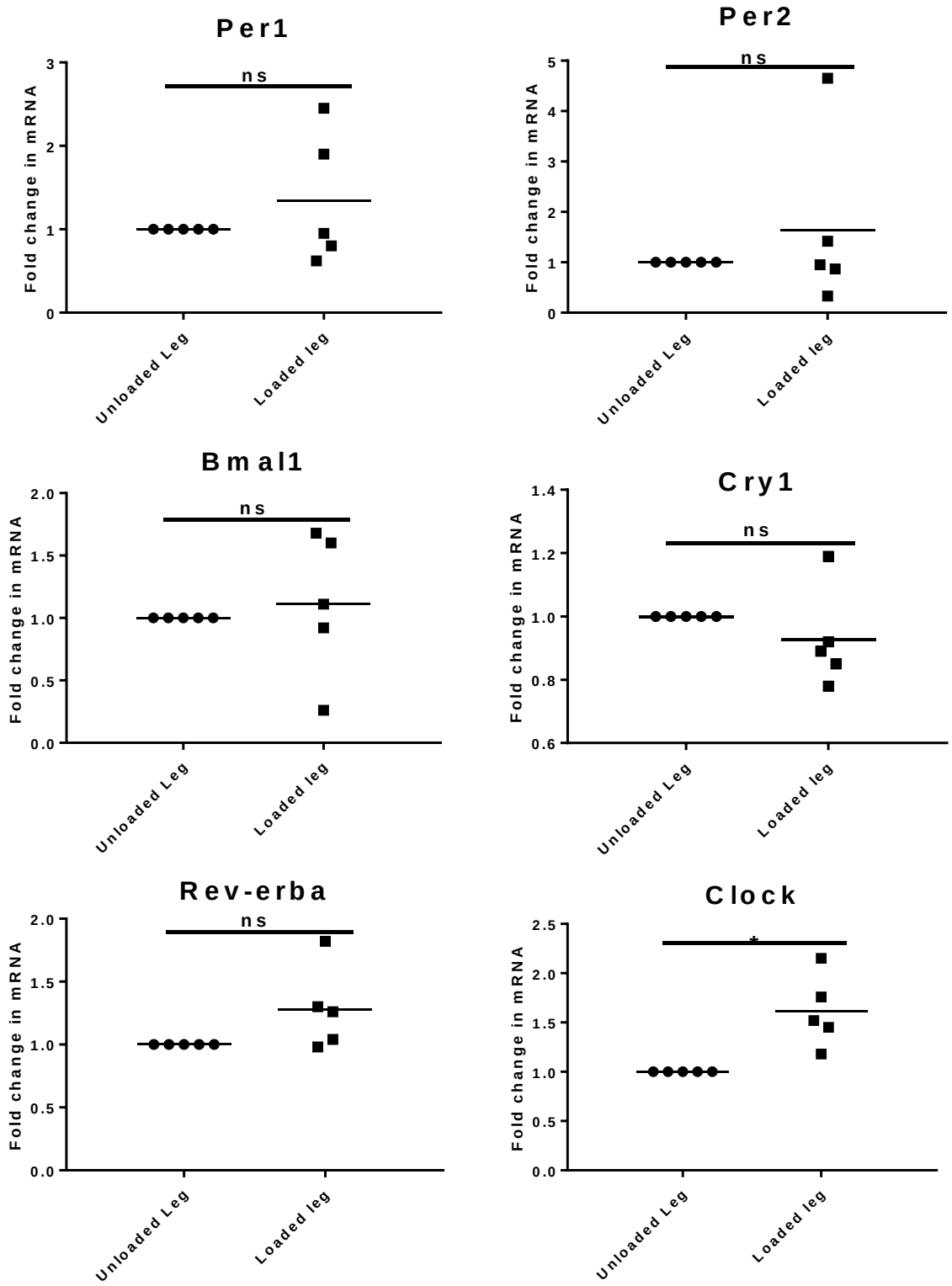

Figure 5.26. Circadian clock gene expression in Quadricep samples from male WT mice subject to chronic *in vivo* loading protocol, demonstrate *Clock* upregulation. Circadian mRNA was analysed by qRT-PCR using the Pfaffl method and normalised to house-keeping gene *β-actin* (Pfaffl, 2001). Data were expressed as fold change relative to unloaded leg which was expressed as 1 and presented as means (unpaired t-test, *p≤0.05, ns= p>0.05, n=5).

5.4.6.3 Chronic loading of male Gastrocnemius, no change in lamin A

To measure *Lmna* expression and compare male Gas samples from the chronic loaded right leg with the unloaded left leg, qRT-PCR analysis was used. No change was demonstrated in *Lmna* expression between loaded and unloaded Gas, normalised to *β-Actin* (Figure 5.27).

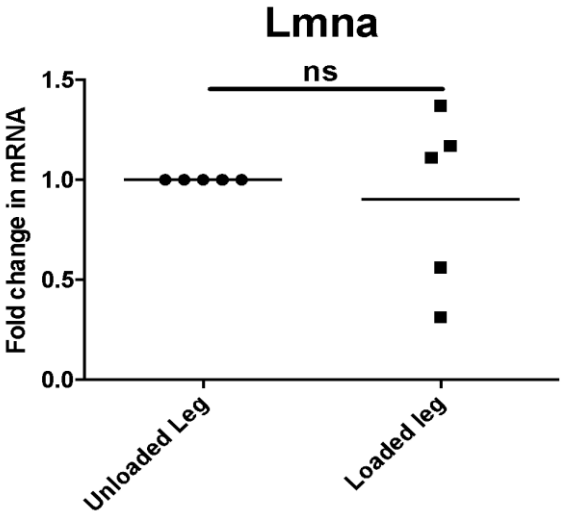

Figure 5.27. Lamin A gene expression in Gastrocnemius from male WT mice subject to chronic *in vivo* loading protocol, no change in *Lmna* expression. *Lmna* mRNA was analysed by qRT-PCR using the Pfaffl method and normalised to house-keeping gene *β-actin* (Pfaffl, 2001). Data were expressed as fold change relative to unloaded leg which was expressed as 1 and presented as means (unpaired t-test, ns= p>0.05, n=5).

5.4.6.4 Chronic loading of male Gastrocnemius, no change in circadian gene expression

Next, the circadian clock gene response in chronic loaded male Gas muscle was investigated. qRT-PCR analysis was used to compare circadian gene expression between the unloaded left leg and the loaded right leg, and demonstrated no change in the circadian genes tested (Figure 5.28). This is consistent with *Lmna* qRT-PCR expression for chronic loading of male Gas (Figure 5.27).

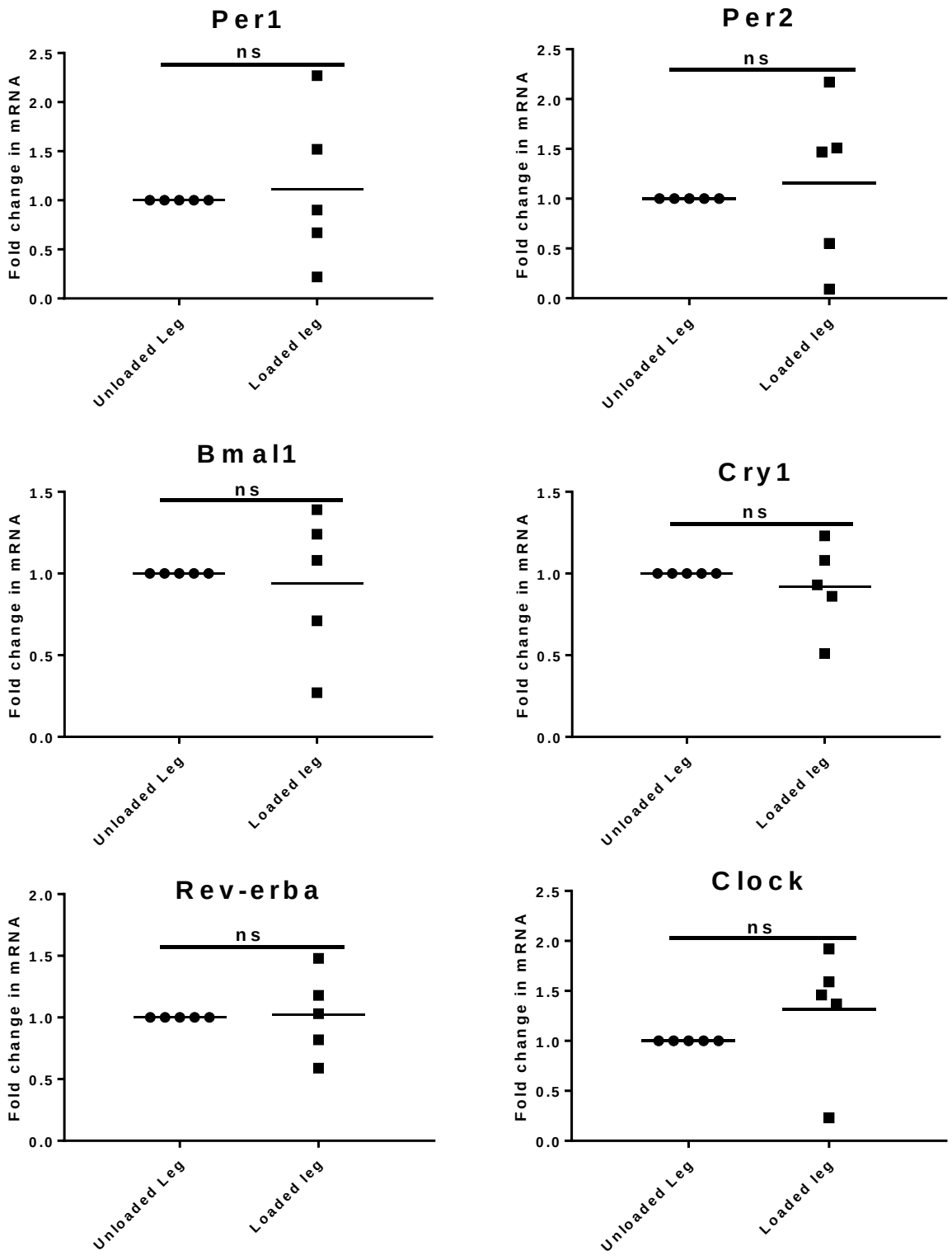

Figure 5.28. Circadian clock gene expression in Gastrocnemius samples from male WT mice subject to chronic *in vivo* loading protocol, no change in expression. Circadian mRNA was analysed by qRT-PCR using the Pfaffl method and normalised to house-keeping gene *β-actin* (Pfaffl, 2001). Data were expressed as fold change relative to unloaded leg which was expressed as 1 and presented as means (unpaired t-test, ns= p>0.05, n=5).

5.4.7 Female Quadricep subject to *in vivo* chronic loading reveals no change in circadian or *Lmna* gene expression

5.4.7.1 Chronic loading of female Quadricep, no change in *Lmna*

The next aim was to investigate whether the response of circadian clock genes and *Lmna* expression in Quad and Gas is less variable or heightened in female mice. Consistent with the acute protocol study and chronic loading protocol in male mice, Quad and Gas muscle samples were collected for analysis. The muscle was homogenised in Purezol and qRT-PCR analysis completed to measure gene expression changes between muscles of the loaded, right leg with the unloaded, left leg. qRT-PCR analysis identified no change in *Lmna* expression between loaded and unloaded Quad (Figure 5.30).

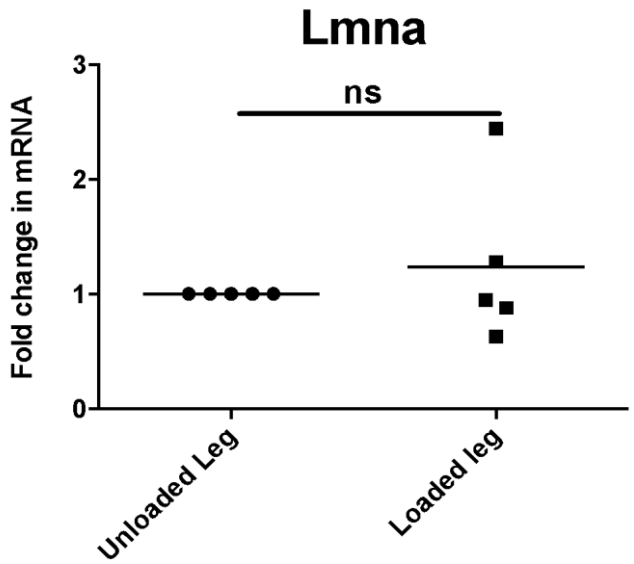

Figure 5.29. Lamin A gene expression in Quadricep from female WT mice subject to chronic *in vivo* loading protocol, no change in *Lmna* expression. *Lmna* mRNA was analysed by qRT-PCR using the Pfaffl method and normalised to house-keeping gene *β-actin* (Pfaffl, 2001). Data were expressed as fold change relative to unloaded leg which was expressed as 1 and presented as means (unpaired t-test, ns= p>0.05, n=5).

5.4.7.2 Chronic loading of female Quadricep, no change in circadian gene expression

To determine whether circadian clock genes in Quad muscle are responsive to the chronic loading in female mice, qRT-PCR was utilised to analyse changes in gene expression. qRT-PCR analysis of circadian clock genes identified no change in expression between loaded Quad muscle from the right leg and unloaded control Quad muscle form the left leg, normalised to *β-Actin* (Figure 5.30).

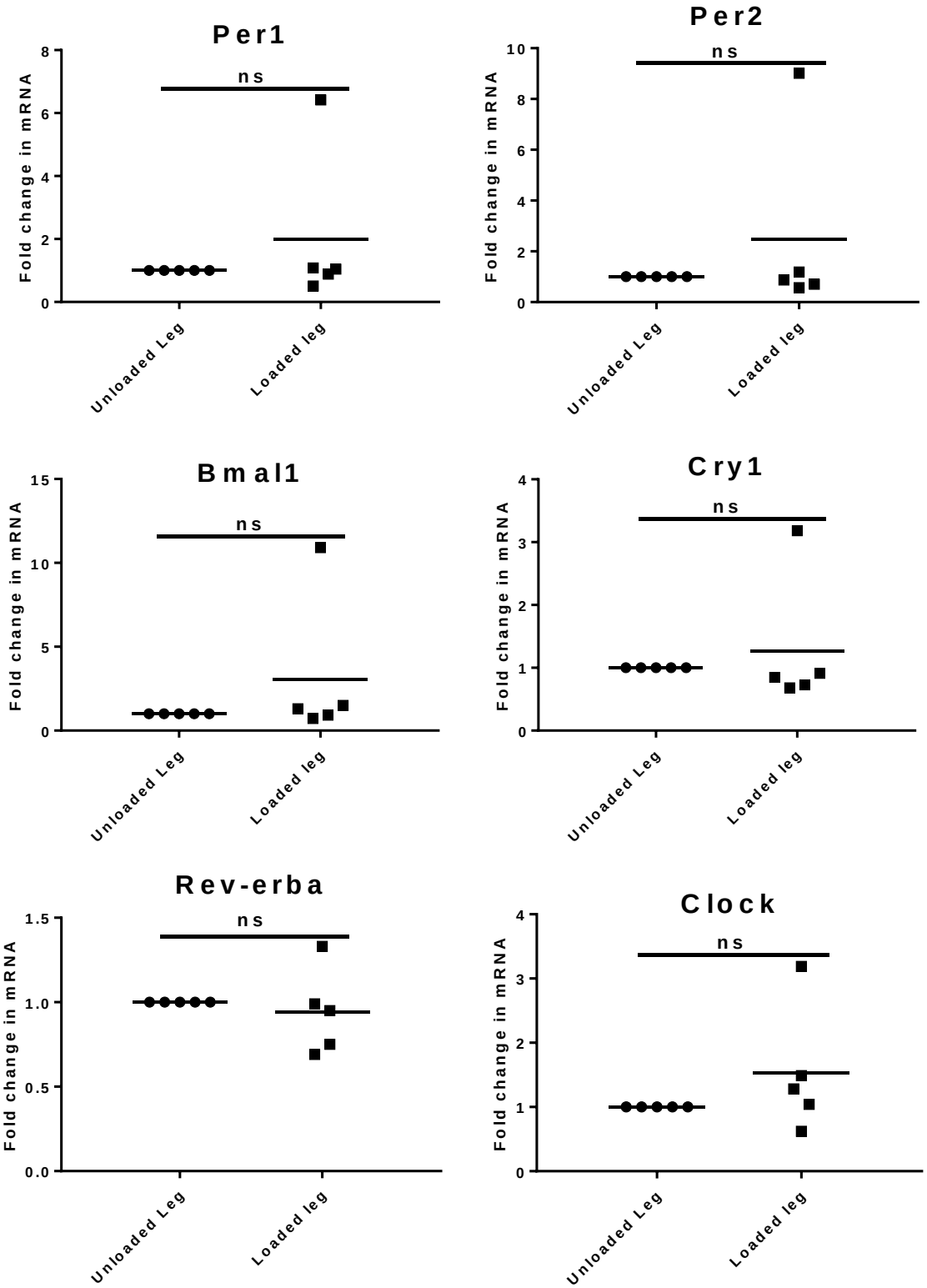

Figure 5.30. Circadian clock gene expression in Quadricep samples from female WT mice subject to chronic *in vivo* loading protocol, no change in expression. Circadian mRNA was analysed by qRT-PCR using the Pfaffl method and normalised to house-keeping gene *β-actin* (Pfaffl, 2001). Data were expressed as fold change relative to unloaded leg which was expressed as 1 and presented as means (unpaired t-test, ns= p>0.05, n=5).

5.4.7.3 Chronic loading of female Gastrocnemius, no change in *Lmna* gene expression

Next, Gas tissue from female mice subject to *in vivo* loading following the chronic protocol was investigated to determine whether there was a response observed in *Lmna* gene expression. qRT-PCR analysis of *Lmna* identified no change in expression between loaded Gas muscle on the right leg and unloaded Gas on the left leg (Figure 5.31).

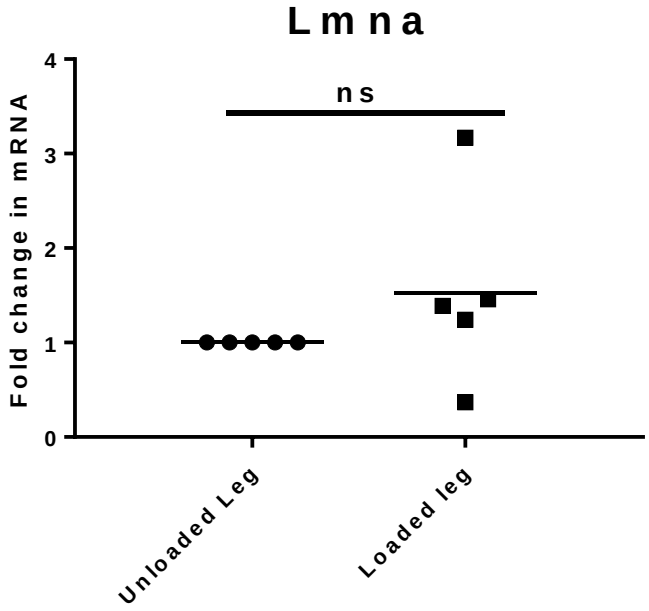

Figure 5.31. Lamin A gene expression in Gastrocnemius from female WT mice subject to chronic *in* vivo loading protocol, no change in *Lmna* expression. *Lmna* mRNA was analysed by qRT-PCR using the Pfaffl method and normalised to house-keeping gene *β-actin* (Pfaffl, 2001). Data were expressed as fold change relative to unloaded leg which was expressed as 1 and presented as means (unpaired t-test, ns= p>0.05, n=5).

5.4.7.4 Chronic loading of female Gastrocnemius, no change in circadian gene expression

To investigate whether circadian clock genes in Gas muscle from female mice are responsive to a loading regime following the chronic protocol, qRT-PCR was used to analyse circadian gene expression. There was no change in the expression of circadian clock genes between the loaded right leg and the unloaded left leg (Figure 5.32).

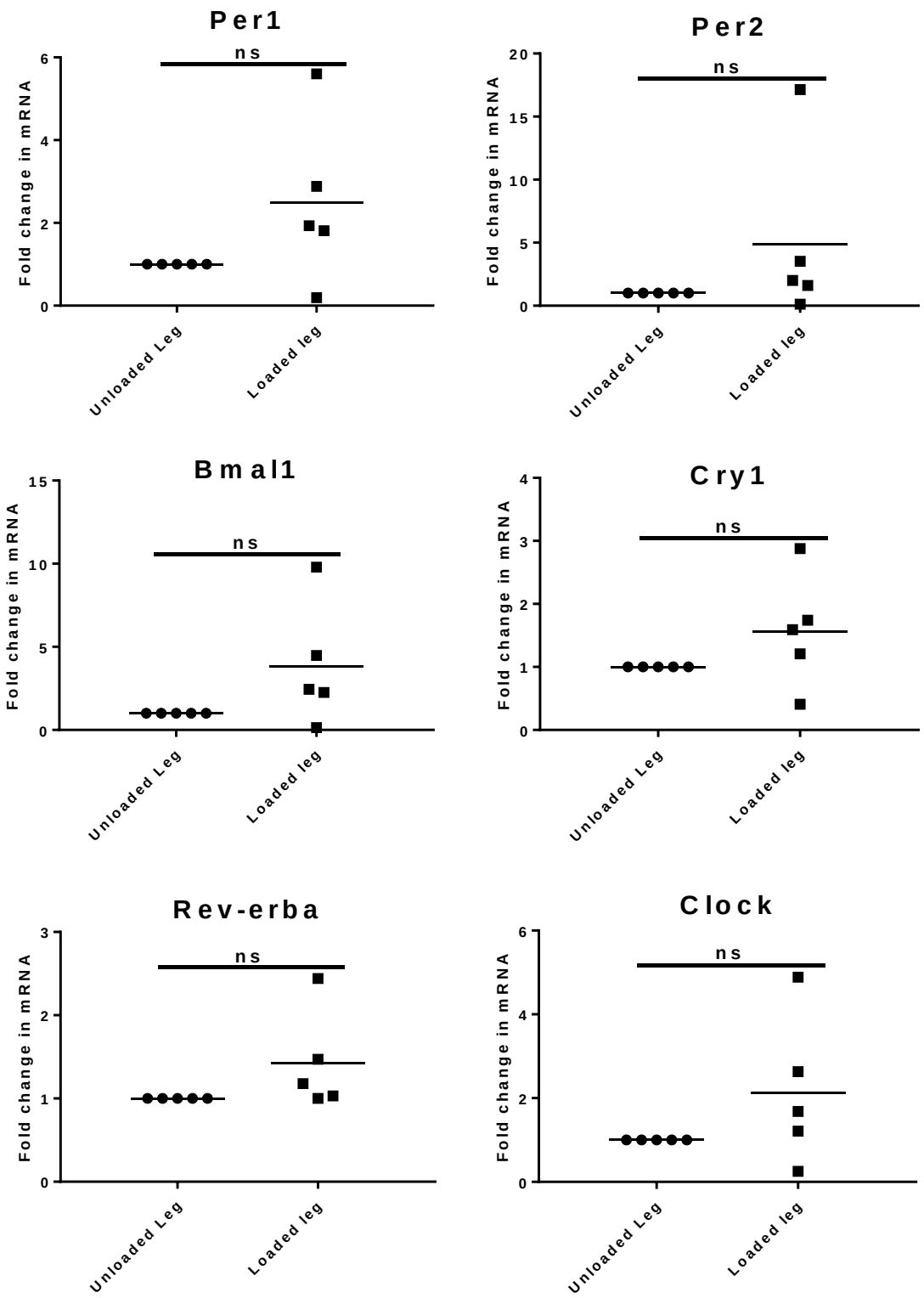

Figure 5.32. Circadian clock gene expression in Gastrocnemius samples from female WT mice subject to chronic *in vivo* loading protocol, no change in expression. Circadian mRNA was analysed by qRT-PCR using the Pfaffl method and normalised to house-keeping gene *β-actin* (Pfaffl, 2001). Data were expressed as fold change relative to unloaded leg which was expressed as 1 and presented as means (unpaired t-test, ns= p>0.05, n=5).

5.5 Discussion

Exercise is capable of synchronising the molecular clock within the SCN and peripheral tissues, independently from the hierarchical synchronisation signals released from the master regulator in the SCN (Wolff and Esser, 2012; Schroeder, *et al*., 2012; Sasaki, *et al*., 2016). Human re-entrainment to a phase advanced sleep-wake cycle was accelerated by timed physical exercise (Yamanaka, *et al*., 2010). Moreover, physical exercise in the evening phase-delayed nocturnal rise in melatonin levels and suppressed the decline of rectal body temperature during sleep (Yamanaka, *et al*., 2015). The timing of exercise regimes are important; mis-timed wheel running activity in mice prevented the entrainment of peripheral clocks in muscle and lung tissue (Yamanaka, *et al*., 2016). Thus, exercise is an entrainment cue for circadian rhythms, and exercise regimes can be used to entrain the master and peripheral clocks. Recently, exciting avenues have been discussed for the use of exercise to shift or regulate the circadian clock involvement in risk markers for cardiovascular disease, hormone regulation, blood pressure, and disorders such as delayed sleep-wake phase disorder and Amnestic Mild Cognitive Impairment (Scheer, *et al*., 2010; Hackney, Davis, and Lane, 2015; Leonardo-Mendonça, *et al*., 2015; de Brito, *et al*., 2015; Tortosa-Martínez, *et al*., 2015; Richardson, *et al*., 2017).

The mechanism of exercise induced entrainment and phase-shifting of the circadian clock has yet to be identified; however, studies have suggested that peripheral clock re-synchronisation in response to exercise is due to changes in hormones, the timing of food consumption or stress (Terzibasi-Tozzini, *et al*., 2017). Exercise increases the release of hormones including prolactin, cortisol, melatonin, and corticosterone (Heaney, Carroll, and Phillips, 2014; Hackney, Davis, and Lane, 2015; Leonardo-Mendonça, *et al*., 2015; Sasaki, *et al*., 2016). One study identified that hormone regulation in response to exercise is sufficient to synchronise the circadian clock, lower blood pressure, lower heart rate, and improve sleep (Melancon, Lorrain, and Dionne, 2014). Additionally, scheduling the timing of food-intake regulated and synchronised the circadian clock in peripheral tissues through insulin-dependent regulation of *Bmal1* (Dang, *et al*., 2016). Skeletal muscle in fasting mice lost the

circadian expression of *Myod1* and *Atrogin1*; supporting food-intake as a synchronisation method for the peripheral clocks in skeletal muscle in response to exercise (Shavlakadze, *et al*., 2013). In contrast, circadian gene expression in mice with time-scheduled restricted access to food and unlimited access to a running wheel did not synchronise to their feeding schedule in the peripheral clocks of skeletal muscle, unlike other peripheral clocks (Yasumoto, *et al*., 2016). Exercise regimes elicit a stress response through the release of reactive oxygen species (ROS) (He, *et al*., 2016). Circadian rhythms are responsible for orchestrating protective responses to oxidative stress. The antioxidant peroxiredoxin oscillates with a circadian rhythm and is involved in peripheral clock synchronisation (Kil, *et al*., 2012; Rhee, 2016). Additionally, the accumulation of ROS feedback to resets the circadian clock (Tamaru, *et al*., 2013; Schippers, *et al*., 2013). Interestingly, lamin A is also correlated with the suppression of oxidative stress and ROS. Patients suffering with laminopathies such as Emery-Dreifuss muscular dystrophy and progeria, have elevated levels of ROS and an increased sensitivity to oxidative stress (Richards, *et al*., 2011; Sieprath, *et al*., 2015; Niebroj-Dobosz, *et al*., 2017). In this regard, hormones, the timing of food consumption, and stress are potential modifiers for communicating mechanical signals to the circadian clock; nevertheless, it was predicted that lamin A is a vital regulator in this pathway.

Knowledge of how this entrainment signal is communicated to the clock may facilitate the manipulation of this pathway to reset desynchronised clocks. Future research can optimise pharmaceutical intervention to stimulate these pathways, eliminating the need for individuals to undergo daily exercise regimes. Individuals who experience jet-lag or shift-work have their SCN and peripheral clocks desynchronised from the external environment. Accordingly, this affects many tissue-specific processes and is linked to sleep, metabolic and psychological disorders, and cancer (Khan, *et al*., 2018). Thus, in these individuals, relevant time-of-day administration of a pharmaceutical intervention to activate these unknown synchronisation pathways has the potential to rapidly synchronise dysfunctional peripheral clocks. Identifying the mechanism and optimising a

method of pharmaceutical activation to quickly reset peripheral clocks will therefore be extremely useful and may alleviate these disorders linked to clock de-synchronisation.

The research in this thesis predicted that the circadian clock is dysfunctional in the peripheral tissues of laminopathy patients due to a lack of feedback regulation by lamin A. Within these tissues, the clock may therefore become arrhythmic. Circadian rhythms are vital in the physiology and maintenance of many tissues such as fat, skeletal muscle, and cardiac tissue (Jung and Feldman, 2018; Crnko, *et al*., 2018). These are tissues that are commonly affected in the pathology of various laminopathy diseases (Kang, Yoon, and Park, 2018). Consequently, this research warrants further study into deciphering whether circadian rhythms are dysfunctional in the peripheral tissues of patients suffering with laminopathies. In addition, further research should be targeted to investigate whether the synchronisation and re-entrainment of the circadian clock will improve tissue-specific pathologies observed in these patients.

To further investigate a relationship between the circadian clock and exercise, research focused on studying the mechanical stimulation of myoblasts, myotubes, and muscle. The investigation began by utilising the Flexcell instrument, an *in vitro* cell culture loading machine (Banes, *et al*., 1985). The Flexcell machine applies biaxial strain to cells seeded onto a flexible silicone membrane; the membrane is stretched across a loading post through vacuum pressure applied via a baseplate.

Previous studies have utilised the Flexcell for studying the response of musculoskeletal cells, including C2C12 myoblasts, to mechanical stimulation. Through experiments utilising the Flexcell system, Shradhanjali *et al*. investigated the role of strain in the development of pluripotent murine embryonic (P19) stem cells into cardiomyocytes (Shradhanjali, *et al*., 2017). Yao *et al*. investigated the involvement of mechanosensitive long noncoding RNAs in hypertension induced vascular remodelling through subjecting vascular smooth muscle cells to cyclical strain (Yao, *et al*., 2017). In addition, Wang *et al*. investigated the effect of heat shock protein 27 on cytoskeletal dynamics and contractile function in human bladder muscle smooth cells (Wang, *et al*., 2015). Finally, Fu *et al*. used

the Flexcell machine to investigate strain induced C2C12 myoblast proliferation and uncovered regulation by IGF-1 through changes in PI3K/Akt and MAPK activation (Fu, *et al*., 2018).

Despite a large body of research utilising the Flexcell machine for mechanobiology research, one drawback of the loading machine is non-uniform strain across the membrane as it is pulled concave by the vacuum either side of the loading post (Delaine-Smith, *et al*., 2015). This results in heterogeneous strain across the membrane. The cells seeded on membrane that remains on the loading post during loading experience different radial and biaxial strain fields compared to those seeded onto the areas of the membrane that are located off the loading post (Vande Geest, *et al*., 2004). This research loaded primary myoblasts on the Flexcell machine, for 24 hours at 6.66% strain and at a frequency of 1Hz, and identified an increase in *Lmna** and a decrease in *Cry1*** expression (Figure 5.7 and Figure 5.9; unpaired t-test, *p≤0.05, **p≤0.01). In response to overexpression of lamin A in C2C12 myoblasts, through transfection with lamin A plasmid, there was a significant decrease in *Cry1* expression (Figure 4.11; unpaired t-test, P≤0.01). Hence, primary Per2::Luc Flexcell data are consistent with previous results, as lamin A up-regulation reduces the expression of the core clock gene *Cry1*. Although there was no significant change in the expression of the remaining clock genes, between static and loaded samples, they showed a tendency to increase and may be significant with an increase in *n* numbers (Figure 5.9). The remaining Flexcell work remains variable, non-significant, and inconsistent. This may be due to cells receiving different percentages of strain, based on the varying locations on the silicone membrane. Other research has identified similar, variable results when using the Flexcell system to subject cells to strain in culture (Bader and Wagoner, 2010).

To further examine the role of lamin A in the circadian clock response to mechanical stimulation, the next aim was to knockdown lamin A in myoblasts and observe the response to *in vitro* Flexcell strain. The response of *Per1* and *Per2* expression followed *Lmna* expression in response to the different experimental conditions; lamin A was knocked-down through transfection with validated lamin A

siRNA and *Per1* and *Per2* also demonstrated down regulation in both static and loaded myoblasts (Figure 5.21). Moreover, the expression of *Rev-erba* was downregulated in static samples with lamin A knockdown, but was decreased in both scrambled and lamin A knockdown myoblasts in response to mechanical loading (Figure 5.21).

Table 5.1 Flexcell loading Experimental Data Summary. Table summarising significant gene changes in cell culture Flexcell loading at 6.66% strain, *p≤0.05, **p≤0.01.

	Lamin A	**Circadian Clock**
C2C12 myoblasts	ns	ns
Per2::Luc myoblasts	Increase in *Lmna**	Decrease in *Cry1***
C2C12 myotubes	ns	Increase in *Cry1*** and *Bma1l***
Per2::Luc myotubes	Increase in lamin A**	ns
lamin A siRNA	Decrease with siRNA*,**	*Per1**, *Per2**,** and *Rev-erbα** follow lamin A knockdown

This research had the opportunity to collect samples of muscle from mice in an *in vivo* loading study to mechanically inducing OA through two different loading regimes. This research incorporated these muscle samples and through qRT-PCR analysis, determined whether lamin A and the circadian clock genes are responsive to acute and chronic mechanical strain. By incorporating acute and chronic loading regimes, it was determined whether increased strain applied to muscles of interest elicits a different response in circadian gene expression. Moreover, this is an interesting model to study as there is a proposed link between muscle mass function and OA progression (Roos, *et al*., 2011). Furthermore, the circadian clock has previously been linked to the progression of OA in cartilage. This model enables us to observe whether a similar disease process may be occurring in muscle, and uncover a potential circadian element.

The circadian clock is linked to cartilage tissue homeostasis, and dysregulated clocks have been identified in the pathogenesis of OA in cartilage (Gosson, *et al*., 2013; Dudek and Meng, 2014). During the destabilisation of the medial meniscus (DMM) model of OA, a lesion is created in the

medial meniscotibial ligament to generate destabilisation, and post-surgery this progresses to mild-to-moderate OA by 4 weeks and moderate-to-severe OA by 8 weeks (Glasson, Blanchet, and Morris, 2007). Mice induced to develop OA through the DMM model study have disrupted clock genes in cartilage during the early stages of development, with the expression of *Bmal1* being significantly increased at 1, 2, and 6-weeks post-DMM (Gosson, *et al*., 2013). This study predicted that clock disruption has a role in the development of OA and the highest increase in *Bmal1* overexpression was at the 2-week time-point (Gosson, *et al*., 2013). In rats, low-intensity pulsed ultrasound treatment of temporomandibular joint osteoarthritis upregulated the expression of *Per2* and *Dbp,* and downregulated the expression of *Bmal1* and *Npas2* (He, *et al*., 2018). Human studies have also reinforced this murine research. Cartilage samples from OA sufferers have decreased levels of *Bmal1* and manipulation of the circadian clock effects cartilage homeostasis through *Sirt1* (Yang, *et al*., 2016). In addition, a study investigating OA cartilage samples identified circadian rhythms as one of fifteen significantly perturbed pathways, and one of five pathways most significantly dysregulated (Fisch, *et al*., 2018). Furthermore, two studies identified dysregulation of circadian clock genes and TGFβ in cartilage samples from patients suffering with OA (Akagi, *et al*., 2017; Soul, *et al*., 2018). Interestingly, TGFβ is regulated by both the circadian clock and by lamin A (Kon, *et al*., 2008).

Therefore, this investigation is an exploratory application. The current hypothesis is that *in vivo* mechanical loading, which results in the progression of OA in mice, will also result in clock gene dysregulation in muscle. In muscle, transcription factors involved in mechanotransduction pathways, such as MAPK, NF-κB, and TGF-β, are both regulated by lamin A and the circadian clock (Obrietan, Impey, and Storm, 1998; Spengler, *et al*., 2012; Kon, *et al*., 2008; Lammerding, *et al*., 2004; Ho, *et al*., 2013; Van Berlo, *et al*., 2005). It was predicted that muscle mechanical strain, activating mechanotransduction pathways, will also provide feedback regulation to the circadian clock via a lamin A-regulated pathway. Currently, the *in vivo* loading model used in this research is used to study articular structures of the knee joint, and the role of muscles in this process in not fully understood. This study collected Gas and Quad muscle, these were chosen as they include one

muscle from each side of the knee and one muscle from the front and the back of the leg; it was predicted that they will be strained and compressed, respectively. These results identified highly variable, non-significant mRNA changes in *Lmna* and circadian clock genes on comparison of loaded muscle with static control. Male Gas samples subject to acute loading, and male Quad samples subject to chronic loading had significant upregulation in *Clock** expression (Figure 5.25 and Figure 5.27, *p≤0.05). These results are consistent with previous research as the expression of *Clock* is mechanosensitive (Kanbe, *et al*., 2006).

Table 5.2 *In vivo* loading model Experimental Data Summary. Table summarising significant gene changes from Quadricep and Gastrocnemius muscle collected from an *in vivo* loading model study following two protocols ad completed on wild-type mice, *p≤0.05.

	Lamin A	**Circadian Clock**
Male Acute Quad	ns	ns
Male Acute Gas	ns	increase *Clock**
Male Chronic Quad	ns	increase *Clock**
Male Chronic Gas	ns	ns
Female Chronic Quad	ns	ns
Female Chronic Gas	ns	ns

Therefore, these results highlight the potential for further research to uncover a novel pathway of feedback regulation to the circadian clock in response to mechanical stimulation in muscle.

5.6 Conclusion

To conclude, this chapter demonstrates data to support the existence of a mechanosensitive circadian clock in myoblasts and muscle. Primary myoblasts isolated from Per2::Luc mice, male Gastrocnemius muscle, and male Quadricep muscle responded to mechanical strain in the expression of circadian clock genes (Figure 5.9, Figure 5.25, and Figure 5.27). Moreover, myoblasts transfected with lamin A siRNA and subject to *in vitro* loading exhibit a dampening of *Per1* and *Per2* expression despite being subject to strain (Figure 5.21). This is an exciting and exploratory area of research that warrants further study to determine the pathway of circadian clock mechanical feedback regulation and the potential involvement of lamin A.

6 Mathematical Modelling of lamin A Regulation of the Circadian Clock

6.1 Mathematical Models

6.1.1 Why use Models?

Mathematical models are used to produce simulations and predict biological outcomes to accelerate investigations and discovery within biomedical research. Experimental data are used to inform computational models to accurately simulate complex biological processes. Models focus on the relationship of how genes, and their respective proteins, are connected, as these proteins do not work in isolation of one another. For example, the development of a complex disease is not likely to be the cause of a single gene and protein, although a particular gene may be necessary for the disease development. Thus, to understand the development of the disease, an understanding of many interactions of genes and proteins is required- relating to numerous variables. Together, these interactions and variables are known as a system. In addition, there are other difficulties involved in studying complex systems such as cell structure, compartmentalisation, stochastic effects or nonlinear reaction kinetics (Fischer, 2008). Mathematical modelling accounts for these problems and can be implemented to study complex systems and how they respond to distinctive conditions.

In order to model a system a general design process is followed and may be repeated numerous times until a suitable and trusted model can be obtained, this includes: formulation, calibration, analysis, and evaluation. Formulation involves accumulating current data and knowledge of the system, identifying objectives for the model to achieve, designing a suitable model to describe the relationships within a system, and developing a hypothesis for the model.

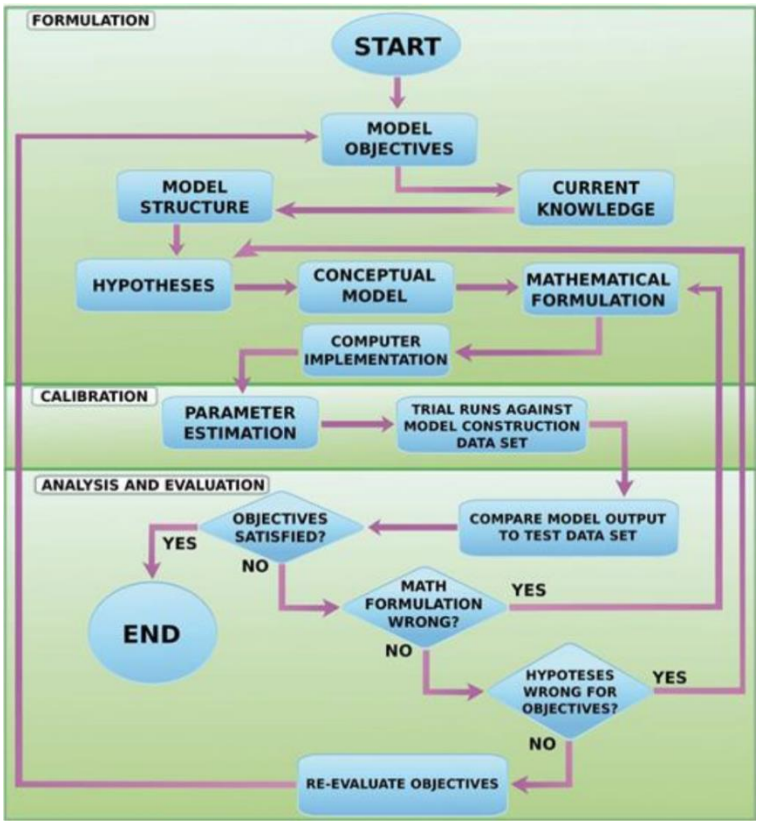

Figure 6.1 Schematic diagram demonstrating the process of model formation using experimental data in order to validate and improve conceptual models, taken from (Motta and Pappalardo, 2013).

Calibration involves choosing suitable parameters and species for implementing the model and can then be used to predict the behaviour of the system under a certain condition. Finally, analysis and evaluation involve utilising experimental data to evaluate whether the prediction from the model was correct. If the model prediction was incorrect the process can be repeated with the objective of adapting the model to fit the results achieved under the condition and data set. If the model was correct and the prediction under the condition was supported by the experimental data, this indicates that the model is robust. In order to test the model further, the process can be repeated with the objective of testing the model under a new condition- to further validate the model. This process is represented as a flow diagram in Figure 6.1.

6.1.2 Mathematical Modelling of Circadian Rhythms

The circadian molecular clockwork consists of numerous gene and protein biochemical reactions; naturally, this makes it a complex system and a mathematical model will assist investigations and analysis. Circadian models were initially implemented in studies aiming to understand how clock proteins synchronise and oscillate with 24-hour cycles (Winfree, 1967). Robust models of the circadian molecular clock are valuable in circadian research as they allow: the identification of important interactions and components within the system, the exploration of clock-controlled regulation in various conditions, and the exploration of conditions which shift oscillatory patterns-such as, period, phase, and amplitude (Podkolodnaya, Tverdokhleb, and Podkolodnyy, 2017).

The generation of experimental molecular data on the clock proteins facilitated the formulation of mathematical models representing the interactions of the clock proteins. Hypothesis-driven adjustments to these models can validate or invalidate working hypotheses and explore potential mechanistic relationships between the clock proteins and downstream genes and proteins.

6.1.3 Circadian Models

Circadian molecular clock models were first constructed for *Drosophila* and *Neurospora*; these models began theoretically exploring the interactions of the core clock proteins and the potential relationships between them. Hence, the *Drosophila* clock model was used with the aim of understanding the mechanism of how *Per*, *Tim*, PER, TIM, and their phosphorylated proteins can oscillate (Goldbeter, 1995; Leloup, Gonze, and Goldbeter, 1999; Smolen, Baxter, and Byrne, 2001). To evaluate models of circadian oscillation, sensitivity analysis can be carried out, this includes: state perturbation – add in extra clock protein, parameter change – a knockout model, or temporary parameter perturbation – light pulse to photosensitive cells (Podkolodnaya, Tverdokhleb, and Podkolodnyy, 2017). A deterministic model by Leloup and Goldbeter was designed to model the gene expression and protein of the mammalian core clock genes and proteins: Bmal, Per, Cry, and

Clock (Leloup and Goldbeter, 2003). The model incorporated phosphorylation and light induced post-translational regulation of this feedback loop, shown in Figure 6.2.

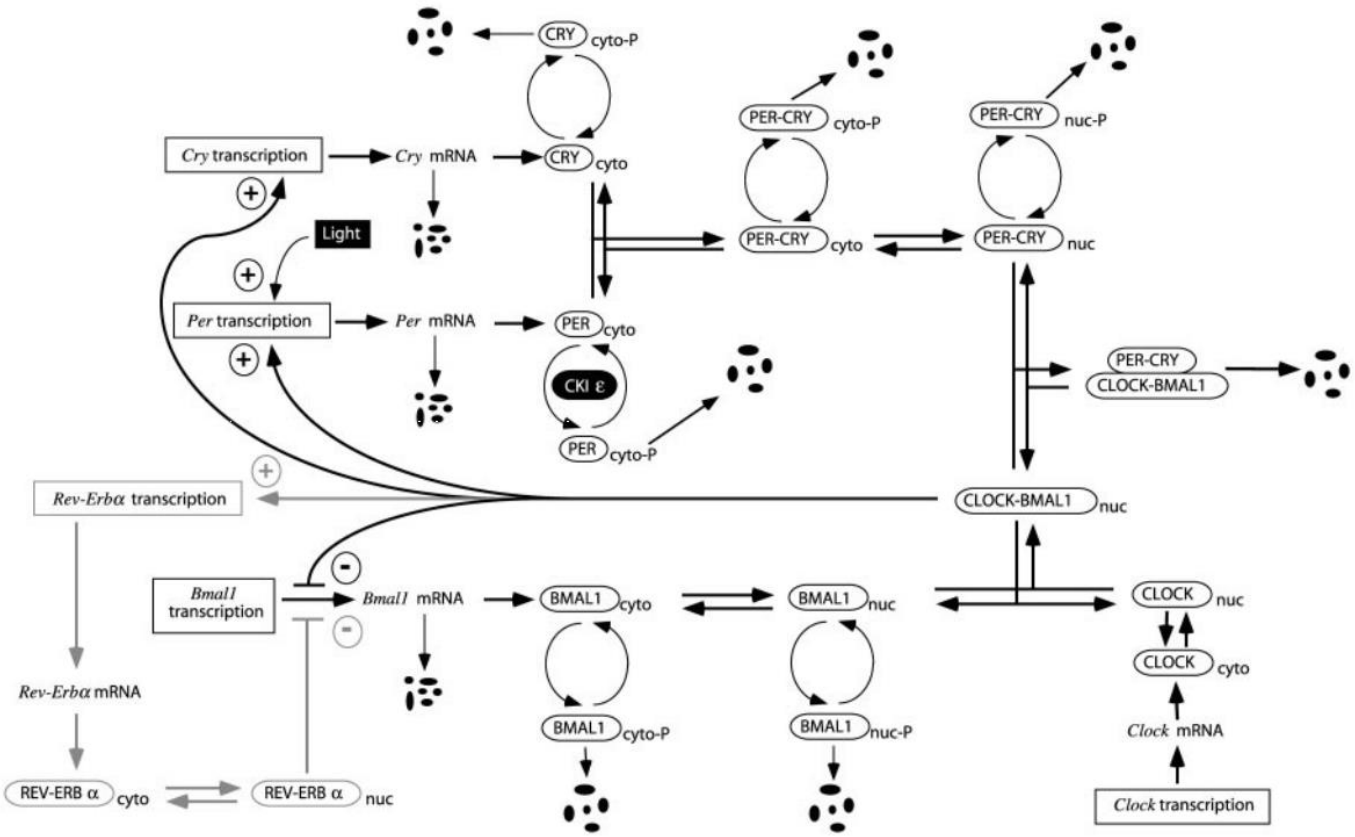

Figure 6.2. Schematic diagram of the interactions modelled in the Leloup and Goldbeter mathematical model, taken from (Leloup and Goldbeter, 2003).

6.2 Objectives

6.2.1 Model Objectives

The aim was to produce a model of the circadian molecular clock and to add in a further component into the system – lamin A. This extra component will allow us to explore potential mechanisms by which lamin A may regulate the circadian clock. Models focused on incorporating four methods of potential regulation by lamin A protein: gene up- and down-regulation, transcription factor sequestering, and nucleo-cytoplasmic shuttling of transcription factors. The mechanisms by which lamin A may undergo gene regulation and particularly, how laminopathies can result in severe tissue

specific effects have been discussed and these four gene-regulation mechanisms are favoured (Camozzi, *et al*., 2014; Maggi, *et al*., 2016). This research predicts that when lamin A is mutated, an aspect of circadian regulation is lost, facilitating the loss of tissue-specific maintenance observed. As with lamin A regulation, it is well known that the circadian clock is responsible for tissue-specific gene expression, important in the development and maintenance of tissues – such as muscle (Markiewicz, Ledran, and Hutchison, 2005). Therefore, these models will facilitate the studies of potential mechanistic methods by which lamin A may be interacting with the circadian clock. Once these models are generated, specific conditions of lamin A will be modelled and the response observed in the expression of clock genes and proteins can be predicted. As outlined above, experimental studies can then determine if these models correctly predicted the response and whether the mechanism modelled may be correct. The objective of these models was to guide the design of future experiments that investigate potential mechanisms and computationally visualise how they may interact. The aim was to utilise model simulations to highlight relevant mechanisms of regulation, which may be acting on the complex system of the circadian clockwork.

6.2.2 Hypothesis

These models will predict the response of clock genes and proteins to lamin A genetic modification within different mechanisms of feedback regulation exerted by lamin A onto the circadian molecular core clock. It was hypothesised that models incorporating lamin A feedback regulation onto the circadian clock can be produced, and that core clock mRNA and proteins and lamin A mRNA and protein can be simulated to produce oscillating traces. It was predicted that the manipulation of lamin A within these models will alter circadian gene expression and protein levels; any changes to amplitude, phase, and periodicity within these models with lamin A manipulation will be investigated.

6.3 Model Formulation

6.3.1 CellDesigner

CellDesigner is a diagram editing software used to draw gene-regulatory and biochemical networks, using graphical notations (Funahashi, *et al*., 2003). Through visualisation of complex multi-gene and protein interactions it enables mathematical modellers to begin piecing together the complex system and breaking it down into the various reactions required to build the entire system. CellDesigner was used to build the network structure for models that were then simulated using the COPASI software.

6.3.2 COPASI

Simulations to determine mRNA and protein levels for *Per*, *Cry*, *Bmal*, *Rev-erba*, and *Lmna* over 72 hours were ran on COPASI (Hoops, *et al*., 2006). COPASI is a powerful biochemical network simulation software tool which is widely used in systems biology research. The models developed were all extensions of the Leloup and Goldbeter mathematical model (Leloup and Goldbeter, 2003). Parameters for the original model were retained but those defined in the extensions for lamin A were fitted using COPASI. Suitable parameter values were inputted to produce oscillatory expression for lamin A in each of the four models before manipulation of lamin A. In this regard, on manipulation of lamin A, the robustness of each model was also investigated by adapting the overexpression or knockdown to 50%.

6.4 Results

6.4.1 Model Design

6.4.1.1 Model 1: Bidirectional regulation of lamin A and *Per*

In the first model, lamin A expression is upregulated by the BMAL:CLOCK heterodimer and in accordance, is subject to clock control. Lamin A mRNA and protein is upregulated together with *Per*, *Cry*, and *Rev-erbα* (there is only one *Per* and one *Cry* gene in each model). For lamin A to exert feedback regulation onto the core molecular clock, the first model incorporates repression of *Per* expression by the lamin A dimer. Hence, when *Lmna* is upregulated by BMAL:CLOCK and the lamin A dimer is produced, it feeds back to negatively regulate *Per* expression (Figure 6.3).

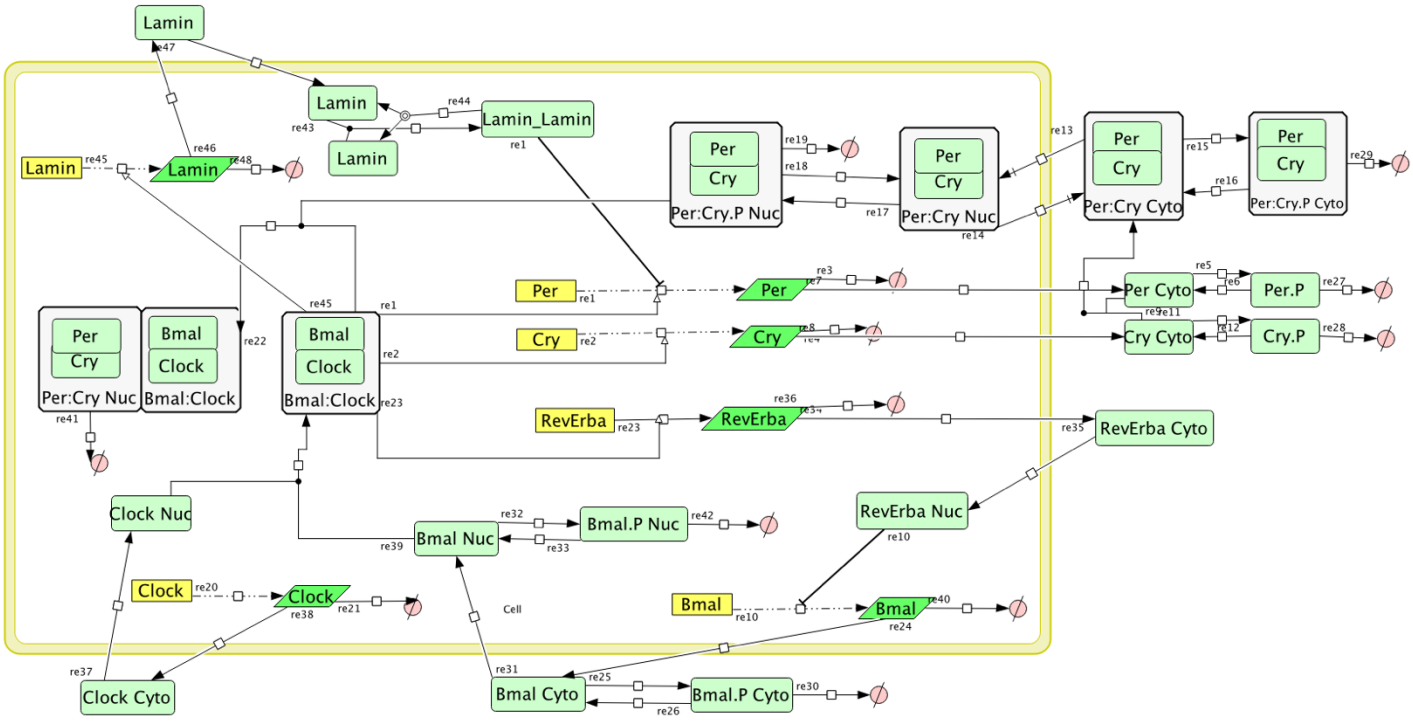

Figure 6.3. Cell Designer regulatory network for Model 1, lamin A is under clock control, through positive regulation by BMAL:CLOCK, and negatively regulates *Per* transcription.

6.4.1.2 Model 2: lamin A upregulates *Per* expression

The second model also involved lamin A providing feedback regulation to the expression of *Per* mRNA. In contrast with the first model, this model observed the effect of lamin A feeding back to positively regulate *Per*. Lamin A mRNA and protein are upregulated by BMAL:CLOCK, in synchronisation with *Per*, *Cry*, and *Rev-erbα*. It was predicted that lamin A will feedback to act as a further 'boost' to upregulate *Per* mRNA and protein levels (Figure 6.4).

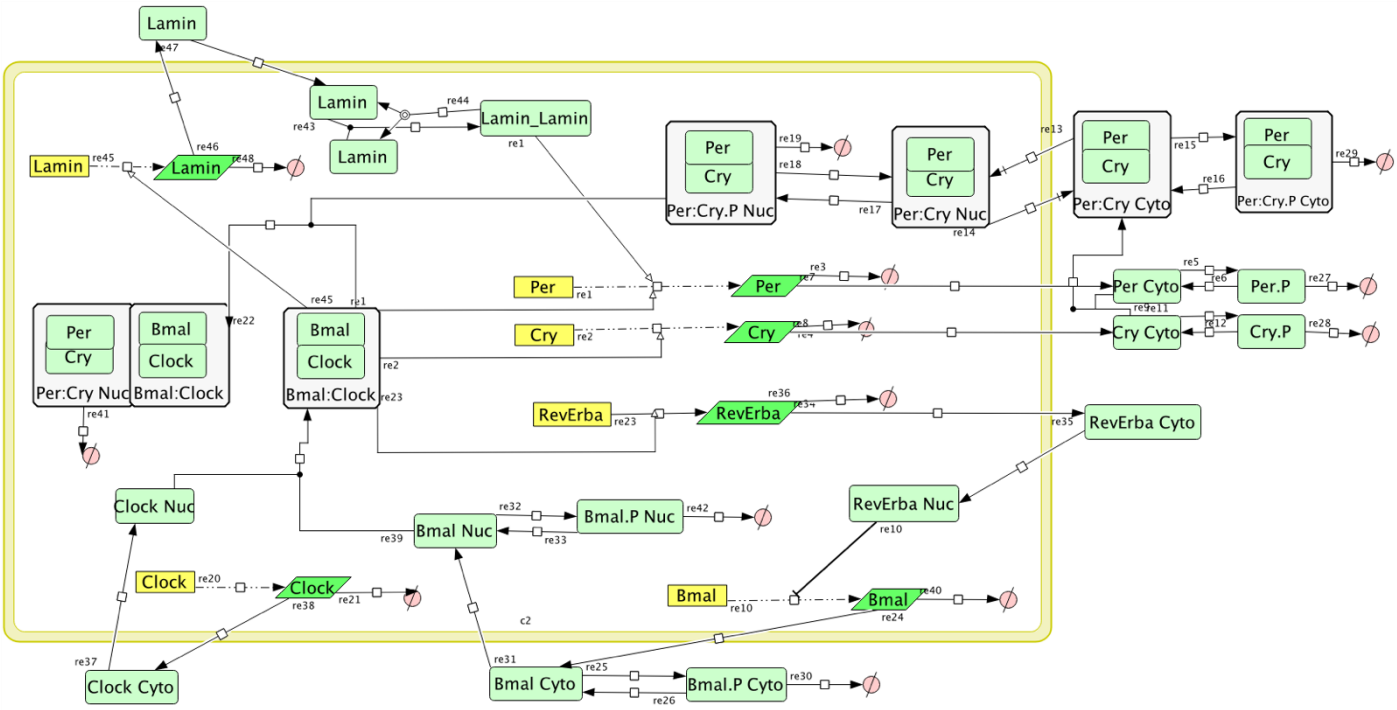

Figure 6.4. Cell Designer regulatory network for Model 2, lamin A is under clock control, through positive regulation by BMAL:CLOCK, and positively regulates *Per* transcription.

6.4.1.3 Model 3: lamin A regulates TF localisation

The third model included lamin A expression positively regulated by the BMAL:CLOCK heterodimer to produce rhythmic lamin A mRNA traces and protein production. In addition, it incorporated the formation of an additional complex: a lamin A dimer bound to PER:CRY (Lm_Lm:PCn). After the production of lamin A dimers, the Lm_Lm:PCn complex is formed and relocates the PER:CRY heterodimer to the nuclear periphery. This re-localisation of the transcription factor complex to the nuclear periphery prevents PER:CRY from binding to the BMAL:CLOCK heterodimer. Subsequently, the BMAL:CLOCK:PER:CRY complex cannot be formed and targeted for degradation. In addition, this localisation prevents the expression of any circadian controlled genes regulated by PER:CRY. Therefore, in this model and by this mechanism of circadian clock feedback regulation, lamin A temporally regulates the activity of PER:CRY within the nucleus through control of its nuclear localisation (Figure 6.5).

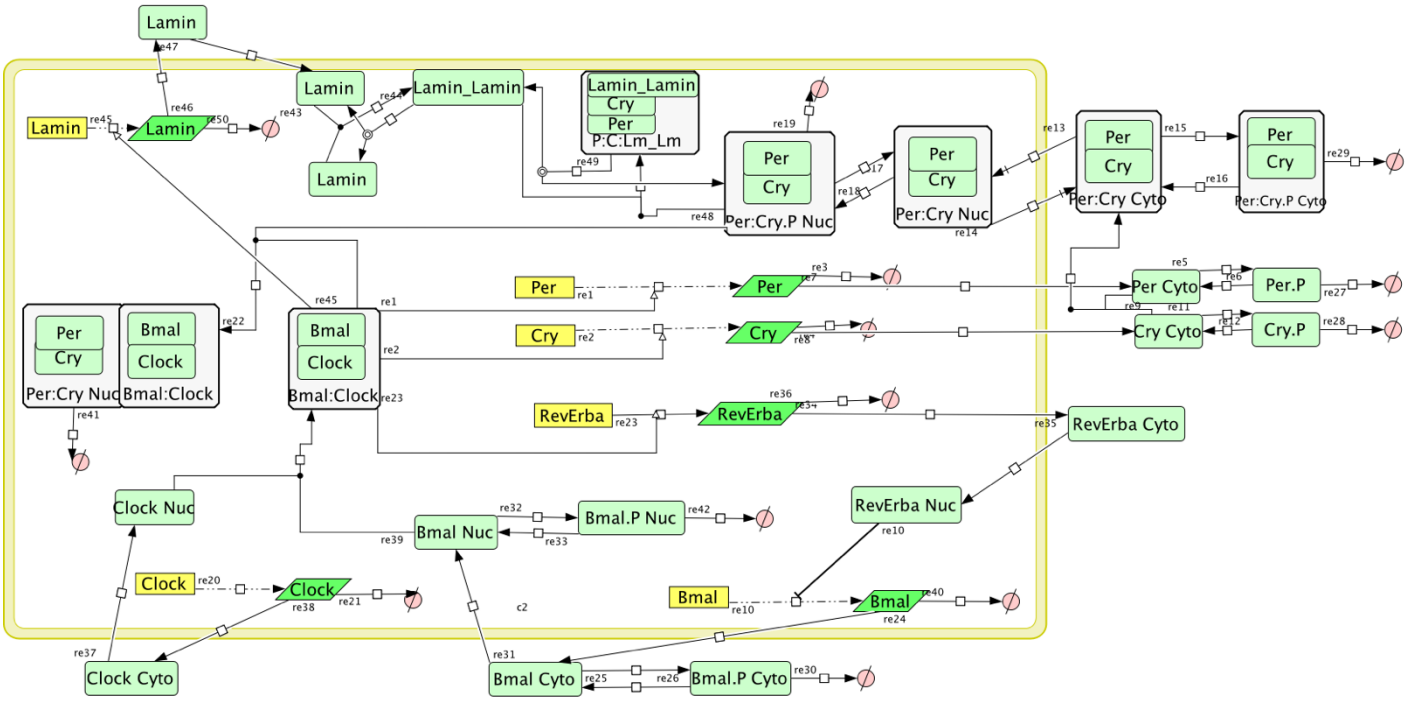

Figure 6.5. Cell Designer regulatory network for Model 3, lamin A is under clock control, through positive regulation by BMAL:CLOCK, and binds to PER:CRY complex in the nucleus to tether it to the nuclear periphery.

6.4.1.4 Model 4: lamin A regulates TF translocation

Our fourth model includes Lamin A expression positively regulated by the BMAL:CLOCK heterodimer to produce rhythmic Lamin A mRNA traces and protein production. This model incorporates negative feedback through inhibiting the translocation of the PER:CRY heterodimer from the cytoplasm into the nucleus, delaying the entry of PER:CRY into the nucleus and preventing it from binding to BMAL:CLOCK. The formation of the PER:CRY:BMAL:CLOCK complex results in subsequent targeting for degradation and thus, translocation inhibition delays PER:CRY degradation and BMAL:CLOCK degradation. This facilitates further positive gene up-regulation by BMAL:CLOCK and prevents clock-controlled gene expression by PER:CRY. Therefore, this model feeds back to regulate the circadian molecular clock through controlling the translocation rate of PER:CRY into the nucleus (Figure 6.5).

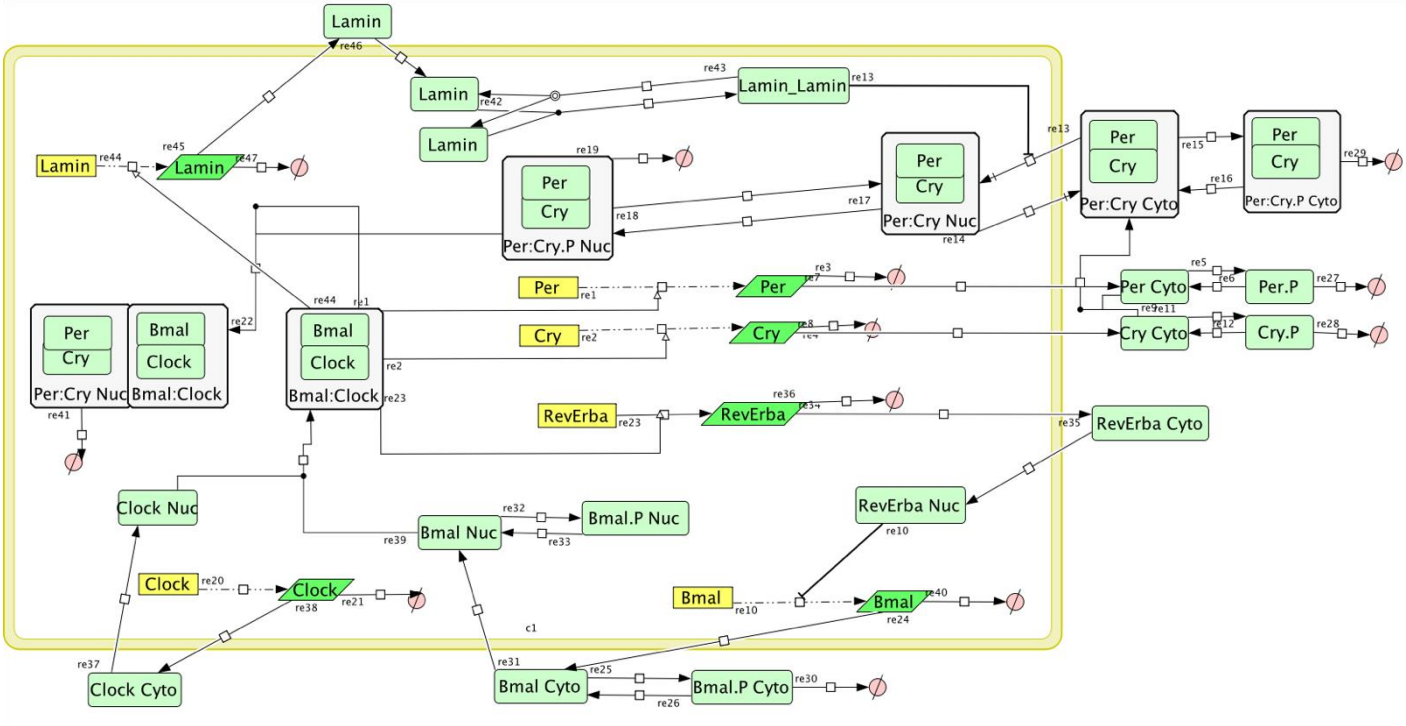

Figure 6.6. Cell Designer regulatory network for Model 4, lamin A is under clock control, being positively regulated by BMAL:CLOCK, and negatively regulates the translocation of PER:CRY into the nucleus.

6.4.2 Model Simulations

6.4.2.1 REV-ERBα model

The mathematical simulation produced by Leloup and Goldbeter incorporated *Bmal*, *Per*, *Cry*, and *Rev-erbα* genes (Leloup and Goldbeter, 2003). The expression of *Bmal* peaks at roughly hours 12, 36, and 60, and has higher amplitude than the expression of the negative core clock genes. The expression of *Per*, *Cry*, and *Rev-erbα* are in synchronisation and peak at roughly hours 21, 45, and 69, shown in Figure 6.7. This model integrates entrainment signals from light: dark diurnal patterns to the circadian clock, through the incorporation of light-induced *Per* expression. The removal of these entrainment signals, under constant dark conditions, does not alter the production of free-running oscillations in the expression of clock genes. Therefore, this mathematical model represents a robust and dynamic representation of the circadian molecular clock.

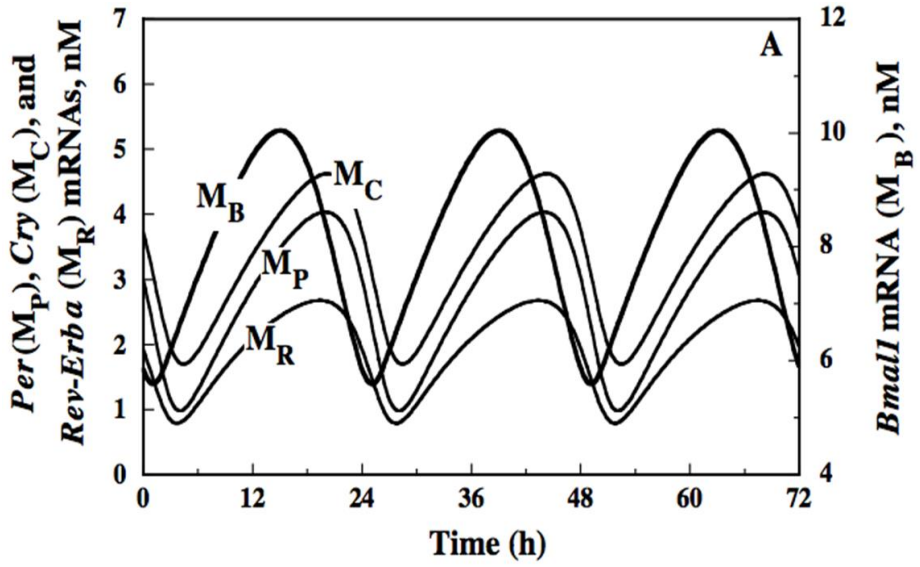

Figure 6.7. Gene expression simulations of the Leloup and Goldbeter Model (Supplementary Figure 8; Leloup and Goldbeter, 2003). mRNA levels over a 72-hour period for the model demonstrating rhythmic expression in *Bmal*, *Per*, *Cry*, and *Rev-erbα*, represented as M_B, M_P, M_C, and M_R, respectively. The mRNA concentration of *Per*, *Cry*, and *Rev-erbα* are shown on the left Y-axis, and *Bmal* mRNA concentration is shown on the right Y-axis.

6.4.2.2 The circadian clock regulates *Lmna*

To begin investigating potential mechanisms that lamin A may use to feedback and regulate the circadian clock, the Leloup and Goldbeter model was reproduced and adapted to include *Lmna* gene expression and protein production. In keeping with previous experimental data that demonstrated rhythmic oscillations in the expression of *Lmna* that are in synchronisation with the genes of the negative arm of the core clock, *Lmna* upregulation by BMAL:CLOCK was incorporated into the model. This produced rhythmic *Lmna* traces that were synchronised with the negative arm core clock genes and *Rev-erbα*, and were anti-phase to *Bmal* expression (Figure 6.8).

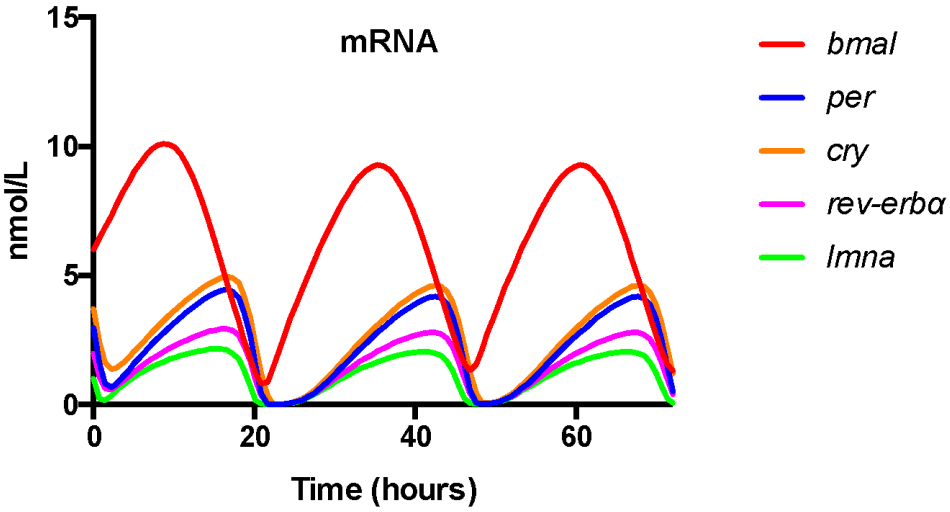

Figure 6.8 COPASI mRNA concentration for the Leloup and Goldbeter model with lamin A incorporated over 72 hours. Lamin A mRNA synthesis is regulated by BMAL:CLOCK, generating oscillating mRNA expression that is in phase with the negative arm of the circadian clock.

The corresponding protein traces for BMAL, PER:CRY, REV-ERBα and LMNA were also produced with rhythmic oscillations (Figure 6.9). Lamin A was in synchronisation with the negative arm proteins, the PER:CRY heterodimer, and REV-ERBα, with LMNA peaking 1-2 hours earlier. BMAL was anti-phase as expected and peaked first.

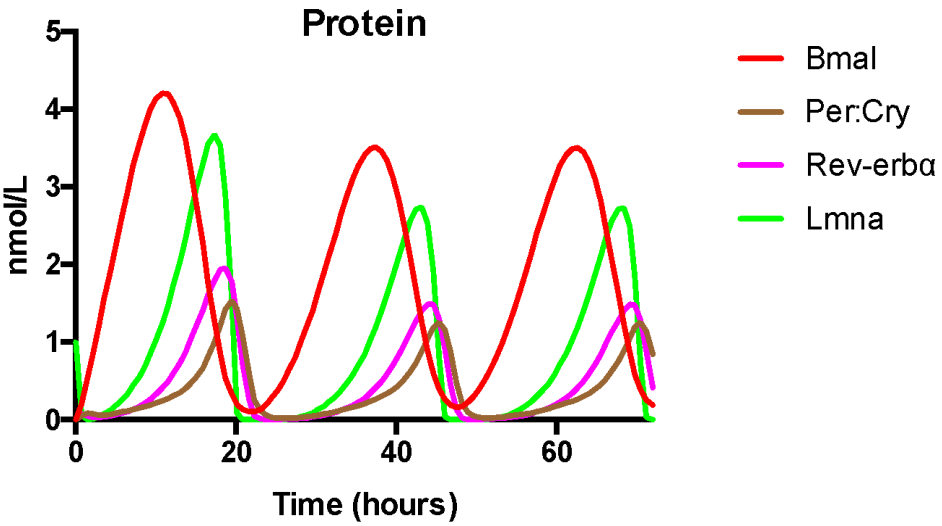

Figure 6.9 COPASI protein concentration for the Leloup and Goldbeter model with lamin A incorporated over 72 hours. BMAL protein in the nucleus was anti-phase with PER:CRY complex in the nucleus and REV-ERBα. Lamin dimer in the nucleus peaked a few hours before PER:CRY complex peaks.

6.4.3 Lamin A Feedback Models

The activity of lamin A in the adapted model was altered to model four mechanisms of lamin A feedback regulation onto the circadian clock, depicted in the Cell Designer Diagrams shown in Figures 6.3, 6.4, 6.5, and 6.6. The ODEs corresponding to each of the four models can be found in the appendix. Once these models were generated and suitable parameter values obtained, lamin A was manipulated to achieve overexpression and knockout conditions. Within these manipulated models the effect on the molecular clock was observed, to further the understanding of potential feedback mechanisms to the clock. In addition, it was evaluated whether the output from these models matched laboratory data, to highlight mechanisms of interest and direct future experiments. As the models were generated by inputting suitable parameter values, the robustness of each model was analysed by adapting the overexpression or knockout to 50%. The effect of a full knockout or overexpression was compared to the 50% manipulation. This ensures that the impact on the clock under each condition is directly related to the corresponding levels of lamin A present, and it can be guaranteed that the effect is robust.

6.4.3.1 Model 1: *Per* synthesis Repression

To model the negative regulation of *Per* mRNA synthesis by lamin A, the mPer synthesis reaction was adapted to include competitive inhibition by the lamin A dimer (Lm_Lm). In the Leloup and Goldbeter model, *Per* mRNA synthesis was only regulated positively by BMAL and oscillations were generated in accordance with BMAL protein levels. In this manner, as BMAL protein oscillated with a circadian rhythm, BMAL could only upregulate *Per* expression in a circadian manner. With the addition of lamin A negative inhibition, once *Lmna* expression is upregulated by BMAL and lamin A levels increase, this will act to repress the expression of *Per.*

Incorporating the repression of *Per* expression by lamin A into the model had no effect on the oscillatory periods of expression, but there was a slight decrease in the amplitude of *Per* expression (Figure 6.10A.). In addition, the protein levels of BMAL decreased from 4 to 3 nmol/L but the levels of PER:CRY complex in the nucleus remained between 1 to 2 nmol/L (Figure 6.10B.).

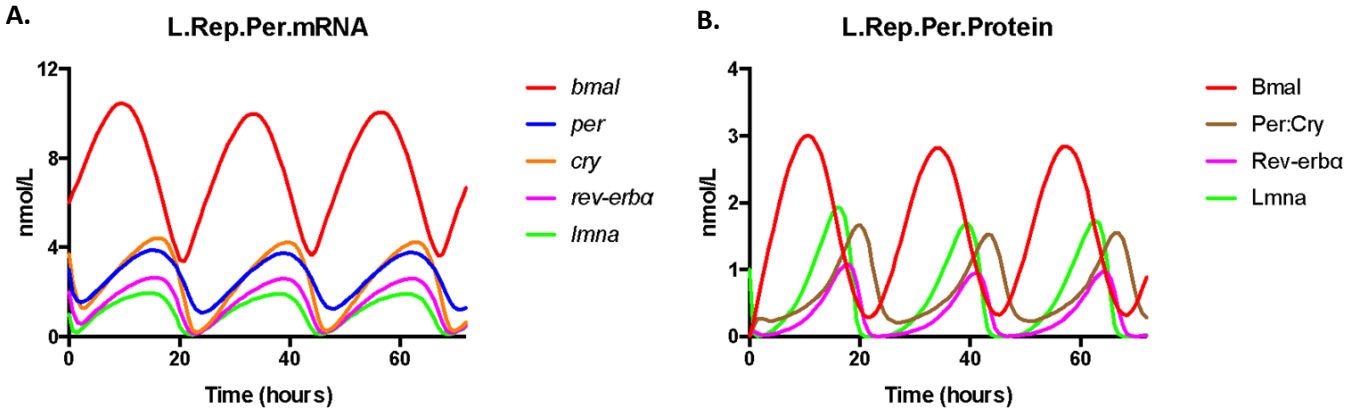

Figure 6.10. mRNA traces and protein concentrations in Model 1, lamin A repressing *Per* synthesis. *Lmna* mRNA and protein oscillate in phase with the negative arm core clock genes, and antiphase to Bmal mRNA expression and protein levels.

6.4.3.2 Model 1: *Per* Repression, lamin A Overexpression

To begin investigating the relationship between lamin A and the circadian clock with lamin A feeding back to repress *Per* synthesis, the next aim was to investigate the effect of lamin A overexpression in this model on circadian mRNA expression and protein concentration. Lamin A was overexpressed; mRNA oscillated at 525 nmol/L and protein concentration was increased to 1000 nmol/L (Figures 6.11A. and 6.11B.). In response, *Per* expression decreased rapidly to 0 nmol/L, *Cry* expression increased by 1 nmol/L, and the period of gene expression increased (Figures 6.11A.). Additionally, the concentration of PER:CRY complex decreased to 0 nmol/L, BMAL and REV-ERBα increased to 7.5 nmol/L and 6 nmol/L, respectively, and the period increased (and 6.11B.). The 50% lamin A overexpression model, where lamin A mRNA and protein concentration were approximately 150nmol/L and 200 nmol/L, respectively, retained the repression of *per* mRNA and PER:CRY complex in the nucleus in a robust manner (Figures 6.11C. and 6.11D.).

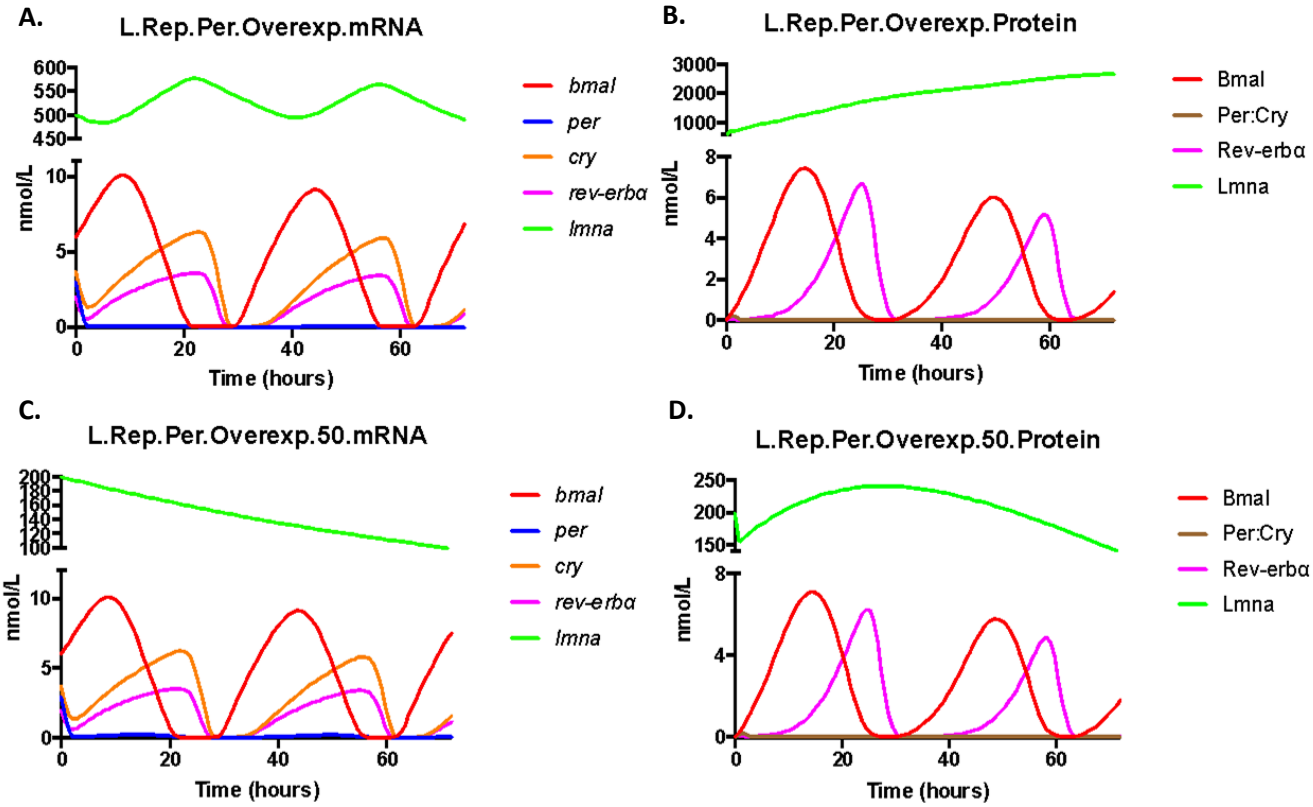

Figure 6.11. mRNA traces and protein concentrations in Model 1 with lamin A overexpression and 50% overexpression, lamin A repressing *Per* synthesis. Lamin A mRNA and protein was overexpressed to around 525 nmol/L and 1000 nmol/L, respectively. 50% overexpression models were reduced to 200 nmol/L mRNA and 200 nmol/L protein levels.

6.4.3.3 Model 1: *Per* Repression, lamin A Knockout

Next, lamin A was knocked out in Model 1 to investigate the effect of lamin A knockout on the circadian molecular clock incorporating a stable feedback loop of lamin A repressing *Per* synthesis. Lamin A mRNA and protein concentration were knocked out to 0 nmol/L (Figure 6.12A. and 6.12B.). The levels of *Per* mRNA under these conditions increased slightly, *Per* mRNA was at the same concentration as *Cry* mRNA, and PER:CRY complex in the nucleus increased at peak concentration from roughly 1.5 nmol/L to 2 nmol/L (Figure 6.12A. and 6.12B.). Robustness of this knockout was investigated through testing conditions with a 50% lamin A knockdown to peak concentration of 1 nmol/L and 0.3 nmol/L for mRNA and protein, respectively (Figure 6.12C. and 6.12D.). The observed effect in *Per* mRNA and protein concentration in the 50% model demonstrated consistent concentrations with the full knockout model (Figure 6.12C. and 6.12D.).

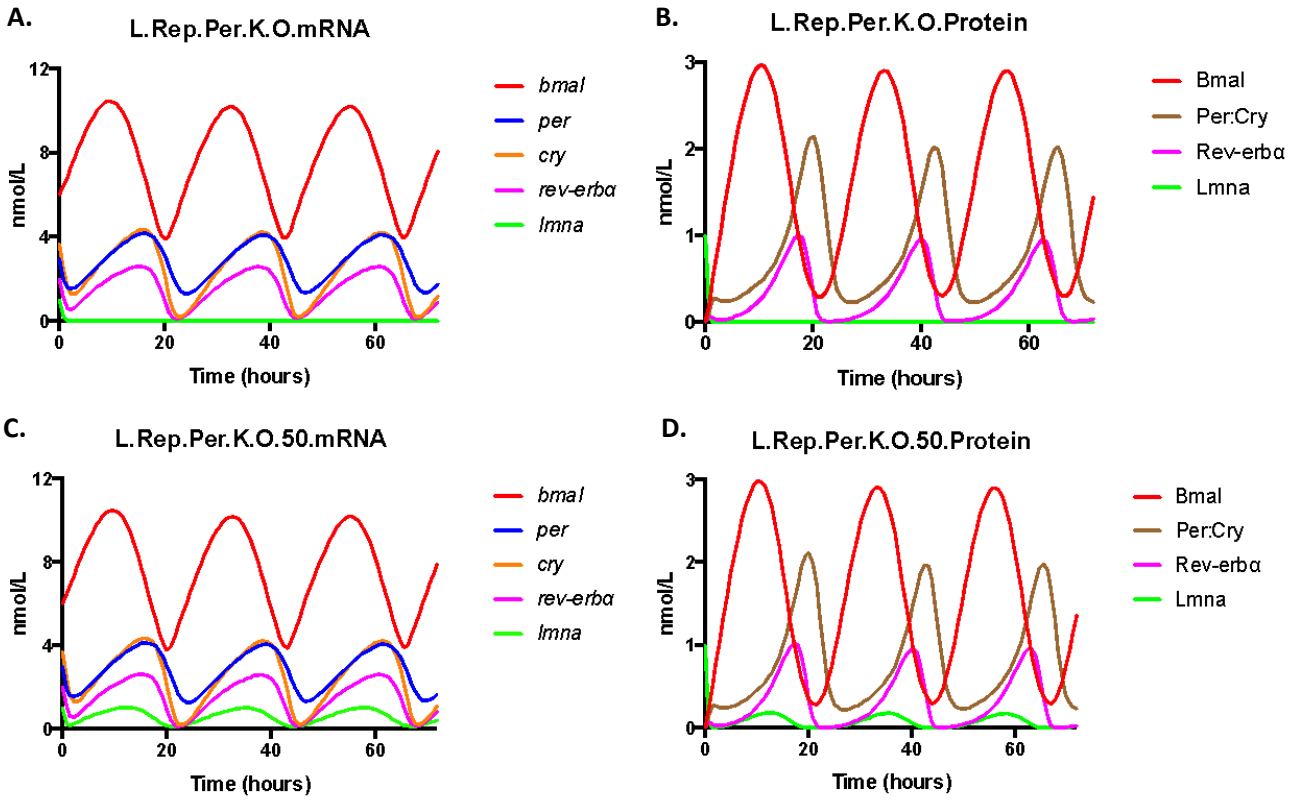

Figure 6.12. mRNA traces and protein concentrations in Model 1 with lamin A knockout and 50% knockdown, lamin A repressing *Per* synthesis. Lamin A mRNA and protein knockout to 0 nmol/L and 50% knockdown to 1 nmol/L and 0.3 nmol/L for mRNA and protein, respectively.

6.4.3.4 Model 2: *Per* synthesis Upregulation

To model lamin A feedback regulation to upregulate *Per*, the mPer synthesis reaction was adapted to include upregulation by the Lm_Lm dimer as a modifier in addition to BMAL. *Bmal* mRNA oscillated with a circadian rhythm antiphase to *Lmna* and *Per*; when BMAL protein levels were high in the nucleus, it upregulated *Lmna* and *Per* expression. In this model, BMAL upregulated the expression of LMNA and in turn, LMNA further increased *Per* expression. Accordingly, the oscillatory increase in levels of lamin A, by BMAL, feedback to boost upregulation of *Per* expression.

Incorporating lamin A upregulation of *Per* synthesis in Model 2 shifted the phase of *Per* expression oscillation earlier and consequently, it was in phase with *Bmal* (Figure 6.13A.). The oscillation of PER:CRY complex in the nucleus dampened in amplitude and exhibited a slight phase shift to peak earlier, just before REV-ERBα; normally PER:CRY complex peaked just after REV-ERBα (Figure 6.13B.; Figure 6.8). Furthermore, the protein concentrations at peak oscillation of BMAL, LMNA, and REV-ERBα were also reduced in this feedback model (Figure 6.13B.).

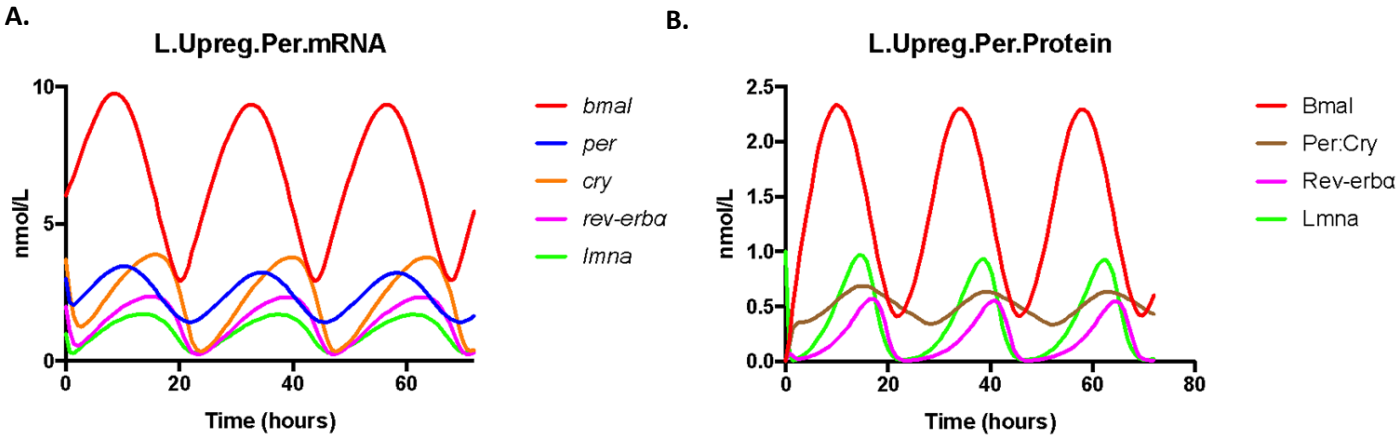

Figure 6.13. mRNA traces and protein concentrations in Model 2, lamin A upregulating *Per* synthesis. Lamin A oscillates in phase with the negative arm core clock genes, and *Per* mRNA and PER:CRY complex peak earlier are have dampened oscillations.

6.4.3.5 Model 2: *Per* Upregulation, lamin A Overexpression

To investigate the response of lamin A manipulation on the circadian clock in Model 2: lamin A upregulating *Per* expression, first, the concentration of lamin A mRNA and protein were overexpressed. Lamin A mRNA increased to around 400 nmol/L and protein increased to 600 nmol/L (Figure 6.14A. and 6.14B.). The expression of *Per* decreased rapidly to 0 nmol/L and *Cry* increased to 6 nom/L; additionally, the concentration of PER:CRY protein complex in the nucleus decreased to 0 nmol/L (Figures 6.14A. and 6.14B.). This effect was demonstrated as robust in the 50% lamin A overexpression model, with lamin A mRNA and protein concentration at roughly 160nmol/L and 200 nmol/L, respectively. Both *Per* mRNA and PER:CRY complex in the nucleus remained repressed to 0 nom/L (Figures 6.14C. and 6.14D.). This result was unexpected, it was predicted that the upregulation of *Per* by lamin A would be heightened and consequently, *Per* mRNA levels would be increased.

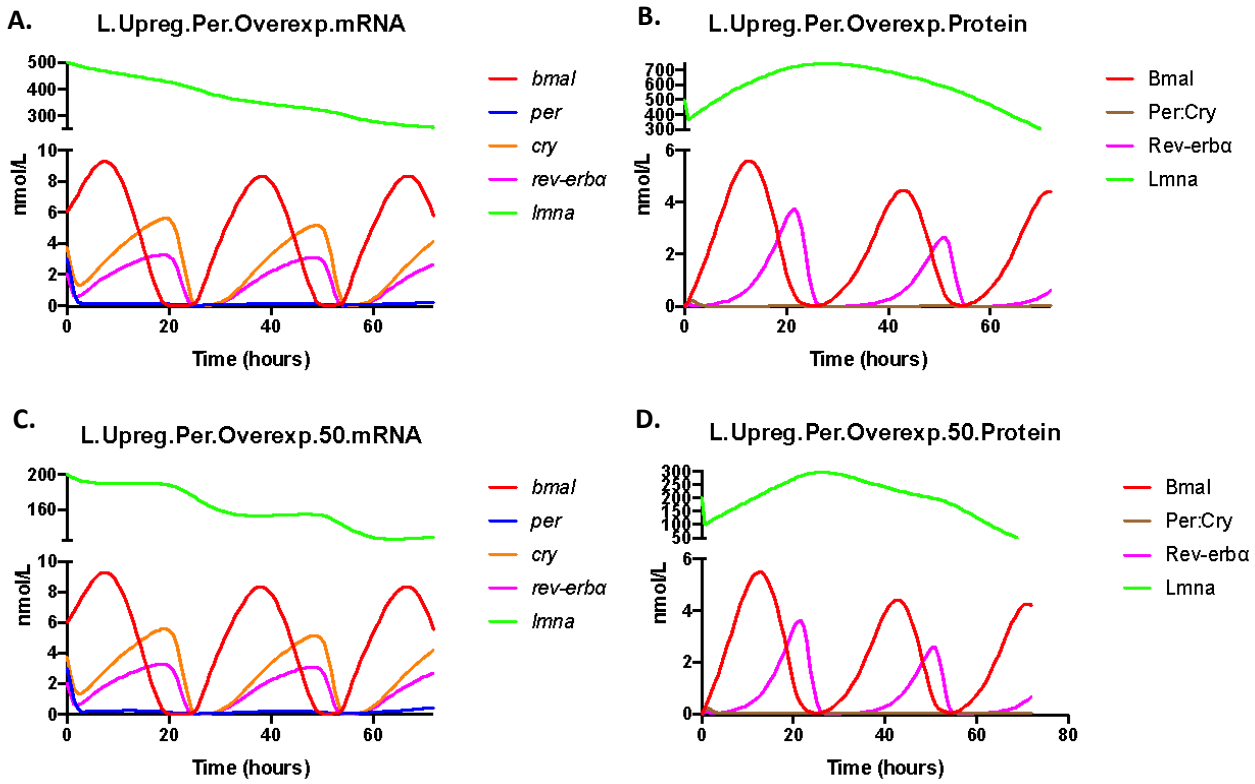

Figure 6.14. mRNA traces and protein concentrations in Model 2 with lamin A overexpression and 50% overexpression, lamin A upregulating *Per* synthesis. Lamin A mRNA was overexpressed to around 500 nmol/L and protein to 500 nmol/L.

5.4.3.6 Model 2: *Per* Upregulation, lamin A Knockout

To investigate whether the response of lamin A knockout in Model 2 mirrors the unusual result observed on overexpression of lamin A, the next aim was to knockout lamin A. Lamin A mRNA and protein were knocked out to 0 nmol/L (Figure 6.15A. and 6.15B.). The concentration of *Per* and *Bmal* mRNA and PER:CRY complex increased, and oscillated with a shorter period, eventually producing a flat line (Figure 6.15A. and 6.15B.). This simulation is robust as when lamin A was knocked down at 50%, the concentration of *Per* and *Bmal* mRNA and PER:CRY complex continued to increase with time and oscillated with a shorter period (Figure 6.15C. and Figure 6.15D.). This result was unexpected, it was predicted that the upregulation of *Per* by lamin A would be lost and consequently, the expression of *Per* would be decreased.

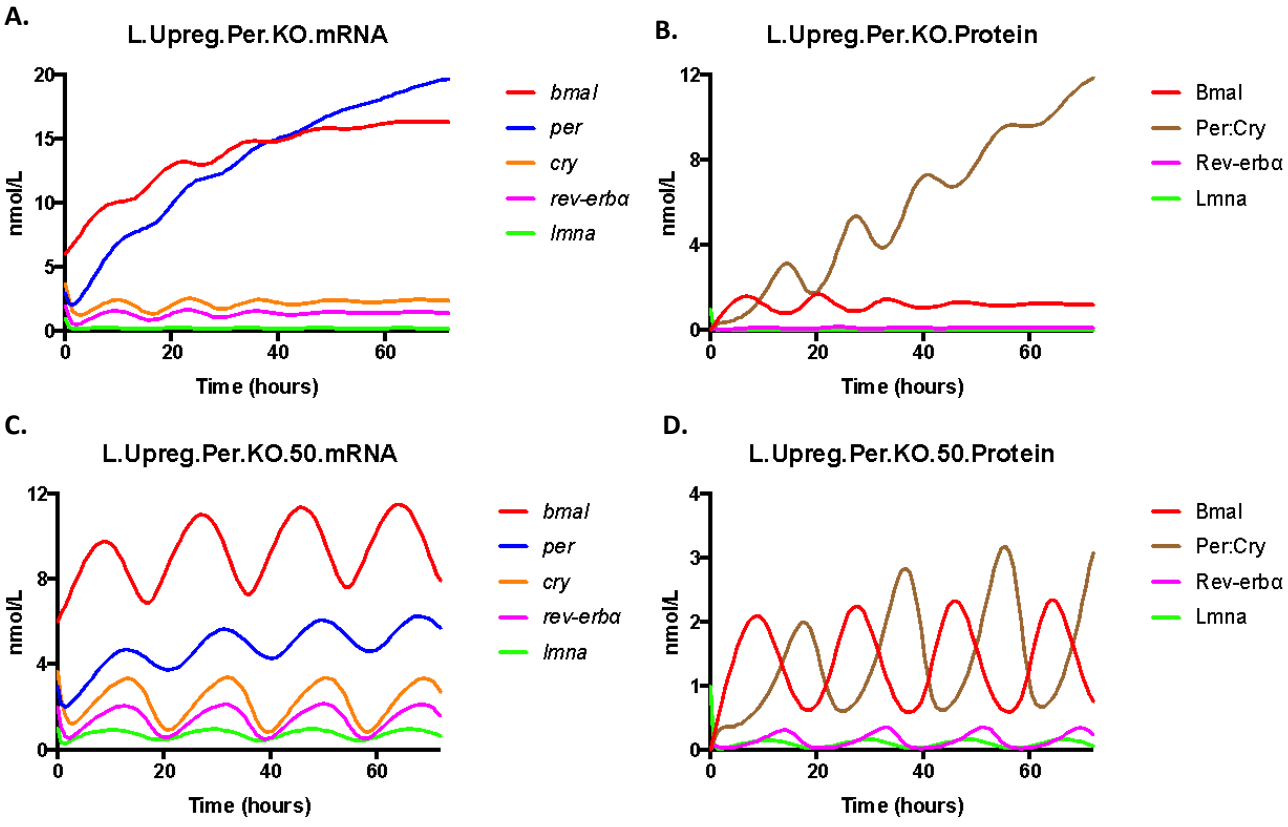

Figure 6.15. mRNA traces and protein concentrations in Model 2 with lamin A knockout and 50% knockdown, lamin A upregulating *Per* synthesis. Lamin A complete knockout, or 50% knockdown to 1 nmol/L and 0.3 nmol/L for mRNA and PER:CRY complex protein, respectively.

6.4.3.7 Model 3: PER:CRY sequestering

To model lamin A sequestering and regulating the activity PER:CRY complex in the nucleus, a new complex was added into Model 3: Lm_LmPCn. This represented the formation of a complex containing a Lamin dimer and the PER:CRY heterodimer in the nucleus. This complex sequesters PER:CRY in the nucleus at the nuclear periphery, where Lamin dimers are located, and as a result, it regulates the activity of PER:CRY. Indeed, this reaction prevents PER:CRY from complexing with BMAL, and prevents the complex being targeted for degradation.

The addition of this complex formation incorporated into the third model did not change the mRNA traces of the core clock genes or *Lmna* (Figure 6.16A.). The oscillation in protein concentrations observed after the integration of the Lm_Lm:PER:CRY complex remained unchanged for BMAL, but the concentration of PER:CRY, REV-ERBα and LMNA were roughly 0.5 nmol/L lower (Figure 6.16B.).

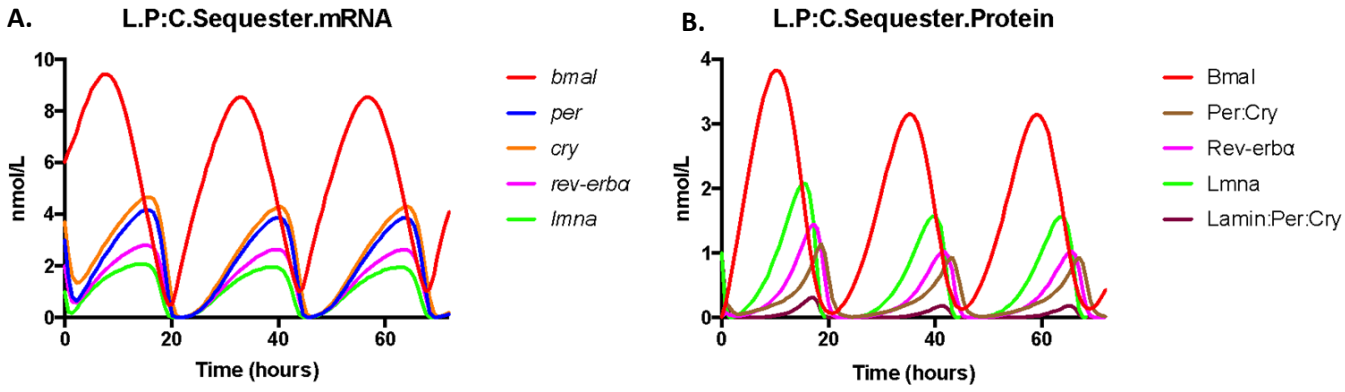

Figure 6.16. mRNA traces and protein concentrations in Model 3, lamin A sequestering PER:CRY complex within the nucleus. Lamin A and the new complex Lm_Lm:PER:CRY are oscillating in phase with the negative arm core clock genes, and are anti-phase to Bmal mRNA and protein oscillation.

6.4.3.8 Model 3: PER:CRY sequestering, lamin A Overexpression

To investigate whether the overexpression of lamin A perturbs the dynamics of the molecular clock in Model 3, the next aim was to overexpress lamin A mRNA and protein. Lamin A mRNA and protein were overexpressed to 500nmol/L and 200nmol/L (Figure 6.17A. and Figure 6.17B.). The concentration of *Per* and *Cry* mRNA increased by 1 nmol/L, and *Per*, *Cry*, and *Rev-erbα* were phase-delayed and peaked 2 hours later (Figure 6.17A.). The protein concentration of BMAL and REV-ERBα in the nucleus increased from 4 to 6nmol/L and 1.5 to 4nmol/L, respectively; PER:CRY in the nucleus was repressed to 0nmol/L (Figure 6.17B.). The response observed in *Per*, *Cry*, and *Rev-erbα* mRNA and BMAL, REV-ERBα, and PER:CRY protein was demonstrated as a robust response as the same oscillations in concentration were observed when the concentration of lamin A overexpression was reduced to 50% (Figure 6.17C. and Figure 6.17D.).

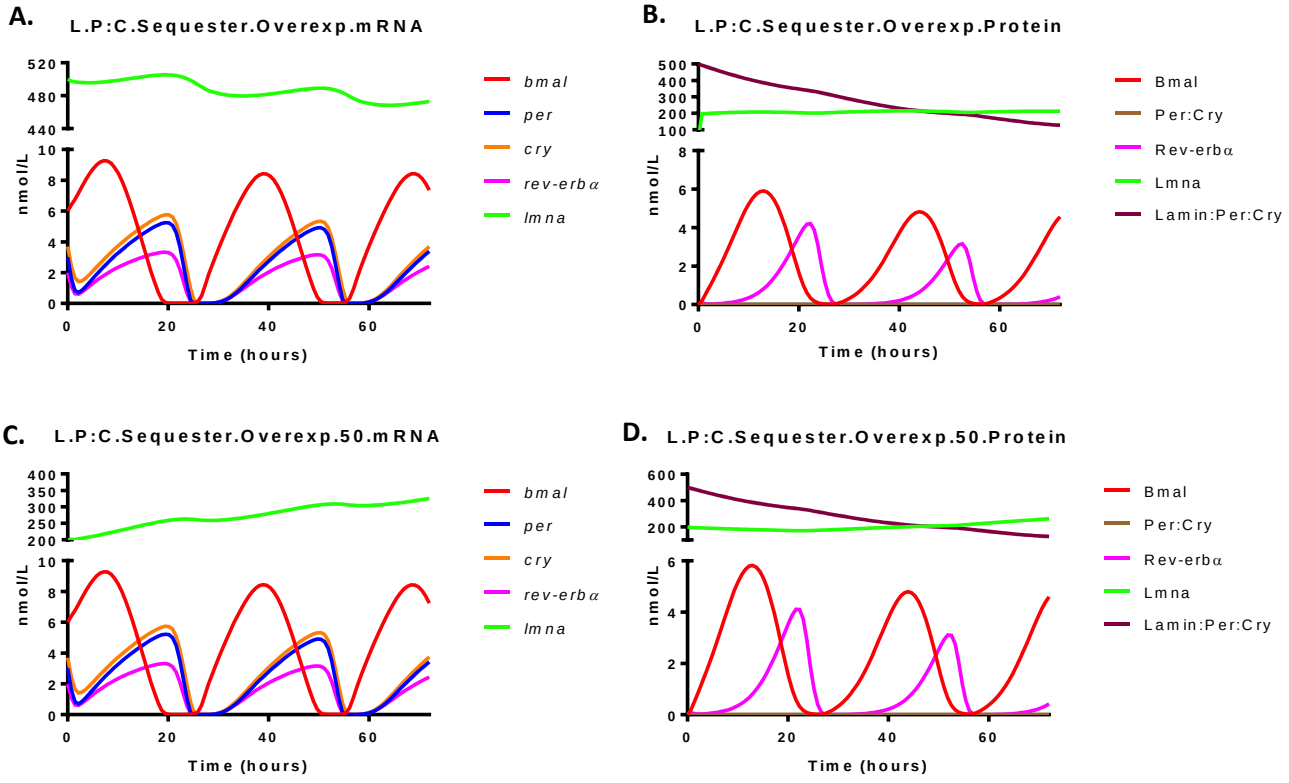

Figure 6.17. mRNA traces and protein concentrations in Model 3 with lamin A overexpression and 50% overexpression, sequestering PER:CRY complex within the nucleus. Lamin A overexpression to 500nmol/L for mRNA and 200nmol/L for protein, and 50% overexpression to 200nmol/L for mRNA and 100nmol for protein.

6.4.3.9 Model 3: PER:CRY sequestering, lamin A Knockout

The next aim was to determine the response of the molecular clock to knockout of lamin A in Model 3, with lamin A sequestering PER:CRY at the nuclear periphery. Lamin A mRNA and protein were knocked out to 0 nmol/L (Figure 6.18A. and Figure 6.18B.). The concentration of *Bmal*, *Per*, *Cry*, and *Rev-erbα* mRNA remained oscillating at similar levels (Figure 6.18A.). In addition, BMAL, REV-ERBα, and PER:CRY protein in the nucleus continued to oscillate at a similar concentration (Figure 6.18B.).

50% knockdown of lamin A in Model 3 also had no effect on the concentration or periodicity of circadian mRNA or protein oscillations (Figure 6.18A. and figure 6.18B.).

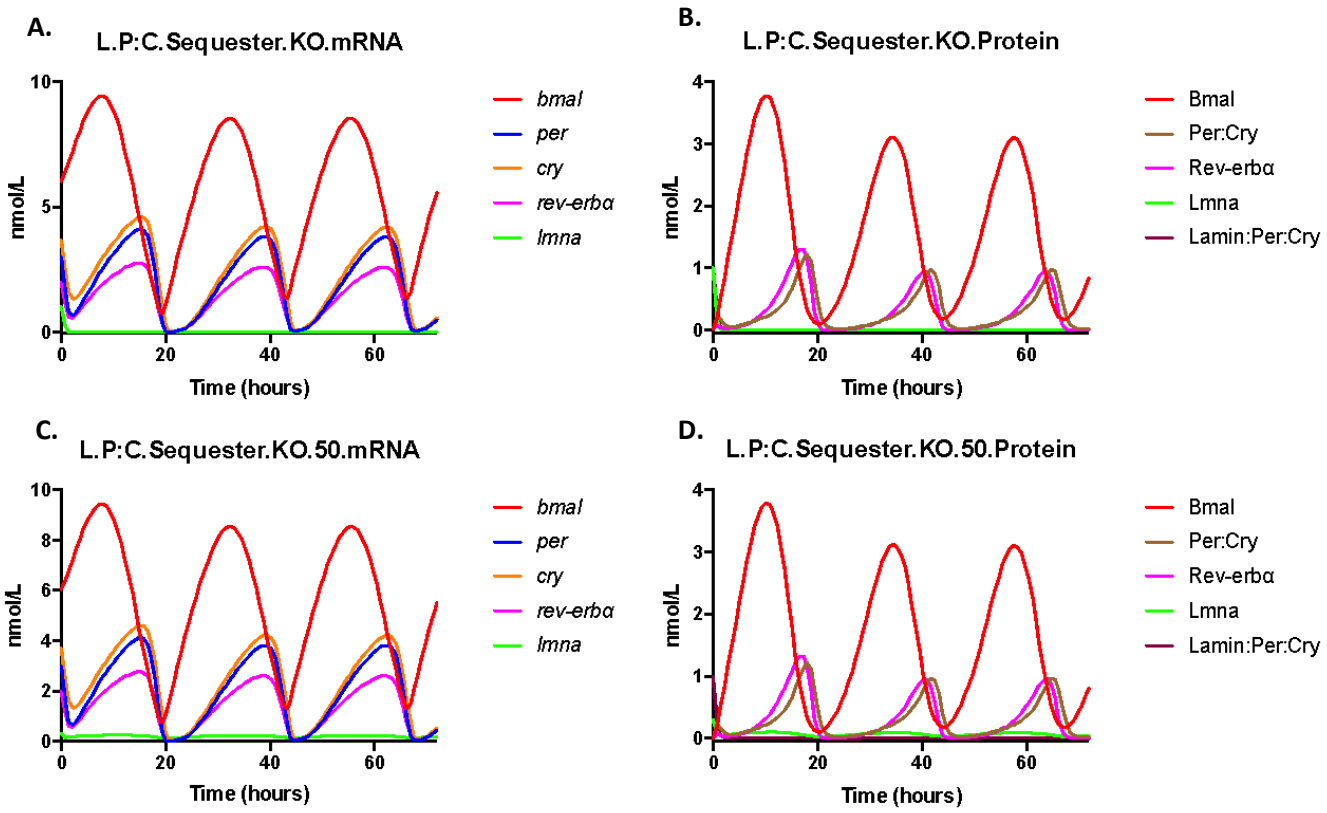

Figure 6.18. mRNA traces and protein concentrations in Model 3 with lamin A knockout and 50% knockdown, sequestering PER:CRY complex within the nucleus. Lamin A complete knockout, or knockdown to 0.5 nmol/L and 0.3 nmol/L for mRNA and protein, respectively.

6.4.3.10 Model 4: PER:CRY translocation regulation

To model the regulation of PER:CRY translocation into the nucleus by lamin A, the translocation of PCc, PER:CRY complex in the cytoplasm, into the nucleus was changed from mass action kinetics to competitive inhibition. The Lamin dimer Lm_Lm was introduced into this reaction as an inhibiting modifier and hence, negatively regulated the translocation of PER:CRY into the nucleus. In this regard, when the concentration of lamin A and lamin A dimers was high, it was predicted that there would be a higher level of negative regulation on PER:CRY complex translocation into the nucleus.

The addition of negative regulation by lamin A acting on PER:CRY translocation into the nucleus disturbed the normal oscillating steady state model. The cycling concentration of *Bmal*, *Per*, *Cry*, and *Rev-erbα* mRNA in this model decreased by roughly 1 nmol/L (Figure 6.19A.). In addition, the cycling protein concentration of BMAL, PER:CRY, and REV-ERBα dampened by roughly 0.5 nmol/L (Figure 6.19B.).

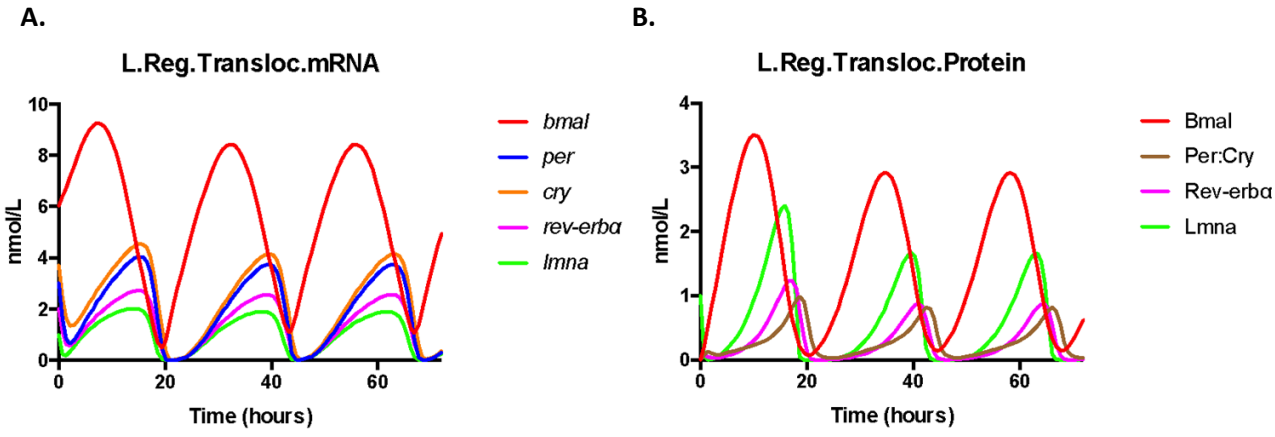

Figure 6.19. mRNA traces and protein concentrations in Model 4, lamin A regulating PER:CRY translocation from the cytoplasm into the nucleus. The oscillating concentration of *Bmal*, *Per*, *Cry*, and *Rev-erbα* mRNA, and BMAL, PER:CRY, and REV-ERBα protein are decreased.

6.4.3.11 Model 4: Regulate PER:CRY translocation, lamin A Overexpression

To investigate whether the manipulation of lamin A perturbs the dynamics of the molecular clock with lamin A regulating PER:CRY nuclear entry, the next aim was to overexpress lamin A. Lamin A mRNA and protein were overexpressed to roughly 520nmol/L and 400nmol/L (Figure 6.20A. and Figure 6.20B.). The oscillation of *Per*, *Cry*, and *Rev-erbα* mRNA increased by roughly 1 nmol/L, and were phase-delayed by a few hours (Figure 6.20A.). In contrast, protein oscillations for BMAL and REV-ERBα were increased by roughly 1.5 nmol/L, and PER:CRY complex in the nucleus decreased from 1 nmol/L to roughly 0.5 nmol/L (Figure 6.20B.).

The oscillating mRNA transcripts remained at the same concentration when the levels of lamin A overexpression were reduced to 100 nmol/L for mRNA and protein (Figure 6.20C.). In contrast, the upregulation of BMAL and REV-ERBα were reduced by 0.5 nmol/L, and PER:CRY complex in the nucleus was increased to 0.75 nmol/L with a dampening of translocation repression (Figure 6.20D.).

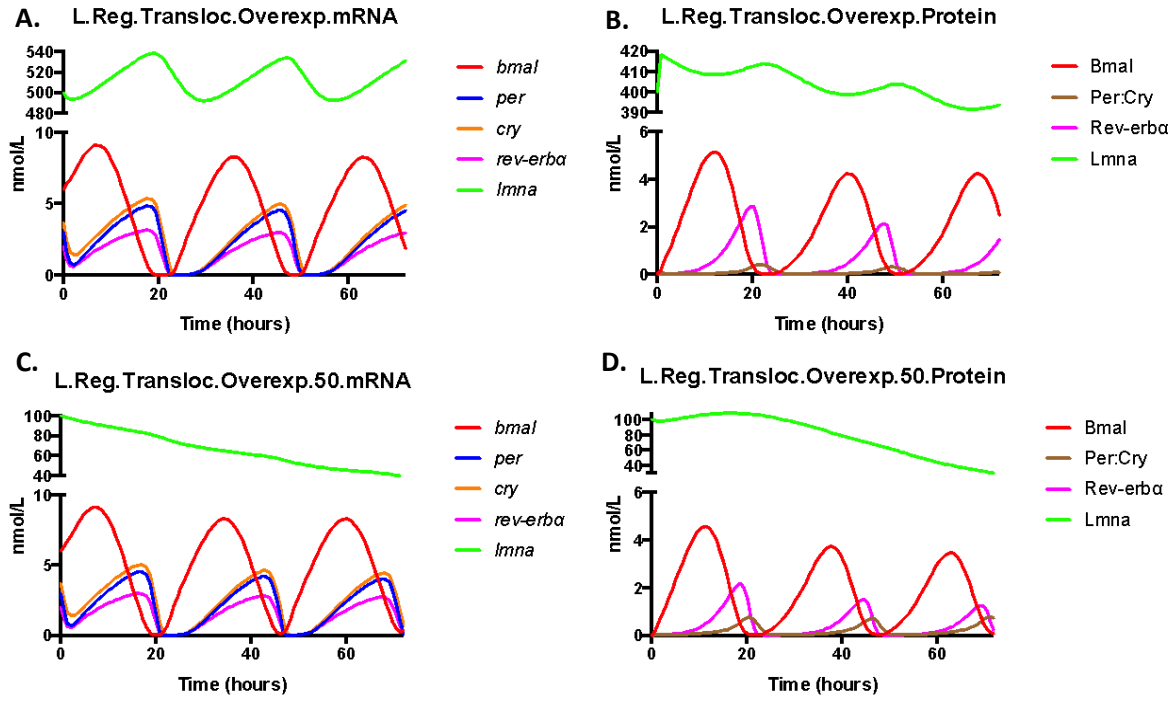

Figure 6.20. mRNA traces and protein concentration in Model 4 with lamin A overexpression and 50% overexpression, regulating PER:CRY translocation. Lamin A is overexpressed to 520nmol/L for mRNA and 410nmol/L for protein, and 50% overexpression concentration is to 100nmol/L for mRNA and 100nmol/L for protein.

6.4.3.12 Model 4: PER:CRY translocation regulation, lamin A Knockout

To investigate whether the response of lamin A knockout in Model 4 elicits a response in circadian molecular clock cycling, the next aim was to knockout lamin A. Lamin A mRNA and protein concentration were knocked out to 0 nmol/L (Figure 6.21A. and 6.21B.). The concentration of *Bmal*, *Per*, *Cry*, and *Rev-erbα* mRNA oscillations remained at the same level (Figure 6.21A.). Additionally, the oscillations of BMAL, PER:CRY, and REV-ERBα in the nucleus continued to oscillate at the same concentration (Figure 6.21B.).

When the levels of lamin A were knocked down by 50% to 0.4 nmol/L and 0.6 nmol/L for mRNA and protein respectively, the concentration of circadian mRNA and proteins continued to oscillate at the same concentration (Figure 6.21C. and Figure 6.21D.). Hence, knockout of lamin A in Model 4 does not disrupt the cycling of the molecular core clock.

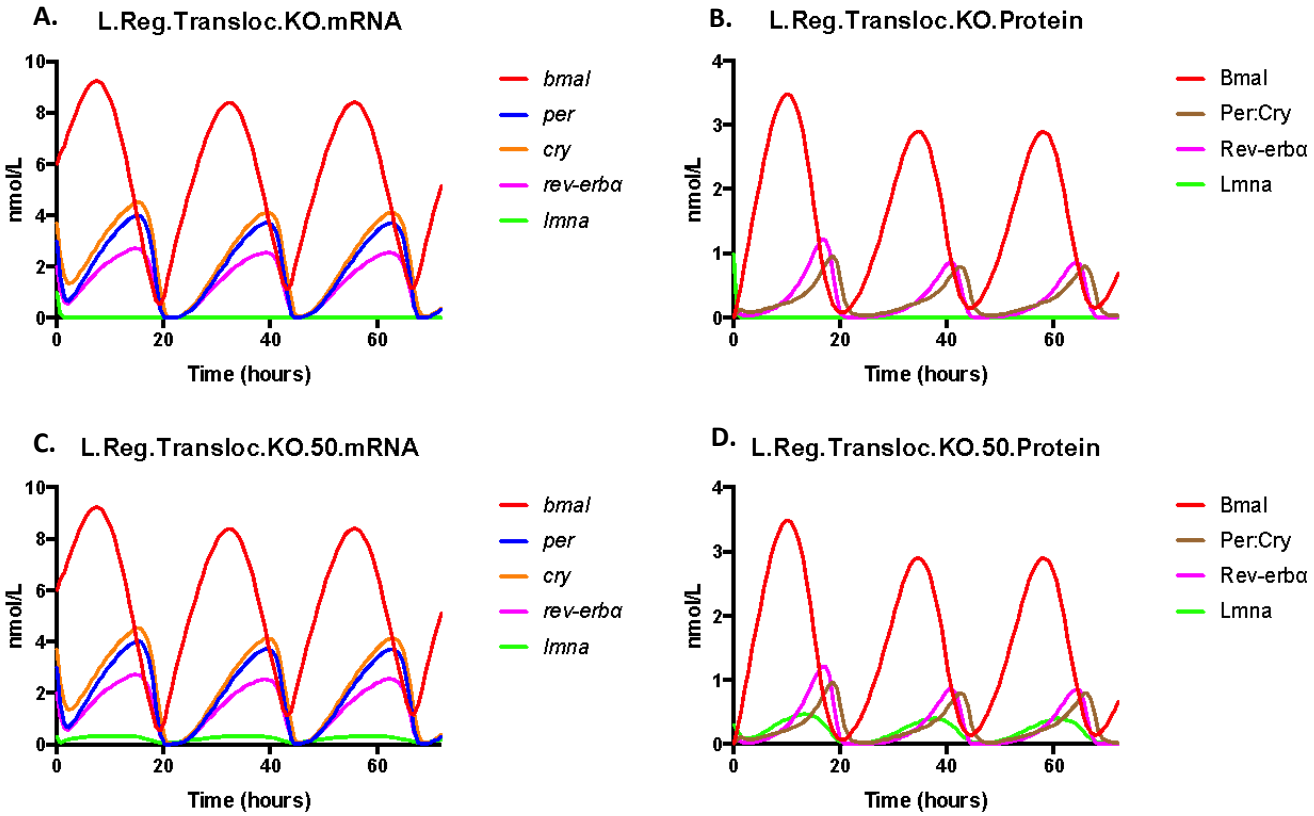

Figure 6.21. mRNA traces and protein concentration in Model 4 with lamin A knockout and 50% knockdown, regulating PER:CRY translocation. Lamin A complete knockout, or knockdown to 0.5 nmol/L and 0.5 nmol/L for mRNA and protein, respectively.

6.5 Model Evaluation- Model Output to Data set

C2C12 myoblasts overexpressing lamin A, by transfection with lamin A plasmid, demonstrated increased expression of *Per1, Per2*, *Bmal1*, and *Rev-erbα*, and reduced the expression of *Cry1* (Figures 4.9 and 4.11). Increased expression of *Per1* and *Bmal1* were also observed over a 24-hour circadian time-course in myoblasts overexpressing lamin A (Figures 4.12 and 4.14). Furthermore, C2C12 myoblasts with a knockdown of lamin A, by transfection with validated siRNA, demonstrated repression in the expression of *Per1*, *Per2*, *Cry1*, *Bmal1*, and *Rev-erbα* (Figures 4.1 and 4.3). The repression of circadian lock gene expression, in response to lamin A knockdown in myoblasts, was also observed over a circadian time-course for 24 hours (Figures 4.4 and 4.6).

Table 6.1 Summary of Circadian clock gene expression in response to lamin A manipulation for Models 1-4.

	Circadian Clock gene expression	Data Match
Model1 Overexpression	*Per* repression, *Cry* upregulation, period lengthening	✘
Model1 Knockout	*Per* upregulation	✘
Model2 Overexpression	*Per* repression, *Cry* upregulation, period lengthening	✘
Model2 Knockout	*Per* upregulation, *Bmal* upregulation, period shortening	✘
Model3 Overexpression	*Per* and *Cry* upregulation, *Per*, *Cry* and *Rev-erbα* phase delay	✓ (not *Cry*)
Model3 Knockout	No change	✘
Model4 Overexpression	*Per, Cry,* and *Rev—erbα* upregulation and slight phase delay	✓ (not *Cry*)
Model4 Knockout	No change	✘

Models 1 and 2 incorporated lamin A regulation to repress and upregulate *Per* expression, respectively. In response to lamin A overexpression, both Model 1 and Model 2 resulted in repressed *Per* expression, upregulated *Cry* expression, and the period of the cycling clock lengthened (Figures 6.11a. and 6.14A.). In addition, lamin A knockout in both Models 1 and 2 upregulated the expression of *Per*, and in Model 2, *Bmal* expression was also upregulated and the period of the cycling clock was shortened (Figures 6.12A. and 6.15A.). In response to lamin A gain-of and loss-of function in myoblast experimental data, *Per1*, *Per2*, and *Bmal1* expression was upregulated and *Cry1* expression was repressed, and *Per1*, *Per2*, *Bmal1*, and *Cry1* expression was repressed, respectively (Figures 4.11

and 4.14; Figures 4.3 and 4.6). Hence, Models 1 and 2 produce the opposite result. It was predicted that Model 2 would best match the laboratory generated data in response to lamin A manipulation; lamin A overexpression was predicted to increase *Per* expression further and lamin A knockout to reduce *Per* expression, due to increased and lost *Per* upregulation by lamin A, respectively. Unfortunately, Model 2 output data did not fit with the Model hypothesis.

Model 3 regulated PER:CRY nuclear localisation through the formation of a complex with Lamin dimers, altering PER:CRY activity. Lamin A overexpression upregulated the expression of *Per* and *Cry*, and *Per*, *Cry*, and *Rev-erbα* displayed a phase delay in mRNA oscillation (Figure 6.17A). In addition, lamin A knockout produced no change to core clock cycling in response to lamin A knockout (Figure 6.18A). Clock gene expression in response to the manipulation of lamin A in Model 3 was not supported by myoblast experimental data; overexpression of lamin A repressed *Cry* expression and did not phase delay in clock cycling, and lamin A knockout repressed clock gene expression (Figures 4.3 and 4.11).

Model 4 regulated PER:CRY translocation and appeared more promising, most closely matching experimental data generated in this thesis. In response to lamin A overexpression, *Per*, *Cry*, and *Rev-erbα* mRNA were up-regulated; myoblasts with an overexpression of lamin A also demonstrated an increase in *Per1*, *Per2*, and *Rev-erbα* expression, but demonstrated repressed *Cry1* expression (Figures 6.20A., 4.11, and 4.14). In contrast, there was no change in gene expression when lamin A was knocked out, unlike C2C12 myoblasts with lamin A knockdown which demonstrated a repression in clock gene expression (Figure 6.21A., and 4.3).

Future research may include fine-tuning and improving Models 2 and 4 with aim of generating circadian clock gene expression in response to lamin A manipulation that reflects experiments data. Moreover, further experimental investigations may be conducted to produce data that supports one of these potential feedback mechanisms of regulation by lamin A.

6.6 Discussion

Over the past decade, research has highlighted the role of the circadian clock in disease progression, and the need for therapeutic disease treatment to incorporate aspects of circadian rhythm research. This was accentuated in 2007 as the WHO released a statement classifying night shift-work as 'probably carcinogenic' due to circadian clock disruption (Straif, *et al*., 2007). Studies have now determined a link between circadian clock disruption and cancer, diabetes, cardiovascular disease, asthma, and many more diseases (Papagiannakopoulos, *et al*., 2016; Onaolapo and Onaolapo, 2018; Kervezee, Kosmadopoulos, and Boivin, 2018; Ehlers, *et al*., 2018). In this regard, the treatment of sleep disorders, including disorders observed in patients suffering Huntington's disease, has been adapted to include circadian clock synchronising methods such as bright light therapy and treatment with a melatonin agonist (Van Wamelen, Roos, and Aziz, 2015).

The development of mathematical models was prompted to aid in elucidating a clearer understanding of circadian mechanisms and initially, was aimed at investigating how the molecular clock was able to cycle, become entrained, and free-run. Furthermore, mathematical models were developed and applied to investigate potential feedback mechanisms to the circadian molecular clock. The research in this chapter is consistent with previous work incorporating mathematical models to investigate feedback mechanisms to the circadian clock. As early as 1991, mathematical models were used as a tool to begin investigating how temperature changes are sufficient to re-set the circadian clock (Lakin-Thomas, Brody, and Coté, 1991). Models combined mechanisms of potential amplitude and period resetting to produce testable predications in response to temperature changes as a single parameter (Lakin-Thomas, Brody, and Coté, 1991; Ruoff, *et al*., 1997; Leloup and Goldbeter, 1997). Furthermore, the relationship between the circadian clock and the cell cycle has been investigated through mathematical models. Feillet *et al*. investigated the temporal co-ordination of the cell cycle and the circadian clock through data collection with single live cells, computational methods and mathematical models (Feillet, *et al*., 2014). Additionally,

Woller *et al*. designed a mathematical model to investigate the potential link between specific diets and cycling of the liver molecular clock (Woller, *et al*., 2016). They included parameters to model a normal, fasting, and high-fat diet, and investigated mechanisms of clock disruption (Woller, *et al*., 2016). A further mathematical model investigated morning and evening oscillators for *Per1* and *Per2* respectively, comprising single-cell dual oscillators and incorporated a coupling signal of vasoactive intestinal polypeptide (VIP) and arginine vasopressin (AVP) (Sriram, 2017). Finally, recent research used a model to further investigate temperature compensation by the circadian clock and revealed underlying mechanisms involving the affinity with CKIδ-ATP complex, a temperature dependant kinase (Shinohara, *et al*., 2017).

These models incorporated iterations of laboratory generated data to refine and improve models until a singular, best-fitting model was chosen; driving future research. Indeed, the research in this chapter follows the study design of these research papers, a mathematical model was produced and this was compared to initial experimental data generated in the laboratory to probe and investigate the relationship between lamin A and the circadian clock.

Incorporating chronotherapy and awareness of the circadian clock into treatment plans for patients suffering with cancer or hypertension improves the treatment outcome (Innominato, Lévi, and Bjarnason, 2010; Bowles, *et al*., 2018). Comparison of Roscovitine, a selective Cdk-inhibitor, delivery at Zeitgeber time 3 (ZT3) to ZT19 identified higher systemic exposure at ZT3 to adipose tissue, testis, kidney, and lungs, and higher exposure at ZT19 in the lungs (Sallam, *et al*., 2015). Similarly, the pharmacokinetics of levofloxacin demonstrate a circadian rhythm in the pattern of drug absorption (Kervezee, *et al*., 2016). These data provide a strong basis for promoting future research identifying the circadian regulation involved in drug delivery, and for therapeutic strategies to incorporate chronotherapy.

The development of mathematical models for chronotherapy enables the predication and testing of potential input, output, and feedback pathways involved in the treatment of disease. Consequently,

circadian models have been developed aiming to facilitate this research (Becker-Weimann, *et al*., 2004; Wang, *et al*., 2017b; Podkolodnaya, Tverdokhleb, and Podkolodnyy, 2017; Mavroudis, *et al*., 2018). Leloup and Goldbeter used a molecular clock mathematical model to investigate the involvement of circadian rhythms in physiological disorders and jet lag. The entrainment to light-dark cycles was investigated for circadian-related physiological disorders familial advanced sleep phase syndrome (FASPS) and delayed sleep phase syndrome (DSPS), demonstrating phase advance and phase delay, respectively (Leloup and Goldbeter, 2008). In addition, they investigated re-entrainment of the molecular clock in response to jet lag and identified that the type and timing of re-entrainment required depends on the autonomous clock period, light intensity, biochemical kinetic parameters, and the direction and magnitude of the phase shift (Leloup and Goldbeter, 2013). Mathematical models for pharmaceutical chronotherapy, otherwise known as chronopharmacology, aim to enhance the efficacy of drugs through improving and optimising drug delivery. Circadian rhythms have already been linked to the efficacy of drug delivery for diseases such as arthritis, metabolic disorders, and cancer. Hadaeghi *et al*. used a mathematical model of the circadian clock and neurotransmitter functioning in the brain to investigate the role of desynchronised clocks in bipolar disorder; this research observed output sleep/wake cycles to identify whether the model replicates deviations observed during manic and depressive episodes (Hadaeghi, *et al*., 2016). The role of the circadian clock in the progression of arthritis pathology has also been discussed and a mathematical model was designed to incorporate two hypothesis-driven potential mechanisms through which the circadian clock may be involved in arthritis disease progression (Rao, *et al*., 2016). Furthermore, the mathematical model designed by Woller *et al*. to investigate mechanisms of clock disruption by high-fat or fasting diets also predicted mechanisms of pharmacological rescue by Rev-erbα administration (Woller, *et al*., 2016). Studies utilising *in vitro* data and a mathematical model for cancer chronotherapy demonstrated circadian rhythms in irinotecan, a topoisomerase I inhibitor, bioactivation, detoxification, transport, and targeting to colorectal cancer cells (Dulong, *et al*., 2015). A further mathematical model identified a circadian

rhythm of pharmacokinetics for the cancer drug 5-fluorouracil following administration at different time points, observed through plasma concentrations in rats (Kobuchi, *et al*., 2016). Peak clearance of 5-fluorouracil is observed roughly 2 hours after light onset and trough clearance levels are 14 hours post-light onset (Kobuchi, *et al*., 2016). Ayyar *et al*. investigated the dosage of methylprednisolone (MPL) on the anti-inflammatory mediator glucocorticoid-induced leucine zipper in multiple tissues through a mathematical model and identified tissue-specific circadian rhythms in pharmacodynamics (Ayyar, *et al*., 2017). Finally, glucocorticoids are produced by the hypothalamic-pituitary-adrenal (HPA) axis in a circadian manner and feedback to regulate the circadian clock; synthetic glucocorticoids are administered as an anti-inflammatory and immunospressor (Coutinho and Chapman, 2011). A mathematical model was created to investigate the response of glucocorticoid administration on endogenous cortisol rhythms and identified a time-dependant effect on the amplitude and acrophase (Rao, Scherholz, and Androulakis, 2018).

The four hypothesis-driven Models 1-4 of this chapter have produced dynamic simulations that enable the generation of predications for future investigations into potential interactions between lamin A and the circadian clock. These models allow us to highlight mechanisms of interest, fine-tune and adjust parameter values, and direct future experimental data collection. The overall research hypothesis for this thesis predicts that lamin A and the circadian clock have a bi-directional feedback relationship, and that both LMNA and the core molecular clock proteins are required to ensure that there are correct concentrations of the other present within a single cell. Furthermore, it is predicted that the loss of lamin A in laminopathy patients has dramatic consequences on circadian molecular clock cycling; contributing to pathogenesis of tissue-specific defects in laminopathy disorders, such as muscle-wasting diseases and lipodystrophies. To test this prediction further, and investigate potential pharmacological routes of treatment, a functioning mathematical model of the lamin A and molecular clock relationship would prove invaluable.

6.7 Conclusion

These mathematical models provided predictions for clock gene and protein concentrations in response to lamin A manipulation within different mechanistic feedback relationships, in which the clock upregulated lamin A and lamin A was feeding back to regulate the circadian clock. The model that matched laboratory generated data in this thesis most closely was Model 4. Paired with lab work to highlight mechanisms that are aligned to experimental output data, refining of these mathematical models will enable us to predict potential feedback mechanisms of interest and direct laminopathy and circadian biology research accordingly.

7 General Discussion

7.1 Summary of Main Findings

The main findings of this thesis were:

1. Time-course data from muscle cell lines, primary muscle cells, and murine muscle identified a circadian rhythm in lamin A mRNA expression and protein levels. Examined through collecting myoblasts, myotubes, and muscle in a circadian time-course, lamin A was investigated using qRT-PCR, western blotting, and immunocytochemistry. Expression of *Lmna* was in the same phase as the expression of the negative arm core clock genes and *Rev-erbα*, and antiphase to *Bmal1* expression.

2. Rhythmic *Lmna* expression qRT-PCR data were observed in WT MEFs collected around the clock at both mRNA expression and protein levels. Consistent with previous data, *Lmna* expression was in the same phase as the expression of *Per2*, and anti-phase to *Bmal1*. The rhythmic expression of *Lmna* was lost in the Cry1 and Cry2 double knockout. Expression of *Lmna* followed the pattern of *Per2* expression in response to Cry1 and Cry2 knockout, and was arrhythmic and upregulated.

3. Data from C2C12 myoblasts with a lamin A knockdown identified a reduction in the expression of circadian clock genes: *Per1*, *Per2, Bmal1*, *Cry1*, and *Rev-erbα*. C2C12 myoblasts transfected with 5nmol validated lamin A siRNA were examined for clock gene expression through qRT-PCR. In addition, C2C12 myoblasts were stably transfected with Bmal1::Luc reporter plasmid. The dampening of *Bmal1* expression in response to transfection with validated lamin A siRNA was observed in real-time through bioluminescent imaging in the LumiCycle.

4. Data from C2C12 myoblasts transfected with 1µg lamin A plasmid, overexpressing lamin A, demonstrated a reduction in the expression of *Cry1* and an increase in the expression of *Per1*, *Per2*, and *Bmal1*. C2C12 myoblasts with a stable Bmal1::Luc transfection were utilised to observe the

increase of *Bmal1* expression in response to transfection with lamin A plasmid in real-time in the LumiCycle.

5. Cell-line and primary myoblasts loaded for 24 hours on the Flexcell machine at 6.66% strain presented variable but supportive data for the response of the circadian clock to mechanical stimulation. Primary myoblasts responded to 24-hour strain with an increase in *Lmna* expression, and a decrease in *Cry1* expression. C2C12 myotubes had an increased *Bmal1* and *Cry1* expression after being subject to 24-hour Flexcell loading.

6. WT mouse muscle collected from mice in an *in vivo* loading study demonstrated, through qRT-PCR data, that samples from acute loaded male Gas and chronic loaded male Quad both have an upregulation in *Clock* expression. No change was observed in the expression of the other circadian clock genes or lamin A.

7. Production of a mathematical model to facilitate future studies elucidating the relationship between lamin A and the circadian molecular clock. The model incorporated light: dark signals and included the auxiliary loop comprising REV-ERBα regulation on *Bmal1*. These studies manipulated a circadian mathematical model by Leloup and Goldbeter, incorporating lamin A regulation into 4 models that aimed to investigate potential feedback regulatory mechanisms to the molecular clock; the fourth model (lamin A regulating the translocation of PER:CRY into the nucleus) matched the experimental research generated in this thesis most closely.

7.2 General Discussion of the Data Presented

7.2.1 Rhythmic *Lmna* in musculoskeletal cells.

The circadian clock ensures that the levels of proteins throughout the cell are present at the correct time-of-day, through regulating many pathways and processes these manifest as circadian rhythms in metabolism, physiology and behaviour. Functioning circadian molecular clocks have been identified across multiple tissues and are responsible for regulating tissue and differentiation-

specific gene expression, which demonstrate rhythmicity (Andrews, *et al*., 2010; Gale, *et al*., 2011). Within the nucleus, lamin A is responsible for providing structural support to the nucleus, organising the genome, and regulating transcription factors, including regulators of signalling pathways involved in stress, mechanical stimulation, and muscle differentiation (Lammerding, *et al*., 2004; Ivorra, *et al*., 2006; Lattanzi, *et al*., 2012; Lee, Lee, and Shim, 2017; Gonzalez-Suarez and Gonzalo, 2010). Given that the circadian clock plays an important role in the homeostasis of muscle and the regulation of muscle-specific genes, mechanosensitive and stress-response transcription factors, it was predicted that lamin A is also regulated by the circadian clock (Kon, *et al*., 2008; Andrews, *et al*., 2010; Shavlakadze, *et al*., 2013).

To begin investigating whether lamin A is regulated by the circadian clock, time-course samples were collected for analysis from a range of musculoskeletal cells. Oscillating *Lmna* transcripts were identified in circadian time-course samples collected from cell-line C2C12 myoblasts and myotubes, Per2::Luc primary isolated myotubes, and WT Gastrocnemius muscle, measured through qRT-PCR (Figure 3.1, 3.3, 3.12, 3.15, and 3.20). Moreover, oscillatory levels were identified in protein samples collected from these circadian time-courses, although less defined (Figure 3.2, 3.4, 3.13, and 3.16). Cosinor Periodogram circadian analysis was used to analyse the mRNA and protein traces; oscillatory traces for *Lmna* transcripts were in phase with the negative arm core clock genes (Refinetti, 2016). To further analyse transcript oscillation of lamin A, the next aim was to determine whether synchronised WT MEF cells also have oscillating *Lmna* expression, and investigate whether knocking out the core clock gene *Cry1* and *Cry2* impairs this oscillatory expression. Time-course data from WT MEF cells confirmed the oscillatory behaviour of lamin A (Figure 3.21). Furthermore, when *Cry1* and *Cry2* were knocked out in MEF cells, time-course data demonstrated that the oscillation in *Lmna* expression was lost and followed the pattern of *Per2* expression (Figure 3.21). Although further work is necessary to confirm that lamin A is regulated by the circadian clock, this research supports the hypothesis that lamin A is a clock-controlled gene. In this regard, this highlights the importance of

considering temporal regulation by the circadian clock whilst completing research to decipher and understand the role of lamin A.

7.2.2 Lamin A and molecular clock regulation

The research in this thesis predicts that the pathogenesis of laminopathy disorders, which often have tissue-specific features, are partly due to dysfunctional circadian clocks that result from a loss of lamin A feedback regulation. The hypothesis is that lamin A and the circadian clock bi-directionally regulate one-another, forming a feedback loop. Since the discovery that lamin A mutations result in laminopathies, such as muscular dystrophy, there has been considerable interest and research around laminopathy pathogenesis (Ho and Hegele, 2019). Research has since focused on deciphering the role played by lamin A within the nucleus and understanding how these mutations can lead to the broad spectrum of diseases encompassed by laminopathies. Despite this interest, a clear understanding of laminopathy pathogenesis is yet to be uncovered. This research predicts that the current understanding is lacking the regulatory involvement of the circadian molecular clock in the roles played by lamin A, and the dependency of functioning circadian rhythms and in tissue-specific homeostasis.

To investigate whether lamin A feeds-back to regulate the circadian clock, the levels of lamin A were perturbed within musculoskeletal cells and the response in circadian gene expression was observed. The expression of core clock circadian genes are regulated within the transcription-translation feedback loop; negative arm core clock genes (*Per* and *Cry1*) are expressed antiphase to the positive arm core clock genes (*Bmal1* and *Clock*) (Griffin, *et al*., 1999; Kume, *et al*., 1999; Sato, *et al*., 2006). In this regard, the core clock genes are highly regulated and are expressed only at specific times of day. Therefore, if lamin A feeds-back to regulate the circadian clock, an overexpression or knockdown of lamin A should enhance or alleviate circadian clock gene expression repression or upregulation.

The first aim was to investigate the effect of lamin A knockdown on the expression of the circadian clock genes. C2C12 myoblasts were knocked-down for lamin A by transfection with 5nM validated

siRNA, and this reduced the expression of circadian clock genes: *Per1*, *Per2*, *Bmal1*, *Cry1*, and *Rev-erbα* (Figure 4.3). The next aim focused on whether overexpressing lamin A also impacts core clock gene expression. C2C12 myoblasts were transfected with 1µg lamin A plasmid and demonstrated a reduction in the expression of *Cry1* and an increase in the expression of *Per1*, *Per2*, and *Bmal1* (Figure 4.11).

Furthermore, to dynamically visualise the effects of lamin A manipulation of the circadian clock, C2C12 myoblasts were stably transfected with Bmal1::Luc reporter plasmid. Myoblasts with a stable Bmal1::Luc transfection were further transfected with lamin A siRNA or lamin A plasmid (Figure 4.17 and 4.18). In the LumiCycle, the effect of lamin A knockdown and overexpression was observed in real-time to reduce and increase the expression of *Bmal1*, respectively; consistent with the previous results (Figure 4.19 and 4.20).

These results support the research hypothesis that lamin A feeds-back to regulate the circadian clock. Highlighting a potential important link between the lamin A regulation and functioning circadian rhythms; a level of regulation previously overlooked in laminopathy research.

7.2.3 The clock and mechanobiology

The circadian clock is synchronised to its external environment through zeitgebers, including light, food-intake, and exercise. Exercise is sufficient to synchronise the master circadian clock in the SCN and the peripheral clocks in tissues, such as skeletal muscle (Yamanaka, *et al*., 2008). Currently, it is unknown how exercise can synchronise the molecular clock. Lamin A increases with tissue stiffness, it is responsible for structurally supporting the nucleus and regulating mechanosensitive responses to the nucleus (Swift, *et al*., 2013). Indeed, both the circadian clock and lamin A are involved in orchestrating the response of musculoskeletal tissue to mechanical stimulation; the research in this thesis predicts that these synchronisation signals to the circadian clock are communicated through lamin A.

The Flexcell machine, an *in vitro* cell culture loading system, was used to subject myoblasts and myotubes, from cell-line C2C12 and isolated primary Per2::Luc cells, to 6.66% strain for 24 hours. Primary myoblasts, isolated from Per2::Luc mice, responded to 24 hour Flexcell strain with an increase in *Lmna* expression, and a decrease in *Cry1* expression; there was no change in the remaining clock genes (Figure 5.7 and 5.9). C2C12 myotubes subject to 24-hour Flexcell strain demonstrated an increase in *Bmal1* and *Cry1* expression but no change in the expression of *Lmna* or the remaining clock genes (Figure 5.11 and 5.13).

Furthermore, an *in vivo* loading rig subjected the right hind limb of mice to cycles of loading, following acute or chronic protocols, and the response in gene expression was examined in Gastrocnemius and Quadricep muscle samples (muscle samples kindly available for collection from mice in a study conducted by Dr Blandine Poulet; Poulet, *et al*., 2011). qRT-PCR data from acute loaded male Gas and chronic loaded male Quad both demonstrated an upregulation in *Clock* expression; there was no change in expression observed in *Lmna* or the remaining circadian clock genes (Figure 5.24, 5.25, 5.26, and 5.27).

This research supports the hypothesis that the expression of circadian clock genes are responsive to mechanical stimulation. This is consistent with previous research that identified exercise as a sufficient signal to entrain circadian rhythms in the peripheral clocks of mouse skeletal muscle (Wolff and Esser, 2012).

7.2.4 Mathematical models to direct laminopathy and circadian biology research

Mathematical models are an aid to facilitate wet laboratory work. Circadian models were developed to begin investigating the dynamics of circadian feedback loops and downstream gene regulation (Podkolodnaya, Tverdokhleb, and Podkolodnyy, 2017).

The first aim was to adapt a model from Leloup and Goldbeter; this model incorporates light:dark signals and includes the auxiliary loop whereby REV-ERBα feeds-back to repress *Bmal1* (Leloup and Goldbeter, 2003). The model was adapted to include the production of lamin A mRNA, lamin A protein and lamin A dimers, and was manipulated to produce 4 variations of different potential bi-directional regulatory relationship between lamin A and the circadian clock. In each of the 4 models, lamin A was upregulated by the BMAL1:CLOCK heterodimer so that it was a clock-controlled gene. The first model included lamin A negatively regulating the expression of *Per* (there is only one Per and one Cry component in the model representing both Per1 and Per2 genes, and Cry1 and Cry2 genes, respectively); the second model included lamin A positively regulating the expression of *Per*; the third included lamin A tethering the PER:CRY complex at the nuclear periphery; the fourth model included lamin A regulating the translocation of PER:CRY into the nucleus from the cytoplasm. After generating these models, the circadian clock and lamin A gene expression and protein levels were simulated over 72 hours in COPASI.

To test the 4 models and generate output data that could enable us to identify mechanisms that may appear more supported than others, lamin A was knocked out and overexpressed within each model. To observe whether this perturbs core clock cycling, each model was ran to simulate gene expression and protein levels over 72 hours. The output simulations from these models can be compared to laboratory data to identify potential pathways of regulation that should be further explored. When the models were compared with lab generated data from this thesis, Model 4 (lamin A regulating the translocation of PER:CRY into the nucleus) was the most promising. In response to the overexpression of lamin A in this model, *Per*, *Cry*, and *Rev-erbα* mRNA were up-regulated; myoblasts with an overexpression of lamin A also demonstrated an increase in *Per1*, *Per2*, and *Rev-erbα* expression (Figures 6.20A., 4.11, and 4.14). In contrast, there was no change in gene expression when lamin A was knocked out, unlike C2C12 myoblasts with lamin A knockdown which demonstrated a repression in clock gene expression (Figure 6.21A., and 4.3). Further laboratory data can be generated to contribute to iterations of fine-tuning and improving of these models. This will

ultimately highlight regulatory pathways that closely align with laboratory produced data and hence, may be the mechanism responsible for lamin A and molecular clock bi-directional regulation.

7.3 Clinical Relevance

Currently, it remains unclear how laminopathy disorders progress from mutation to phenotype despite much interest and research focused on clarifying the pathogenesis pathway in the development of the disease. Muscular dystrophy has no cure and the only treatment option currently available aims at reducing the symptoms and slowing the progression of the disease (Brull, *et al*., 2018). Lamin A is responsible for many different roles within the nucleus, these roles can be grouped into and support the "gene expression" or "mechanical stress" hypotheses, or both (Worman, 2012). The research hypothesis for this thesis predicts that the circadian clock is of vital importance in the development of these disorders, and that lamin A and the circadian clock feedback to bi-directionally regulate one another. In this regard, in laminopathy diseases, it is predicted that the circadian clock is disrupted in response to lamin A mutations and contributes to the tissue-specific pathogenesis observed across laminopathy disorders.

To treat and alleviate laminopathy disorders, it is required that the precise pathway leading to disease formation is understood. To dynamically understand lamin A in the nucleus, the research in this thesis indicates that circadian rhythms have to be studied also. Uncovering the lamin A and circadian clock regulatory pathway will facilitate future studies exploring pharmacological intervention and potential effective treatment options.

7.4 Limitations

The limitations of this project included the lack of available antibodies directed to circadian clock proteins, and the success of the lamin A antibody to study LMNA protein from mouse tissue samples. With circadian antibodies available, lamin A protein oscillations could have been compared to core clock protein oscillations from circadian time-course samples. Their availability would further the analysis of lamin A oscillations through comparing whether lamin A protein is also in

synchronisation with core clock proteins of the negative arm. Additionally, if lamin A antibody suitable to study LMNA protein from mouse tissue samples was available, it would have facilitated the analysis of LMNA protein from the murine dark: dark circadian time-course, and the Gastrocnemius and Quadricep samples from the *in vivo* loading study.

A further limitation was the opportunity to collect additional animal model tissue samples for circadian time-course data analysis. Further *in vivo* analysis of lamin A mRNA cyclical behaviour in murine samples under light: dark conditions, and across different types of muscle tissue, would have provided an interesting comparison to the dark: dark time-course analysed in Chapter 3.

Additionally, the Flexcell machine subjected musculoskeletal cells to *in vitro* strain through vacuum-induced pulling of a silicone membrane, seeded with the musculoskeletal cells, either side of a loading post, applying strain across the membrane. A limitation of this study was that this machine generates non-uniform, heterogeneous strain across the membrane (Delaine-Smith, *et al*., 2015). The cells seeded onto the membrane that remained on the loading post during loading experience different radial and biaxial strain fields compared to those seeded onto the areas of the membrane that were pulled concave and off the loading post (Vande Geest, *et al*., 2004).

Finally, the *in vivo* loading model used to study the response of the circadian clock to mechanical loading in murine muscle, in Chapter 5, was part of a study observing osteoarthritis (OA) in the murine joint. This model applied load to the murine hind knee joint to initiate and observe OA development. A limitation of this *in vivo* model is the limited knowledge of the degree in which the skeletal muscle of the loaded hind limb will experience strain, and a resultant biological response, in response to the acute and chronic loading protocols.

7.5 Future Studies

There are a number of potential future studies that may be used to further investigate the findings in this thesis.

7.5.1 Lamin A is a CCG

Our data provides evidence for oscillating lamin A mRNA expression and protein levels in musculoskeletal tissues. To conclude that lamin A is a circadian clock-controlled gene further studies are required to identify lamin A up- or down-regulation by a core circadian clock protein. These studies may include ChIP-seq, EMSAs, and promoter mutation studies with a reporter construct (Elnitski, *et al*., 2006). These experimental techniques can provide data to identify core or auxiliary clock proteins that may bind to and regulate the lamin A promoter. Furthermore, future data may show that abolishing this regulation results in a loss of oscillatory *Lmna* transcript expression due to a loss of clock gene regulation.

Currently, the mathematical models are designed with BMAL1:CLOCK heterodimer upregulating the expression of *Lmna*. mRNA circadian time-course data analysed in this thesis indicated that lamin A oscillation is in phase with the negative arm core clock genes, supporting this hypothesis. Data uncovering which protein within the molecular clock up- or down-regulates lamin A, and by what mechanism of interaction, would enable us to improve the models, and assist in future investigations into feedback mechanisms by lamin A that regulate the molecular clock.

7.5.2 Lamin A and Circadian Feedback Regulation

In order to confirm the relationship between lamin A and the musculoskeletal molecular clock, future work may include investigating the effects of loss-of and gain-of lamin A function on clock gene expression and temporal dynamics in C2C12 differentiated myotubes. In comparison to lamin A manipulation experiments in myoblasts, this study would enable the observation of whether the effect on clock gene expression is more profound in differentiated myotubes compared to undifferentiated myoblasts. In addition, further experimental data are needed to identify mechanisms of regulatory interaction between lamin A and any potential core clock gene promoters or transcription factors. Future studies to investigate this potential regulation may also utilise ChIP-seq, EMSAs, FISH, and promoter mutation studies with a reporter construct to study whether lamin

A regulates core clock gene promoter expression (Elnitski, *et al*., 2006). To observe whether lamin A regulates circadian transcription factor location or activity, experiments may include studies investigating whether circadian transcription factors and lamin A interact at the nuclear periphery. Experiments may include yeast two-hybrid screening, utilising circadian protein and lamin A antibodies to study protein location around the clock, or co-immunoprecipitation (Stasi, Luca and Bucci, 2015).

Theses experimental studies will facilitate the identification of interactions between lamin A and the circadian clock, aiding the discovery of regulatory feedback pathways. As further experimental data are developed to identify gene or protein interactions, the lamin A and circadian clock mathematical model can be adapted to include any supported molecular interactions. Future iterations to develop the mathematical model will facilitate the refining of laboratory work to explore pathways of particular interest. This will accelerate research exploring feedback pathways between lamin A and the circadian clock.

7.5.3 Lamin A, Mechanobiology and the Clock

The work in this thesis supports the hypothesis that the circadian clock is responsive to mechanical stimulation. Further research may include incorporating a different *in vivo* model in which mouse muscle will experience high proportions of mechanical strain. A future study may include exercising mice on a forced treadmill (Sasaki, *et al*., 2016). Through the collection of different muscle samples and analysis of circadian clock gene and protein levels, it can be observed whether the circadian clock is responsive to mechanical strain, exerted through exercise, across different muscle samples. In addition, the response of circadian clock gene and proteins levels can be compared when forced exercise is subject to mice at different times of day and for different periods of time.

Furthermore, once a suitable *in vivo* model is identified, future research may aim to investigate whether the circadian clock response to *in vivo* mechanical strain is altered in a mouse model of muscular dystrophy. Mice such as the transgenic $Lmna^{H222P/H222P}$ mice exhibit pathologies similar to

human striated muscle laminopathies and demonstrate skeletal muscle degeneration (Arimura, *et al*., 2005). These mice would make a useful comparison to wild type mice after subjecting them to forced exercise on a treadmill. If the cycling of the molecular clock responds differently to mechanical strain within these mice, this will support the research hypothesis that lamin A and the circadian clock exhibit bi-directional regulation, and that this pathway of regulation is utilised to communicate mechanosensitive information and signals to the circadian clock.

8 References

Aaronson, R.P. & Blobel, G. (1975) 'Isolation of nuclear pore complexes in association with a lamina', *Proc Natl Acad Sci U S A*, vol. 72, no. 3, pp. 1007-1011.

Abercrombie, M. & Dunn, G.A. (1975) 'Adhesions of fibroblasts to substratum during contact inhibition observed by interference reflection microscopy', *Exp Cell Res*, vol. 92, no. 1, pp. 57-62.

Abraham, U., Schlichting, J.K., Kramer, A. & Herzel, H. (2018) 'Quantitative analysis of circadian single cell oscillations in response to temperature', *PLoS One*, vol. 13, no. 1, p. e0190004.

Adolph, K.W. (1987) 'ADPribosylation of nuclear proteins labeled with [3H]adenosine: changes during the HeLa cycle', *Biochim Biophys Acta*, vol. 909, no. 3, pp. 222-230.

Aebi, U., Cohn, J., Buhle, L. & Gerace, L. (1986) 'The nuclear lamina is a meshwork of intermediate-type filaments', *Nature*, vol. 323, no. 6088, pp. 560-564.

Aguilar-Arnal, L., Hakim, O., Patel, V.R., Baldi, P., Hager, G.L. & Sassone-Corsi, P. (2013) 'Cycles in spatial and temporal chromosomal organization driven by the circadian clock', *Nat Struct Mol Biol*, vol. 20, no. 10, pp. 1206-1213.

Akagi, R., Akatsu, Y., Fisch, K.M., Alvarez-Garcia, O., Teramura, T., Muramatsu, Y., Saito, M., Sasho, T., Su, A.I. & Lotz, M.K. (2017) 'Dysregulated circadian rhythm pathway in human osteoarthritis: NR1D1 and BMAL1 suppression alters TGF-β signaling in chondrocytes', *Osteoarthritis Cartilage*, vol. 25, no. 6, pp. 943-951.

Akashi, M. & Takumi, T. (2005) 'The orphan nuclear receptor RORalpha regulates circadian transcription of the mammalian core-clock Bmal1', *Nat Struct Mol Biol*, vol. 12, no. 5, pp. 441-448.

Akashi, M., Tsuchiya, Y., Yoshino, T. & Nishida, E. (2002) 'Control of intracellular dynamics of mammalian period proteins by casein kinase I epsilon (CKIepsilon) and CKIdelta in cultured cells', *Mol Cell Biol*, vol. 22, no. 6, pp. 1693-1703.

Al-Haboubi, T., Shumaker, D.K., Köser, J., Wehnert, M. & Fahrenkrog, B. (2011) 'Distinct association of the nuclear pore protein Nup153 with A- and B-type lamins', *Nucleus*, vol. 2, no. 5, pp. 500-509.

Albers, H.E. & Ferris, C.F. (1984) 'Neuropeptide Y: role in light-dark cycle entrainment of hamster circadian rhythms', *Neurosci Lett*, vol. 50, no. 1-3, pp. 163-168.

Albrecht, U., Sun, Z.S., Eichele, G. & Lee, C.C. (1997) 'A differential response of two putative mammalian circadian regulators, mper1 and mper2, to light', *Cell*, vol. 91, no. 7, pp. 1055-1064.

Altman, B.J., Hsieh, A.L., Sengupta, A., Krishnanaiah, S.Y., Stine, Z.E., Walton, Z.E., Gouw, A.M., Venkataraman, A., Li, B., Goraksha-Hicks, P., Diskin, S.J., Bellovin, D.I., Simon, M.C., Rathmell, J.C., Lazar, M.A., Maris, J.M., Felsher, D.W., Hogenesch, J.B., Weljie, A.M. & Dang, C.V. (2015) 'MYC Disrupts the Circadian Clock and Metabolism in Cancer Cells', *Cell Metab*, vol. 22, no. 6, pp. 1009-1019.

Andrews, J.L., Zhang, X., McCarthy, J.J., McDearmon, E.L., Hornberger, T.A., Russell, B., Campbell, K.S., Arbogast, S., Reid, M.B., Walker, J.R., Hogenesch, J.B., Takahashi, J.S. & Esser, K.A. (2010) 'CLOCK and BMAL1 regulate MyoD and are necessary for maintenance of skeletal muscle phenotype and function', *Proc Natl Acad Sci U S A*, vol. 107, no. 44, pp. 19090-19095.

Angori, S., Capanni, C., Faulkner, G., Bean, C., Boriani, G., Lattanzi, G. & Cenni, V. (2017) 'Emery-Dreifuss Muscular Dystrophy-Associated Mutant Forms of lamin A Recruit the Stress Responsive Protein Ankrd2 into the Nucleus, Affecting the Cellular Response to Oxidative Stress', *Cell Physiol Biochem*, vol. 42, no. 1, pp. 169-184.

Arimura, T., Helbling-Leclerc, A., Massart, C., Varnous, S., Niel, F., Lacène, E., Fromes, Y., Toussaint, M., Mura, A.M., Keller, D.I., Amthor, H., Isnard, R., Malissen, M., Schwartz, K. & Bonne, G. (2005) 'Mouse model carrying H222P-Lmna mutation develops muscular dystrophy and

dilated cardiomyopathy similar to human striated muscle laminopathies', *Hum Mol Genet*, vol. 14, no. 1, pp. 155-169.

Aronson, D., Dufresne, S.D. & Goodyear, L.J. (1997) 'Contractile activity stimulates the c-Jun NH2-terminal kinase pathway in rat skeletal muscle', *J Biol Chem*, vol. 272, no. 41, pp. 25636-25640.

Arvind, V. & Huang, A.H. (2017) 'Mechanobiology of limb musculoskeletal development', *Ann N Y Acad Sci*, vol. 1409, no. 1, pp. 18-32.

Aschoff, J. (1969) 'Desynchronization and resynchronization of human circadian rhythms', *Aerosp Med*, vol. 40, no. 8, pp. 844-849.

Aschoff, J., Daan, S., Figala, J. & Müller, K. (1972) 'Precision of entrained circadian activity rhythms under natural photoperiodic conditions', *Naturwissenschaften*, vol. 59, no. 6, pp. 276-277.

Athar, F. & Parnaik, V.K. (2015) 'Association of lamin A/C with muscle gene-specific promoters in myoblasts', *Biochem Biophys Rep*, vol. 4, pp. 76-82.

Ayyar, V.S., DuBois, D.C., Almon, R.R. & Jusko, W.J. (2017) 'Mechanistic Multi-Tissue Modeling of Glucocorticoid-Induced Leucine Zipper Regulation: Integrating Circadian Gene Expression with Receptor-Mediated Corticosteroid Pharmacodynamics', *J Pharmacol Exp Ther*, vol. 363, no. 1, pp. 45-57.

Bader, R.A. & Wagoner, K.L. (2010) 'Modulation of the response of rheumatoid arthritis synovial fibroblasts to proinflammatory stimulants with cyclic tensile strain', *Cytokine*, vol. 51, no. 1, pp. 35-41.

Bae, K., Lee, K., Seo, Y., Lee, H., Kim, D. & Choi, I. (2006) 'Differential effects of two period genes on the physiology and proteomic profiles of mouse anterior tibialis muscles', *Mol Cells*, vol. 22, no. 3, pp. 275-284.

Bakay, M., Wang, Z., Melcon, G., Schiltz, L., Xuan, J., Zhao, P., Sartorelli, V., Seo, J., Pegoraro, E., Angelini, C., Shneiderman, B., Escolar, D., Chen, Y.W., Winokur, S.T., Pachman, L.M., Fan, C., Mandler, R., Nevo, Y., Gordon, E., Zhu, Y., Dong, Y., Wang, Y. & Hoffman, E.P. (2006) 'Nuclear envelope dystrophies show a transcriptional fingerprint suggesting disruption of Rb-MyoD pathways in muscle regeneration', *Brain*, vol. 129, no. Pt 4, pp. 996-1013.

Balan, M. & Locke, M. (2011) 'Acute exercise activates myocardial nuclear factor kappa B', *Cell Stress Chaperones*, vol. 16, no. 1, pp. 105-111.

Balsalobre, A., Brown, S.A., Marcacci, L., Tronche, F., Kellendonk, C., Reichardt, H.M., Schütz, G. & Schibler, U. (2000) 'Resetting of circadian time in peripheral tissues by glucocorticoid signaling', *Science*, vol. 289, no. 5488, pp. 2344-2347.

Balsalobre, A., Damiola, F. & Schibler, U. (1998) 'A serum shock induces circadian gene expression in mammalian tissue culture cells', *Cell*, vol. 93, no. 6, pp. 929-937.

Balsalobre, A., Marcacci, L. & Schibler, U. (2000) 'Multiple signaling pathways elicit circadian gene expression in cultured Rat-1 fibroblasts', *Curr Biol*, vol. 10, no. 20, pp. 1291-1294.

Banes, A.J., Gilbert, J., Taylor, D. & Monbureau, O. (1985) 'A new vacuum-operated stress-providing instrument that applies static or variable duration cyclic tension or compression to cells in vitro', *J Cell Sci*, vol. 75, pp. 35-42.

Barger, L.K., Wright, K.P., Hughes, R.J. & Czeisler, C.A. (2004) 'Daily exercise facilitates phase delays of circadian melatonin rhythm in very dim light', *Am J Physiol Regul Integr Comp Physiol*, vol. 286, no. 6, pp. R1077-1084.

Becker-Weimann, S., Wolf, J., Herzel, H. & Kramer, A. (2004) 'Modeling feedback loops of the Mammalian circadian oscillator', *Biophys J*, vol. 87, no. 5, pp. 3023-3034.

Belkin, A.M., Zhidkova, N.I. & Koteliansky, V.E. (1986) 'Localization of talin in skeletal and cardiac muscles', *FEBS Lett*, vol. 200, no. 1, pp. 32-36.

Bellisle, F. & Le Magnen, J. (1981) 'The structure of meals in humans: eating and drinking patterns in lean and obese subjects', *Physiol Behav*, vol. 27, no. 4, pp. 649-658.

Belmont, A.S., Zhai, Y. & Thilenius, A. (1993) 'Lamin B distribution and association with peripheral chromatin revealed by optical sectioning and electron microscopy tomography', *J Cell Biol*,

vol. 123, no. 6 Pt 2, pp. 1671-1685.
Ben-Harush, K., Wiesel, N., Frenkiel-Krispin, D., Moeller, D., Soreq, E., Aebi, U., Herrmann, H., Gruenbaum, Y. & Medalia, O. (2009) 'The supramolecular organization of the C. elegans nuclear lamin filament', *J Mol Biol*, vol. 386, no. 5, pp. 1392-1402.
Bergo, M.O., Gavino, B., Ross, J., Schmidt, W.K., Hong, C., Kendall, L.V., Mohr, A., Meta, M., Genant, H., Jiang, Y., Wisner, E.R., Van Bruggen, N., Carano, R.A., Michaelis, S., Griffey, S.M. & Young, S.G. (2002) 'Zmpste24 deficiency in mice causes spontaneous bone fractures, muscle weakness, and a prelamin A processing defect', *Proc Natl Acad Sci U S A*, vol. 99, no. 20, pp. 13049-13054.
Bieler, J., Cannavo, R., Gustafson, K., Gobet, C., Gatfield, D. & Naef, F. (2014) 'Robust synchronization of coupled circadian and cell cycle oscillators in single mammalian cells', *Mol Syst Biol*, vol. 10, p. 739.
Biello, S.M., Janik, D. & Mrosovsky, N. (1994) 'Neuropeptide Y and behaviorally induced phase shifts', *Neuroscience*, vol. 62, no. 1, pp. 273-279.
Bikkul M., Clements C., Godwin L., Goldberg M., Kill I. & Bridger J. (2018) 'Farnesyltransferase inhibitor and rapamycin correct aberrant genome organisation and decrease DNA damage respectively, in Hutchinson-Gilford progeria syndrome fibroblasts', *Biogerontology*, vol. 19, no.6, pp. 579-602.
Bione, S., Maestrini, E., Rivella, S., Mancini, M., Regis, S., Romeo, G. & Toniolo, D. (1994) 'Identification of a novel X-linked gene responsible for Emery-Dreifuss muscular dystrophy', *Nat Genet*, vol. 8, no. 4, pp. 323-327.
Bishopric, N.H., Jayasena, V. & Webster, K.A. (1992) 'Positive regulation of the skeletal alpha-actin gene by Fos and Jun in cardiac myocytes', *J Biol Chem*, vol. 267, no. 35, pp. 25535-25540.
Bloch, R.J. & Gonzalez-Serratos, H. (2003) 'Lateral force transmission across costameres in skeletal muscle', *Exerc Sport Sci Rev*, vol. 31, no. 2, pp. 73-78.
Boguslavsky, R., Stewart, C. & Worman, H. (2006) 'Nuclear lamin A inhibits adipocyte differentiation: implications for Dunnigan-type familial partial lipodystrophy', *Hum Mol Genet*, vol. 15, no. 4, pp. 653-663.
Bonne, G., Di Barletta, M.R., Varnous, S., Bécane, H.M., Hammouda, E.H., Merlini, L., Muntoni, F., Greenberg, C.R., Gary, F., Urtizberea, J.A., Duboc, D., Fardeau, M., Toniolo, D. & Schwartz, K. (1999) 'Mutations in the gene encoding lamin A/C cause autosomal dominant Emery-Dreifuss muscular dystrophy', *Nat Genet*, vol. 21, no. 3, pp. 285-288.
Bonner, W.M. (1975) 'Protein migration into nuclei. II. Frog oocyte nuclei accumulate a class of microinjected oocyte nuclear proteins and exclude a class of microinjected oocyte cytoplasmic proteins', *J Cell Biol*, vol. 64, no. 2, pp. 431-437.
Borbély, A.A. (1982) 'A two process model of sleep regulation', *Hum Neurobiol*, vol. 1, no. 3, pp. 195-204.
Borovik, L., Modaff, P., Waterham, H.R., Krentz, A.D. & Pauli, R.M. (2013) 'Pelger-huet anomaly and a mild skeletal phenotype secondary to mutations in LBR', *Am J Med Genet A*, vol. 161A, no. 8, pp. 2066-2073.
Bosler, O. & Beaudet, A. (1985) 'VIP neurons as prime synaptic targets for serotonin afferents in rat suprachiasmatic nucleus: a combined radioautographic and immunocytochemical study', *J Neurocytol*, vol. 14, no. 5, pp. 749-763.
Boveri, T. (1888) *Die Befruchtung und Teilung des Eies vonAscaris megalocephala.*, vol. 22, In Z Naturw (Jena), pp. 685-882.
Boveri, T. (1909) *Die Blastomerenkerne von Ascaris megalocephala und dieTheorie der Chromosomenindividualität.*, no 3, Arch Ze llforsch, pp. 181-268.
Bowles, N.P., Thosar, S.S., Herzig, M.X. & Shea, S.A. (2018) 'Chronotherapy for Hypertension', *Curr Hypertens Rep*, vol. 20, no. 11, p. 97.
Boyartchuk, V.L., Ashby, M.N. & Rine, J. (1997) 'Modulation of Ras and a-factor function by carboxyl-terminal proteolysis', *Science*, vol. 275, no. 5307, pp. 1796-1800.

Boyle, S., Gilchrist, S., Bridger, J., Mahy, N., Ellis, J. & Bickmore, W., (2001) 'The spatial organization of human chromosomes within the nuclei of normal and emerin-mutant cells', *Human Molecular Genetics*, vol. 10, no. 3, pp. 211-220.

Brachner, A. & Foisner, R. (2014) 'Lamina-associated polypeptide (LAP)2α and other LEM proteins in cancer biology', *Adv Exp Med Biol*, vol. 773, pp. 143-163.

Briand, N. & Collas, P. (2018) 'Laminopathy-causing lamin A mutations reconfigure lamina-associated domains and local spatial chromatin conformation', *Nucleus*, vol. 9, no. 1, pp. 216-226.

Bridger, J.M., Foeger, N., Kill, I.R. & Herrmann, H. (2007) 'The nuclear lamina. Both a structural framework and a platform for genome organization', *FEBS J*, vol. 274, no. 6, pp. 1354-1361.

Bridger, J., Kill, I., O'Farrell, M. & Hutchison, C. (1993) 'Internal lamin structures within G1 nuclei of human dermal fibroblasts', *J Cell Sci*, vol. 104, pp. 297-306.

Broers, J.L., Machiels, B.M., Kuijpers, H.J., Smedts, F., van den Kieboom, R., Raymond, Y. & Ramaekers, F.C. (1997) 'A- and B-type lamins are differentially expressed in normal human tissues', *Histochem Cell Biol*, vol. 107, no. 6, pp. 505-517.

Bruce, V.G. (1972) 'Mutants of the biological clock in Chlamydomonas reinhardi', *Genetics*, vol. 70, no. 4, pp. 537-548.

Brull, A., Morales Rodriguez, B., Bonne, G., Muchir, A. & Bertrand, A.T. (2018) 'The Pathogenesis and Therapies of Striated Muscle Laminopathies', *Front Physiol*, vol. 9, p. 1533.

Brunt, L.H., Begg, K., Kague, E., Cross, S. & Hammond, C.L. (2017) 'Wnt signalling controls the response to mechanical loading during zebrafish joint development', *Development*, vol. 144, no. 15, pp. 2798-2809.

Buhr, E.D. & Takahashi, J.S. (2013) 'Molecular components of the Mammalian circadian clock', *Handb Exp Pharmacol*, no. 217, pp. 3-27.

Buhr, E.D., Yoo, S.H. & Takahashi, J.S. (2010) 'Temperature as a universal resetting cue for mammalian circadian oscillators', *Science*, vol. 330, no. 6002, pp. 379-385.

Bunger, M.K., Wilsbacher, L.D., Moran, S.M., Clendenin, C., Radcliffe, L.A., Hogenesch, J.B., Simon, M.C., Takahashi, J.S. & Bradfield, C.A. (2000) 'Mop3 is an essential component of the master circadian pacemaker in mammals', *Cell*, vol. 103, no. 7, pp. 1009-1017.

Burr, D.B. (2002) 'Bone material properties and mineral matrix contributions to fracture risk or age in women and men', *J Musculoskelet Neuronal Interact*, vol. 2, no. 3, pp. 201-204.

Burridge, K. & Chrzanowska-Wodnicka, M. (1996) 'Focal adhesions, contractility, and signaling', *Annu Rev Cell Dev Biol*, vol. 12, pp. 463-518.

Burridge, K. & Mangeat, P. (1984) 'An interaction between vinculin and talin', *Nature*, vol. 308, no. 5961, pp. 744-746.

Busino, L., Bassermann, F., Maiolica, A., Lee, C., Nolan, P.M., Godinho, S.I., Draetta, G.F. & Pagano, M. (2007) 'SCFFbxl3 controls the oscillation of the circadian clock by directing the degradation of cryptochrome proteins', *Science*, vol. 316, no. 5826, pp. 900-904.

Butcher, G.Q., Lee, B., Cheng, H.Y. & Obrietan, K. (2005) 'Light stimulates MSK1 activation in the suprachiasmatic nucleus via a PACAP-ERK/MAP kinase-dependent mechanism', *J Neurosci*, vol. 25, no. 22, pp. 5305-5313.

Buxton, O.M., Frank, S.A., L'Hermite-Balériaux, M., Leproult, R., Turek, F.W. & Van Cauter, E. (1997) 'Roles of intensity and duration of nocturnal exercise in causing phase delays of human circadian rhythms', *Am J Physiol*, vol. 273, no. 3 Pt 1, pp. E536-542.

Cai, M., Huang, Y., Ghirlando, R., Wilson, K.L., Craigie, R. & Clore, G.M. (2001) 'Solution structure of the constant region of nuclear envelope protein LAP2 reveals two LEM-domain structures: one binds BAF and the other binds DNA', *EMBO J*, vol. 20, no. 16, pp. 4399-4407.

Callan, H.G. & Tomlin, S.G. (1950) 'Experimental studies on amphibian oocyte nuclei. I. Investigation of the structure of the nuclear membrane by means of the electron microscope', *Proc R Soc Lond B Biol Sci*, vol. 137, no. 888, pp. 367-378.

Camozzi, D., Capanni, C., Cenni, V., Mattioli, E., Columbaro, M., Squarzoni, S. & Lattanzi, G. (2014) 'Diverse lamin-dependent mechanisms interact to control chromatin dynamics. Focus on

laminopathies', *Nucleus*, vol. 5, no. 5, pp. 427-440.
Cao, H. & Hegele, R.A. (2000) 'Nuclear lamin A/C R482Q mutation in canadian kindreds with Dunnigan-type familial partial lipodystrophy', *Hum Mol Genet*, vol. 9, no. 1, pp. 109-112.
Capanni, C., Cenni, V., Haraguchi, T., Squarzoni, S., Schüchner, S., Ogris, E., Novelli, G., Maraldi, N. & Lattanzi, G. (2010) 'lamin A precursor induces barrier-to-autointegration factor nuclear localization', *Cell Cycle*, vol. 9, no. 13, pp. 2600-2610.
Cenik, B.K., Liu, N., Chen, B., Bezprozvannaya, S., Olson, E.N. & Bassel-Duby, R. (2016) 'Myocardin-related transcription factors are required for skeletal muscle development', *Development*, vol. 143, no. 15, pp. 2853-2861.
Cenni, V., Bavelloni, A., Beretti, F., Tagliavini, F., Manzoli, L., Lattanzi, G., Maraldi, N.M., Cocco, L. & Marmiroli, S. (2011) 'Ankrd2/ARPP is a novel Akt2 specific substrate and regulates myogenic differentiation upon cellular exposure to H(2)O(2)', *Mol Biol Cell*, vol. 22, no. 16, pp. 2946-2956.
Cesarini, E., Mozzetta, C., Marullo, F., Gregoretti, F., Gargiulo, A., Columbaro, M., Cortesi, A., Antonelli, L., Di Pelino, S., Squarzoni, S., Palacios, D., Zippo, A., Bodega, B., Oliva, G. & Lanzuolo, C. (2015) 'Lamin A/C sustains PcG protein architecture, maintaining transcriptional repression at target genes', *J Cell Biol*, vol. 211, no. 3, pp. 533-551.
Chambeyron, S. & Bickmore, W.A. (2004) 'Chromatin decondensation and nuclear reorganization of the HoxB locus upon induction of transcription', *Genes Dev*, vol. 18, no. 10, pp. 1119-1130.
Chang, Y.J., Chen, Y.J., Huang, C.W., Fan, S.C., Huang, B.M., Chang, W.T., Tsai, Y.S., Su, F.C. & Wu, C.C. (2016) 'Cyclic Stretch Facilitates Myogenesis in C2C12 Myoblasts and Rescues Thiazolidinedione-Inhibited Myotube Formation', *Front Bioeng Biotechnol*, vol. 4, p. 27.
Chaouch, M., Allal, Y., De Sandre-Giovannoli, A., Vallat, J.M., Amer-el-Khedoud, A., Kassouri, N., Chaouch, A., Sindou, P., Hammadouche, T., Tazir, M., Lévy, N. & Grid, D. (2003) 'The phenotypic manifestations of autosomal recessive axonal Charcot-Marie-Tooth due to a mutation in lamin A/C gene', *Neuromuscul Disord*, vol. 13, no. 1, pp. 60-67.
Chatterjee, S. & Ma, K. (2016) 'Circadian clock regulation of skeletal muscle growth and repair', *F1000Res*, vol. 5, p. 1549.
Chatterjee, S., Nam, D., Guo, B., Kim, J.M., Winnier, G.E., Lee, J., Berdeaux, R., Yechoor, V.K. & Ma, K. (2013) 'Brain and muscle Arnt-like 1 is a key regulator of myogenesis', *J Cell Sci*, vol. 126, no. Pt 10, pp. 2213-2224.
Chen, H., Chen, J., Muir, L.A., Ronquist, S., Meixner, W., Ljungman, M., Ried, T., Smale, S. & Rajapakse, I. (2015a) 'Functional organization of the human 4D Nucleome', *Proc Natl Acad Sci U S A*, vol. 112, no. 26, pp. 8002-8007.
Chen, I.H., Huber, M., Guan, T., Bubeck, A. & Gerace, L. (2006) 'Nuclear envelope transmembrane proteins (NETs) that are up-regulated during myogenesis', *BMC Cell Biol*, vol. 7, p. 38.
Chen, L., Jiang, F., Qiao, Y., Li, H., Wei, Z., Huang, T., Lan, J., Xia, Y. & Li, J. (2018) 'Nucleoskeletal stiffness regulates stem cell migration and differentiation through lamin A/C', *J Cell Physiol*, vol. 233, no. 7, pp. 5112-5118.
Chen, R., Feng, L., Ruan, M., Liu, X., Adriouch, S. & Liao, H. (2013) 'Mechanical-stretch of C2C12 myoblasts inhibits expression of Toll-like receptor 3 (TLR3) and of autoantigens associated with inflammatory myopathies', *PLoS One*, vol. 8, no. 11, p. e79930.
Chen, W.D., Yeh, J.K., Peng, M.T., Shie, S.S., Lin, S.L., Yang, C.H., Chen, T.H., Hung, K.C., Wang, C.C., Hsieh, I.C., Wen, M.S. & Wang, C.Y. (2015b) 'Circadian CLOCK Mediates Activation of Transforming Growth Factor-β Signaling and Renal Fibrosis through Cyclooxygenase 2', *Am J Pathol*, vol. 185, no. 12, pp. 3152-3163.
Cheng, M.Y., Bullock, C.M., Li, C., Lee, A.G., Bermak, J.C., Belluzzi, J., Weaver, D.R., Leslie, F.M. & Zhou, Q.Y. (2002) 'Prokineticin 2 transmits the behavioural circadian rhythm of the suprachiasmatic nucleus', *Nature*, vol. 417, no. 6887, pp. 405-410.
Cho, H., Zhao, X., Hatori, M., Yu, R.T., Barish, G.D., Lam, M.T., Chong, L.W., DiTacchio, L., Atkins, A.R., Glass, C.K., Liddle, C., Auwerx, J., Downes, M., Panda, S. & Evans, R.M. (2012) 'Regulation of

circadian behaviour and metabolism by REV-ERB-α and REV-ERB-β', *Nature*, vol. 485, no. 7396, pp. 123-127.

Clarke, S., Vogel, J.P., Deschenes, R.J. & Stock, J. (1988) 'Posttranslational modification of the Ha-ras oncogene protein: evidence for a third class of protein carboxyl methyltransferases', *Proc Natl Acad Sci U S A*, vol. 85, no. 13, pp. 4643-4647.

Constantinescu, D., Gray, H.L., Sammak, P.J., Schatten, G.P. & Csoka, A.B. (2006) 'lamin A/C expression is a marker of mouse and human embryonic stem cell differentiation', *Stem Cells*, vol. 24, no. 1, pp. 177-185.

Conway, J.F. & Parry, D.A. (1990) 'Structural features in the heptad substructure and longer range repeats of two-stranded alpha-fibrous proteins', *Int J Biol Macromol*, vol. 12, no. 5, pp. 328-334.

Corne, T.D.J., Sieprath, T., Vandenbussche, J., Mohammed, D., Te Lindert, M., Gevaert, K., Gabriele, S., Wolf, K. & De Vos, W.H. (2017) 'Deregulation of focal adhesion formation and cytoskeletal tension due to loss of A-type lamins', *Cell Adh Migr*, vol. 11, no. 5-6, pp. 447-463.

Coutinho, A.E. & Chapman, K.E. (2011) 'The anti-inflammatory and immunosuppressive effects of glucocorticoids, recent developments and mechanistic insights', *Mol Cell Endocrinol*, vol. 335, no. 1, pp. 2-13.

Cremer, T., Cremer, C., Baumann, H., Luedtke, E.K., Sperling, K., Teuber, V. & Zorn, C. (1982) 'Rabl's model of the interphase chromosome arrangement tested in Chinese hamster cells by premature chromosome condensation and laser-UV-microbeam experiments', *Hum Genet*, vol. 60, no. 1, pp. 46-56.

Crisp, M., Liu, Q., Roux, K., Rattner, J.B., Shanahan, C., Burke, B., Stahl, P.D. & Hodzic, D. (2006) 'Coupling of the nucleus and cytoplasm: role of the LINC complex', *J Cell Biol*, vol. 172, no. 1, pp. 41-53.

Crnko, S., Cour, M., Van Laake, L.W. & Lecour, S. (2018) 'Vasculature on the clock: Circadian rhythm and vascular dysfunction', *Vascul Pharmacol*, vol. 108, pp. 1-7.

Croft, J.A., Bridger, J.M., Boyle, S., Perry, P., Teague, P. & Bickmore, W.A. (1999) 'Differences in the localization and morphology of chromosomes in the human nucleus', *J Cell Biol*, vol. 145, no. 6, pp. 1119-1131.

Cronshaw, J.M., Krutchinsky, A.N., Zhang, W., Chait, B.T. & Matunis, M.J. (2002) 'Proteomic analysis of the mammalian nuclear pore complex', *J Cell Biol*, vol. 158, no. 5, pp. 915-927.

Crosthwaite, S.K., Dunlap, J.C. & Loros, J.J. (1997) 'Neurospora wc-1 and wc-2: transcription, photoresponses, and the origins of circadian rhythmicity', *Science*, vol. 276, no. 5313, pp. 763-769.

Dai, H., Zhang, L., Cao, M., Song, F., Zheng, H., Zhu, X., Wei, Q., Zhang, W. & Chen, K. (2011) 'The role of polymorphisms in circadian pathway genes in breast tumorigenesis', *Breast Cancer Res Treat*, vol. 127, no. 2, pp. 531-540.

Dai, Q., Choy, E., Chiu, V., Romano, J., Slivka, S.R., Steitz, S.A., Michaelis, S. & Philips, M.R. (1998) 'Mammalian prenylcysteine carboxyl methyltransferase is in the endoplasmic reticulum', *J Biol Chem*, vol. 273, no. 24, pp. 15030-15034.

Dang, F., Sun, X., Ma, X., Wu, R., Zhang, D., Chen, Y., Xu, Q., Wu, Y. & Liu, Y. (2016) 'Insulin post-transcriptionally modulates Bmal1 protein to affect the hepatic circadian clock', *Nat Commun*, vol. 7, p. 12696.

Danowski, B.A., Imanaka-Yoshida, K., Sanger, J.M. & Sanger, J.W. (1992) 'Costameres are sites of force transmission to the substratum in adult rat cardiomyocytes', *J Cell Biol*, vol. 118, no. 6, pp. 1411-1420.

de Brito, L.C., Rezende, R.A., da Silva Junior, N.D., Tinucci, T., Casarini, D.E., Cipolla-Neto, J. & Forjaz, C.L. (2015) 'Post-Exercise Hypotension and Its Mechanisms Differ after Morning and Evening Exercise: A Randomized Crossover Study', *PLoS One*, vol. 10, no. 7, p. e0132458.

De Sandre-Giovannoli, A., Bernard, R., Cau, P., Navarro, C., Amiel, J., Boccaccio, I., Lyonnet, S., Stewart, C.L., Munnich, A., Le Merrer, M. & Lévy, N. (2003) 'Lamin a truncation in

Hutchinson-Gilford progeria', *Science*, vol. 300, no. 5628, p. 2055.
De Sandre-Giovannoli, A., Chaouch, M., Kozlov, S., Vallat, J.M., Tazir, M., Kassouri, N., Szepetowski, P., Hammadouche, T., Vandenberghe, A., Stewart, C.L., Grid, D. & Lévy, N. (2002) 'Homozygous defects in LMNA, encoding lamin A/C nuclear-envelope proteins, cause autosomal recessive axonal neuropathy in human (Charcot-Marie-Tooth disorder type 2) and mouse', *Am J Hum Genet*, vol. 70, no. 3, pp. 726-736.
Dechat, T., Shimi, T., Adam, S.A., Rusinol, A.E., Andres, D.A., Spielmann, H.P., Sinensky, M.S. & Goldman, R.D. (2007) 'Alterations in mitosis and cell cycle progression caused by a mutant lamin A known to accelerate human aging', *Proc Natl Acad Sci U S A*, vol. 104, no. 12, pp. 4955-4960.
Dechat, T., Vlcek, S. & Foisner, R. (2000) 'Review: lamina-associated polypeptide 2 isoforms and related proteins in cell cycle-dependent nuclear structure dynamics', *J Struct Biol*, vol. 129, no. 2-3, pp. 335-345.
Delaine-Smith, R., Javaheri, B., Helen Edwards, J., Vazquez, M. & Rumney, R.M. (2015) 'Preclinical models for in vitro mechanical loading of bone-derived cells', *Bonekey Rep*, vol. 4, p. 728.
Dhe-Paganon, S., Werner, E.D., Chi, Y.I. & Shoelson, S.E. (2002) 'Structure of the globular tail of nuclear lamin', *J Biol Chem*, vol. 277, no. 20, pp. 17381-17384.
Dialynas, G., Shrestha, O.K., Ponce, J.M., Zwerger, M., Thiemann, D.A., Young, G.H., Moore, S.A., Yu, L., Lammerding, J. & Wallrath, L.L. (2015) 'Myopathic lamin mutations cause reductive stress and activate the nrf2/keap-1 pathway', *PLoS Genet*, vol. 11, no. 5, p. e1005231.
Dierickx, P., Van Laake, L.W. & Geijsen, N. (2018) 'Circadian clocks: from stem cells to tissue homeostasis and regeneration', *EMBO Rep*, vol. 19, no. 1, pp. 18-28.
Dixon, J., Selvaraj, S., Yue, F., Kim, A., Li, Y., Shen, Y., Hu, M., Liu, J. & Ren, B. (2012) 'Topological Domains in Mammalian Genomes Identified by Analysis of Chromatin Interactions', *Nature*, vol. 485, no. 7398, pp. 376-380.
Dong, C., Gongora, R., Sosulski, M.L., Luo, F. & Sanchez, C.G. (2016) 'Regulation of transforming growth factor-beta1 (TGF-β1)-induced pro-fibrotic activities by circadian clock gene BMAL1', *Respir Res*, vol. 17, p. 4.
Dreuillet, C., Harper, M., Tillit, J., Kress, M. & Ernoult-Lange, M. (2008) 'Mislocalization of human transcription factor MOK2 in the presence of pathogenic mutations of lamin A/C', *Biol Cell*, vol. 100, no. 1, pp. 51-61.
Dreuillet, C., Tillit, J., Kress, M. & Ernoult-Lange, M. (2002) 'In vivo and in vitro interaction between human transcription factor MOK2 and nuclear lamin A/C', *Nucleic Acids Res*, vol. 30, no. 21, pp. 4634-4642.
Duband-Goulet, I. & Courvalin, J.C. (2000) 'Inner nuclear membrane protein LBR preferentially interacts with DNA secondary structures and nucleosomal linker', *Biochemistry*, vol. 39, no. 21, pp. 6483-6488.
Dudek, M. & Meng, Q.J. (2014) 'Running on time: the role of circadian clocks in the musculoskeletal system', *Biochem J*, vol. 463, no. 1, pp. 1-8.
Dulong, S., Ballesta, A., Okyar, A. & Lévi, F. (2015) 'Identification of Circadian Determinants of Cancer Chronotherapy through In Vitro Chronopharmacology and Mathematical Modeling', *Mol Cancer Ther*, vol. 14, no. 9, pp. 2154-2164.
Eckel-Mahan, K. & Sassone-Corsi, P. (2015) 'Phenotyping Circadian Rhythms in Mice', *Curr Protoc Mouse Biol*, vol. 5, no. 3, pp. 271-281.
Edelstein, K. & Amir, S. (1999) 'The intergeniculate leaflet does not mediate the disruptive effects of constant light on circadian rhythms in the rat', *Neuroscience*, vol. 90, no. 3, pp. 1093-1101.
Edgar, D.M. & Dement, W.C. (1991) 'Regularly scheduled voluntary exercise synchronizes the mouse circadian clock', *Am J Physiol*, vol. 261, no. 4 Pt 2, pp. R928-933.
Ehlers, A., Xie, W., Agapov, E., Brown, S., Steinberg, D., Tidwell, R., Sajol, G., Schutz, R., Weaver, R., Yu, H., Castro, M., Bacharier, L.B., Wang, X., Holtzman, M.J. & Haspel, J.A. (2018) 'BMAL1 links the circadian clock to viral airway pathology and asthma phenotypes', *Mucosal*

Immunol, vol. 11, no. 1, pp. 97-111.
Eide, E.J., Vielhaber, E.L., Hinz, W.A. & Virshup, D.M. (2002) 'The circadian regulatory proteins BMAL1 and cryptochromes are substrates of casein kinase Iepsilon', *J Biol Chem*, vol. 277, no. 19, pp. 17248-17254.
Eide, E.J., Woolf, M.F., Kang, H., Woolf, P., Hurst, W., Camacho, F., Vielhaber, E.L., Giovanni, A. & Virshup, D.M. (2005) 'Control of mammalian circadian rhythm by CKIepsilon-regulated proteasome-mediated PER2 degradation', *Mol Cell Biol*, vol. 25, no. 7, pp. 2795-2807.
Elnitski, L., Jin, V.X., Farnham, P.J. & Jones, S.J. (2006) 'Locating mammalian transcription factor binding sites: a survey of computational and experimental techniques', *Genome Res*, vol. 16, no. 12, pp. 1455-1464.
Ervasti, J.M. & Campbell, K.P. (1993) 'A role for the dystrophin-glycoprotein complex as a transmembrane linker between laminin and actin', *J Cell Biol*, vol. 122, no. 4, pp. 809-823.
Fanin, M., Savarese, M., Nascimbeni, A.C., Di Fruscio, G., Pastorello, E., Tasca, E., Trevisan, C.P., Nigro, V. & Angelini, C. (2015) 'Dominant muscular dystrophy with a novel SYNE1 gene mutation', *Muscle Nerve*, vol. 51, no. 1, pp. 145-147.
Farnsworth, C.C., Wolda, S.L., Gelb, M.H. & Glomset, J.A. (1989) 'Human lamin B contains a farnesylated cysteine residue', *J Biol Chem*, vol. 264, no. 34, pp. 20422-20429.
Fatkin, D., MacRae, C., Sasaki, T., Wolff, M.R., Porcu, M., Frenneaux, M., Atherton, J., Vidaillet, H.J., Spudich, S., De Girolami, U., Seidman, J.G., Seidman, C., Muntoni, F., Müehle, G., Johnson, W. & McDonough, B. (1999) 'Missense mutations in the rod domain of the lamin A/C gene as causes of dilated cardiomyopathy and conduction-system disease', *N Engl J Med*, vol. 341, no. 23, pp. 1715-1724.
Fawcett, D.W. (1966) 'On the occurrence of a fibrous lamina on the inner aspect of the nuclear envelope in certain cells of vertebrates', *Am J Anat*, vol. 119, no. 1, pp. 129-145.
Feillet, C., Krusche, P., Tamanini, F., Janssens, R.C., Downey, M.J., Martin, P., Teboul, M., Saito, S., Lévi, F.A., Bretschneider, T., van der Horst, G.T., Delaunay, F. & Rand, D.A. (2014) 'Phase locking and multiple oscillating attractors for the coupled mammalian clock and cell cycle', *Proc Natl Acad Sci U S A*, vol. 111, no. 27, pp. 9828-9833.
Feldman, J.F. & Hoyle, M.N. (1973) 'Isolation of circadian clock mutants of Neurospora crassa', *Genetics*, vol. 75, no. 4, pp. 605-613.
Ferraro, A., Eufemi, M., Cervoni, L., Marinetti, R. & Turano, C. (1989) 'Glycosylated forms of nuclear lamins', *FEBS Lett*, vol. 257, no. 2, pp. 241-246.
Ferri, G., Storti, B. & Bizzarri, R. (2017) 'Nucleocytoplasmic transport in cells with progerin-induced defective nuclear lamina', *Biophys Chem*, vol. 229, pp. 77-83.
Fisch, K.M., Gamini, R., Alvarez-Garcia, O., Akagi, R., Saito, M., Muramatsu, Y., Sasho, T., Koziol, J.A., Su, A.I. & Lotz, M.K. (2018) 'Identification of transcription factors responsible for dysregulated networks in human osteoarthritis cartilage by global gene expression analysis', *Osteoarthritis Cartilage*, vol. 26, no. 11, pp. 1531-1538.
Fischer, H.P. (2008) 'Mathematical modeling of complex biological systems: from parts lists to understanding systems behavior', *Alcohol Res Health*, vol. 31, no. 1, pp. 49-59.
Fisher, D.Z., Chaudhary, N. & Blobel, G. (1986) 'cDNA sequencing of nuclear lamins A and C reveals primary and secondary structural homology to intermediate filament proteins', *Proc Natl Acad Sci U S A*, vol. 83, no. 17, pp. 6450-6454.
Fitzgerald, K. & Zucker, I. (1976) 'Circadian organization of the estrous cycle of the golden hamster', *Proc Natl Acad Sci U S A*, vol. 73, no. 8, pp. 2923-2927.
Foisner, R. (2001) 'Inner nuclear membrane proteins and the nuclear lamina', *J Cell Sci*, vol. 114, no. Pt 21, pp. 3791-3792.
Foisner, R. & Gerace, L. (1993) 'Integral membrane proteins of the nuclear envelope interact with lamins and chromosomes, and binding is modulated by mitotic phosphorylation', *Cell*, vol. 73, no. 7, pp. 1267-1279.
Franke, W.W. (1987) 'Nuclear lamins and cytoplasmic intermediate filament proteins: a growing

multigene family', *Cell*, vol. 48, no. 1, pp. 3-4.
Frock, R.L., Kudlow, B.A., Evans, A.M., Jameson, S.A., Hauschka, S.D. & Kennedy, B.K. (2006) 'lamin A/C and emerin are critical for skeletal muscle satellite cell differentiation', *Genes Dev*, vol. 20, no. 4, pp. 486-500.
Fu, S., Yin, L., Lin, X., Lu, J. & Wang, X. (2018) 'Effects of Cyclic Mechanical Stretch on the Proliferation of L6 Myoblasts and Its Mechanisms: PI3K/Akt and MAPK Signal Pathways Regulated by IGF-1 Receptor', *Int J Mol Sci*, vol. 19, no. 6.
Funahashi, A. (2003) *CellDesigner: a process diagram editor for gene-regulatory and biochemical networks*, in N. Tanimura (ed.).
Furukawa, K., Panté, N., Aebi, U. & Gerace, L. (1995) 'Cloning of a cDNA for lamina-associated polypeptide 2 (LAP2) and identification of regions that specify targeting to the nuclear envelope', *EMBO J*, vol. 14, no. 8, pp. 1626-1636.
Gale, J.E., Cox, H.I., Qian, J., Block, G.D., Colwell, C.S. & Matveyenko, A.V. (2011) 'Disruption of circadian rhythms accelerates development of diabetes through pancreatic beta-cell loss and dysfunction', *J Biol Rhythms*, vol. 26, no. 5, pp. 423-433.
Garg, A., Peshock, R.M. & Fleckenstein, J.L. (1999) 'Adipose tissue distribution pattern in patients with familial partial lipodystrophy (Dunnigan variety)', *J Clin Endocrinol Metab*, vol. 84, no. 1, pp. 170-174.
Gaucher, J., Montellier, E. & Sassone-Corsi, P. (2018) 'Molecular Cogs: Interplay between Circadian Clock and Cell Cycle', *Trends Cell Biol*, vol. 28, no. 5, pp. 368-379.
Gekakis, N., Staknis, D., Nguyen, H.B., Davis, F.C., Wilsbacher, L.D., King, D.P., Takahashi, J.S. & Weitz, C.J. (1998) 'Role of the CLOCK protein in the mammalian circadian mechanism', *Science*, vol. 280, no. 5369, pp. 1564-1569.
Gerace, L., Blum, A. & Blobel, G. (1978) 'Immunocytochemical localization of the major polypeptides of the nuclear pore complex-lamina fraction. Interphase and mitotic distribution', *J Cell Biol*, vol. 79, no. 2 Pt 1, pp. 546-566.
Gerber, A., Esnault, C., Aubert, G., Treisman, R., Pralong, F. & Schibler, U. (2013) 'Blood-borne circadian signal stimulates daily oscillations in actin dynamics and SRF activity', *Cell*, vol. 152, no. 3, pp. 492-503.
Geusz, M.E., Fletcher, C., Block, G.D., Straume, M., Copeland, N.G., Jenkins, N.A., Kay, S.A. & Day, R.N. (1997) 'Long-term monitoring of circadian rhythms in c-fos gene expression from suprachiasmatic nucleus cultures', *Curr Biol*, vol. 7, no. 10, pp. 758-766.
Glass, C.A., Glass, J.R., Taniura, H., Hasel, K.W., Blevitt, J.M. & Gerace, L. (1993) 'The alpha-helical rod domain of human lamins A and C contains a chromatin binding site', *EMBO J*, vol. 12, no. 11, pp. 4413-4424.
Glasson, S.S., Blanchet, T.J. & Morris, E.A. (2007) 'The surgical destabilization of the medial meniscus (DMM) model of osteoarthritis in the 129/SvEv mouse', *Osteoarthritis Cartilage*, vol. 15, no. 9, pp. 1061-1069.
Goldberg, M.W. & Allen, T.D. (1996) 'The nuclear pore complex and lamina: three-dimensional structures and interactions determined by field emission in-lens scanning electron microscopy', *J Mol Biol*, vol. 257, no. 4, pp. 848-865.
Goldbeter, A. (1995) 'A model for circadian oscillations in the Drosophila period protein (PER)', *Proc Biol Sci*, vol. 261, no. 1362, pp. 319-324.
Goldman, R.D., Gruenbaum, Y., Moir, R.D., Shumaker, D.K. & Spann, T.P. (2002) 'Nuclear lamins: building blocks of nuclear architecture', *Genes Dev*, vol. 16, no. 5, pp. 533-547.
Goldman, R.D., Shumaker, D.K., Erdos, M.R., Eriksson, M., Goldman, A.E., Gordon, L.B., Gruenbaum, Y., Khuon, S., Mendez, M., Varga, R. & Collins, F.S. (2004) 'Accumulation of mutant lamin A causes progressive changes in nuclear architecture in Hutchinson-Gilford progeria syndrome', *Proc Natl Acad Sci U S A*, vol. 101, no. 24, pp. 8963-8968.
Goldsmith, C.S. & Bell-Pedersen, D. (2013) 'Diverse roles for MAPK signaling in circadian clocks', *Adv Genet*, vol. 84, pp. 1-39.

Gonzalez-Suarez, I. & Gonzalo, S. (2010) 'Nurturing the genome: A-type lamins preserve genomic stability', *Nucleus*, vol. 1, no. 2, pp. 129-135.

González, J.M., Navarro-Puche, A., Casar, B., Crespo, P. & Andrés, V. (2008) 'Fast regulation of AP-1 activity through interaction of lamin A/C, ERK1/2, and c-Fos at the nuclear envelope', *J Cell Biol*, vol. 183, no. 4, pp. 653-666.

Goodyear, L.J., Chang, P.Y., Sherwood, D.J., Dufresne, S.D. & Moller, D.E. (1996) 'Effects of exercise and insulin on mitogen-activated protein kinase signaling pathways in rat skeletal muscle', *Am J Physiol*, vol. 271, no. 2 Pt 1, pp. E403-408.

Gossan, N., Zeef, L., Hensman, J., Hughes, A., Bateman, J.F., Rowley, L., Little, C.B., Piggins, H.D., Rattray, M., Boot-Handford, R.P. & Meng, Q.J. (2013) 'The circadian clock in murine chondrocytes regulates genes controlling key aspects of cartilage homeostasis', *Arthritis Rheum*, vol. 65, no. 9, pp. 2334-2345.

Griffin, E.A., Staknis, D. & Weitz, C.J. (1999) 'Light-independent role of CRY1 and CRY2 in the mammalian circadian clock', *Science*, vol. 286, no. 5440, pp. 768-771.

Grinnell, F. & Geiger, B. (1986) 'Interaction of fibronectin-coated beads with attached and spread fibroblasts. Binding, phagocytosis, and cytoskeletal reorganization', *Exp Cell Res*, vol. 162, no. 2, pp. 449-461.

Grossi, A., Yadav, K. & Lawson, M.A. (2007) 'Mechanical stimulation increases proliferation, differentiation and protein expression in culture: stimulation effects are substrate dependent', *J Biomech*, vol. 40, no. 15, pp. 3354-3362.

Gruenbaum, Y., Goldman, R.D., Meyuhas, R., Mills, E., Margalit, A., Fridkin, A., Dayani, Y., Prokocimer, M. & Enosh, A. (2003) 'The nuclear lamina and its functions in the nucleus', *Int Rev Cytol*, vol. 226, pp. 1-62.

Gréchez-Cassiau, A., Rayet, B., Guillaumond, F., Teboul, M. & Delaunay, F. (2008) 'The circadian clock component BMAL1 is a critical regulator of p21WAF1/CIP1 expression and hepatocyte proliferation', *J Biol Chem*, vol. 283, no. 8, pp. 4535-4542.

Guelen, L., Pagie, L., Brasset, E., Meuleman, W., Faza, M.B., Talhout, W., Eussen, B.H., de Klein, A., Wessels, L., de Laat, W. & van Steensel, B. (2008) 'Domain organization of human chromosomes revealed by mapping of nuclear lamina interactions', *Nature*, vol. 453, no. 7197, pp. 948-951.

Guillaumond, F., Dardente, H., Giguère, V. & Cermakian, N. (2005) 'Differential control of Bmal1 circadian transcription by REV-ERB and ROR nuclear receptors', *J Biol Rhythms*, vol. 20, no. 5, pp. 391-403.

Hackney, A.C., Davis, H.C. & Lane, A.R. (2015) 'Exercise augments the nocturnal prolactin rise in exercise-trained men', *Ther Adv Endocrinol Metab*, vol. 6, no. 5, pp. 217-222.

Hadaeghi, F., Hashemi Golpayegani, M.R., Jafari, S. & Murray, G. (2016) 'Toward a complex system understanding of bipolar disorder: A chaotic model of abnormal circadian activity rhythms in euthymic bipolar disorder', *Aust N Z J Psychiatry*, vol. 50, no. 8, pp. 783-792.

Halberg, F., Halberg, E., Barnum, C. & Bittner, J. (1959) 'Photoperiodism and related phenomena in plants and animals', *AAAS 1959*.

Hamasaki, K., Mimura, T., Furuya, H., Morino, N., Yamazaki, T., Komuro, I., Yazaki, Y. & Nojima, Y. (1995) 'Stretching mesangial cells stimulates tyrosine phosphorylation of focal adhesion kinase pp125FAK', *Biochem Biophys Res Commun*, vol. 212, no. 2, pp. 544-549.

Hanks, S.K., Calalb, M.B., Harper, M.C. & Patel, S.K. (1992) 'Focal adhesion protein-tyrosine kinase phosphorylated in response to cell attachment to fibronectin', *Proc Natl Acad Sci U S A*, vol. 89, no. 18, pp. 8487-8491.

Hanukoglu, I. & Fuchs, E. (1982) 'The cDNA sequence of a human epidermal keratin: divergence of sequence but conservation of structure among intermediate filament proteins', *Cell*, vol. 31, no. 1, pp. 243-252.

Haque, F., Lloyd, D.J., Smallwood, D.T., Dent, C.L., Shanahan, C.M., Fry, A.M., Trembath, R.C. & Shackleton, S. (2006) 'SUN1 interacts with nuclear lamin A and cytoplasmic nesprins to

provide a physical connection between the nuclear lamina and the cytoskeleton', *Mol Cell Biol*, vol. 26, no. 10, pp. 3738-3751.
Haque, W.A., Vuitch, F. & Garg, A. (2002) 'Post-mortem findings in familial partial lipodystrophy, Dunnigan variety', *Diabet Med*, vol. 19, no. 12, pp. 1022-1025.
Harrington, M.E., Nance, D.M. & Rusak, B. (1985) 'Neuropeptide Y immunoreactivity in the hamster geniculo-suprachiasmatic tract', *Brain Res Bull*, vol. 15, no. 5, pp. 465-472.
Harrington, M.E. & Rusak, B. (1986) 'Lesions of the thalamic intergeniculate leaflet alter hamster circadian rhythms', *J Biol Rhythms*, vol. 1, no. 4, pp. 309-325.
Harris, M.J., Wirtz, D. & Wu, P.H. (2018) 'Dissecting cellular mechanics: Implications for aging, cancer, and immunity', *Semin Cell Dev Biol*.
He, D., An, Y., Li, Y., Wang, J., Wu, G., Chen, L. & Zhu, G. (2018) 'RNA sequencing reveals target genes of temporomandibular joint osteoarthritis in rats after the treatment of low-intensity pulsed ultrasound', *Gene*, vol. 672, pp. 126-136.
He, F., Li, J., Liu, Z., Chuang, C.C., Yang, W. & Zuo, L. (2016) 'Redox Mechanism of Reactive Oxygen Species in Exercise', *Front Physiol*, vol. 7, p. 486.
Heald, R. & McKeon, F. (1990) 'Mutations of phosphorylation sites in lamin A that prevent nuclear lamina disassembly in mitosis', *Cell*, vol. 61, no. 4, pp. 579-589.
Heaney, J.L., Carroll, D. & Phillips, A.C. (2014) 'Physical activity, life events stress, cortisol, and DHEA: preliminary findings that physical activity may buffer against the negative effects of stress', *J Aging Phys Act*, vol. 22, no. 4, pp. 465-473.
Helbling-Leclerc, A., Bonne, G. & Schwartz, K. (2002) 'Emery-Dreifuss muscular dystrophy', *Eur J Hum Genet*, vol. 10, no. 3, pp. 157-161.
Hellemans, J., Preobrazhenska, O., Willaert, A., Debeer, P., Verdonk, P.C., Costa, T., Janssens, K., Menten, B., Van Roy, N., Vermeulen, S.J., Savarirayan, R., Van Hul, W., Vanhoenacker, F., Huylebroeck, D., De Paepe, A., Naeyaert, J.M., Vandesompele, J., Speleman, F., Verschueren, K., Coucke, P.J. & Mortier, G.R. (2004) 'Loss-of-function mutations in LEMD3 result in osteopoikilosis, Buschke-Ollendorff syndrome and melorheostosis', *Nat Genet*, vol. 36, no. 11, pp. 1213-1218.
Hirano, H. & Matsuura, Y. (2011) 'Sensing actin dynamics: structural basis for G-actin-sensitive nuclear import of MAL', *Biochem Biophys Res Commun*, vol. 414, no. 2, pp. 373-378.
Ho, C.Y., Jaalouk, D.E., Vartiainen, M.K. & Lammerding, J. (2013) 'lamin A/C and emerin regulate MKL1-SRF activity by modulating actin dynamics', *Nature*, vol. 497, no. 7450, pp. 507-511.
Ho, R. & Hegele, R.A. (2019) 'Complex effects of laminopathy mutations on nuclear structure and function', *Clin Genet*, vol. 95, no. 2, pp. 199-209.
Ho, R.C., Hirshman, M.F., Li, Y., Cai, D., Farmer, J.R., Aschenbach, W.G., Witczak, C.A., Shoelson, S.E. & Goodyear, L.J. (2005) 'Regulation of IkappaB kinase and NF-kappaB in contracting adult rat skeletal muscle', *Am J Physiol Cell Physiol*, vol. 289, no. 4, pp. C794-801.
Hodzic, D.M., Yeater, D.B., Bengtsson, L., Otto, H. & Stahl, P.D. (2004) 'Sun2 is a novel mammalian inner nuclear membrane protein', *J Biol Chem*, vol. 279, no. 24, pp. 25805-25812.
Hoops, S., Sahle, S., Gauges, R., Lee, C., Pahle, J., Simus, N., Singhal, M., Xu, L., Mendes, P. & Kummer, U. (2006) 'COPASI--a COmplex PAthway SImulator', *Bioinformatics*, vol. 22, no. 24, pp. 3067-3074.
Hutchison, C.J., Alvarez-Reyes, M. & Vaughan, O.A. (2001) 'Lamins in disease: why do ubiquitously expressed nuclear envelope proteins give rise to tissue-specific disease phenotypes?', *J Cell Sci*, vol. 114, no. Pt 1, pp. 9-19.
Ihara, T., Mitsui, T., Nakamura, Y., Kira, S., Miyamoto, T., Nakagomi, H., Sawada, N., Hirayama, Y., Shibata, K., Shigetomi, E., Shinozaki, Y., Yoshiyama, M., Andersson, K.E., Nakao, A., Takeda, M. & Koizumi, S. (2017) 'The Clock mutant mouse is a novel experimental model for nocturia and nocturnal polyuria', *Neurourol Urodyn*, vol. 36, no. 4, pp. 1034-1038.
Ingber, D.E. (2006) 'Cellular mechanotransduction: putting all the pieces together again', *FASEB J*, vol. 20, no. 7, pp. 811-827.

Innominato, P.F., Lévi, F.A. & Bjarnason, G.A. (2010) 'Chronotherapy and the molecular clock: Clinical implications in oncology', *Adv Drug Deliv Rev*, vol. 62, no. 9-10, pp. 979-1001.

Ishiura, M., Kutsuna, S., Aoki, S., Iwasaki, H., Andersson, C.R., Tanabe, A., Golden, S.S., Johnson, C.H. & Kondo, T. (1998) 'Expression of a gene cluster kaiABC as a circadian feedback process in cyanobacteria', *Science*, vol. 281, no. 5382, pp. 1519-1523.

Ivorra, C., Kubicek, M., González, J.M., Sanz-González, S.M., Alvarez-Barrientos, A., O'Connor, J.E., Burke, B. & Andrés, V. (2006) 'A mechanism of AP-1 suppression through interaction of c-Fos with lamin A/C', *Genes Dev*, vol. 20, no. 3, pp. 307-320.

Jainchill, J.L., Aaronson, S.A. & Todaro, G.J. (1969) 'Murine sarcoma and leukemia viruses: assay using clonal lines of contact-inhibited mouse cells', *J Virol*, vol. 4, no. 5, pp. 549-553.

Janik, D. & Mrosovsky, N. (1994) 'Intergeniculate leaflet lesions and behaviorally-induced shifts of circadian rhythms', *Brain Res*, vol. 651, no. 1-2, pp. 174-182.

Johnson, B.R., Nitta, R.T., Frock, R.L., Mounkes, L., Barbie, D.A., Stewart, C.L., Harlow, E. & Kennedy, B.K. (2004) 'A-type lamins regulate retinoblastoma protein function by promoting subnuclear localization and preventing proteasomal degradation', *Proc Natl Acad Sci U S A*, vol. 101, no. 26, pp. 9677-9682.

Jung, Y. & Feldman, B.J. (2018) 'A context-specific circadian clock in adipocyte precursor cells modulates adipogenesis', *Adipocyte*, pp. 1-4.

Kalsbeek, A., Buijs, R.M., van Heerikhuize, J.J., Arts, M. & van der Woude, T.P. (1992) 'Vasopressin-containing neurons of the suprachiasmatic nuclei inhibit corticosterone release', *Brain Res*, vol. 580, no. 1-2, pp. 62-67.

Kanbe, K., Inoue, K., Xiang, C. & Chen, Q. (2006) 'Identification of clock as a mechanosensitive gene by large-scale DNA microarray analysis: downregulation in osteoarthritic cartilage', *Mod Rheumatol*, vol. 16, no. 3, pp. 131-136.

Kang, S.M., Yoon, M.H. & Park, B.J. (2018) 'Laminopathies; Mutations on single gene and various human genetic diseases', *BMB Rep*, vol. 51, no. 7, pp. 327-337.

Keesler, G.A., Camacho, F., Guo, Y., Virshup, D., Mondadori, C. & Yao, Z. (2000) 'Phosphorylation and destabilization of human period I clock protein by human casein kinase I epsilon', *Neuroreport*, vol. 11, no. 5, pp. 951-955.

Kervezee, L., Kosmadopoulos, A. & Boivin, D.B. (2018) 'Metabolic and cardiovascular consequences of shift work: the role of circadian disruption and sleep disturbances', *Eur J Neurosci*.

Kervezee, L., Stevens, J., Birkhoff, W., Kamerling, I.M., de Boer, T., Dröge, M., Meijer, J.H. & Burggraaf, J. (2016) 'Identifying 24 h variation in the pharmacokinetics of levofloxacin: a population pharmacokinetic approach', *Br J Clin Pharmacol*, vol. 81, no. 2, pp. 256-268.

Khan, S., Nabi, G., Yao, L., Siddique, R., Sajjad, W., Kumar, S., Duan, P. & Hou, H. (2018) 'Health risks associated with genetic alterations in internal clock system by external factors', *Int J Biol Sci*, vol. 14, no. 7, pp. 791-798.

Kil, I.S., Lee, S.K., Ryu, K.W., Woo, H.A., Hu, M.C., Bae, S.H. & Rhee, S.G. (2012) 'Feedback control of adrenal steroidogenesis via H2O2-dependent, reversible inactivation of peroxiredoxin III in mitochondria', *Mol Cell*, vol. 46, no. 5, pp. 584-594.

Kim, Y.H., Marhon, S.A., Zhang, Y., Steger, D.J., Won, K.J. & Lazar, M.A. (2018) 'Rev-erbα dynamically modulates chromatin looping to control circadian gene transcription', *Science*, vol. 359, no. 6381, pp. 1274-1277.

King, D.P., Zhao, Y., Sangoram, A.M., Wilsbacher, L.D., Tanaka, M., Antoch, M.P., Steeves, T.D., Vitaterna, M.H., Kornhauser, J.M., Lowrey, P.L., Turek, F.W. & Takahashi, J.S. (1997) 'Positional cloning of the mouse circadian clock gene', *Cell*, vol. 89, no. 4, pp. 641-653.

Kobuchi, S., Ito, Y., Nakano, Y. & Sakaeda, T. (2016) 'Population pharmacokinetic modelling and simulation of 5-fluorouracil incorporating a circadian rhythm in rats', *Xenobiotica*, vol. 46, no. 7, pp. 597-604.

Kohrt, W.M., Barry, D.W. & Schwartz, R.S. (2009) 'Muscle forces or gravity: what predominates mechanical loading on bone?', *Med Sci Sports Exerc*, vol. 41, no. 11, pp. 2050-2055.

Kojima, S., Sher-Chen, E.L. & Green, C.B. (2012) 'Circadian control of mRNA polyadenylation dynamics regulates rhythmic protein expression', *Genes Dev*, vol. 26, no. 24, pp. 2724-2736.

Kojima, S., Shingle, D.L. & Green, C.B. (2011) 'Post-transcriptional control of circadian rhythms', *J Cell Sci*, vol. 124, no. Pt 3, pp. 311-320.

Kon, N., Hirota, T., Kawamoto, T., Kato, Y., Tsubota, T. & Fukada, Y. (2008) 'Activation of TGF-beta/activin signalling resets the circadian clock through rapid induction of Dec1 transcripts', *Nat Cell Biol*, vol. 10, no. 12, pp. 1463-1469.

Kondratov, R.V., Kondratova, A.A., Gorbacheva, V.Y., Vykhovanets, O.V. & Antoch, M.P. (2006) 'Early aging and age-related pathologies in mice deficient in BMAL1, the core componentof the circadian clock', *Genes Dev*, vol. 20, no. 14, pp. 1868-1873.

Konopka, R.J. & Benzer, S. (1971) 'Clock mutants of Drosophila melanogaster', *Proc Natl Acad Sci U S A*, vol. 68, no. 9, pp. 2112-2116.

Korge, S., Maier, B., Brüning, F., Ehrhardt, L., Korte, T., Mann, M., Herrmann, A., Robles, M.S. & Kramer, A. (2018) 'The non-classical nuclear import carrier Transportin 1 modulates circadian rhythms through its effect on PER1 nuclear localization', *PLoS Genet*, vol. 14, no. 1, p. e1007189.

Kovary, K. & Bravo, R. (1991) 'The jun and fos protein families are both required for cell cycle progression in fibroblasts', *Mol Cell Biol*, vol. 11, no. 9, pp. 4466-4472.

Kowalska, E., Ripperger, J.A., Hoegger, D.C., Bruegger, P., Buch, T., Birchler, T., Mueller, A., Albrecht, U., Contaldo, C. & Brown, S.A. (2013) 'NONO couples the circadian clock to the cell cycle', *Proc Natl Acad Sci U S A*, vol. 110, no. 5, pp. 1592-1599.

Kraves, S. & Weitz, C.J. (2006) 'A role for cardiotrophin-like cytokine in the circadian control of mammalian locomotor activity', *Nat Neurosci*, vol. 9, no. 2, pp. 212-219.

Krohne, G., Wolin, S.L., McKeon, F.D., Franke, W.W. & Kirschner, M.W. (1987) 'Nuclear lamin LI of Xenopus laevis: cDNA cloning, amino acid sequence and binding specificity of a member of the lamin B subfamily', *EMBO J*, vol. 6, no. 12, pp. 3801-3808.

Kubben, N., Zhang, W., Wang, L., Voss, T.C., Yang, J., Qu, J., Liu, G.H. & Misteli, T. (2016) 'Repression of the Antioxidant NRF2 Pathway in Premature Aging', *Cell*, vol. 165, no. 6, pp. 1361-1374.

Kumar, A., Murphy, R., Robinson, P., Wei, L. & Boriek, A. (2004) 'Cyclic mechanical strain inhibits skeletal myogenesis through activation of focal adhesion kinase, Rac-1 GTPase, and NF-κB transcription factor', *FASEB J*, vol. 18., pp. 1524-1535.

Kumari, S.R. & Alvarez-Gonzalez, R. (2000) 'Expression of c-jun and c-fos in apoptotic cells after DNA damage', *Cancer Invest*, vol. 18, no. 8, pp. 715-721.

Kume, K., Zylka, M.J., Sriram, S., Shearman, L.P., Weaver, D.R., Jin, X., Maywood, E.S., Hastings, M.H. & Reppert, S.M. (1999) 'mCRY1 and mCRY2 are essential components of the negative limb of the circadian clock feedback loop', *Cell*, vol. 98, no. 2, pp. 193-205.

Kurz, A., Lampel, S., Nickolenko, J.E., Bradl, J., Benner, A., Zirbel, R.M., Cremer, T. & Lichter, P. (1996) 'Active and inactive genes localize preferentially in the periphery of chromosome territories', *J Cell Biol*, vol. 135, no. 5, pp. 1195-1205.

Köbberling, J. & Dunnigan, M.G. (1986) 'Familial partial lipodystrophy: two types of an X linked dominant syndrome, lethal in the hemizygous state', *J Med Genet*, vol. 23, no. 2, pp. 120-127.

Lakin-Thomas, P.L., Brody, S. & Coté, G.G. (1991) 'Amplitude model for the effects of mutations and temperature on period and phase resetting of the Neurospora circadian oscillator', *J Biol Rhythms*, vol. 6, no. 4, pp. 281-297.

Lamia, K.A., Storch, K.F. & Weitz, C.J. (2008) 'Physiological significance of a peripheral tissue circadian clock', *Proc Natl Acad Sci U S A*, vol. 105, no. 39, pp. 15172-15177.

Lammerding, J., Schulze, P.C., Takahashi, T., Kozlov, S., Sullivan, T., Kamm, R.D., Stewart, C.L. & Lee, R.T. (2004) 'lamin A/C deficiency causes defective nuclear mechanics and mechanotransduction', *J Clin Invest*, vol. 113, no. 3, pp. 370-378.

Lange-Carter, C.A., Pleiman, C.M., Gardner, A.M., Blumer, K.J. & Johnson, G.L. (1993) 'A divergence in

the MAP kinase regulatory network defined by MEK kinase and Raf', *Science*, vol. 260, no. 5106, pp. 315-319.
Langille, B.L. (1996) 'Arterial remodeling: relation to hemodynamics', *Can J Physiol Pharmacol*, vol. 74, no. 7, pp. 834-841.
Laranjeiro, R., Tamai, T.K., Letton, W., Hamilton, N. & Whitmore, D. (2018) 'Circadian Clock Synchronization of the Cell Cycle in Zebrafish Occurs through a Gating Mechanism Rather Than a Period-phase Locking Process', *J Biol Rhythms*, vol. 33, no. 2, pp. 137-150.
Lattanzi, G., Marmiroli, S., Facchini, A. & Maraldi, N.M. (2012) 'Nuclear damages and oxidative stress: new perspectives for laminopathies', *Eur J Histochem*, vol. 56, no. 4, p. e45.
Le Dour, C., Macquart, C., Sera, F., Homma, S., Bonne, G., Morrow, J.P., Worman, H.J. & Muchir, A. (2017) 'Decreased WNT/β-catenin signalling contributes to the pathogenesis of dilated cardiomyopathy caused by mutations in the lamin a/C gene', *Hum Mol Genet*, vol. 26, no. 2, pp. 333-343.
Lee, B., Lee, T.H. & Shim, J. (2017) 'Emerin suppresses Notch signaling by restricting the Notch intracellular domain to the nuclear membrane', *Biochim Biophys Acta Mol Cell Res*, vol. 1864, no. 2, pp. 303-313.
Lee, K.K., Haraguchi, T., Lee, R.S., Koujin, T., Hiraoka, Y. & Wilson, K.L. (2001) 'Distinct functional domains in emerin bind lamin A and DNA-bridging protein BAF', *J Cell Sci*, vol. 114, no. Pt 24, pp. 4567-4573.
Leloup, J.C. & Goldbeter, A. (1997) 'Temperature compensation of circadian rhythms: control of the period in a model for circadian oscillations of the per protein in Drosophila', *Chronobiol Int*, vol. 14, no. 5, pp. 511-520.
Leloup, J.C. & Goldbeter, A. (2003) 'Toward a detailed computational model for the mammalian circadian clock', *Proc Natl Acad Sci U S A*, vol. 100, no. 12, pp. 7051-7056.
Leloup, J.C. & Goldbeter, A. (2008) 'Modeling the circadian clock: from molecular mechanism to physiological disorders', *Bioessays*, vol. 30, no. 6, pp. 590-600.
Leloup, J.C. & Goldbeter, A. (2013) 'Critical phase shifts slow down circadian clock recovery: implications for jet lag', *J Theor Biol*, vol. 333, pp. 47-57.
Leloup, J.C., Gonze, D. & Goldbeter, A. (1999) 'Limit cycle models for circadian rhythms based on transcriptional regulation in Drosophila and Neurospora', *J Biol Rhythms*, vol. 14, no. 6, pp. 433-448.
Lenz-Böhme, B., Wismar, J., Fuchs, S., Reifegerste, R., Buchner, E., Betz, H. & Schmitt, B. (1997) 'Insertional mutation of the Drosophila nuclear lamin Dm0 gene results in defective nuclear envelopes, clustering of nuclear pore complexes, and accumulation of annulate lamellae', *J Cell Biol*, vol. 137, no. 5, pp. 1001-1016.
Leonardo-Mendonça, R.C., Martinez-Nicolas, A., de Teresa Galván, C., Ocaña-Wilhelmi, J., Rusanova, I., Guerra-Hernández, E., Escames, G. & Acuña-Castroviejo, D. (2015) 'The benefits of four weeks of melatonin treatment on circadian patterns in resistance-trained athletes', *Chronobiol Int*, vol. 32, no. 8, pp. 1125-1134.
Lewis, J.M. & Schwartz, M.A. (1995) 'Mapping in vivo associations of cytoplasmic proteins with integrin beta 1 cytoplasmic domain mutants', *Mol Biol Cell*, vol. 6, no. 2, pp. 151-160.
Li, Q., Ye, F., Shi, Y., Zhang, L., Wang, W., Tu, Z., Qiu, J., Wang, J., Li, S., Bu, H. & Li, Y. (2006) 'Nuclear translocation of SMAD3 may enhance the TGF-beta/SMADS pathway in high glucose circumstances', *Transplant Proc*, vol. 38, no. 7, pp. 2158-2160.
Lin, F., Blake, D.L., Callebaut, I., Skerjanc, I.S., Holmer, L., McBurney, M.W., Paulin-Levasseur, M. & Worman, H.J. (2000) 'MAN1, an inner nuclear membrane protein that shares the LEM domain with lamina-associated polypeptide 2 and emerin', *J Biol Chem*, vol. 275, no. 7, pp. 4840-4847.
Lin, F., Noyer, C.M., Ye, Q., Courvalin, J.C. & Worman, H.J. (1996) 'Autoantibodies from patients with primary biliary cirrhosis recognize a region within the nucleoplasmic domain of inner nuclear membrane protein LBR', *Hepatology*, vol. 23, no. 1, pp. 57-61.

Lin, F. & Worman, H.J. (1993) 'Structural organization of the human gene encoding nuclear lamin A and nuclear lamin C', *J Biol Chem*, vol. 268, no. 22, pp. 16321-16326.

Lin, S.T., Zhang, L., Lin, X., Zhang, L.C., Garcia, V.E., Tsai, C.W., Ptáček, L. & Fu, Y.H. (2014) 'Nuclear envelope protein MAN1 regulates clock through BMAL1', *Elife*, vol. 3, p. e02981.

Lipton, J.O., Yuan, E.D., Boyle, L.M., Ebrahimi-Fakhari, D., Kwiatkowski, E., Nathan, A., Güttler, T., Davis, F., Asara, J.M. & Sahin, M. (2015) 'The Circadian Protein BMAL1 Regulates Translation in Response to S6K1-Mediated Phosphorylation', *Cell*, vol. 161, no. 5, pp. 1138-1151.

Liu, A.C., Tran, H.G., Zhang, E.E., Priest, A.A., Welsh, D.K. & Kay, S.A. (2008) 'Redundant function of REV-ERBalpha and beta and non-essential role for Bmal1 cycling in transcriptional regulation of intracellular circadian rhythms', *PLoS Genet*, vol. 4, no. 2, p. e1000023.

Liu, D., Black, B.L. & Derynck, R. (2001) 'TGF-beta inhibits muscle differentiation through functional repression of myogenic transcription factors by Smad3', *Genes Dev*, vol. 15, no. 22, pp. 2950-2966.

Liu, G.H., Guan, T., Datta, K., Coppinger, J., Yates, J. & Gerace, L. (2009) 'Regulation of myoblast differentiation by the nuclear envelope protein NET39', *Mol Cell Biol*, vol. 29, no. 21, pp. 5800-5812.

Lloyd, D.J., Trembath, R.C. & Shackleton, S. (2002) 'A novel interaction between lamin A and SREBP1: implications for partial lipodystrophy and other laminopathies', *Hum Mol Genet*, vol. 11, no. 7, pp. 769-777.

Loerakker, S., Stassen, O.M.J.A., Ter Huurne, F.M., Boareto, M., Bouten, C.V.C. & Sahlgren, C.M. (2018) 'Mechanosensitivity of Jagged-Notch signaling can induce a switch-type behavior in vascular homeostasis', *Proc Natl Acad Sci U S A*, vol. 115, no. 16, pp. E3682-E3691.

Lowrey, P.L. & Takahashi, J.S. (2000) 'Genetics of the mammalian circadian system: Photic entrainment, circadian pacemaker mechanisms, and posttranslational regulation', *Annu Rev Genet*, vol. 34, pp. 533-562.

Lutz, R.J., Trujillo, M.A., Denham, K.S., Wenger, L. & Sinensky, M. (1992) 'Nucleoplasmic localization of prelamin A: implications for prenylation-dependent lamin A assembly into the nuclear lamina', *Proc Natl Acad Sci U S A*, vol. 89, no. 7, pp. 3000-3004.

Lévi, F., Canon, C., Dipalma, M., Florentin, I. & Misset, J.L. (1991) 'When should the immune clock be reset? From circadian pharmacodynamics to temporally optimized drug delivery', *Ann N Y Acad Sci*, vol. 618, pp. 312-329.

Ma, H., Siegel, A.J. & Berezney, R. (1999) 'Association of chromosome territories with the nuclear matrix. Disruption of human chromosome territories correlates with the release of a subset of nuclear matrix proteins', *J Cell Biol*, vol. 146, no. 3, pp. 531-542.

Machiels, B.M., Zorenc, A.H., Endert, J.M., Kuijpers, H.J., van Eys, G.J., Ramaekers, F.C. & Broers, J.L. (1996) 'An alternative splicing product of the lamin A/C gene lacks exon 10', *J Biol Chem*, vol. 271, no. 16, pp. 9249-9253.

Maggi, L., Carboni, N. & Bernasconi, P. (2016) 'Skeletal Muscle Laminopathies: A Review of Clinical and Molecular Features', *Cells*, vol. 5, no. 3.

Mahy, N.L., Perry, P.E. & Bickmore, W.A. (2002) 'Gene density and transcription influence the localization of chromatin outside of chromosome territories detectable by FISH', *J Cell Biol*, vol. 159, no. 5, pp. 753-763.

Malone, C.J., Fixsen, W.D., Horvitz, H.R. & Han, M. (1999) 'UNC-84 localizes to the nuclear envelope and is required for nuclear migration and anchoring during C. elegans development', *Development*, vol. 126, no. 14, pp. 3171-3181.

Maniotis, A.J., Chen, C.S. & Ingber, D.E. (1997) 'Demonstration of mechanical connections between integrins, cytoskeletal filaments, and nucleoplasm that stabilize nuclear structure', *Proc Natl Acad Sci U S A*, vol. 94, no. 3, pp. 849-854.

Mansharamani, M. & Wilson, K.L. (2005) 'Direct binding of nuclear membrane protein MAN1 to emerin in vitro and two modes of binding to barrier-to-autointegration factor', *J Biol Chem*, vol. 280, no. 14, pp. 13863-13870.

Manuelidis, L. (1984) 'Different central nervous system cell types display distinct and nonrandom arrangements of satellite DNA sequences', *Proc Natl Acad Sci U S A*, vol. 81, no. 10, pp. 3123-3127.

Marchant, E.G. & Mistlberger, R.E. (1996) 'Entrainment and phase shifting of circadian rhythms in mice by forced treadmill running', *Physiol Behav*, vol. 60, no. 2, pp. 657-663.

Margalit, A., Segura-Totten, M., Gruenbaum, Y. & Wilson, K.L. (2005) 'Barrier-to-autointegration factor is required to segregate and enclose chromosomes within the nuclear envelope and assemble the nuclear lamina', *Proc Natl Acad Sci U S A*, vol. 102, no. 9, pp. 3290-3295.

Markiewicz, E., Dechat, T., Foisner, R., Quinlan, R.A. & Hutchison, C.J. (2002a) 'lamin A/C binding protein LAP2alpha is required for nuclear anchorage of retinoblastoma protein', *Mol Biol Cell*, vol. 13, no. 12, pp. 4401-4413.

Markiewicz, E., Ledran, M. & Hutchison, C.J. (2005) 'Remodelling of the nuclear lamina and nucleoskeleton is required for skeletal muscle differentiation in vitro', *J Cell Sci*, vol. 118, no. Pt 2, pp. 409-420.

Markiewicz, E., Tilgner, K., Barker, N., van de Wetering, M., Clevers, H., Dorobek, M., Hausmanowa-Petrusewicz, I., Ramaekers, F.C., Broers, J.L., Blankesteijn, W.M., Salpingidou, G., Wilson, R.G., Ellis, J.A. & Hutchison, C.J. (2006) 'The inner nuclear membrane protein emerin regulates beta-catenin activity by restricting its accumulation in the nucleus', *EMBO J*, vol. 25, no. 14, pp. 3275-3285.

Markiewicz, E., Venables, R., Mauricio-Alvarez-Reyes, Quinlan, R., Dorobek, M., Hausmanowa-Petrucewicz, I. & Hutchison, C. (2002b) 'Increased solubility of lamins and redistribution of lamin C in X-linked Emery-Dreifuss muscular dystrophy fibroblasts', *J Struct Biol*, vol. 140, no. 1-3, pp. 241-253.

Martin, L., Crimaudo, C. & Gerace, L. (1995) 'cDNA cloning and characterization of lamina-associated polypeptide 1C (LAP1C), an integral protein of the inner nuclear membrane', *J Biol Chem*, vol. 270, no. 15, pp. 8822-8828.

Matsu-Ura, T., Dovzhenok, A., Aihara, E., Rood, J., Le, H., Ren, Y., Rosselot, A.E., Zhang, T., Lee, C., Obrietan, K., Montrose, M.H., Lim, S., Moore, S.R. & Hong, C.I. (2016) 'Intercellular Coupling of the Cell Cycle and Circadian Clock in Adult Stem Cell Culture', *Mol Cell*, vol. 64, no. 5, pp. 900-912.

Matsuo, T., Yamaguchi, S., Mitsui, S., Emi, A., Shimoda, F. & Okamura, H. (2003) 'Control mechanism of the circadian clock for timing of cell division in vivo', *Science*, vol. 302, no. 5643, pp. 255-259.

Mattout, A., Pike, B.L., Towbin, B.D., Bank, E.M., Gonzalez-Sandoval, A., Stadler, M.B., Meister, P., Gruenbaum, Y. & Gasser, S.M. (2011) 'An EDMD mutation in C. elegans lamin blocks muscle-specific gene relocation and compromises muscle integrity', *Curr Biol*, vol. 21, no. 19, pp. 1603-1614.

Mauvoisin, D., Wang, J., Jouffe, C., Martin, E., Atger, F., Waridel, P., Quadroni, M., Gachon, F. & Naef, F. (2014) 'Circadian clock-dependent and -independent rhythmic proteomes implement distinct diurnal functions in mouse liver', *Proc Natl Acad Sci U S A*, vol. 111, no. 1, pp. 167-172.

Mavroudis, P.D., DuBois, D.C., Almon, R.R. & Jusko, W.J. (2018) 'Modeling circadian variability of core-clock and clock-controlled genes in four tissues of the rat', *PLoS One*, vol. 13, no. 6, p. e0197534.

Maywood, E.S., Mrosovsky, N., Field, M.D. & Hastings, M.H. (1999) 'Rapid down-regulation of mammalian period genes during behavioral resetting of the circadian clock', *Proc Natl Acad Sci U S A*, vol. 96, no. 26, pp. 15211-15216.

Mazumder, A. & Shivashankar, G.V. (2010) 'Emergence of a prestressed eukaryotic nucleus during cellular differentiation and development', *J R Soc Interface*, vol. 7 Suppl 3, pp. S321-330.

McCarthy, J.J., Andrews, J.L., McDearmon, E.L., Campbell, K.S., Barber, B.K., Miller, B.H., Walker, J.R., Hogenesch, J.B., Takahashi, J.S. & Esser, K.A. (2007) 'Identification of the circadian

transcriptome in adult mouse skeletal muscle', *Physiol Genomics*, vol. 31, no. 1, pp. 86-95.
McCord, R.P., Nazario-Toole, A., Zhang, H., Chines, P.S., Zhan, Y., Erdos, M.R., Collins, F.S., Dekker, J. & Cao, K. (2013) 'Correlated alterations in genome organization, histone methylation, and DNA-lamin A/C interactions in Hutchinson-Gilford progeria syndrome', *Genome Res*, vol. 23, no. 2, pp. 260-269.
McDearmon, E.L., Patel, K.N., Ko, C.H., Walisser, J.A., Schook, A.C., Chong, J.L., Wilsbacher, L.D., Song, E.J., Hong, H.K., Bradfield, C.A. & Takahashi, J.S. (2006) 'Dissecting the functions of the mammalian clock protein BMAL1 by tissue-specific rescue in mice', *Science*, vol. 314, no. 5803, pp. 1304-1308.
McGlincy, N.J., Valomon, A., Chesham, J.E., Maywood, E.S., Hastings, M.H. & Ule, J. (2012) 'Regulation of alternative splicing by the circadian clock and food related cues', *Genome Biol*, vol. 13, no. 6, p. R54.
McKeon, F.D., Kirschner, M.W. & Caput, D. (1986) 'Homologies in both primary and secondary structure between nuclear envelope and intermediate filament proteins', *Nature*, vol. 319, no. 6053, pp. 463-468.
Meaburn, K., Cabuy, E., Bonne, G., Levy, N., Morris, G., Novelli, G., Kill, I. & Bridger, J. (2007) 'Primary laminopathy fibroblasts display altered genome organization and apoptosis', *Ageing Cell*, vol. 6, no. 2, pp. 139-153.
Mehta I., Eskiw C., Arican H., Kill I. & Bridger J. (2011) 'Farnesyltransferase inhibitor treatment restores chromosome territory positions and active chromosome dynamics in Hutchinson-Gilford progeria syndrome cells', *Genome Biol*, vol. 12, no. 8, p. R74
Meier, J., Campbell, K.H., Ford, C.C., Stick, R. & Hutchison, C.J. (1991) 'The role of lamin LIII in nuclear assembly and DNA replication, in cell-free extracts of Xenopus eggs', *J Cell Sci*, vol. 98 (Pt 3), pp. 271-279.
Melancon, M.O., Lorrain, D. & Dionne, I.J. (2014) 'Exercise and sleep in aging: emphasis on serotonin', *Pathol Biol (Paris)*, vol. 62, no. 5, pp. 276-283.
Meng, Q.J., McMaster, A., Beesley, S., Lu, W.Q., Gibbs, J., Parks, D., Collins, J., Farrow, S., Donn, R., Ray, D. & Loudon, A. (2008) 'Ligand modulation of REV-ERBalpha function resets the peripheral circadian clock in a phasic manner', *J Cell Sci*, vol. 121, no. Pt 21, pp. 3629-3635.
Merideth, M.A., Gordon, L.B., Clauss, S., Sachdev, V., Smith, A.C., Perry, M.B., Brewer, C.C., Zalewski, C., Kim, H.J., Solomon, B., Brooks, B.P., Gerber, L.H., Turner, M.L., Domingo, D.L., Hart, T.C., Graf, J., Reynolds, J.C., Gropman, A., Yanovski, J.A., Gerhard-Herman, M., Collins, F.S., Nabel, E.G., Cannon, R.O., Gahl, W.A. & Introne, W.J. (2008) 'Phenotype and course of Hutchinson-Gilford progeria syndrome', *N Engl J Med*, vol. 358, no. 6, pp. 592-604.
Mermet, J., Yeung, J., Hurni, C., Mauvoisin, D., Gustafson, K., Jouffe, C., Nicolas, D., Emmenegger, Y., Gobet, C., Franken, P., Gachon, F. & Naef, F. (2018) 'Clock-dependent chromatin topology modulates circadian transcription and behavior', *Genes Dev*, vol. 32, no. 5-6, pp. 347-358.
Mewborn, S.K., Puckelwartz, M.J., Abuisneineh, F., Fahrenbach, J.P., Zhang, Y., MacLeod, H., Dellefave, L., Pytel, P., Selig, S., Labno, C.M., Reddy, K., Singh, H. & McNally, E. (2010) 'Altered chromosomal positioning, compaction, and gene expression with a lamin A/C gene mutation', *PLoS One*, vol. 5, no. 12, p. e14342.
Meyer-Bernstein, E.L. & Morin, L.P. (1996) 'Differential serotonergic innervation of the suprachiasmatic nucleus and the intergeniculate leaflet and its role in circadian rhythm modulation', *J Neurosci*, vol. 16, no. 6, pp. 2097-2111.
Miller, B.H., McDearmon, E.L., Panda, S., Hayes, K.R., Zhang, J., Andrews, J.L., Antoch, M.P., Walker, J.R., Esser, K.A., Hogenesch, J.B. & Takahashi, J.S. (2007) 'Circadian and CLOCK-controlled regulation of the mouse transcriptome and cell proliferation', *Proc Natl Acad Sci U S A*, vol. 104, no. 9, pp. 3342-3347.
Miralles, F., Posern, G., Zaromytidou, A.I. & Treisman, R. (2003) 'Actin dynamics control SRF activity by regulation of its coactivator MAL', *Cell*, vol. 113, no. 3, pp. 329-342.
Miyamoto, S., Teramoto, H., Coso, O.A., Gutkind, J.S., Burbelo, P.D., Akiyama, S.K. & Yamada, K.M.

(1995) 'Integrin function: molecular hierarchies of cytoskeletal and signaling molecules', *J Cell Biol*, vol. 131, no. 3, pp. 791-805.

Moen, P.T., Johnson, C.V., Byron, M., Shopland, L.S., de la Serna, I.L., Imbalzano, A.N. & Lawrence, J.B. (2004) 'Repositioning of muscle-specific genes relative to the periphery of SC-35 domains during skeletal myogenesis', *Mol Biol Cell*, vol. 15, no. 1, pp. 197-206.

Moiseeva, O., Lessard, F., Acevedo-Aquino, M., Vernier, M., Tsantrizos, Y.S. & Ferbeyre, G. (2015) 'Mutant lamin A links prophase to a p53 independent senescence program', *Cell Cycle*, vol. 14, no. 15, pp. 2408-2421.

Mokalled, M.H., Johnson, A.N., Creemers, E.E. & Olson, E.N. (2012) 'MASTR directs MyoD-dependent satellite cell differentiation during skeletal muscle regeneration', *Genes Dev*, vol. 26, no. 2, pp. 190-202.

Mondello, M.R., Bramanti, P., Cutroneo, G., Santoro, G., Di Mauro, D. & Anastasi, G. (1996) 'Immunolocalization of the costameres in human skeletal muscle fibers: confocal scanning laser microscope investigations', *Anat Rec*, vol. 245, no. 3, pp. 481-487.

Moore, R.Y. & Eichler, V.B. (1972) 'Loss of a circadian adrenal corticosterone rhythm following suprachiasmatic lesions in the rat', *Brain Res*, vol. 42, no. 1, pp. 201-206.

Moore, R.Y. & Speh, J.C. (1994) 'A putative retinohypothalamic projection containing substance P in the human', *Brain Res*, vol. 659, no. 1-2, pp. 249-253.

Moore-Ede, M.C., Sulzman, F.M. & Fuller, C.A. (1982) *The clocks that time us : physiology of the circadian timing system*, Harvard University Press, Cambridge, Mass.

Morse, D., Pischke, S.E., Zhou, Z., Davis, R.J., Flavell, R.A., Loop, T., Otterbein, S.L., Otterbein, L.E. & Choi, A.M. (2003) 'Suppression of inflammatory cytokine production by carbon monoxide involves the JNK pathway and AP-1', *J Biol Chem*, vol. 278, no. 39, pp. 36993-36998.

Motta, S. & Pappalardo, F. (2013) 'Mathematical modeling of biological systems', *Brief Bioinform*, vol. 14, no. 4, pp. 411-422.

Muchir, A., Bonne, G., van der Kooi, A.J., van Meegen, M., Baas, F., Bolhuis, P.A., de Visser, M. & Schwartz, K. (2000) 'Identification of mutations in the gene encoding lamins A/C in autosomal dominant limb girdle muscular dystrophy with atrioventricular conduction disturbances (LGMD1B)', *Hum Mol Genet*, vol. 9, no. 9, pp. 1453-1459.

Muchir, A., Pavlidis, P., Decostre, V., Herron, A.J., Arimura, T., Bonne, G. & Worman, H.J. (2007) 'Activation of MAPK pathways links LMNA mutations to cardiomyopathy in Emery-Dreifuss muscular dystrophy', *J Clin Invest*, vol. 117, no. 5, pp. 1282-1293.

Muchir, A., Wu, W. & Worman, H. (2009) 'Reduced expression of A-type lamins and emerin activates extracellular signal-regulated kinase in cultured cells', *Biochim Biophys Acta, 2009 Jan; 1792(1): 75–81.*

Naetar, N., Ferraioli, S. & Foisner, R. (2017) 'Lamins in the nuclear interior - life outside the lamina', *J Cell Sci*, vol. 130, no. 13, pp. 2087-2096.

Nagano, A., Koga, R., Ogawa, M., Kurano, Y., Kawada, J., Okada, R., Hayashi, Y.K., Tsukahara, T. & Arahata, K. (1996) 'Emerin deficiency at the nuclear membrane in patients with Emery-Dreifuss muscular dystrophy', *Nat Genet*, vol. 12, no. 3, pp. 254-259.

Nagoshi, E., Saini, C., Bauer, C., Laroche, T., Naef, F. & Schibler, U. (2004) 'Circadian gene expression in individual fibroblasts: cell-autonomous and self-sustained oscillators pass time to daughter cells', *Cell*, vol. 119, no. 5, pp. 693-705.

Nakai, N., Kawano, F., Oke, Y., Nomura, S., Ohira, T., Fujita, R. & Ohira, Y. (2010) 'Mechanical stretch activates signaling events for protein translation initiation and elongation in C2C12 myoblasts', *Mol Cells*, vol. 30, no. 6, pp. 513-518.

Nakashima, A., Kawamoto, T., Honda, K.K., Ueshima, T., Noshiro, M., Iwata, T., Fujimoto, K., Kubo, H., Honma, S., Yorioka, N., Kohno, N. & Kato, Y. (2008) 'DEC1 modulates the circadian phase of clock gene expression', *Mol Cell Biol*, vol. 28, no. 12, pp. 4080-4092.

Newport, J.W. & Forbes, D.J. (1987) 'The nucleus: structure, function, and dynamics', *Annu Rev Biochem*, vol. 56, pp. 535-565.

Niebroj-Dobosz, I., Sokołowska, B., Madej-Pilarczyk, A., Marchel, M. & Hausmanowa-Petrusewicz, I. (2017) 'Dysfunctional lamins as mediators of oxidative stress in Emery-Dreifuss muscular dystrophy', *Folia Neuropathol*, vol. 55, no. 3, pp. 193-198.

Nigg, E.A. (1989) 'The nuclear envelope', *Curr Opin Cell Biol*, vol. 1, no. 3, pp. 435-440.

Nitta, R.T., Jameson, S.A., Kudlow, B.A., Conlan, L.A. & Kennedy, B.K. (2006) 'Stabilization of the retinoblastoma protein by A-type nuclear lamins is required for INK4A-mediated cell cycle arrest', *Mol Cell Biol*, vol. 26, no. 14, pp. 5360-5372.

O'Keefe, R.T., Henderson, S.C. & Spector, D.L. (1992) 'Dynamic organization of DNA replication in mammalian cell nuclei: spatially and temporally defined replication of chromosome-specific alpha-satellite DNA sequences', *J Cell Biol*, vol. 116, no. 5, pp. 1095-1110.

Obrietan, K., Impey, S. & Storm, D.R. (1998) 'Light and circadian rhythmicity regulate MAP kinase activation in the suprachiasmatic nuclei', *Nat Neurosci*, vol. 1, no. 8, pp. 693-700.

Onaolapo, A.Y. & Onaolapo, O.J. (2018) 'Circadian dysrhythmia-linked diabetes mellitus: Examining melatonin's roles in prophylaxis and management', *World J Diabetes*, vol. 9, no. 7, pp. 99-114.

Osmanagic-Myers, S., Dechat, T. & Foisner, R. (2015) 'Lamins at the crossroads of mechanosignaling', *Genes Dev*, vol. 29, no. 3, pp. 225-237.

Ostlund, C., Ellenberg, J., Hallberg, E., Lippincott-Schwartz, J. & Worman, H.J. (1999) 'Intracellular trafficking of emerin, the Emery-Dreifuss muscular dystrophy protein', *J Cell Sci*, vol. 112 (Pt 11), pp. 1709-1719.

Ottaviano, Y. & Gerace, L. (1985) 'Phosphorylation of the nuclear lamins during interphase and mitosis', *J Biol Chem*, vol. 260, no. 1, pp. 624-632.

Otto, J.C., Kim, E., Young, S.G. & Casey, P.J. (1999) 'Cloning and characterization of a mammalian prenyl protein-specific protease', *J Biol Chem*, vol. 274, no. 13, pp. 8379-8382.

Ozaki, T., Saijo, M., Murakami, K., Enomoto, H., Taya, Y. & Sakiyama, S. (1994) 'Complex formation between lamin A and the retinoblastoma gene product: identification of the domain on lamin A required for its interaction', *Oncogene*, vol. 9, no. 9, pp. 2649-2653.

Paddy, M.R., Belmont, A.S., Saumweber, H., Agard, D.A. & Sedat, J.W. (1990) 'Interphase nuclear envelope lamins form a discontinuous network that interacts with only a fraction of the chromatin in the nuclear periphery', *Cell*, vol. 62, no. 1, pp. 89-106.

Padmakumar, V.C., Libotte, T., Lu, W., Zaim, H., Abraham, S., Noegel, A.A., Gotzmann, J., Foisner, R. & Karakesisoglou, I. (2005) 'The inner nuclear membrane protein Sun1 mediates the anchorage of Nesprin-2 to the nuclear envelope', *J Cell Sci*, vol. 118, no. Pt 15, pp. 3419-3430.

Pahl, H.L. (1999) 'Activators and target genes of Rel/NF-kappaB transcription factors', *Oncogene*, vol. 18, no. 49, pp. 6853-6866.

Papachroni, K.K., Karatzas, D.N., Papavassiliou, K.A., Basdra, E.K. & Papavassiliou, A.G. (2009) 'Mechanotransduction in osteoblast regulation and bone disease', *Trends Mol Med*, vol. 15, no. 5, pp. 208-216.

Papagiannakopoulos, T., Bauer, M.R., Davidson, S.M., Heimann, M., Subbaraj, L., Bhutkar, A., Bartlebaugh, J., Vander Heiden, M.G. & Jacks, T. (2016) 'Circadian Rhythm Disruption Promotes Lung Tumorigenesis', *Cell Metab*, vol. 24, no. 2, pp. 324-331.

Pardo, J.V., Siliciano, J.D. & Craig, S.W. (1983) 'A vinculin-containing cortical lattice in skeletal muscle: transverse lattice elements ("costameres") mark sites of attachment between myofibrils and sarcolemma', *Proc Natl Acad Sci U S A*, vol. 80, no. 4, pp. 1008-1012.

Partch, C.L., Shields, K.F., Thompson, C.L., Selby, C.P. & Sancar, A. (2006) 'Posttranslational regulation of the mammalian circadian clock by cryptochrome and protein phosphatase 5', *Proc Natl Acad Sci U S A*, vol. 103, no. 27, pp. 10467-10472.

Paulsen, J., Sekelja, M., Oldenburg, A.R., Barateau, A., Briand, N., Delbarre, E., Shah, A., Sørensen, A.L., Vigouroux, C., Buendia, B. & Collas, P. (2017) 'Chrom3D: three-dimensional genome modeling from Hi-C and nuclear lamin-genome contacts', *Genome Biol*, vol. 18, no. 1, p. 21.

Pekovic, V., Harborth, J., Broers, J.L., Ramaekers, F.C., van Engelen, B., Lammens, M., von Zglinicki, T., Foisner, R., Hutchison, C. & Markiewicz, E. (2007) 'Nucleoplasmic LAP2alpha-lamin A complexes are required to maintain a proliferative state in human fibroblasts', *J Cell Biol*, vol. 176, no. 2, pp. 163-172.

Pekovic-Vaughan, V., Gibbs, J., Yoshitane, H., Yang, N., Pathiranage, D., Guo, B., Sagami, A., Taguchi, K., Bechtold, D., Loudon, A., Yamamoto, M., Chan, J., van der Horst, G.T., Fukada, Y. & Meng, Q.J. (2014) 'The circadian clock regulates rhythmic activation of the NRF2/glutathione-mediated antioxidant defense pathway to modulate pulmonary fibrosis', *Genes Dev*, vol. 28, no. 6, pp. 548-560.

Pendergast, J.S., Yeom, M., Reyes, B.A., Ohmiya, Y. & Yamazaki, S. (2010) 'Disconnected circadian and cell cycles in a tumor-driven cell line', *Commun Integr Biol*, vol. 3, no. 6, pp. 536-539.

Pendás, A.M., Zhou, Z., Cadiñanos, J., Freije, J.M., Wang, J., Hultenby, K., Astudillo, A., Wernerson, A., Rodríguez, F., Tryggvason, K. & López-Otín, C. (2002) 'Defective prelamin A processing and muscular and adipocyte alterations in Zmpste24 metalloproteinase-deficient mice', *Nat Genet*, vol. 31, no. 1, pp. 94-99.

Penton, C.M., Badarinarayana, V., Prisco, J., Powers, E., Pincus, M., Allen, R.E. & August, P.R. (2016) 'Laminin 521 maintains differentiation potential of mouse and human satellite cell-derived myoblasts during long-term culture expansion', *Skelet Muscle*, vol. 6, no. 1, p. 44.

Peter, M., Nakagawa, J., Dorée, M., Labbé, J.C. & Nigg, E.A. (1990) 'In vitro disassembly of the nuclear lamina and M phase-specific phosphorylation of lamins by cdc2 kinase', *Cell*, vol. 61, no. 4, pp. 591-602.

Pfaffl, M.W. (2001) 'A new mathematical model for relative quantification in real-time RT-PCR', *Nucleic Acids Res*, vol. 29, no. 9, p. e45.

Pickard, G.E. (1985) 'Bifurcating axons of retinal ganglion cells terminate in the hypothalamic suprachiasmatic nucleus and the intergeniculate leaflet of the thalamus', *Neurosci Lett*, vol. 55, no. 2, pp. 211-217.

Pickard, G.E., Ralph, M.R. & Menaker, M. (1987) 'The intergeniculate leaflet partially mediates effects of light on circadian rhythms', *J Biol Rhythms*, vol. 2, no. 1, pp. 35-56.

Pittendrigh, C.S. (1960) 'Circadian rhythms and the circadian organization of living systems', *Cold Spring Harb Symp Quant Biol*, vol. 25, pp. 159-184.

Plotnikov, A., Zehorai, E., Procaccia, S. & Seger, R. (2011) 'The MAPK cascades: signaling components, nuclear roles and mechanisms of nuclear translocation', *Biochim Biophys Acta*, vol. 1813, no. 9, pp. 1619-1633.

Podkolodnaya, O.A., Tverdokhleb, N.N. & Podkolodnyy, N.L. (2017) 'Computational modeling of the cell-autonomous mammalian circadian oscillator', *BMC Syst Biol*, vol. 11, no. Suppl 1, p. 379.

Poulet, B., de Souza, R., Kent, A.V., Saxon, L., Barker, O., Wilson, A., Chang, Y.M., Cake, M. & Pitsillides, A.A. (2015) 'Intermittent applied mechanical loading induces subchondral bone thickening that may be intensified locally by contiguous articular cartilage lesions', *Osteoarthritis Cartilage*, vol. 23, no. 6, pp. 940-948.

Poulet, B., Hamilton, R.W., Shefelbine, S. & Pitsillides, A.A. (2011) 'Characterizing a novel and adjustable noninvasive murine joint loading model', *Arthritis Rheum*, vol. 63, no. 1, pp. 137-147.

Preitner, N., Damiola, F., Lopez-Molina, L., Zakany, J., Duboule, D., Albrecht, U. & Schibler, U. (2002) 'The orphan nuclear receptor REV-ERBalpha controls circadian transcription within the positive limb of the mammalian circadian oscillator', *Cell*, vol. 110, no. 2, pp. 251-260.

Prolo, L.M., Takahashi, J.S. & Herzog, E.D. (2005) 'Circadian rhythm generation and entrainment in astrocytes', *J Neurosci*, vol. 25, no. 2, pp. 404-408.

Puckelwartz, M.J., Kessler, E., Zhang, Y., Hodzic, D., Randles, K.N., Morris, G., Earley, J.U., Hadhazy, M., Holaska, J.M., Mewborn, S.K., Pytel, P. & McNally, E.M. (2009) 'Disruption of nesprin-1 produces an Emery Dreifuss muscular dystrophy-like phenotype in mice', *Hum Mol Genet*, vol. 18, no. 4, pp. 607-620.

Puri, P.L., Iezzi, S., Stiegler, P., Chen, T.T., Schiltz, R.L., Muscat, G.E., Giordano, A., Kedes, L., Wang, J.Y. & Sartorelli, V. (2001) 'Class I histone deacetylases sequentially interact with MyoD and pRb during skeletal myogenesis', *Mol Cell*, vol. 8, no. 4, pp. 885-897.

Putker, M. & O'Neill, J.S. (2016) 'Reciprocal Control of the Circadian Clock and Cellular Redox State - a Critical Appraisal', *Mol Cells*, vol. 39, no. 1, pp. 6-19.

Qi, L. & Boateng, S.Y. (2006) 'The circadian protein Clock localizes to the sarcomeric Z-disk and is a sensor of myofilament cross-bridge activity in cardiac myocytes', *Biochem Biophys Res Commun*, vol. 351, no. 4, pp. 1054-1059.

Rabl, C. (1885) *Uber Zelltheilung.*, vol. 10, *Morphol. Jahrb*, pp. 214–330.

Radin, E.L., Ehrlich, M.G., Chernack, R., Abernethy, P., Paul, I.L. & Rose, R.M. (1978) 'Effect of repetitive impulsive loading on the knee joints of rabbits', *Clin Orthop Relat Res*, no. 131, pp. 288-293.

Raffaele Di Barletta, M., Ricci, E., Galluzzi, G., Tonali, P., Mora, M., Morandi, L., Romorini, A., Voit, T., Orstavik, K.H., Merlini, L., Trevisan, C., Biancalana, V., Housmanowa-Petrusewicz, I., Bione, S., Ricotti, R., Schwartz, K., Bonne, G. & Toniolo, D. (2000) 'Different mutations in the LMNA gene cause autosomal dominant and autosomal recessive Emery-Dreifuss muscular dystrophy', *Am J Hum Genet*, vol. 66, no. 4, pp. 1407-1412.

Rao, R., DuBois, D., Almon, R., Jusko, W.J. & Androulakis, I.P. (2016) 'Mathematical modeling of the circadian dynamics of the neuroendocrine-immune network in experimentally induced arthritis', *Am J Physiol Endocrinol Metab*, vol. 311, no. 2, pp. E310-324.

Rao, R.T., Scherholz, M.L. & Androulakis, I.P. (2018) 'Modeling the influence of chronopharmacological administration of synthetic glucocorticoids on the hypothalamic-pituitary-adrenal axis', *Chronobiol Int*, vol. 35, no. 12, pp. 1619-1636.

Reddy, A.B., Karp, N.A., Maywood, E.S., Sage, E.A., Deery, M., O'Neill, J.S., Wong, G.K., Chesham, J., Odell, M., Lilley, K.S., Kyriacou, C.P. & Hastings, M.H. (2006) 'Circadian orchestration of the hepatic proteome', *Curr Biol*, vol. 16, no. 11, pp. 1107-1115.

Reddy, K.L., Zullo, J.M., Bertolino, E. & Singh, H. (2008) 'Transcriptional repression mediated by repositioning of genes to the nuclear lamina', *Nature*, vol. 452, no. 7184, pp. 243-247.

Refinetti, R., Lissen, G.C. & Halberg, F. (2007) 'Procedures for numerical analysis of circadian rhythms', *Biol Rhythm Res*, vol. 38, no. 4, pp. 275-325.

Refinetti, R. (2016) 'Circadian Physiology' 3rd Edition, Boca Raton, Fla.: CRC Press.

Reibman, J., Meixler, S., Lee, T.C., Gold, L.I., Cronstein, B.N., Haines, K.A., Kolasinski, S.L. & Weissmann, G. (1991) 'Transforming growth factor beta 1, a potent chemoattractant for human neutrophils, bypasses classic signal-transduction pathways', *Proc Natl Acad Sci U S A*, vol. 88, no. 15, pp. 6805-6809.

Reischl, S., Vanselow, K., Westermark, P.O., Thierfelder, N., Maier, B., Herzel, H. & Kramer, A. (2007) 'Beta-TrCP1-mediated degradation of PERIOD2 is essential for circadian dynamics', *J Biol Rhythms*, vol. 22, no. 5, pp. 375-386.

Rey, G., Cesbron, F., Rougemont, J., Reinke, H., Brunner, M. & Naef, F. (2011) 'Genome-wide and phase-specific DNA-binding rhythms of BMAL1 control circadian output functions in mouse liver', *PLoS Biol*, vol. 9, no. 2, p. e1000595.

Rhee, S.G. (2016) 'Overview on Peroxiredoxin', *Mol Cells*, vol. 39, no. 1, pp. 1-5.

Richards, S.A., Muter, J., Ritchie, P., Lattanzi, G. & Hutchison, C.J. (2011) 'The accumulation of un-repairable DNA damage in laminopathy progeria fibroblasts is caused by ROS generation and is prevented by treatment with N-acetyl cysteine', *Hum Mol Genet*, vol. 20, no. 20, pp. 3997-4004.

Richardson, C.E., Gradisar, M., Short, M.A. & Lang, C. (2017) 'Can exercise regulate the circadian system of adolescents? Novel implications for the treatment of delayed sleep-wake phase disorder', *Sleep Med Rev*, vol. 34, pp. 122-129.

Robson, M.I., de Las Heras, J.I., Czapiewski, R., Lê Thành, P., Booth, D.G., Kelly, D.A., Webb, S., Kerr, A.R.W. & Schirmer, E.C. (2016) 'Tissue-Specific Gene Repositioning by Muscle Nuclear

Membrane Proteins Enhances Repression of Critical Developmental Genes during Myogenesis', *Mol Cell*, vol. 62, no. 6, pp. 834-847.
Roos, E.M., Herzog, W., Block, J.A. & Bennell, K.L. (2011) 'Muscle weakness, afferent sensory dysfunction and exercise in knee osteoarthritis', *Nat Rev Rheumatol*, vol. 7, no. 1, pp. 57-63.
Ruoff, P., Rensing, L., Kommedal, R. & Mohsenzadeh, S. (1997) 'Modeling temperature compensation in chemical and biological oscillators', *Chronobiol Int*, vol. 14, no. 5, pp. 499-510.
Rusak, B. & Boulos, Z. (1981) 'Pathways for photic entrainment of mammalian circadian rhythms', *Photochem Photobiol*, vol. 34, no. 2, pp. 267-273.
Rusak, B., Meijer, J.H. & Harrington, M.E. (1989) 'Hamster circadian rhythms are phase-shifted by electrical stimulation of the geniculo-hypothalamic tract', *Brain Res*, vol. 493, no. 2, pp. 283-291.
Röber, R.A., Weber, K. & Osborn, M. (1989) 'Differential timing of nuclear lamin A/C expression in the various organs of the mouse embryo and the young animal: a developmental study', *Development*, vol. 105, no. 2, pp. 365-378.
Rønningen, T., Shah, A., Oldenburg, A., Vekterud, K., Delbarre, E., Moskaug, J. & Collas, P. (2015) 'Prepatterning of differentiation-driven nuclear lamin A/C-associated chromatin domains by GlcNAcylated histone H2B', *Genome Res*, vol. 25, no. 12, pp. 1825-1835.
S, S. & Sriram, K. (2017) 'Hypothesis driven single cell dual oscillator mathematical model of circadian rhythms', *PLoS One*, vol. 12, no. 5, p. e0177197.
Saifur Rohman, M., Emoto, N., Nonaka, H., Okura, R., Nishimura, M., Yagita, K., van der Horst, G.T., Matsuo, M., Okamura, H. & Yokoyama, M. (2005) 'Circadian clock genes directly regulate expression of the Na(+)/H(+) exchanger NHE3 in the kidney', *Kidney Int*, vol. 67, no. 4, pp. 1410-1419.
Sakaki, M., Koike, H., Takahashi, N., Sasagawa, N., Tomioka, S., Arahata, K. & Ishiura, S. (2001) 'Interaction between emerin and nuclear lamins', *J Biochem*, vol. 129, no. 2, pp. 321-327.
Sallam, H., El-Serafi, A.T., Filipski, E., Terelius, Y., Lévi, F. & Hassan, M. (2015) 'The effect of circadian rhythm on pharmacokinetics and metabolism of the Cdk inhibitor, roscovitine, in tumor mice model', *Chronobiol Int*, vol. 32, no. 5, pp. 608-614.
Samson, C., Celli, F., Hendriks, K., Zinke, M., Essawy, N., Herrada, I., Arteni, A.A., Theillet, F.X., Alpha-Bazin, B., Armengaud, J., Coirault, C., Lange, A. & Zinn-Justin, S. (2017) 'Emerin self-assembly mechanism: role of the LEM domain', *FEBS J*, vol. 284, no. 2, pp. 338-352.
Santhi, N., Lazar, A.S., McCabe, P.J., Lo, J.C., Groeger, J.A. & Dijk, D.J. (2016) 'Sex differences in the circadian regulation of sleep and waking cognition in humans', *Proc Natl Acad Sci U S A*, vol. 113, no. 19, pp. E2730-2739.
Sasaki, H., Hattori, Y., Ikeda, Y., Kamagata, M., Iwami, S., Yasuda, S., Tahara, Y. & Shibata, S. (2016) 'Forced rather than voluntary exercise entrains peripheral clocks via a corticosterone/noradrenaline increase in PER2::LUC mice', *Sci Rep*, vol. 6, p. 27607.
Sastry, S.K. & Burridge, K. (2000) 'Focal adhesions: a nexus for intracellular signaling and cytoskeletal dynamics', *Exp Cell Res*, vol. 261, no. 1, pp. 25-36.
Sato, F., Kawamoto, T., Fujimoto, K., Noshiro, M., Honda, K.K., Honma, S., Honma, K. & Kato, Y. (2004) 'Functional analysis of the basic helix-loop-helix transcription factor DEC1 in circadian regulation. Interaction with BMAL1', *Eur J Biochem*, vol. 271, no. 22, pp. 4409-4419.
Sato, T.K., Yamada, R.G., Ukai, H., Baggs, J.E., Miraglia, L.J., Kobayashi, T.J., Welsh, D.K., Kay, S.A., Ueda, H.R. & Hogenesch, J.B. (2006) 'Feedback repression is required for mammalian circadian clock function', *Nat Genet*, vol. 38, no. 3, pp. 312-319.
Scaffidi, P. & Misteli, T. (2008) 'lamin A-dependent misregulation of adult stem cells associated with accelerated ageing', *Nat Cell Biol*, vol. 10, no. 4, pp. 452-459.
Scheer, F.A., Hu, K., Evoniuk, H., Kelly, E.E., Malhotra, A., Hilton, M.F. & Shea, S.A. (2010) 'Impact of the human circadian system, exercise, and their interaction on cardiovascular function', *Proc Natl Acad Sci U S A*, vol. 107, no. 47, pp. 20541-20546.

Schippers, J.H., Lai, A.G., Mueller-Roeber, B. & Dijkwel, P.P. (2013) 'Could ROS signals drive tissue-specific clocks?', *Transcription*, vol. 4, no. 5, pp. 206-208.

Schirmer, E.C., Florens, L., Guan, T., Yates, J.R. & Gerace, L. (2003) 'Nuclear membrane proteins with potential disease links found by subtractive proteomics', *Science*, vol. 301, no. 5638, pp. 1380-1382.

Schroeder, A.M., Truong, D., Loh, D.H., Jordan, M.C., Roos, K.P. & Colwell, C.S. (2012) 'Voluntary scheduled exercise alters diurnal rhythms of behaviour, physiology and gene expression in wild-type and vasoactive intestinal peptide-deficient mice', *J Physiol*, vol. 590, no. 23, pp. 6213-6226.

Schwartz, W.J. & Gainer, H. (1977) 'Suprachiasmatic nucleus: use of 14C-labeled deoxyglucose uptake as a functional marker', *Science*, vol. 197, no. 4308, pp. 1089-1091.

Segura-Totten, M., Kowalski, A.K., Craigie, R. & Wilson, K.L. (2002) 'Barrier-to-autointegration factor: major roles in chromatin decondensation and nuclear assembly', *J Cell Biol*, vol. 158, no. 3, pp. 475-485.

Senior, A. & Gerace, L. (1988) 'Integral membrane proteins specific to the inner nuclear membrane and associated with the nuclear lamina', *J Cell Biol*, vol. 107, no. 6 Pt 1, pp. 2029-2036.

Sewry, C.A., Brown, S.C., Mercuri, E., Bonne, G., Feng, L., Camici, G., Morris, G.E. & Muntoni, F. (2001) 'Skeletal muscle pathology in autosomal dominant Emery-Dreifuss muscular dystrophy with lamin A/C mutations', *Neuropathol Appl Neurobiol*, vol. 27, no. 4, pp. 281-290.

Shah, S., Tugendreich, S. & Forbes, D. (1998) 'Major binding sites for the nuclear import receptor are the internal nucleoporin Nup153 and the adjacent nuclear filament protein Tpr', *J Cell Biol*, vol. 141, no. 1, pp. 31-49.

Shavlakadze, T., Anwari, T., Soffe, Z., Cozens, G., Mark, P.J., Gondro, C. & Grounds, M.D. (2013) 'Impact of fasting on the rhythmic expression of myogenic and metabolic factors in skeletal muscle of adult mice', *Am J Physiol Cell Physiol*, vol. 305, no. 1, pp. C26-35.

Shin, J.Y., Méndez-López, I., Wang, Y., Hays, A.P., Tanji, K., Lefkowitch, J.H., Schulze, P.C., Worman, H.J. & Dauer, W.T. (2013) 'Lamina-associated polypeptide-1 interacts with the muscular dystrophy protein emerin and is essential for skeletal muscle maintenance', *Dev Cell*, vol. 26, no. 6, pp. 591-603.

Shinohara, K., Tominaga, K., Fukuhara, C., Otori, Y. & Inouye, S.I. (1993) 'Processing of photic information within the intergeniculate leaflet of the lateral geniculate body: assessed by neuropeptide Y immunoreactivity in the suprachiasmatic nucleus of rats', *Neuroscience*, vol. 56, no. 4, pp. 813-822.

Shinohara, Y., Koyama, Y.M., Ukai-Tadenuma, M., Hirokawa, T., Kikuchi, M., Yamada, R.G., Ukai, H., Fujishima, H., Umehara, T., Tainaka, K. & Ueda, H.R. (2017) 'Temperature-Sensitive Substrate and Product Binding Underlie Temperature-Compensated Phosphorylation in the Clock', *Mol Cell*, vol. 67, no. 5, pp. 783-798.e720.

Shostak, A., Ruppert, B., Ha, N., Bruns, P., Toprak, U.H., Eils, R., Schlesner, M., Diernfellner, A., Brunner, M. & Project, I.M.-S. (2016) 'MYC/MIZ1-dependent gene repression inversely coordinates the circadian clock with cell cycle and proliferation', *Nat Commun*, vol. 7, p. 11807.

Shradhanjali, A., Riehl, B.D., Lee, J.S., Ha, L. & Lim, J.Y. (2017) 'Enhanced cardiomyogenic induction of mouse pluripotent cells by cyclic mechanical stretch', *Biochem Biophys Res Commun*, vol. 488, no. 4, pp. 590-595.

Shumaker, D.K., Lee, K.K., Tanhehco, Y.C., Craigie, R. & Wilson, K.L. (2001) 'LAP2 binds to BAF.DNA complexes: requirement for the LEM domain and modulation by variable regions', *EMBO J*, vol. 20, no. 7, pp. 1754-1764.

Siepka, S.M., Yoo, S.H., Park, J., Song, W., Kumar, V., Hu, Y., Lee, C. & Takahashi, J.S. (2007) 'Circadian mutant Overtime reveals F-box protein FBXL3 regulation of cryptochrome and period gene expression', *Cell*, vol. 129, no. 5, pp. 1011-1023.

Sieprath, T., Corne, T.D., Nooteboom, M., Grootaert, C., Rajkovic, A., Buysschaert, B., Robijns, J., Broers, J.L., Ramaekers, F.C., Koopman, W.J., Willems, P.H. & De Vos, W.H. (2015) 'Sustained accumulation of prelamin A and depletion of lamin A/C both cause oxidative stress and mitochondrial dysfunction but induce different cell fates', *Nucleus*, vol. 6, no. 3, pp. 236-246.

Simoni, A., Wolfgang, W., Topping, M.P., Kavlie, R.G., Stanewsky, R. & Albert, J.T. (2014) 'A mechanosensory pathway to the Drosophila circadian clock', *Science*, vol. 343, no. 6170, pp. 525-528.

Sinensky, M., Fantle, K., Trujillo, M., McLain, T., Kupfer, A. & Dalton, M. (1994) 'The processing pathway of prelamin A', *J Cell Sci*, vol. 107 (Pt 1), pp. 61-67.

Sloin, H.E., Ruggiero, G., Rubinstein, A., Smadja Storz, S., Foulkes, N.S. & Gothilf, Y. (2018) 'Interactions between the circadian clock and TGF-β signaling pathway in zebrafish', *PLoS One*, vol. 13, no. 6, p. e0199777.

Smith, A. & Benavente, R. (1992) 'Identification of a short nuclear lamin protein selectively expressed during meiotic stages of rat spermatogenesis', *Differentiation*, vol. 52, no. 1, pp. 55-60.

Smolen, P., Baxter, D.A. & Byrne, J.H. (2001) 'Modeling circadian oscillations with interlocking positive and negative feedback loops', *J Neurosci*, vol. 21, no. 17, pp. 6644-6656.

Solovei, I., Wang, A.S., Thanisch, K., Schmidt, C.S., Krebs, S., Zwerger, M., Cohen, T.V., Devys, D., Foisner, R., Peichl, L., Herrmann, H., Blum, H., Engelkamp, D., Stewart, C.L., Leonhardt, H. & Joffe, B. (2013) 'LBR and lamin A/C sequentially tether peripheral heterochromatin and inversely regulate differentiation', *Cell*, vol. 152, no. 3, pp. 584-598.

Soriano-Arroquia, A., Clegg, P.D., Molloy, A.P. & Goljanek-Whysall, K. (2017) 'Preparation and Culture of Myogenic Precursor Cells/Primary Myoblasts from Skeletal Muscle of Adult and Aged Humans', *J Vis Exp*, no. 120.

Soul, J., Dunn, S.L., Anand, S., Serracino-Inglott, F., Schwartz, J.M., Boot-Handford, R.P. & Hardingham, T.E. (2018) 'Stratification of knee osteoarthritis: two major patient subgroups identified by genome-wide expression analysis of articular cartilage', *Ann Rheum Dis*, vol. 77, no. 3, p. 423.

Spann, T.P., Moir, R.D., Goldman, A.E., Stick, R. & Goldman, R.D. (1997) 'Disruption of nuclear lamin organization alters the distribution of replication factors and inhibits DNA synthesis', *J Cell Biol*, vol. 136, no. 6, pp. 1201-1212.

Spengler, M.L., Kuropatwinski, K.K., Comas, M., Gasparian, A.V., Fedtsova, N., Gleiberman, A.S., Gitlin, I.I., Artemicheva, N.M., Deluca, K.A., Gudkov, A.V. & Antoch, M.P. (2012) 'Core circadian protein CLOCK is a positive regulator of NF-κB-mediated transcription', *Proc Natl Acad Sci U S A*, vol. 109, no. 37, pp. E2457-2465.

Stables, G.I. & Morley, W.N. (1994) 'Hutchinson-Gilford syndrome', *J R Soc Med*, vol. 87, no. 4, pp. 243-244.

Stasi, M., De Luca, M. & Bucci, C. (2015) 'Two-hybrid-based systems: powerful tools for investigation of membrane traffic machineries', *J Biotechnol*, vol. 202, pp. 105-117.

Stephan, F.K. & Zucker, I. (1972) 'Circadian rhythms in drinking behavior and locomotor activity of rats are eliminated by hypothalamic lesions', *Proc Natl Acad Sci U S A*, vol. 69, no. 6, pp. 1583-1586.

Stewart, C. & Burke, B. (1987) 'Teratocarcinoma stem cells and early mouse embryos contain only a single major lamin polypeptide closely resembling lamin B', *Cell*, vol. 51, no. 3, pp. 383-392.

Stierlé, V., Couprie, J., Ostlund, C., Krimm, I., Zinn-Justin, S., Hossenlopp, P., Worman, H.J., Courvalin, J.C. & Duband-Goulet, I. (2003) 'The carboxyl-terminal region common to lamins A and C contains a DNA binding domain', *Biochemistry*, vol. 42, no. 17, pp. 4819-4828.

Straif, K., Baan, R., Grosse, Y., Secretan, B., El Ghissassi, F., Bouvard, V., Altieri, A., Benbrahim-Tallaa, L., Cogliano, V. & Group, W.I.A.F.R.o.C.M.W. (2007) 'Carcinogenicity of shift-work, painting, and fire-fighting', *Lancet Oncol*, vol. 8, no. 12, pp. 1065-1066.

Strelkov, S.V., Schumacher, J., Burkhard, P., Aebi, U. & Herrmann, H. (2004) 'Crystal structure of the human lamin A coil 2B dimer: implications for the head-to-tail association of nuclear lamins',

J Mol Biol, vol. 343, no. 4, pp. 1067-1080.

Stroud, M., Feng, W., Zhang, J., Veevers, J., Fang, X., Gerace, L. & Chen, J. (2017) 'Nesprin 1α2 is essential for mouse postnatal viability and nuclear positioning in skeletal muscle', *J Cell Biol*, vol. 216, no. 7, pp. 1915-1924.

Sullivan, T., Escalante-Alcalde, D., Bhatt, H., Anver, M., Bhat, N., Nagashima, K., Stewart, C.L. & Burke, B. (1999) 'Loss of A-type lamin expression compromises nuclear envelope integrity leading to muscular dystrophy', *J Cell Biol*, vol. 147, no. 5, pp. 913-920.

Sun, Z.S., Albrecht, U., Zhuchenko, O., Bailey, J., Eichele, G. & Lee, C.C. (1997) 'RIGUI, a putative mammalian ortholog of the Drosophila period gene', *Cell*, vol. 90, no. 6, pp. 1003-1011.

Swift, J., Ivanovska, I.L., Buxboim, A., Harada, T., Dingal, P.C., Pinter, J., Pajerowski, J.D., Spinler, K.R., Shin, J.W., Tewari, M., Rehfeldt, F., Speicher, D.W. & Discher, D.E. (2013) 'Nuclear lamin-A scales with tissue stiffness and enhances matrix-directed differentiation', *Science*, vol. 341, no. 6149, p. 1240104.

Synofzik, M., Smets, K., Mallaret, M., Di Bella, D., Gallenmüller, C., Baets, J., Schulze, M., Magri, S., Sarto, E., Mustafa, M., Deconinck, T., Haack, T., Züchner, S., Gonzalez, M., Timmann, D., Stendel, C., Klopstock, T., Durr, A., Tranchant, C., Sturm, M., Hamza, W., Nanetti, L., Mariotti, C., Koenig, M., Schöls, L., Schüle, R., de Jonghe, P., Anheim, M., Taroni, F. & Bauer, P. (2016) 'SYNE1 ataxia is a common recessive ataxia with major non-cerebellar features: a large multi-centre study', *Brain*, vol. 139, no. Pt 5, pp. 1378-1393.

Takahashi, J.S. (2015) 'Molecular components of the circadian clock in mammals', *Diabetes Obes Metab*, vol. 17 Suppl 1, pp. 6-11.

Takano, A., Shimizu, K., Kani, S., Buijs, R.M., Okada, M. & Nagai, K. (2000) 'Cloning and characterization of rat casein kinase 1epsilon', *FEBS Lett*, vol. 477, no. 1-2, pp. 106-112.

Tamaru, T., Hattori, M., Ninomiya, Y., Kawamura, G., Varès, G., Honda, K., Mishra, D.P., Wang, B., Benjamin, I., Sassone-Corsi, P., Ozawa, T. & Takamatsu, K. (2013) 'ROS stress resets circadian clocks to coordinate pro-survival signals', *PLoS One*, vol. 8, no. 12, p. e82006.

Taniura, H., Glass, C. & Gerace, L. (1995) 'A chromatin binding site in the tail domain of nuclear lamins that interacts with core histones', *J Cell Biol*, vol. 131, no. 1, pp. 33-44.

Tataroglu, O. & Emery, P. (2014) 'Studying circadian rhythms in Drosophila melanogaster', *Methods*, vol. 68, no. 1, pp. 140-150.

Taylor, M.R., Slavov, D., Gajewski, A., Vlcek, S., Ku, L., Fain, P.R., Carniel, E., Di Lenarda, A., Sinagra, G., Boucek, M.M., Cavanaugh, J., Graw, S.L., Ruegg, P., Feiger, J., Zhu, X., Ferguson, D.A., Bristow, M.R., Gotzmann, J., Foisner, R., Mestroni, L. & Group, F.C.R.R. (2005) 'Thymopoietin (lamina-associated polypeptide 2) gene mutation associated with dilated cardiomyopathy', *Hum Mutat*, vol. 26, no. 6, pp. 566-574.

Tei, H., Okamura, H., Shigeyoshi, Y., Fukuhara, C., Ozawa, R., Hirose, M. & Sakaki, Y. (1997) 'Circadian oscillation of a mammalian homologue of the Drosophila period gene', *Nature*, vol. 389, no. 6650, pp. 512-516.

Terzibasi-Tozzini, E., Martinez-Nicolas, A. & Lucas-Sánchez, A. (2017) 'The clock is ticking. Ageing of the circadian system: From physiology to cell cycle', *Semin Cell Dev Biol*, vol. 70, pp. 164-176.

Thanos, D. & Maniatis, T. (1995) 'NF-kappa B: a lesson in family values', *Cell*, vol. 80, no. 4, pp. 529-532.

Tortosa-Martínez, J., Clow, A., Caus-Pertegaz, N., González-Caballero, G., Abellán-Miralles, I. & Saenz, M.J. (2015) 'Exercise Increases the Dynamics of Diurnal Cortisol Secretion and Executive Function in People With Amnestic Mild Cognitive Impairment', *J Aging Phys Act*, vol. 23, no. 4, pp. 550-558.

Treisman, R. (1996) 'Regulation of transcription by MAP kinase cascades', *Curr Opin Cell Biol*, vol. 8, no. 2, pp. 205-215.

Triqueneaux, G., Thenot, S., Kakizawa, T., Antoch, M.P., Safi, R., Takahashi, J.S., Delaunay, F. & Laudet, V. (2004) 'The orphan receptor Rev-erbalpha gene is a target of the circadian clock pacemaker', *J Mol Endocrinol*, vol. 33, no. 3, pp. 585-608.

Trott, A.J. & Menet, J.S. (2018) 'Regulation of circadian clock transcriptional output by CLOCK:BMAL1', *PLoS Genet*, vol. 14, no. 1, p. e1007156.

Ueda, H.R., Chen, W., Adachi, A., Wakamatsu, H., Hayashi, S., Takasugi, T., Nagano, M., Nakahama, K., Suzuki, Y., Sugano, S., Iino, M., Shigeyoshi, Y. & Hashimoto, S. (2002) 'A transcription factor response element for gene expression during circadian night', *Nature*, vol. 418, no. 6897, pp. 534-539.

Unsal-Kaçmaz, K., Mullen, T.E., Kaufmann, W.K. & Sancar, A. (2005) 'Coupling of human circadian and cell cycles by the timeless protein', *Mol Cell Biol*, vol. 25, no. 8, pp. 3109-3116.

van Berlo, J.H., de Voogt, W.G., van der Kooi, A.J., van Tintelen, J.P., Bonne, G., Yaou, R.B., Duboc, D., Rossenbacker, T., Heidbüchel, H., de Visser, M., Crijns, H.J. & Pinto, Y.M. (2005) 'Meta-analysis of clinical characteristics of 299 carriers of LMNA gene mutations: do lamin A/C mutations portend a high risk of sudden death?', *J Mol Med (Berl)*, vol. 83, no. 1, pp. 79-83.

van der Horst, G.T., Muijtjens, M., Kobayashi, K., Takano, R., Kanno, S., Takao, M., de Wit, J., Verkerk, A., Eker, A.P., van Leenen, D., Buijs, R., Bootsma, D., Hoeijmakers, J.H. & Yasui, A. (1999) 'Mammalian Cry1 and Cry2 are essential for maintenance of circadian rhythms', *Nature*, vol. 398, no. 6728, pp. 627-630.

van Engelen, B.G., Muchir, A., Hutchison, C.J., van der Kooi, A.J., Bonne, G. & Lammens, M. (2005) 'The lethal phenotype of a homozygous nonsense mutation in the lamin A/C gene', *Neurology*, vol. 64, no. 2, pp. 374-376.

Van Reeth, O., Sturis, J., Byrne, M.M., Blackman, J.D., L'Hermite-Balériaux, M., Leproult, R., Oliner, C., Refetoff, S., Turek, F.W. & Van Cauter, E. (1994) 'Nocturnal exercise phase delays circadian rhythms of melatonin and thyrotropin secretion in normal men', *Am J Physiol*, vol. 266, no. 6 Pt 1, pp. E964-974.

van Steensel, B. & Belmont, A.S. (2017) 'Lamina-Associated Domains: Links with Chromosome Architecture, Heterochromatin, and Gene Repression', *Cell*, vol. 169, no. 5, pp. 780-791.

van Wamelen, D.J., Roos, R.A. & Aziz, N.A. (2015) 'Therapeutic strategies for circadian rhythm and sleep disturbances in Huntington disease', *Neurodegener Dis Manag*, vol. 5, no. 6, pp. 549-559.

Vande Geest, J.P., Di Martino, E.S. & Vorp, D.A. (2004) 'An analysis of the complete strain field within Flexercell membranes', *J Biomech*, vol. 37, no. 12, pp. 1923-1928.

Vandenburgh, H., Chromiak, J., Shansky, J., Del Tatto, M. & Lemaire, J. (1999) 'Space travel directly induces skeletal muscle atrophy', *FASEB J*, vol. 13, no. 9, pp. 1031-1038.

Vatine, G., Vallone, D., Gothilf, Y. & Foulkes, N.S. (2011) 'It's time to swim! Zebrafish and the circadian clock', *FEBS Lett*, vol. 585, no. 10, pp. 1485-1494.

Vaughan, A., Alvarez-Reyes, M., Bridger, J.M., Broers, J.L., Ramaekers, F.C., Wehnert, M., Morris, G.E., Whitfield WGF & Hutchison, C.J. (2001) 'Both emerin and lamin C depend on lamin A for localization at the nuclear envelope', *J Cell Sci*, vol. 114, no. Pt 14, pp. 2577-2590.

Vitaterna, M.H., King, D.P., Chang, A.M., Kornhauser, J.M., Lowrey, P.L., McDonald, J.D., Dove, W.F., Pinto, L.H., Turek, F.W. & Takahashi, J.S. (1994) 'Mutagenesis and mapping of a mouse gene, Clock, essential for circadian behavior', *Science*, vol. 264, no. 5159, pp. 719-725.

Vlcek, S., Just, H., Dechat, T. & Foisner, R. (1999) 'Functional diversity of LAP2alpha and LAP2beta in postmitotic chromosome association is caused by an alpha-specific nuclear targeting domain', *EMBO J*, vol. 18, no. 22, pp. 6370-6384.

Vollmers, C., Panda, S. & DiTacchio, L. (2008) 'A high-throughput assay for siRNA-based circadian screens in human U2OS cells', *PLoS One*, vol. 3, no. 10, p. e3457.

Wagner, N. & Krohne, G. (2007) 'LEM-Domain proteins: new insights into lamin-interacting proteins', *Int Rev Cytol*, vol. 261, pp. 1-46.

Walsh, K. (1997) 'Coordinate regulation of cell cycle and apoptosis during myogenesis', *Prog Cell Cycle Res*, vol. 3, pp. 53-58.

Wang, D., Chang, P.S., Wang, Z., Sutherland, L., Richardson, J.A., Small, E., Krieg, P.A. & Olson, E.N. (2001) 'Activation of cardiac gene expression by myocardin, a transcriptional cofactor for

serum response factor', *Cell*, vol. 105, no. 7, pp. 851-862.
Wang, J., Mauvoisin, D., Martin, E., Atger, F., Galindo, A.N., Dayon, L., Sizzano, F., Palini, A., Kussmann, M., Waridel, P., Quadroni, M., Dulić, V., Naef, F. & Gachon, F. (2017a) 'Nuclear Proteomics Uncovers Diurnal Regulatory Landscapes in Mouse Liver', *Cell Metab*, vol. 25, no. 1, pp. 102-117.
Wang, X., Tang, J., Xing, L., Shi, G., Ruan, H., Gu, X., Liu, Z., Wu, X., Gao, X. & Xu, Y. (2010) 'Interaction of MAGED1 with nuclear receptors affects circadian clock function', *EMBO J*, vol. 29, no. 8, pp. 1389-1400.
Wang, Y., Ni, X., Yan, J. & Yang, L. (2017b) 'Modeling transcriptional co-regulation of mammalian circadian clock', *Math Biosci Eng*, vol. 14, no. 5-6, pp. 1447-1462.
Wang, Y., Song, L., Liu, M., Ge, R., Zhou, Q., Liu, W., Li, R., Qie, J., Zhen, B., He, F., Qin, J. & Ding, C. (2018) 'A proteomics landscape of circadian clock in mouse liver', *Nat Commun*, vol. 9, no. 1, p. 1553.
Wang, Y., Xiong, Z., Gong, W., Zhou, P., Xie, Q., Zhou, Z. & Lu, G. (2015) 'Expression of heat shock protein 27 correlates with actin cytoskeletal dynamics and contractility of cultured human bladder smooth muscle cells', *Exp Cell Res*, vol. 338, no. 1, pp. 39-44.
Wang, Z.Y. & Tobin, E.M. (1998) 'Constitutive expression of the CIRCADIAN CLOCK ASSOCIATED 1 (CCA1) gene disrupts circadian rhythms and suppresses its own expression', *Cell*, vol. 93, no. 7, pp. 1207-1217.
Watts, A.G., Swanson, L.W. & Sanchez-Watts, G. (1987) 'Efferent projections of the suprachiasmatic nucleus: I. Studies using anterograde transport of Phaseolus vulgaris leucoagglutinin in the rat', *J Comp Neurol*, vol. 258, no. 2, pp. 204-229.
Weitzman, E.D. (1976) 'Biologic rhythms and hormone secretion patterns', *Hosp Pract*, vol. 11, no. 8, pp. 79-86.
Welsh, D.K., Logothetis, D.E., Meister, M. & Reppert, S.M. (1995) 'Individual neurons dissociated from rat suprachiasmatic nucleus express independently phased circadian firing rhythms', *Neuron*, vol. 14, no. 4, pp. 697-706.
Wheeler, M.A., Warley, A., Roberts, R.G., Ehler, E. & Ellis, J.A. (2010) 'Identification of an emerin-beta-catenin complex in the heart important for intercalated disc architecture and beta-catenin localisation', *Cell Mol Life Sci*, vol. 67, no. 5, pp. 781-796.
Widegren, U., Jiang, X.J., Krook, A., Chibalin, A.V., Björnholm, M., Tally, M., Roth, R.A., Henriksson, J., Wallberg-henriksson, H. & Zierath, J.R. (1998) 'Divergent effects of exercise on metabolic and mitogenic signaling pathways in human skeletal muscle', *FASEB J*, vol. 12, no. 13, pp. 1379-1389.
Wilson, K.L. & Foisner, R. (2010) 'Lamin-binding Proteins', *Cold Spring Harb Perspect Biol*, vol. 2, no. 4, p. a000554.
Winfree, A.T. (1967) 'Biological rhythms and the behavior of populations of coupled oscillators', *J Theor Biol*, vol. 16, no. 1, pp. 15-42.
Wolff, G. & Esser, K.A. (2012) 'Scheduled exercise phase shifts the circadian clock in skeletal muscle', *Med Sci Sports Exerc*, vol. 44, no. 9, pp. 1663-1670.
Woller, A., Duez, H., Staels, B. & Lefranc, M. (2016) 'A Mathematical Model of the Liver Circadian Clock Linking Feeding and Fasting Cycles to Clock Function', *Cell Rep*, vol. 17, no. 4, pp. 1087-1097.
Worman, H.J. (2012) 'Nuclear lamins and laminopathies', *J Pathol*, vol. 226, no. 2, pp. 316-325.
Worman, H.J. & Courvalin, J.C. (2004) 'How do mutations in lamins A and C cause disease?', *J Clin Invest*, vol. 113, no. 3, pp. 349-351.
Worman, H.J., Yuan, J., Blobel, G. & Georgatos, S.D. (1988) 'A lamin B receptor in the nuclear envelope', *Proc Natl Acad Sci U S A*, vol. 85, no. 22, pp. 8531-8534.
Xanthoudakis, S., Miao, G., Wang, F., Pan, Y.C. & Curran, T. (1992) 'Redox activation of Fos-Jun DNA binding activity is mediated by a DNA repair enzyme', *EMBO J*, vol. 11, no. 9, pp. 3323-3335.
Yaffe, D. & Saxel, O. (1977) 'Serial passaging and differentiation of myogenic cells isolated from

dystrophic mouse muscle', *Nature*, vol. 270, no. 5639, pp. 725-727.
Yagita, K., Tamanini, F., van Der Horst, G.T. & Okamura, H. (2001) 'Molecular mechanisms of the biological clock in cultured fibroblasts', *Science*, vol. 292, no. 5515, pp. 278-281.
Yagita, K., Yamanaka, I., Emoto, N., Kawakami, K. & Shimada, S. (2010) 'Real-time monitoring of circadian clock oscillations in primary cultures of mammalian cells using Tol2 transposon-mediated gene transfer strategy', *BMC Biotechnol*, vol. 10, p. 3.
Yamanaka, Y., Hashimoto, S., Takasu, N.N., Tanahashi, Y., Nishide, S.Y., Honma, S. & Honma, K. (2015) 'Morning and evening physical exercise differentially regulate the autonomic nervous system during nocturnal sleep in humans', *Am J Physiol Regul Integr Comp Physiol*, vol. 309, no. 9, pp. R1112-1121.
Yamanaka, Y., Hashimoto, S., Tanahashi, Y., Nishide, S.Y., Honma, S. & Honma, K. (2010) 'Physical exercise accelerates reentrainment of human sleep-wake cycle but not of plasma melatonin rhythm to 8-h phase-advanced sleep schedule', *Am J Physiol Regul Integr Comp Physiol*, vol. 298, no. 3, pp. R681-691.
Yamanaka, Y., Honma, S. & Honma, K. (2008) 'Scheduled exposures to a novel environment with a running-wheel differentially accelerate re-entrainment of mice peripheral clocks to new light-dark cycles', *Genes Cells*, vol. 13, no. 5, pp. 497-507.
Yamanaka, Y., Honma, S. & Honma, K. (2016) 'Mistimed wheel running interferes with re-entrainment of circadian Per1 rhythms in the mouse skeletal muscle and lung', *Genes Cells*, vol. 21, no. 3, pp. 264-274.
Yamazaki, S., Numano, R., Abe, M., Hida, A., Takahashi, R., Ueda, M., Block, G.D., Sakaki, Y., Menaker, M. & Tei, H. (2000) 'Resetting central and peripheral circadian oscillators in transgenic rats', *Science*, vol. 288, no. 5466, pp. 682-685.
Yang, N., Williams, J., Pekovic-Vaughan, V., Wang, P., Olabi, S., McConnell, J., Gossan, N., Hughes, A., Cheung, J., Streuli, C.H. & Meng, Q.J. (2017) 'Cellular mechano-environment regulates the mammary circadian clock', *Nat Commun*, vol. 8, p. 14287.
Yang, W., Kang, X., Liu, J., Li, H., Ma, Z., Jin, X., Qian, Z., Xie, T., Qin, N., Feng, D., Pan, W., Chen, Q., Sun, H. & Wu, S. (2016) 'Clock Gene Bmal1 Modulates Human Cartilage Gene Expression by Crosstalk With Sirt1', *Endocrinology*, vol. 157, no. 8, pp. 3096-3107.
Yao, Q.P., Xie, Z.W., Wang, K.X., Zhang, P., Han, Y., Qi, Y.X. & Jiang, Z.L. (2017) 'Profiles of long noncoding RNAs in hypertensive rats: long noncoding RNA XR007793 regulates cyclic strain-induced proliferation and migration of vascular smooth muscle cells', *J Hypertens*, vol. 35, no. 6, pp. 1195-1203.
Yasumoto, Y., Hashimoto, C., Nakao, R., Yamazaki, H., Hiroyama, H., Nemoto, T., Yamamoto, S., Sakurai, M., Oike, H., Wada, N., Yoshida-Noro, C. & Oishi, K. (2016) 'Short-term feeding at the wrong time is sufficient to desynchronize peripheral clocks and induce obesity with hyperphagia, physical inactivity and metabolic disorders in mice', *Metabolism*, vol. 65, no. 5, pp. 714-727.
Yeom, M., Pendergast, J.S., Ohmiya, Y. & Yamazaki, S. (2010) 'Circadian-independent cell mitosis in immortalized fibroblasts', *Proc Natl Acad Sci U S A*, vol. 107, no. 21, pp. 9665-9670.
Yim, E.K. & Sheetz, M.P. (2012) 'Force-dependent cell signaling in stem cell differentiation', *Stem Cell Res Ther*, vol. 3, no. 5, p. 41.
Yoo, S.H., Ko, C.H., Lowrey, P.L., Buhr, E.D., Song, E.J., Chang, S., Yoo, O.J., Yamazaki, S., Lee, C. & Takahashi, J.S. (2005) 'A noncanonical E-box enhancer drives mouse Period2 circadian oscillations in vivo', *Proc Natl Acad Sci U S A*, vol. 102, no. 7, pp. 2608-2613.
Zambon, A.C., McDearmon, E.L., Salomonis, N., Vranizan, K.M., Johansen, K.L., Adey, D., Takahashi, J.S., Schambelan, M. & Conklin, B.R. (2003) 'Time- and exercise-dependent gene regulation in human skeletal muscle', *Genome Biol*, vol. 4, no. 10, p. R61.
Zhan, M., Jin, B., Chen, S.E., Reecy, J.M. & Li, Y.P. (2007) 'TACE release of TNF-alpha mediates mechanotransduction-induced activation of p38 MAPK and myogenesis', *J Cell Sci*, vol. 120, no. Pt 4, pp. 692-701.

Zhang, Q., Skepper, J.N., Yang, F., Davies, J.D., Hegyi, L., Roberts, R.G., Weissberg, P.L., Ellis, J.A. & Shanahan, C.M. (2001) 'Nesprins: a novel family of spectrin-repeat-containing proteins that localize to the nuclear membrane in multiple tissues', *J Cell Sci*, vol. 114, no. Pt 24, pp. 4485-4498.

Zhang, R., Lahens, N.F., Ballance, H.I., Hughes, M.E. & Hogenesch, J.B. (2014) 'A circadian gene expression atlas in mammals: implications for biology and medicine', *Proc Natl Acad Sci U S A*, vol. 111, no. 45, pp. 16219-16224.

Zhang, Y.Q. & Sarge, K.D. (2008) 'Sumoylation regulates lamin A function and is lost in lamin A mutants associated with familial cardiomyopathies', *J Cell Biol*, vol. 182, no. 1, pp. 35-39.

Zhao, H., Sifakis, E.G., Sumida, N., Millán-Ariño, L., Scholz, B.A., Svensson, J.P., Chen, X., Ronnegren, A.L., Mallet de Lima, C.D., Varnoosfaderani, F.S., Shi, C., Loseva, O., Yammine, S., Israelsson, M., Rathje, L.S., Németi, B., Fredlund, E., Helleday, T., Imreh, M.P. & Göndör, A. (2015) 'PARP1- and CTCF-Mediated Interactions between Active and Repressed Chromatin at the Lamina Promote Oscillating Transcription', *Mol Cell*, vol. 59, no. 6, pp. 984-997.

Zhao, S. & Sancar, A. (1997) 'Human blue-light photoreceptor hCRY2 specifically interacts with protein serine/threonine phosphatase 5 and modulates its activity', *Photochem Photobiol*, vol. 66, no. 5, pp. 727-731.

Zheng, B., Albrecht, U., Kaasik, K., Sage, M., Lu, W., Vaishnav, S., Li, Q., Sun, Z.S., Eichele, G., Bradley, A. & Lee, C.C. (2001) 'Nonredundant roles of the mPer1 and mPer2 genes in the mammalian circadian clock', *Cell*, vol. 105, no. 5, pp. 683-694.

Zheng, R., Ghirlando, R., Lee, M.S., Mizuuchi, K., Krause, M. & Craigie, R. (2000) 'Barrier-to-autointegration factor (BAF) bridges DNA in a discrete, higher-order nucleoprotein complex', *Proc Natl Acad Sci U S A*, vol. 97, no. 16, pp. 8997-9002.

Zhou, C., Li, C., Zhou, B., Sun, H., Koullourou, V., Holt, I., Puckelwartz, M., Warren, D., Hayward, R., Lin, Z., Zhang, L., Morris, G., McNally, E., Shackleton, S., Rao, L., Shanahan, C. & Zhang, Q. (2017) 'Novel nesprin-1 mutations associated with dilated cardiomyopathy cause nuclear envelope disruption and defects in myogenesis', *Hum Mol Genet*, vol. 26, no.12, pp. 2258-2276.

Zuleger, N., Boyle, S., Kelly, D.A., de las Heras, J.I., Lazou, V., Korfali, N., Batrakou, D.G., Randles, K.N., Morris, G.E., Harrison, D.J., Bickmore, W.A. & Schirmer, E.C. (2013) 'Specific nuclear envelope transmembrane proteins can promote the location of chromosomes to and from the nuclear periphery', *Genome Biol*, vol. 14, no. 2, p. R14.

Zuleger, N., Kelly, D.A., Richardson, A.C., Kerr, A.R., Goldberg, M.W., Goryachev, A.B. & Schirmer, E.C. (2011) 'System analysis shows distinct mechanisms and common principles of nuclear envelope protein dynamics', *J Cell Biol*, vol. 193, no. 1, pp. 109-123.

Zullo, J.M., Demarco, I.A., Piqué-Regi, R., Gaffney, D.J., Epstein, C.B., Spooner, C.J., Luperchio, T.R., Bernstein, B.E., Pritchard, J.K., Reddy, K.L. & Singh, H. (2012) 'DNA sequence-dependent compartmentalization and silencing of chromatin at the nuclear lamina', *Cell*, vol. 149, no. 7, pp. 1474-1487.

Zuo, B., Yang, J., Wang, F., Wang, L., Yin, Y., Dan, J., Liu, N. & Liu L. (2012) 'Influences of lamin A levels on induction of pluripotent stem cells', *Biology Open*, vol. 1, pp. 1118-1127.

Zylka, M.J., Shearman, L.P., Weaver, D.R. & Reppert, S.M. (1998) 'Three period homologs in mammals: differential light responses in the suprachiasmatic circadian clock and oscillating transcripts outside of brain', *Neuron*, vol. 20, no. 6, pp. 1103-1110.

9 Appendix

Table 9.1. Variables within the ODE equations and the concentration represented by each variable.

Variable	Variable concentration
Mb	*Bmal* mRNA
Bc	BMAL in cytoplasm
Bcp	Phosphorylated BMAL in cytoplasm
Bn	BMAL in nucleus
Cc	CRY in cytoplasm
Mc	*Cry* mRNA
Ccp	Phosphorylated CRY in cytoplasm
Mp	*Per* mRNA
Pc	PER in cytoplasm
Pcp	Phosphorylated PER in cytoplasm
PCc	PER:CRY in cytoplasm
PCcp	Phosphorylated PER:CRY in cytoplasm
PCn	PER:CRY in nucleus
Bnp	Phosphorylated BMAL in nucleus
PCnp	Phosphorylated PER:CRY in nucleus
In	Inactive complex between PER:CRY and CLOCK:BMAL in the nucleus
Mr	*Rev-erbα* mRNA
Rc	REV-ERBα in cytoplasm
Rn	REV-ERBα in nucleus
Lm	LMNA
Lm_Lm	Lamin A dimer
mLm	*Lmna* mRNA
Lm_LmPCn (model 3 only)	Lamin A dimer bound to PER:CRY (sequestering complex)

9.1 Model 1: lamin A repress *Per* ODEs

$$\frac{d([Mb]\cdot V_{cell})}{dt} = +V_{cell}\cdot\left(\frac{2.04797\cdot 0.401148^{1.525}}{0.401148^{1.525}+[Rn]^{1.525}}\right) - V_{cell}\cdot(0.02\cdot[Mb]) - V_{cell}\cdot\left(\frac{1.3\cdot[Mb]}{0.4+[Mb]}\right)$$

$$\frac{d([Bc]\cdot V_{cell})}{dt} = +V_{cell}\cdot(0.32\cdot[Mb]) - V_{cell}\cdot\left(\frac{1.4\cdot[Bc]}{1.006+[Bc]}\right) - V_{cell}\cdot(0.02\cdot[Bc]) - V_{cell}\cdot((0.8\cdot[Bc]-0.4\cdot[Bn])) + V_{cell}\cdot\left(\frac{0.2\cdot[Bcp]}{0.1+[Bcp]}\right)$$

$$\frac{d([Bcp]\cdot V_{cell})}{dt} = -V_{cell}\cdot(0.02\cdot[Bcp]) + V_{cell}\cdot\left(\frac{1.4\cdot[Bc]}{1.006+[Bc]}\right) - V_{cell}\cdot\left(\frac{3\cdot[Bcp]}{0.3+[Bcp]}\right) - V_{cell}\cdot\left(\frac{0.2\cdot[Bcp]}{0.1+[Bcp]}\right)$$

$$\frac{d([Bn]\cdot V_{cell})}{dt} = -V_{cell}\cdot((1\cdot[PCn]\cdot[Bn]-0.2\cdot[In])) - V_{cell}\cdot\left(\frac{1.4\cdot[Bn]}{1.006+[Bn]}\right) + V_{cell}\cdot((0.8\cdot[Bc]-0.4\cdot[Bn])) - V_{cell}\cdot(0.02\cdot[Bn]) + V_{cell}\cdot\left(\frac{0.4\cdot[Bnp]}{0.1+[Bnp]}\right)$$

$$\frac{d([Cc]\cdot V_{cell})}{dt} = -V_{cell}\cdot((0.8\cdot[Cc]\cdot[Pc]-0.4\cdot[PCc])) - V_{cell}\cdot(0.2\cdot[Cc]) + V_{cell}\cdot\left(\frac{0.2\cdot[Ccp]}{0.1+[Ccp]}\right) + V_{cell}\cdot(3.2\cdot[Mc]) - V_{cell}\cdot\left(\frac{1.2\cdot[Cc]}{1.006+[Cc]}\right)$$

$$\frac{d([Mc]\cdot V_{cell})}{dt} = +V_{cell}\cdot\left(\frac{2.2\cdot[Bn]^2}{0.6^2+[Bn]^2}\right) - V_{cell}\cdot\left(\frac{2\cdot[Mc]}{0.4+[Mc]}\right) - V_{cell}\cdot(0.02\cdot[Mc])$$

$$\frac{d([Ccp]\cdot V_{cell})}{dt} = -V_{cell}\cdot(0.02\cdot[Ccp]) - V_{cell}\cdot\left(\frac{0.2\cdot[Ccp]}{0.1+[Ccp]}\right) + V_{cell}\cdot\left(\frac{1.2\cdot[Cc]}{1.006+[Cc]}\right) - V_{cell}\cdot\left(\frac{1.4\cdot[Ccp]}{0.3+[Ccp]}\right)$$

$$\frac{d([Mp]\cdot V_{cell})}{dt} = -V_{cell}\cdot(0.02\cdot[Mp]) - V_{cell}\cdot\left(\frac{2.2\cdot[Mp]}{0.3+[Mp]}\right) + V_{cell}\cdot\left(\frac{2.5\cdot[Bn]}{0.25+[Bn]+\frac{0.25\cdot[Lm\_Lm]}{5}}\right)$$

$$\frac{d([Pc]\cdot V_{cell})}{dt} = +V_{cell}\cdot(1.2\cdot[Mp]) - V_{cell}\cdot\left(\frac{9.6\cdot[Pc]}{1.006+[Pc]}\right) - V_{cell}\cdot((0.8\cdot[Cc]\cdot[Pc]-0.4\cdot[PCc])) - V_{cell}\cdot(0.02\cdot[Pc]) + V_{cell}\cdot\left(\frac{0.6\cdot[Pcp]}{0.1+[Pcp]}\right)$$

$$\frac{d([Pcp]\cdot V_{cell})}{dt} = -V_{cell}\cdot\left(\frac{3.4\cdot[Pcp]}{0.3+[Pcp]}\right) + V_{cell}\cdot\left(\frac{9.6\cdot[Pc]}{1.006+[Pc]}\right) - V_{cell}\cdot(0.02\cdot[Pcp]) - V_{cell}\cdot\left(\frac{0.6\cdot[Pcp]}{0.1+[Pcp]}\right)$$

$$\frac{d([PCc]\cdot V_{cell})}{dt} = +V_{cell}\cdot((0.8\cdot[Cc]\cdot[Pc]-0.4\cdot[PCc])) - V_{cell}\cdot\left(\frac{2.4\cdot[PCc]}{1.006+[PCc]}\right) - V_{cell}\cdot((3\cdot[PCc]-0.4\cdot[PCn])) - V_{cell}\cdot(0.02\cdot[PCc]) + V_{cell}\cdot\left(\frac{0.2\cdot[PCcp]}{0.1+[PCcp]}\right)$$

$$\frac{d([PCcp]\cdot V_{cell})}{dt} = +V_{cell}\cdot\left(\frac{2.4\cdot[PCc]}{1.006+[PCc]}\right) - V_{cell}\cdot\left(\frac{1.4\cdot[PCcp]}{0.3+[PCcp]}\right) - V_{cell}\cdot(0.02\cdot[PCcp]) - V_{cell}\cdot\left(\frac{0.2\cdot[PCcp]}{0.1+[PCcp]}\right)$$

$$\frac{d([PCn]\cdot V_{cell})}{dt} = +V_{cell}\cdot((3\cdot[PCc]-0.4\cdot[PCn]))$$
$$-V_{cell}\cdot\left(\frac{2.4\cdot[PCn]}{1.006+[PCn]}\right)$$
$$-V_{cell}\cdot((1\cdot[PCn]\cdot[Bn]-0.2\cdot[In]))$$
$$+V_{cell}\cdot\left(\frac{0.2\cdot[PCnp]}{0.1+[PCnp]}\right)$$
$$-V_{cell}\cdot(0.02\cdot[PCn])$$

$$\frac{d([Bnp]\cdot V_{cell})}{dt} = -V_{cell}\cdot(0.02\cdot[Bnp])$$
$$+V_{cell}\cdot\left(\frac{1.4\cdot[Bn]}{1.006+[Bn]}\right)$$
$$-V_{cell}\cdot\left(\frac{3\cdot[Bnp]}{0.3+[Bnp]}\right)$$
$$-V_{cell}\cdot\left(\frac{0.4\cdot[Bnp]}{0.1+[Bnp]}\right)$$

$$\frac{d([PCnp]\cdot V_{cell})}{dt} = -V_{cell}\cdot(0.02\cdot[PCnp])$$
$$+V_{cell}\cdot\left(\frac{2.4\cdot[PCn]}{1.006+[PCn]}\right)$$
$$-V_{cell}\cdot\left(\frac{1.4\cdot[PCnp]}{0.3+[PCnp]}\right)$$
$$-V_{cell}\cdot\left(\frac{0.2\cdot[PCnp]}{0.1+[PCnp]}\right)$$

$$\frac{d([In]\cdot V_{cell})}{dt} = +V_{cell}\cdot((1\cdot[PCn]\cdot[Bn]-0.2\cdot[In]))$$
$$-V_{cell}\cdot(0.02\cdot[In])$$
$$-V_{cell}\cdot\left(\frac{1.6\cdot[In]}{0.3+[In]}\right)$$

$$\frac{d([Mr]\cdot V_{cell})}{dt} = +V_{cell}\cdot\left(\frac{1.6\cdot[Bn]^2}{0.6^2+[Bn]^2}\right)$$
$$-V_{cell}\cdot(0.02\cdot[Mr])$$
$$-V_{cell}\cdot\left(\frac{1.6\cdot[Mr]}{0.4+[Mr]}\right)$$

$$\frac{d([Rc]\cdot V_{cell})}{dt} = +V_{cell}\cdot(1.7\cdot[Mr])$$
$$-V_{cell}\cdot((0.8\cdot[Rc]-0.4\cdot[Rn]))$$
$$-V_{cell}\cdot\left(\frac{4.4\cdot[Rc]}{0.3+[Rc]}\right)$$
$$-V_{cell}\cdot(0.02\cdot[Rc])$$

$$\frac{d([Rn]\cdot V_{cell})}{dt} = +V_{cell}\cdot((0.8\cdot[Rc]-0.4\cdot[Rn]))$$
$$-V_{cell}\cdot\left(\frac{0.8\cdot[Rn]}{0.3+[Rn]}\right)$$
$$-V_{cell}\cdot(0.02\cdot[Rn])$$

$$\frac{d([Lm]\cdot V_{cell})}{dt} = -V_{cell}\cdot(0.01\cdot[Lm])$$
$$-V_{cell}\cdot\left(\frac{3\cdot[Lm]}{0.3+[Lm]}\right)$$
$$-2\cdot V_{cell}\cdot((4\cdot[Lm]\cdot[Lm]-1\cdot[Lm\_Lm]))$$
$$+V_{cell}\cdot(5\cdot[mLm])$$

$$\frac{d([Lm\_Lm]\cdot V_{cell})}{dt} = +V_{cell}\cdot((4\cdot[Lm]\cdot[Lm]-1\cdot[Lm\_Lm])) - V_{cell}\cdot(0.02\cdot[Lm\_Lm]) - V_{cell}\cdot\left(\frac{4\cdot[Lm\_Lm]}{0.3+[Lm\_Lm]}\right)$$

$$\frac{d([mLm]\cdot V_{cell})}{dt} = +V_{cell}\cdot\left(\frac{1.8\cdot[Bn]^2}{0.6^2+[Bn]^2}\right) - V_{cell}\cdot(0.01\cdot[mLm]) - V_{cell}\cdot\left(\frac{2\cdot[mLm]}{0.4+[mLm]}\right)$$

$$LD = ceiling(12, Time)$$

$$vsp = 2.3999999999999999+(3-2.3999999999999999)\cdot LD$$

9.2 Model 2: lamin A upregulate *Per* ODEs

$$\frac{d([Mb]\cdot V_{cell})}{dt} = +V_{cell}\cdot\left(\frac{2.04797\cdot 0.2445^{1.525}}{0.2445^{1.525}+[Rn]^{1.525}}\right) - V_{cell}\cdot(0.02\cdot[Mb]) - V_{cell}\cdot\left(\frac{1.3\cdot[Mb]}{0.4+[Mb]}\right)$$

$$\frac{d([Bc]\cdot V_{cell})}{dt} = -V_{cell}\cdot(0.02\cdot[Bc]) + V_{cell}\cdot\left(\frac{0.2\cdot[Bcp]}{0.1+[Bcp]}\right) + V_{cell}\cdot(0.32\cdot[Mb]) - V_{cell}\cdot\left(\frac{1.4\cdot[Bc]}{1.006+[Bc]}\right) - V_{cell}\cdot((0.8\cdot[Bc]-0.4\cdot[Bn]))$$

$$\frac{d([Bcp]\cdot V_{cell})}{dt} = -V_{cell}\cdot\left(\frac{3\cdot[Bcp]}{0.3+[Bcp]}\right) - V_{cell}\cdot\left(\frac{0.2\cdot[Bcp]}{0.1+[Bcp]}\right) + V_{cell}\cdot\left(\frac{1.4\cdot[Bc]}{1.006+[Bc]}\right) - V_{cell}\cdot(0.02\cdot[Bcp])$$

$$\frac{d([Bn]\cdot V_{cell})}{dt} = -V_{cell}\cdot\left(\frac{1.4\cdot[Bn]}{1.006+[Bn]}\right) - V_{cell}\cdot(0.02\cdot[Bn]) + V_{cell}\cdot\left(\frac{0.4\cdot[Bnp]}{0.1+[Bnp]}\right) + V_{cell}\cdot((0.8\cdot[Bc]-0.4\cdot[Bn])) - V_{cell}\cdot((1\cdot[PCn]\cdot[Bn]-0.2\cdot[In]))$$

$$\frac{d([Cc]\cdot V_{cell})}{dt} = +V_{cell}\cdot\left(\frac{0.2\cdot[Ccp]}{0.1+[Ccp]}\right) +V_{cell}\cdot(3.2\cdot[Mc]) -V_{cell}\cdot\left(\frac{1.2\cdot[Cc]}{1.006+[Cc]}\right) -V_{cell}\cdot((0.8\cdot[Cc]\cdot[Pc]-0.4\cdot[PCc])) -V_{cell}\cdot(0.2\cdot[Cc])$$

$$\frac{d([Mc]\cdot V_{cell})}{dt} = -V_{cell}\cdot(0.02\cdot[Mc]) +V_{cell}\cdot\left(\frac{2.2\cdot[Bn]^2}{0.6^2+[Bn]^2}\right) -V_{cell}\cdot\left(\frac{2\cdot[Mc]}{0.4+[Mc]}\right)$$

$$\frac{d([Ccp]\cdot V_{cell})}{dt} = -V_{cell}\cdot\left(\frac{0.2\cdot[Ccp]}{0.1+[Ccp]}\right) +V_{cell}\cdot\left(\frac{1.2\cdot[Cc]}{1.006+[Cc]}\right) -V_{cell}\cdot\left(\frac{1.4\cdot[Ccp]}{0.3+[Ccp]}\right) -V_{cell}\cdot(0.02\cdot[Ccp])$$

$$\frac{d([Mp]\cdot V_{cell})}{dt} = +V_{cell}\cdot\left(\frac{3.00241\cdot[Bn]^{0.267029}}{0.786553^{0.267029}+[Lm\_Lm]^{0.267029}}\right) -V_{cell}\cdot(0.02\cdot[Mp]) -V_{cell}\cdot\left(\frac{2.2\cdot[Mp]}{0.3+[Mp]}\right)$$

$$\frac{d([Pc]\cdot V_{cell})}{dt} = +V_{cell}\cdot\left(\frac{0.6\cdot[Pcp]}{0.1+[Pcp]}\right) +V_{cell}\cdot(1.2\cdot[Mp]) -V_{cell}\cdot\left(\frac{9.6\cdot[Pc]}{1.006+[Pc]}\right) -V_{cell}\cdot((0.8\cdot[Cc]\cdot[Pc]-0.4\cdot[PCc])) -V_{cell}\cdot(0.02\cdot[Pc])$$

$$\frac{d([Pcp]\cdot V_{cell})}{dt} = -V_{cell}\cdot\left(\frac{0.6\cdot[Pcp]}{0.1+[Pcp]}\right) -V_{cell}\cdot\left(\frac{3.4\cdot[Pcp]}{0.3+[Pcp]}\right) +V_{cell}\cdot\left(\frac{9.6\cdot[Pc]}{1.006+[Pc]}\right) -V_{cell}\cdot(0.02\cdot[Pcp])$$

$$\frac{d([PCc]\cdot V_{cell})}{dt} = +V_{cell}\cdot\left(\frac{0.2\cdot[PCcp]}{0.1+[PCcp]}\right) +V_{cell}\cdot((0.8\cdot[Cc]\cdot[Pc]-0.4\cdot[PCc])) -V_{cell}\cdot\left(\frac{2.4\cdot[PCc]}{1.006+[PCc]}\right) -V_{cell}\cdot((3\cdot[PCc]-0.4\cdot[PCn])) -V_{cell}\cdot(0.02\cdot[PCc])$$

$$\frac{d([PCcp]\cdot V_{cell})}{dt} = -V_{cell}\cdot\left(\frac{0.2\cdot[PCcp]}{0.1+[PCcp]}\right) + V_{cell}\cdot\left(\frac{2.4\cdot[PCc]}{1.006+[PCc]}\right) - V_{cell}\cdot\left(\frac{1.4\cdot[PCcp]}{0.3+[PCcp]}\right) - V_{cell}\cdot(0.02\cdot[PCcp])$$

$$\frac{d([PCn]\cdot V_{cell})}{dt} = +V_{cell}\cdot\left(\frac{0.2\cdot[PCnp]}{0.1+[PCnp]}\right) - V_{cell}\cdot(0.02\cdot[PCn]) + V_{cell}\cdot((3\cdot[PCc]-0.4\cdot[PCn])) - V_{cell}\cdot\left(\frac{2.4\cdot[PCn]}{1.006+[PCn]}\right) - V_{cell}\cdot((1\cdot[PCn]\cdot[Bn]-0.2\cdot[In]))$$

$$\frac{d([Bnp]\cdot V_{cell})}{dt} = +V_{cell}\cdot\left(\frac{1.4\cdot[Bn]}{1.006+[Bn]}\right) - V_{cell}\cdot\left(\frac{3\cdot[Bnp]}{0.3+[Bnp]}\right) - V_{cell}\cdot\left(\frac{0.4\cdot[Bnp]}{0.1+[Bnp]}\right) - V_{cell}\cdot(0.02\cdot[Bnp])$$

$$\frac{d([PCnp]\cdot V_{cell})}{dt} = -V_{cell}\cdot\left(\frac{0.2\cdot[PCnp]}{0.1+[PCnp]}\right) - V_{cell}\cdot(0.02\cdot[PCnp]) + V_{cell}\cdot\left(\frac{2.4\cdot[PCn]}{1.006+[PCn]}\right) - V_{cell}\cdot\left(\frac{1.4\cdot[PCnp]}{0.3+[PCnp]}\right)$$

$$\frac{d([In]\cdot V_{cell})}{dt} = -V_{cell}\cdot(0.02\cdot[In]) - V_{cell}\cdot\left(\frac{1.6\cdot[In]}{0.3+[In]}\right) + V_{cell}\cdot((1\cdot[PCn]\cdot[Bn]-0.2\cdot[In]))$$

$$\frac{d([Mr]\cdot V_{cell})}{dt} = +V_{cell}\cdot\left(\frac{1.6\cdot[Bn]^2}{0.6^2+[Bn]^2}\right) - V_{cell}\cdot(0.02\cdot[Mr]) - V_{cell}\cdot\left(\frac{1.6\cdot[Mr]}{0.4+[Mr]}\right)$$

$$\frac{d([Rc]\cdot V_{cell})}{dt} = +V_{cell}\cdot(1.7\cdot[Mr]) - V_{cell}\cdot((0.8\cdot[Rc]-0.4\cdot[Rn])) - V_{cell}\cdot\left(\frac{4.4\cdot[Rc]}{0.3+[Rc]}\right) - V_{cell}\cdot(0.02\cdot[Rc])$$

$$\frac{d([Rn]\cdot V_{cell})}{dt} = +V_{cell}\cdot((0.8\cdot[Rc]-0.4\cdot[Rn])) - V_{cell}\cdot\left(\frac{0.8\cdot[Rn]}{0.3+[Rn]}\right) - V_{cell}\cdot(0.02\cdot[Rn])$$

$$\frac{d([Lm]\cdot V_{cell})}{dt} = -V_{cell}\cdot(0.01\cdot[Lm]) - V_{cell}\cdot\left(\frac{3\cdot[Lm]}{0.3+[Lm]}\right) - 2\cdot V_{cell}\cdot((4\cdot[Lm]\cdot[Lm]-1\cdot[Lm\_Lm])) + V_{cell}\cdot(5\cdot[mLm])$$

$$\frac{d([Lm\_Lm]\cdot V_{cell})}{dt} = +V_{cell}\cdot((4\cdot[Lm]\cdot[Lm]-1\cdot[Lm\_Lm])) - V_{cell}\cdot(0.02\cdot[Lm\_Lm]) - V_{cell}\cdot\left(\frac{4\cdot[Lm\_Lm]}{0.3+[Lm\_Lm]}\right)$$

$$\frac{d([mLm]\cdot V_{cell})}{dt} = +V_{cell}\cdot\left(\frac{1.9825\cdot[Bn]^{1.21381}}{0.547444^{1.21381}+[Bn]^{1.21381}}\right) - V_{cell}\cdot(0.01\cdot[mLm]) - V_{cell}\cdot\left(\frac{2\cdot[mLm]}{0.4+[mLm]}\right)$$

$$LD = ceiling(12, Time)$$

$$vsp = 2.3999999999999999 + (3 - 2.3999999999999999)\cdot LD$$

9.3 Model 3: lamin A regulate PER:CRY localisation ODEs

$$\frac{d([Mb]\cdot V_{cell})}{dt} = -V_{cell}\cdot\left(\frac{1.3\cdot[Mb]}{0.4+[Mb]}\right) - V_{cell}\cdot(0.02\cdot[Mb]) + V_{cell}\cdot\left(\frac{2.04797\cdot 0.264958^{1.525}}{0.264958^{1.525}+[Rn]^{1.525}}\right)$$

$$\frac{d([Bc]\cdot V_{cell})}{dt} = +V_{cell}\cdot\left(\frac{0.2\cdot[Bcp]}{0.1+[Bcp]}\right) - V_{cell}\cdot(0.02\cdot[Bc]) - V_{cell}\cdot((0.8\cdot[Bc]-0.4\cdot[Bn])) - V_{cell}\cdot\left(\frac{1.4\cdot[Bc]}{1.006+[Bc]}\right) + V_{cell}\cdot(0.32\cdot[Mb])$$

$$\frac{d([Bcp]\cdot V_{cell})}{dt} = -V_{cell}\cdot\left(\frac{0.2\cdot[Bcp]}{0.1+[Bcp]}\right) - V_{cell}\cdot\left(\frac{3\cdot[Bcp]}{0.3+[Bcp]}\right) - V_{cell}\cdot(0.02\cdot[Bcp]) + V_{cell}\cdot\left(\frac{1.4\cdot[Bc]}{1.006+[Bc]}\right)$$

$$\frac{d([Bn]\cdot V_{cell})}{dt} = +V_{cell}\cdot\left(\frac{0.4\cdot[Bnp]}{0.1+[Bnp]}\right) - V_{cell}\cdot(0.02\cdot[Bn]) - V_{cell}\cdot\left(\frac{1.4\cdot[Bn]}{1.006+[Bn]}\right) - V_{cell}\cdot((1\cdot[PCn]\cdot[Bn] - 0.2\cdot[In])) + V_{cell}\cdot((0.8\cdot[Bc] - 0.4\cdot[Bn]))$$

$$\frac{d([Cc]\cdot V_{cell})}{dt} = +V_{cell}\cdot\left(\frac{0.2\cdot[Ccp]}{0.1+[Ccp]}\right) - V_{cell}\cdot(0.2\cdot[Cc]) - V_{cell}\cdot((0.8\cdot[Cc]\cdot[Pc] - 0.4\cdot[PCc])) - V_{cell}\cdot\left(\frac{1.2\cdot[Cc]}{1.006+[Cc]}\right) + V_{cell}\cdot(3.2\cdot[Mc])$$

$$\frac{d([Mc]\cdot V_{cell})}{dt} = -V_{cell}\cdot\left(\frac{2\cdot[Mc]}{0.4+[Mc]}\right) + V_{cell}\cdot\left(\frac{2.2\cdot[Bn]^2}{0.6^2+[Bn]^2}\right) - V_{cell}\cdot(0.02\cdot[Mc])$$

$$\frac{d([Ccp]\cdot V_{cell})}{dt} = -V_{cell}\cdot\left(\frac{0.2\cdot[Ccp]}{0.1+[Ccp]}\right) - V_{cell}\cdot(0.02\cdot[Ccp]) - V_{cell}\cdot\left(\frac{1.4\cdot[Ccp]}{0.3+[Ccp]}\right) + V_{cell}\cdot\left(\frac{1.2\cdot[Cc]}{1.006+[Cc]}\right)$$

$$\frac{d([Mp]\cdot V_{cell})}{dt} = -V_{cell}\cdot\left(\frac{2.2\cdot[Mp]}{0.3+[Mp]}\right) - V_{cell}\cdot(0.02\cdot[Mp]) + V_{cell}\cdot\left(\frac{2.4\cdot[Bn]^2}{0.6^2+[Bn]^2}\right)$$

$$\frac{d([Pc]\cdot V_{cell})}{dt} = +V_{cell}\cdot\left(\frac{0.6\cdot[Pcp]}{0.1+[Pcp]}\right) - V_{cell}\cdot(0.02\cdot[Pc]) - V_{cell}\cdot((0.8\cdot[Cc]\cdot[Pc] - 0.4\cdot[PCc])) - V_{cell}\cdot\left(\frac{9.6\cdot[Pc]}{1.006+[Pc]}\right) + V_{cell}\cdot(1.2\cdot[Mp])$$

$$\frac{d([Pcp]\cdot V_{cell})}{dt} = -V_{cell}\cdot\left(\frac{0.6\cdot[Pcp]}{0.1+[Pcp]}\right) -V_{cell}\cdot(0.02\cdot[Pcp]) +V_{cell}\cdot\left(\frac{9.6\cdot[Pc]}{1.006+[Pc]}\right) -V_{cell}\cdot\left(\frac{3.4\cdot[Pcp]}{0.3+[Pcp]}\right)$$

$$\frac{d([PCc]\cdot V_{cell})}{dt} = +V_{cell}\cdot\left(\frac{0.2\cdot[PCcp]}{0.1+[PCcp]}\right) -V_{cell}\cdot(0.02\cdot[PCc]) -V_{cell}\cdot((0.8\cdot[PCc]-0.4\cdot[PCn])) -V_{cell}\cdot\left(\frac{2.4\cdot[PCc]}{1.006+[PCc]}\right) +V_{cell}\cdot((0.8\cdot[Cc]\cdot[Pc]-0.4\cdot[PCc]))$$

$$\frac{d([PCcp]\cdot V_{cell})}{dt} = -V_{cell}\cdot\left(\frac{0.2\cdot[PCcp]}{0.1+[PCcp]}\right) -V_{cell}\cdot(0.02\cdot[PCcp]) -V_{cell}\cdot\left(\frac{1.4\cdot[PCcp]}{0.3+[PCcp]}\right) +V_{cell}\cdot\left(\frac{2.4\cdot[PCc]}{1.006+[PCc]}\right)$$

$$\frac{d([PCn]\cdot V_{cell})}{dt} = -V_{cell}\cdot((0.5\cdot[Lm\_Lm]\cdot[PCn]-1\cdot[Lm\_LmPCn])) -V_{cell}\cdot(0.02\cdot[PCn]) +V_{cell}\cdot\left(\frac{0.2\cdot[PCnp]}{0.1+[PCnp]}\right) -V_{cell}\cdot((1\cdot[PCn]\cdot[Bn]-0.2\cdot[In])) -V_{cell}\cdot\left(\frac{2.4\cdot[PCn]}{1.006+[PCn]}\right) +V_{cell}\cdot((0.8\cdot[PCc]-0.4\cdot[PCn]))$$

$$\frac{d([Bnp]\cdot V_{cell})}{dt} = -V_{cell}\cdot\left(\frac{0.4\cdot[Bnp]}{0.1+[Bnp]}\right) -V_{cell}\cdot\left(\frac{3\cdot[Bnp]}{0.3+[Bnp]}\right) +V_{cell}\cdot\left(\frac{1.4\cdot[Bn]}{1.006+[Bn]}\right) -V_{cell}\cdot(0.02\cdot[Bnp])$$

$$\frac{d([PCnp]\cdot V_{cell})}{dt} = -V_{cell}\cdot\left(\frac{0.2\cdot[PCnp]}{0.1+[PCnp]}\right) -V_{cell}\cdot\left(\frac{1.4\cdot[PCnp]}{0.3+[PCnp]}\right) +V_{cell}\cdot\left(\frac{2.4\cdot[PCn]}{1.006+[PCn]}\right) -V_{cell}\cdot(0.02\cdot[PCnp])$$

$$\frac{d([In]\cdot V_{cell})}{dt} = -V_{cell}\cdot\left(\frac{1.6\cdot[In]}{0.3+[In]}\right) - V_{cell}\cdot(0.02\cdot[In]) + V_{cell}\cdot((1\cdot[PCn]\cdot[Bn]-0.2\cdot[In]))$$

$$\frac{d([Mr]\cdot V_{cell})}{dt} = -V_{cell}\cdot\left(\frac{1.6\cdot[Mr]}{0.4+[Mr]}\right) - V_{cell}\cdot(0.02\cdot[Mr]) + V_{cell}\cdot\left(\frac{1.6\cdot[Bn]^2}{0.6^2+[Bn]^2}\right)$$

$$\frac{d([Rc]\cdot V_{cell})}{dt} = -V_{cell}\cdot(0.02\cdot[Rc]) - V_{cell}\cdot\left(\frac{4.4\cdot[Rc]}{0.3+[Rc]}\right) - V_{cell}\cdot((0.8\cdot[Rc]-0.4\cdot[Rn])) + V_{cell}\cdot(1.7\cdot[Mr])$$

$$\frac{d([Rn]\cdot V_{cell})}{dt} = -V_{cell}\cdot\left(\frac{0.8\cdot[Rn]}{0.3+[Rn]}\right) + V_{cell}\cdot((0.8\cdot[Rc]-0.4\cdot[Rn])) - V_{cell}\cdot(0.02\cdot[Rn])$$

$$\frac{d([Lm]\cdot V_{cell})}{dt} = +V_{cell}\cdot(5\cdot[mLm]) - 2\cdot V_{cell}\cdot((4\cdot[Lm]\cdot[Lm]-1\cdot[Lm\_Lm])) - V_{cell}\cdot\left(\frac{3\cdot[Lm]}{0.3+[Lm]}\right) - V_{cell}\cdot(0.01\cdot[Lm])$$

$$\frac{d([Lm\_Lm]\cdot V_{cell})}{dt} = -V_{cell}\cdot\left(\frac{4\cdot[Lm\_Lm]}{0.3+[Lm\_Lm]}\right) - V_{cell}\cdot(0.02\cdot[Lm\_Lm]) - V_{cell}\cdot((0.5\cdot[Lm\_Lm]\cdot[PCn]-1\cdot[Lm\_LmPCn])) + V_{cell}\cdot((4\cdot[Lm]\cdot[Lm]-1\cdot[Lm\_Lm]))$$

$$\frac{d([mLm]\cdot V_{cell})}{dt} = -V_{cell}\cdot\left(\frac{2\cdot[mLm]}{0.4+[mLm]}\right) - V_{cell}\cdot(0.01\cdot[mLm]) + V_{cell}\cdot\left(\frac{1.8\cdot[Bn]^2}{0.6^2+[Bn]^2}\right)$$

$$\frac{d([Lm\_LmPCn]\cdot V_{cell})}{dt} = +V_{cell}\cdot((0.5\cdot[Lm\_Lm]\cdot[PCn]-1\cdot[Lm\_LmPCn])) - V_{cell}\cdot(0.02\cdot[Lm\_LmPCn]) - V_{cell}\cdot\left(\frac{0.8\cdot[Lm\_LmPCn]}{0.4+[Lm\_LmPCn]}\right)$$

$$LD = \text{ceiling}(12, Time)$$

$$vsp = 2.3999999999999999 + (3 - 2.3999999999999999)\cdot LD$$

9.4 Model 4: lamin A regulate PER:CRY translocation ODEs

$$\frac{d([Mb]\cdot V_{cell})}{dt} = -V_{cell}\cdot\left(\frac{1.3\cdot[Mb]}{0.4+[Mb]}\right) - V_{cell}\cdot(0.02\cdot[Mb]) + V_{cell}\cdot\left(\frac{2.04797\cdot 0.24^{1.525}}{0.24^{1.525}+[Rn]^{1.525}}\right)$$

$$\frac{d([Bc]\cdot V_{cell})}{dt} = -V_{cell}\cdot((0.8\cdot[Bc]-0.4\cdot[Bn])) - V_{cell}\cdot\left(\frac{1.4\cdot[Bc]}{1.006+[Bc]}\right) + V_{cell}\cdot(0.32\cdot[Mb]) + V_{cell}\cdot\left(\frac{0.2\cdot[Bcp]}{0.1+[Bcp]}\right) - V_{cell}\cdot(0.02\cdot[Bc])$$

$$\frac{d([Bcp]\cdot V_{cell})}{dt} = -V_{cell}\cdot(0.02\cdot[Bcp]) + V_{cell}\cdot\left(\frac{1.4\cdot[Bc]}{1.006+[Bc]}\right) - V_{cell}\cdot\left(\frac{0.2\cdot[Bcp]}{0.1+[Bcp]}\right) - V_{cell}\cdot\left(\frac{3\cdot[Bcp]}{0.3+[Bcp]}\right)$$

$$\frac{d([Bn]\cdot V_{cell})}{dt} = -V_{cell}\cdot((1\cdot[PCn]\cdot[Bn]-0.2\cdot[In])) + V_{cell}\cdot((0.8\cdot[Bc]-0.4\cdot[Bn])) + V_{cell}\cdot\left(\frac{0.4\cdot[Bnp]}{0.1+[Bnp]}\right) - V_{cell}\cdot(0.02\cdot[Bn]) - V_{cell}\cdot\left(\frac{1.4\cdot[Bn]}{1.006+[Bn]}\right)$$

$$\frac{d([Cc]\cdot V_{cell})}{dt} = -V_{cell}\cdot(0.2\cdot[Cc]) - V_{cell}\cdot((0.8\cdot[Cc]\cdot[Pc]-0.4\cdot[PCc])) - V_{cell}\cdot\left(\frac{1.2\cdot[Cc]}{1.006+[Cc]}\right) + V_{cell}\cdot(3.2\cdot[Mc]) + V_{cell}\cdot\left(\frac{0.2\cdot[Ccp]}{0.1+[Ccp]}\right)$$

$$\frac{d([Mc]\cdot V_{cell})}{dt} = -V_{cell}\cdot\left(\frac{2\cdot[Mc]}{0.4+[Mc]}\right) + V_{cell}\cdot\left(\frac{2.2\cdot[Bn]^2}{0.6^2+[Bn]^2}\right) - V_{cell}\cdot(0.02\cdot[Mc])$$

$$\frac{d([Ccp]\cdot V_{cell})}{dt} = -V_{cell}\cdot(0.02\cdot[Ccp])$$
$$-V_{cell}\cdot\left(\frac{1.4\cdot[Ccp]}{0.3+[Ccp]}\right)$$
$$+V_{cell}\cdot\left(\frac{1.2\cdot[Cc]}{1.006+[Cc]}\right)$$
$$-V_{cell}\cdot\left(\frac{0.2\cdot[Ccp]}{0.1+[Ccp]}\right)$$

$$\frac{d([Mp]\cdot V_{cell})}{dt} = -V_{cell}\cdot\left(\frac{2.2\cdot[Mp]}{0.3+[Mp]}\right)$$
$$-V_{cell}\cdot(0.02\cdot[Mp])$$
$$+V_{cell}\cdot\left(\frac{2.4\cdot[Bn]^2}{0.6^2+[Bn]^2}\right)$$

$$\frac{d([Pc]\cdot V_{cell})}{dt} = -V_{cell}\cdot(0.02\cdot[Pc])$$
$$-V_{cell}\cdot((0.8\cdot[Cc]\cdot[Pc]-0.4\cdot[PCc]))$$
$$-V_{cell}\cdot\left(\frac{9.6\cdot[Pc]}{1.006+[Pc]}\right)$$
$$+V_{cell}\cdot(1.2\cdot[Mp])$$
$$+V_{cell}\cdot\left(\frac{0.6\cdot[Pcp]}{0.1+[Pcp]}\right)$$

$$\frac{d([Pcp]\cdot V_{cell})}{dt} = -V_{cell}\cdot(0.02\cdot[Pcp])$$
$$+V_{cell}\cdot\left(\frac{9.6\cdot[Pc]}{1.006+[Pc]}\right)$$
$$-V_{cell}\cdot\left(\frac{3.4\cdot[Pcp]}{0.3+[Pcp]}\right)$$
$$-V_{cell}\cdot\left(\frac{0.6\cdot[Pcp]}{0.1+[Pcp]}\right)$$

$$\frac{d([PCc]\cdot V_{cell})}{dt} = -V_{cell}\cdot\left(\frac{\frac{3.28\cdot[PCc]}{2.005}-\frac{0.505\cdot[PCn]}{1.01}}{1+\frac{[PCc]}{2.005}+\frac{[PCn]}{1.01}+\frac{[Lm\_Lm]}{15.08}}\right)$$
$$-V_{cell}\cdot\left(\frac{2.4\cdot[PCc]}{1.006+[PCc]}\right)$$
$$+V_{cell}\cdot((0.8\cdot[Cc]\cdot[Pc]-0.4\cdot[PCc]))$$
$$+V_{cell}\cdot\left(\frac{0.2\cdot[PCcp]}{0.1+[PCcp]}\right)$$
$$-V_{cell}\cdot(0.02\cdot[PCc])$$

$$\frac{d([PCcp]\cdot V_{cell})}{dt} = -V_{cell}\cdot(0.02\cdot[PCcp])$$
$$-V_{cell}\cdot\left(\frac{1.4\cdot[PCcp]}{0.3+[PCcp]}\right)$$
$$+V_{cell}\cdot\left(\frac{2.4\cdot[PCc]}{1.006+[PCc]}\right)$$
$$-V_{cell}\cdot\left(\frac{0.2\cdot[PCcp]}{0.1+[PCcp]}\right)$$

$$\frac{d([PCn]\cdot V_{cell})}{dt} = -V_{cell}\cdot((1\cdot[PCn]\cdot[Bn]-0.2\cdot[In]))$$
$$-V_{cell}\cdot\left(\frac{2.4\cdot[PCn]}{1.006+[PCn]}\right)$$
$$+V_{cell}\cdot\left(\frac{\frac{3.28\cdot[PCc]}{2.005}-\frac{0.505\cdot[PCn]}{1.01}}{1+\frac{[PCc]}{2.005}+\frac{[PCn]}{1.01}+\frac{[Lm\_Lm]}{15.08}}\right)$$
$$-V_{cell}\cdot(0.02\cdot[PCn])$$
$$+V_{cell}\cdot\left(\frac{0.2\cdot[PCnp]}{0.1+[PCnp]}\right)$$

$$\frac{d([Bnp]\cdot V_{cell})}{dt} = -V_{cell}\cdot(0.02\cdot[Bnp])$$
$$-V_{cell}\cdot\left(\frac{0.4\cdot[Bnp]}{0.1+[Bnp]}\right)$$
$$-V_{cell}\cdot\left(\frac{3\cdot[Bnp]}{0.3+[Bnp]}\right)$$
$$+V_{cell}\cdot\left(\frac{1.4\cdot[Bn]}{1.006+[Bn]}\right)$$

$$\frac{d([PCnp]\cdot V_{cell})}{dt} = +V_{cell}\cdot\left(\frac{2.4\cdot[PCn]}{1.006+[PCn]}\right)$$
$$-V_{cell}\cdot(0.02\cdot[PCnp])$$
$$-V_{cell}\cdot\left(\frac{0.2\cdot[PCnp]}{0.1+[PCnp]}\right)$$
$$-V_{cell}\cdot\left(\frac{1.4\cdot[PCnp]}{0.3+[PCnp]}\right)$$

$$\frac{d([In]\cdot V_{cell})}{dt} = +V_{cell}\cdot((1\cdot[PCn]\cdot[Bn]-0.2\cdot[In]))$$
$$-V_{cell}\cdot\left(\frac{1.6\cdot[In]}{0.3+[In]}\right)$$
$$-V_{cell}\cdot(0.02\cdot[In])$$

$$\frac{d([Mr]\cdot V_{cell})}{dt} = -V_{cell}\cdot\left(\frac{1.6\cdot[Mr]}{0.4+[Mr]}\right)$$
$$-V_{cell}\cdot(0.02\cdot[Mr])$$
$$+V_{cell}\cdot\left(\frac{1.6\cdot[Bn]^2}{0.6^2+[Bn]^2}\right)$$

$$\frac{d([Rc]\cdot V_{cell})}{dt} = -V_{cell}\cdot(0.02\cdot[Rc])$$
$$-V_{cell}\cdot\left(\frac{4.4\cdot[Rc]}{0.3+[Rc]}\right)$$
$$-V_{cell}\cdot((0.8\cdot[Rc]-0.4\cdot[Rn]))$$
$$+V_{cell}\cdot(1.7\cdot[Mr])$$

$$\frac{d([Rn]\cdot V_{cell})}{dt} = -V_{cell}\cdot(0.02\cdot[Rn])$$
$$-V_{cell}\cdot\left(\frac{0.8\cdot[Rn]}{0.3+[Rn]}\right)$$
$$+V_{cell}\cdot((0.8\cdot[Rc]-0.4\cdot[Rn]))$$

$$\frac{d([Lm]\cdot V_{cell})}{dt} = +V_{cell}\cdot(5\cdot[mLm])$$
$$-2\cdot V_{cell}\cdot((4\cdot[Lm]\cdot[Lm]-1\cdot[Lm\_Lm]))$$
$$-V_{cell}\cdot\left(\frac{3\cdot[Lm]}{0.3+[Lm]}\right)$$
$$-V_{cell}\cdot(0.01\cdot[Lm])$$
$$\frac{d([Lm\_Lm]\cdot V_{cell})}{dt} = -V_{cell}\cdot\left(\frac{4\cdot[Lm\_Lm]}{0.3+[Lm\_Lm]}\right)$$
$$-V_{cell}\cdot(0.02\cdot[Lm\_Lm])$$
$$+V_{cell}\cdot((4\cdot[Lm]\cdot[Lm]-1\cdot[Lm\_Lm]))$$
$$\frac{d([mLm]\cdot V_{cell})}{dt} = -V_{cell}\cdot\left(\frac{2\cdot[mLm]}{0.4+[mLm]}\right)$$
$$-V_{cell}\cdot(0.01\cdot[mLm])$$
$$+V_{cell}\cdot\left(\frac{1.8\cdot[Bn]^2}{0.6^2+[Bn]^2}\right)$$
$$LD = ceiling(12, Time)$$
$$vsp = 2.3999999999999999+(3-2.3999999999999999)\cdot LD$$